



**HAL**  
open science

# Modélisation semi-distribuée de la production et du transfert des MES, HAPs et métaux dans les eaux urbaines de temps de pluie

Saja Al Ali

► **To cite this version:**

Saja Al Ali. Modélisation semi-distribuée de la production et du transfert des MES, HAPs et métaux dans les eaux urbaines de temps de pluie. Chimie analytique. Université Paris-Est; École doctorale des Sciences et de Technologie (Beyrouth), 2018. Français. NNT : 2018PESC1012 . tel-01876672

**HAL Id: tel-01876672**

**<https://pastel.hal.science/tel-01876672>**

Submitted on 18 Sep 2018

**HAL** is a multi-disciplinary open access archive for the deposit and dissemination of scientific research documents, whether they are published or not. The documents may come from teaching and research institutions in France or abroad, or from public or private research centers.

L'archive ouverte pluridisciplinaire **HAL**, est destinée au dépôt et à la diffusion de documents scientifiques de niveau recherche, publiés ou non, émanant des établissements d'enseignement et de recherche français ou étrangers, des laboratoires publics ou privés.

**Thèse en cotutelle**

Pour obtenir le grade de Docteur délivré par

**L'UNIVERSITE PARIS-EST**

ECOLE DOCTORALE : Sciences, Ingénierie et Environnement

*Spécialité Sciences et Techniques de l'Environnement*

Et

**L'UNIVERSITE LIBANAISE**

ECOLE DOCTORALE : Sciences et Technologies

Présentée et soutenue publiquement le 22 janvier 2018 par

**Saja Al Ali**

**MODELISATION SEMI-DISTRIBUEE DE LA PRODUCTION  
ET DU TRANSFERT DES MES, HAPS ET METAUX DANS LES EAUX  
URBAINES DE TEMPS DE PLUIE**

**Membres du jury**

M. Gislain Lipeme-Kouyi  
M. Patrick Willems  
M. Fabrice Rodriguez  
M. Yelva Roustan  
Mme. Céline Bonhomme

Insa de Lyon  
KU Leuven  
IFSTTAR  
Ecole des Ponts ParisTech  
Ministère de la transition écologique et  
solidaire  
Université Libanaise  
Université Libanaise

Rapporteur  
Rapporteur (Président du jury)  
Examineur  
Examineur  
Co-Directeur de thèse  
Directeur de thèse (France)  
Directeur de thèse (Liban)



*A mes parents,*

*A mes sœurs...*

# Résumé

La maîtrise de la contamination générée par temps de pluie en milieu urbain constitue un enjeu environnemental important pour limiter la dégradation des milieux aquatiques superficiels. Les outils de modélisation traditionnelle utilisés pour estimer les flux de polluants dans les eaux de ruissellement sont jugés insuffisants dans leur capacité à reproduire les dynamiques des polluants à l'exutoire. Cela est souvent lié au manque de connaissances précises sur les processus en jeu d'une part, et d'autre part aux difficultés d'acquérir des bases de données représentatives et en continu sur des sites réels. Cette thèse a donc pour objectif d'améliorer l'état de la modélisation de la qualité. Elle vise en particulier le développement d'un outil de modélisation conceptuelle de la qualité des eaux de ruissellement à l'échelle du quartier, à partir d'une compréhension approfondie des processus d'accumulation et de lessivage. La simulation des pollutogrammes de matières en suspension (MES) à l'avaloir du bassin versant routier avec les modèles conceptuels d'accumulation-lessivage montre la faible performance des modèles pour estimer les dynamiques d'émissions de MES pour des longues périodes ; la variabilité du processus d'accumulation est le responsable principal de l'inadéquation de ces modèles. L'évaluation de la contribution des retombées atmosphériques sèches à la contamination des eaux de ruissellement en hydrocarbures aromatiques polycycliques (HAPs) et métaux montrent que l'atmosphère ne joue qu'un rôle très mineur dans la contamination des eaux de ruissellement par ces substances. Ainsi le couplage des modèles atmosphériques, qui ne tiennent pas compte des émissions directes liées au trafic, avec les modèles de qualité de l'eau, ne semble pas très pertinent dans l'objectif d'améliorer la prédiction de la contamination des eaux pluviales à l'exutoire. L'investigation à la micro-échelle du mécanisme de lessivage montre que les particules fines sont les plus susceptibles d'être mobilisées par le ruissellement. Cette étude a été menée en utilisant un simulateur de pluie innovant qui présente les avantages d'être mobile et léger, et la possibilité d'avoir des enregistrements en ligne du débit et de la turbidité. Les nouvelles connaissances acquises sur les processus soulignent une grande variabilité qui remet en cause l'intérêt de leur modélisation avec des approches déterministes. Ces connaissances sont intégrées à l'échelle du quartier pour développer un outil de modélisation conceptuelle basé sur une approche

stochastique d'estimation de la concentration moyenne de MES et des paramètres de qualité. Le modèle développé est intégré dans le modèle hydrologique URBS. L'application de ce modèle permet d'intégrer la variabilité spatiale et temporelle des émissions en distinguant les contributions de chaque occupation du sol. Les résultats sont prometteurs en termes d'estimation des niveaux de concentration de MES à l'exutoire du bassin versant et de réplique du comportement général de la dynamique de MES, cependant des améliorations peuvent être envisagées pour consolider l'approche et améliorer ses prédictions. La comparaison de ce modèle avec des approches de modélisation empirique globale, conceptuelle semi-distribuée et physique distribuée, montre qu'en termes de pouvoir prédictif et de fiabilité, l'approche URBS-stochastique en parallèle avec l'approche de modélisation physique distribuée sont les plus performantes. En termes de simplicité d'implémentation et d'ajustement entre les observations et les simulations, les approches de modélisation empirique globale et conceptuelle semi-distribuée sont les plus puissantes. A l'issue de cette comparaison, il est clair qu'il n'existe pas un modèle parfait qui couvre toutes les caractéristiques de la modélisation de la qualité des eaux de ruissellement. Le choix de l'approche de modélisation la plus appropriée doit se faire en fonction des objectifs attendus par le modélisateur.

**Mots-clés :** Modélisation conceptuelle ; stochastique ; accumulation ; lessivage ; particules fines ; simulateur de pluie ; retombées atmosphériques ; polluants particuliers.

# Abstract

Urban runoff contamination is recognized as a major source of the deterioration of the quality of surface water. Commonly used stormwater quality models have poor performance in predicting the pollutant dynamics at the surface outlet, mainly due to the lack of precise knowledge on the governing processes and the difficulties of acquiring representative and continuous databases on real sites. The main purpose of this Ph.D. thesis is to improve the state of stormwater quality modeling. It aims in particular to develop a conceptual modeling tool for stormwater quality prediction at the scale of a city district catchment, based on a deep understanding of the build-up and the wash-off. The application of commonly used stormwater build-up/wash-off models to simulate the dynamics of total suspended solids (TSS) at the outlet of the road catchment suggests that the models poorly replicate the temporal variability of the TSS concentrations unless short periods are considered. The unpredictable nature of the accumulation is largely responsible for the model failure. The evaluation of the contribution of atmospheric dry deposition to stormwater loads for polycyclic aromatic hydrocarbons (PAHs) and metals shows that atmospheric deposition is not a major source of contaminants in stormwater runoff. Thus, linking the air and water compartment in a modeling chain to have more accurate estimates of pollutant loads in stormwater runoff may not be relevant unless the direct traffic emissions are accounted for. The investigation of the wash-off process on elementary surfaces shows that the fine particles are the most likely to be mobilized and transported during a rainfall event. Stormwater samples were collected for this study using an innovative rainfall simulator that allows continuous, on-site monitoring of instantaneous flow and turbidity and that can be easily transported and used on real sites. The new knowledge acquired on the build-up and wash-off processes underlines the great variability of these processes and calls into question their modeling with deterministic approaches. Hence, this knowledge is incorporated into developing a new conceptual stormwater quality model based on the stochastic drawing of event mean concentrations (EMC) of TSS and water quality parameters. The model is integrated within the hydrological model URBS. The application of this approach accounts for the spatial and temporal variability of pollutant emissions by distinguishing the contributions of each land use separately. The

obtained results are promising in terms of estimating the concentration levels of TSS at the outlet of the city district catchment and replicating the general behavior of the TSS dynamics. However, improvements can be envisaged to consolidate the approach and improve its predictions. Comparison of this model with global empirical, semi-distributed conceptual and distributed physical modeling approaches shows that in terms of predictive power and stability, the stochastic-URBS and the physically distributed approaches are the most efficient. However, in terms of ease of implementation and best fit between observations and simulations, the global empirical and semi-distributed conceptual modeling approaches are the most powerful. This comparison shows that the perfect model that covers all aspects of stormwater quality modeling does not exist. The choice of the most appropriate modeling approach should mainly be driven by modeling objectives.

**Keywords:** Conceptual modeling; stochastic; build-up; wash-off; fine particles; rainfall simulator; atmospheric deposition; particulate pollutants.



# Remerciements

Ce travail de recherche a été réalisé au Laboratoire Eau Environnement et Systèmes Urbains (LEESU), laboratoire commun de l'École Nationale des Ponts et Chaussées, de l'Université Paris Est et de l'Institut des sciences et industries du vivant et de l'environnement (AgroParisTech). Je souhaiterais tout d'abord remercier son directeur, Monsieur Régis Moilleron, de m'avoir accueilli au sein du laboratoire et d'avoir veillé au bon déroulement de la thèse durant ces trois longues et enrichissantes années.

Je souhaiterais remercier l'association « Azm & Saade » du Liban et le programme de recherche OPUR (Observatoire des Polluants Urbains) d'avoir financé cette thèse, réalisée en cotutelle entre le Liban et la France.

Ma reconnaissance va également à Monsieur Gislain Lipeme-Kouyi et Monsieur Patrick Willems d'avoir accepté de rapporter cette thèse, ainsi que Messieurs Fabrice Rodriguez et Yelva Roustan pour leur rôle d'examinateurs. Leur intérêt porté à ce travail ainsi que leurs remarques et critiques m'ont permis de prendre du recul sur ces trois années.

Cette thèse a été réalisée sous la direction de Monsieur Ghassan Chebbo en France et Madame Véronique Kazpard au Liban, et l'encadrement de Madame Céline Bonhomme en France. Je tiens à leur exprimer mes plus sincères remerciements pour leur confiance, leur implication, leur enthousiasme et leur soutien tout au long de ce travail. J'ai appris à leur côté la persévérance, la rigueur et la curiosité scientifique indispensable à tout travail de recherche. Sans eux, ce travail ne serait certainement pas ce qu'il est aujourd'hui. Je souhaiterais en particulier remercier Monsieur Ghassan Chebbo pour m'avoir permis d'intégrer le programme de recherche passionnant OPUR et pour toutes les idées intéressantes qu'il apportait à nos réunions. Je souhaiterais également saluer l'investissement considérable de Madame Céline Bonhomme qui était disponible tout au long de la thèse pour m'orienter, me guider et pour répondre à mes nombreuses interrogations. Je tiens par ailleurs à remercier Madame Véronique Kazpard pour m'avoir accompagné avec mes démarches au Liban.

Je tiens à remercier chaleureusement Monsieur Fabrice Rodriguez, et lui exprimer ma gratitude pour son implication dans cette thèse, ses conseils et sa bonne humeur. A travers cette collaboration, j'ai eu l'occasion d'approfondir considérablement le volet modélisation de ce travail de recherche.

Certains résultats de cette thèse s'appuient sur les contributions des stagiaires Xavier Debade et Edric Clayton à qui je souhaiterais adresser mes remerciements. Je tiens aussi à remercier Madame Béatrice Béchet qui a été impliquée dans le stage de Xavier Debade, et Yi Hong avec qui j'ai collaboré sur une partie de cette thèse.

Une partie de ce travail s'est appuyée sur des résultats expérimentaux acquis durant ma thèse. Je tiens par conséquent à remercier Messieurs Philippe Dubois et Mohamed Saad, pour leur aide, s'agissant de soutien méthodologique comme logistique. Je souhaiterais en particulier adresser ma gratitude à Monsieur Philippe Dubois, pour son appui précieux, sa disponibilité et sa patience lors des expérimentations que nous avons menées ensemble.

Un grand merci à Mesdames Annick Piazza, Catherine Charleux et Cécile Blachemanche pour leur soutien administratif mais surtout leur gentillesse et leurs sourires quotidiens.

Je tiens à remercier l'ensemble des membres (ou anciens membres) du LEESU avec qui j'ai partagé ces trois années de thèse. A Kelsey Flanagan et Tala Kanso, avec qui j'ai partagé des moments inoubliables qui resteront à jamais gravés dans ma mémoire, un très grand merci. A tous les doctorants du LEESU : Mohamad, Najwa, Jérémie, Steven, Claire, Damien, Neng, Yujie, Natalie, Yi, Fabien, Francesco... Un grand merci pour la bonne humeur, les discussions autour d'un café, les gâteaux, les galettes des rois, les tisanes, les chocolats, les sorties et surtout les encouragements dans la dernière ligne droite de cette thèse !

Je souhaiterais également remercier mes copines au Liban pour leur soutien inconditionnel : May, Lara, Roua, Zahraa, Sarah M., Sarah H., Nadine, Sabrine, Zeinab, Fatima F., Fatima D., Feda et Elissa.

Je souhaiterais adresser un merci très particulier à Walaa Issa et Mohamad Hobballah, je n'y serai jamais arrivée sans vous, votre amitié a été plus qu'un soutien.

Pour finir, je dois dire un grand MERCI à ma famille qui m'a soutenue, à mes sœurs, May et Nada, qui m'ont encouragé sans cesse, et particulièrement à mes parents, Sawsan et Mohamad, qui m'ont donné le goût pour les études et m'ont permis de suivre la voie que j'ai choisie. Je vous suis éternellement reconnaissante !



# Table des matières

Résumé .....	4
Abstract .....	6
Remerciements .....	8
Table des matières .....	11
Partie 1. Introduction.....	16
1.1. Contexte .....	16
1.2. Projets de recherche.....	18
1.2.1. OPUR.....	18
1.2.2. Trafipollu .....	19
1.3. Objectifs de la thèse .....	19
1.4. Structure du manuscrit.....	19
1.5. Références .....	22
Partie 2. Présentation des sites expérimentaux et de la base de données .....	24
2.1. Echelle locale : le bassin versant routier.....	25
2.1.1. Description du site.....	25
2.1.2. Mesures des paramètres quantitatifs et qualitatifs des eaux de ruissellement	25
2.1.3. Dépôts secs .....	26
2.1.4. Analyse granulométrique.....	28
2.1.5. Mesures des concentrations atmosphériques .....	28
2.2. Méso-Echelle : le bassin versant quartier .....	29
2.2.1. Description du site.....	29
2.2.2. Mesures des paramètres quantitatifs et qualitatifs des eaux à l'exutoire .	29

2.3.	Station pluviométrique.....	30
2.4.	L'expérimentation de lessivage.....	30
2.5.	Récapitulatif.....	31
Partie 3.	Etat de l'art.....	34
3.1.	Le ruissellement en milieu urbain.....	34
3.1.1.	Effets de l'urbanisation.....	35
3.1.2.	Pollution des eaux de ruissellement.....	39
3.2.	Processus d'accumulation et de lessivage.....	48
3.2.1.	Accumulation.....	49
3.2.2.	Lessivage.....	54
3.3.	Modélisation.....	57
3.3.1.	Modélisation hydrologique et fonction de production.....	57
3.3.2.	Modélisation de qualité.....	59
3.4.	Conclusion.....	69
3.5.	Références.....	70
Partie 4.	Compréhension des processus de production et de mobilisation des contaminants à l'échelle locale : modélisation et études expérimentales.....	87
Chapitre 1.	Evaluation of the Performance and the Predictive Capacity of Build-Up and Wash-Off Models on Different Temporal Scales.....	93
1.	Introduction.....	93
2.	Materials and Methods.....	96
3.	Results and discussion.....	105
4.	Conclusions and perspectives.....	122
5.	References.....	125
Chapitre 2.	Contribution of atmospheric dry deposition to stormwater loads for PAHs and trace metals in a small and highly trafficked urban road catchment.....	129

1. Introduction.....	129
2. Materials and methods .....	132
3. Results.....	138
4. Discussion.....	148
5. Conclusion.....	151
6. References.....	152
Chapitre 3. Investigation of the wash-off process using an innovative portable rainfall simulator allowing continuous monitoring of flow and turbidity at the urban surface outlet	157
1. Introduction.....	157
2. Materials and methods .....	160
3. Results.....	166
4. Discussion.....	173
5. Conclusion.....	179
6. References.....	183
Chapitre 4. Bilan des messages principaux dans cette partie.....	187
Partie 5. Modélisation de la production et du transfert de la contamination dans les eaux de ruissellement à l'échelle du quartier .....	189
Chapitre 5. Accounting for the spatio-temporal variability of pollutant processes in stormwater quality modelling based on stochastic approaches.....	193
1. Introduction.....	193
2. Materials and methods .....	196
3. Results and discussion.....	205
4. Conclusion.....	215
5. References.....	217

Chapitre 6. Benchmarking urban stormwater quality models of varying spatial discretization: A case study with lumped, sub-catchments based, urban hydrological element based and grid-based models .....	220
1. Introduction.....	220
2. Study site and data availability .....	222
3. Modelling approaches .....	227
4. Benchmarking different modelling approaches.....	231
5. Results and discussion.....	238
6. Future outlook for urban stormwater quality modelling practice .....	242
7. Conclusion.....	245
8. References.....	248
Chapitre 7. Bilan des messages principaux dans cette partie.....	252
Partie 6. Conclusions et Perspectives .....	254
6.1. Rappel des objectifs.....	254
6.2. Principaux résultats.....	254
6.2.1. Synthèse sur les connaissances acquises sur les processus d'accumulation et de lessivage.....	254
6.2.2. Synthèse sur la modélisation à l'échelle du quartier .....	255
6.3. Perspectives.....	257
6.3.1. Pour une meilleure compréhension des processus.....	257
6.3.2. Modélisation de la qualité : où va t'on ?.....	258





# Partie 1. Introduction

## 1.1. Contexte

L'urbanisation a connu un accroissement sans précédent depuis la moitié du XXème siècle dans la plupart des régions du monde. Selon un rapport de l'ONU sur l'urbanisation, 54% de la population mondiale vivait dans les zones urbaines en 2014, une fraction qui est supposée passer à 66% en 2050. L'expansion du développement urbain s'est traduite par la transformation progressive des zones rurales accompagnée de la construction intensive de bâtiments et infrastructures, et en conséquence par l'augmentation des surfaces imperméables (Paul and Meyer, 2001).

La modification de l'occupation du sol liée à l'urbanisation exerce des pressions directes sur le cycle de l'eau. Celles-ci se manifestent non seulement par l'augmentation des volumes ruisselés par temps de pluie mais aussi par l'augmentation des débits de pointe et la diminution du temps de réponse du bassin versant (Chocat, 1997; Schueler, 1994). En plus de l'altération du cycle hydrologique, s'ajoute la dégradation des milieux aquatiques récepteurs en raison de la forte contamination diffuse véhiculée par les eaux de ruissellement (Miller et al., 2014; Paul and Meyer, 2001).

La mise en place des stratégies pour limiter et contrôler les impacts des rejets urbains sur la qualité des milieux récepteurs imposée par les textes réglementaires (Directive cadre sur l'eau DCE/2000/60/CE) fait de la maîtrise de la contamination des rejets urbains par temps de pluie un enjeu environnemental important. Pour cette raison, des expérimentations sont mises en place sur les systèmes d'assainissement et les milieux récepteurs pour surveiller et quantifier les flux de polluants ; par ailleurs, les modèles mathématiques constituent des outils de gestion et de prédiction très importants car ils permettent d'avoir des estimations des masses et des flux rejetés.

Dès les années 1970, les modèles de calcul des rejets urbains par temps de pluie ont été développés et ils comprennent généralement deux modules : quantitatif et qualitatif. Les modèles hydrologiques quantitatifs basés sur la transformation pluie-débit ont largement évolué au cours du temps avec l'intégration des connaissances détaillées sur les processus

hydrologiques qui permettent d'avoir des estimations précises des flux d'eau (Fletcher et al., 2013). Cependant, l'évolution des modèles de qualité des rejets de polluants ne s'est pas faite au même rythme que celle des modèles quantitatifs. Les processus dominants vis-à-vis de la production et du transfert des contaminants dans le milieu urbain sont mal compris et leur description dans les modèles n'a pas évolué depuis une quarantaine d'années. La modélisation de la qualité des rejets urbains par temps de pluie reste alors un grand défi pour les chercheurs dans le domaine de l'hydrologie urbaine (Dotto et al., 2011; Freni et al., 2009). Cela est dû à plusieurs raisons notamment i) la complexité des processus de génération des polluants, ii) la difficulté de mesurer les processus directement in situ, iii) la quantité limitée de données de pollution des eaux à cause des contraintes économiques et logistiques, iv) les réactions physiques, chimiques, biologiques et biochimiques qui se passent dans le réseau, v) la variabilité extrême, spatiale et temporelle, des phénomènes liés à la pollution des eaux de ruissellement.

Les résultats obtenus dans le cadre des travaux antérieurs engagés sur le thème de la modélisation des contaminants en milieu urbain menés au LEESU soulignent les lacunes des modèles conceptuels de qualité. Dans la thèse de (Kanso, 2004), les principales conclusions montrent que les modèles traditionnels d'accumulation-lessivage, basés sur les équations de (Sartor et al., 1974), sont incapables de reproduire les pollutogrammes à l'exutoire du bassin versant « Le Marais » à Paris. Le calage de ces modèles en appliquant la méthode de Monte Carlo par Chaîne de Markov, a mis en évidence la grande incertitude liée à l'estimation des valeurs des paramètres de qualité et l'insensibilité des modèles aux valeurs optimales des paramètres, en particulier pour les paramètres d'accumulation. Ce travail s'appuyait sur une base de données événementielle où les prélèvements et les analyses n'ont été effectués que sur un nombre limité d'événements. Dans la thèse de (Sage, 2016), la performance de ces modèles a été évaluée mais cette fois ci en utilisant des données de débit et de turbidité acquises en continu sur 11 mois à l'avaloir d'une chaussée urbaine sur un bassin versant de 0.08 ha. Les résultats montrent encore une fois que les modèles conceptuels exponentiels d'accumulation-lessivage ont un pouvoir prédictif très faible. La capacité de ces modèles à estimer les dynamiques de MES est limitée pour des longues périodes ce qui est en majorité expliqué par la faiblesse de la formulation d'accumulation. Les travaux de modélisation de qualité en milieu urbain conduits au LEESU, ne se sont pas limités à la modélisation conceptuelle. Dans la thèse

de (Hong, 2016), une plateforme de modélisation de la qualité distribuée à base physique a été développée. L'application de cette approche de modélisation a contribué à l'amélioration des connaissances sur les processus, et a réussi à donner des niveaux de performance satisfaisants en termes de réplication de la dynamique des particules et des polluants. Cependant, cette approche nécessite l'acquisition d'importantes bases de données pour sa mise en œuvre et elle est très coûteuse en termes d'expérimentation et de temps de calcul ce qui empêche son application dans un contexte opérationnel.

Une étude plus approfondie sur les processus impliqués dans la génération et le transport des contaminants dans le milieu urbain semble donc nécessaire pour une meilleure compréhension des mécanismes et pour le développement des outils de modélisation qui seront fiables et faciles à utiliser par les opérationnels.

## 1.2. Projets de recherche

Cette thèse s'inscrit dans le cadre du thème 11 de la quatrième phase du programme de recherche OPUR lancée en 2012 et qui porte sur la modélisation intégrée. Elle bénéficie également des bases de données quantitatives et qualitatives acquises dans le cadre du projet ANR « Trafipollu », associé au programme OPUR, ainsi que des résultats expérimentaux mis en œuvre dans ce projet pour l'implémentation, le calage et la validation des modèles utilisés.

### 1.2.1. OPUR

OPUR est un observatoire de terrain en hydrologie urbaine créé en 1994 et installé en Ile de France. OPUR regroupe les acteurs scientifiques et opérationnels autour des enjeux principaux relatifs à la production, au transfert et la gestion de la contamination des eaux pluviales. Les principaux volets de la quatrième phase de ce projet incluent la maîtrise à la source de la contamination des eaux pluviales, l'utilisation des ressources alternatives à l'eau potable en ville, le développement de nouvelles méthodes pour le suivi et la caractérisation des contaminants et la modélisation intégrée des flux de polluants.

L'objectif du thème 11 sur la modélisation intégrée est de développer un modèle à l'échelle d'un quartier urbain capable de reproduire la variabilité spatiale et temporelle des flux de polluants à l'exutoire d'un bassin versant, mais aussi en différents points clés du bassin versant, avec une attention particulière aux processus de surface et en réseau.

### 1.2.2. Trafipollu

Ce projet ANR a été lancé en Avril 2013 et clôturé en Septembre 2016. Le focus du projet « Trafipollu » portait sur les polluants générés par le trafic routier. Son objectif principal était de développer des outils de modélisation qui permettent de réaliser des cartographies pour déterminer dynamiquement la localisation de ces polluants dans un milieu urbain. Pour atteindre cet objectif, il a fallu mettre en œuvre des chaînes de modélisation à l'échelle de la rue, le quartier et la ville dans le but de prévoir (i) le comportement du trafic, (ii) les émissions de polluants associées, (iii) la dispersion des polluants dans l'atmosphère, (iv) le dépôt des polluants sur les surfaces urbaines et (v) leur transfert dans l'eau et dans les sols.

### 1.3. Objectifs de la thèse

L'objectif principal de cette thèse est de contribuer au développement d'un outil de modélisation de la qualité des eaux de ruissellement à l'échelle du quartier à partir d'une compréhension approfondie des processus primaires de production et de transfert de contaminants dans le milieu urbain, notamment l'accumulation et le lessivage.

Ce travail de recherche vise à :

1. Améliorer les connaissances sur les processus primaires de génération des contaminants dans le milieu urbain qui sont l'accumulation et le lessivage à l'échelle locale d'un petit bassin versant urbain routier et à l'échelle d'une surface élémentaire en se basant sur l'interprétation des bases de données expérimentales.

2. Développer un outil de modélisation conceptuelle de la qualité des eaux de ruissellement à l'échelle du quartier, en se basant sur les connaissances acquises à l'échelle locale, afin de mieux appréhender la prédiction des niveaux de contamination à l'exutoire.

### 1.4. Structure du manuscrit

Ce manuscrit correspond à une thèse sur articles et il s'organise en six parties :

**Partie 1. Introduction** : Cette première partie donne d'une part le contexte général de la thèse et présente les projets de recherche dans lesquels elle s'inscrit. D'autre part, elle détaille les objectifs de la thèse et la méthodologie de recherche qui a été suivie.

**Partie 2. Etat de l'art :** Cette partie synthétise les principales connaissances sur la contamination des eaux pluviales, la modélisation hydrologique et de qualité dans le milieu urbain, en se focalisant sur les processus d'accumulation et de mobilisation des contaminants. Elle permet de récapituler les recherches précédentes menées sur ces questions et met en évidence les lacunes en termes de performances des modèles de qualité.

**Partie 3. Présentation des sites expérimentaux et de la base de données :** l'objectif de cette partie est de décrire les sites expérimentaux à l'échelle locale ainsi qu'à l'échelle du quartier, les équipements qui sont mis en place et les bases de données qui sont acquises. Elle détaille aussi les procédures d'échantillonnages et les analyses faites sur les échantillons récupérés. L'expérimentation de lessivage qui été mise en place sur la surface élémentaire est aussi présentée.

**Partie 4. Compréhension des processus de production et de mobilisation des contaminants à l'échelle locale : modélisation et études expérimentales :** Dans cette partie, les bases de données présentées dans la partie précédente sont exploitées pour approfondir les connaissances sur les processus. Cette partie comprend trois chapitres. Dans le **chapitre 1**, la possibilité de simuler les concentrations en matières en suspension (MES) dans le ruissellement à l'avaloir du bassin versant routier est évaluée en considérant les modèles traditionnels d'accumulation-lessivage. Dans le **chapitre 2**, les transferts de polluants entre les compartiments air-eau sont quantifiés en évaluant la contribution des retombées atmosphériques sèches à la contamination des eaux de ruissellement en hydrocarbures aromatiques polycycliques (HAPs) et métaux. Le **chapitre 3** est consacré à l'étude à la micro échelle des surfaces élémentaires du mécanisme de mobilisation des particules lors d'un événement pluvieux, et de la relation qui existe entre le stock accumulé et le stock mobilisable. La conception et la mise en point d'un simulateur de pluie innovant qui a été utilisé pour obtenir les échantillons de ruissellement sont aussi détaillées. Le **chapitre 4** donne le bilan des messages principaux obtenus dans cette partie.

Cette partie s'appuie sur les articles suivants :

**Article 1-** Al Ali, S., Bonhomme, C., Chebbo, G., 2016. Evaluation of the Performance and the Predictive Capacity of Build-Up and Wash-Off Models on Different Temporal Scales. *Water*,8,(8),312.

**Article 2-** Al Ali, S., Debade, X., Chebbo, G., Béchet, B., Bonhomme, C., 2017. Contribution of atmospheric dry deposition to stormwater loads for PAHs and trace metals in a small and highly trafficked urban road catchment. *Environmental Science and Pollution Research*, doi:10.1007/s11356-017-0238-1.

**Article 3-** Al Ali, S., Bonhomme, C., Dubois, P., Chebbo, G., 2017. Investigation of the wash-off process using an innovative portable rainfall simulator allowing continuous monitoring of flow and turbidity at the urban surface outlet. *Science of the Total Environment*. 609, 17–26.

**Partie 5. Modélisation de la production et du transfert de la contamination dans les eaux de ruissellement à l'échelle du quartier** : Cette partie est consacrée à la modélisation à l'échelle du quartier et comprend deux chapitres. Les nouvelles connaissances relatives sur la contamination des eaux de ruissellement sont intégrées pour proposer un outil de modélisation de la qualité basé sur une approche stochastique afin d'évaluer les niveaux de contamination en MES à l'exutoire. Ce module de qualité est intégré au modèle hydrologique URBS (Rodriguez et al., 2008). Ce travail est présenté dans le **chapitre 6**. Afin d'évaluer la robustesse de cette approche et ce qu'elle apporte par rapport à d'autres approches de modélisation de la qualité ayant des degrés de complexité variables (globale, semi distribuée conceptuelle et distribuée à base physique) et qui ont été appliquées sur le même bassin versant du quartier, un travail de comparaison des différentes approches de modélisation est fait en collaboration avec Yi Hong au LEESU et il est décrit dans le **chapitre 7**. Les messages principaux de cette partie sont résumés dans le **chapitre 8**.

Cette partie s'appuie sur les articles :

**Article 4-** Al Ali, S., Rodriguez, F., Bonhomme, C., Chebbo, G., 2017. Accounting for the spatial-temporal variability of Pollutant processes in stormwater quality modelling based on stochastic approaches. *Soumis*.

**Article 5-** Benchmarking urban stormwater quality models of varying spatial discretization: lumped, sub-catchments based, urban hydrological element based and grid-based.

**Partie 6. Conclusions et perspectives :** Dans cette dernière partie, les principales conclusions tirées de ce travail sont présentées avec une mise en perspectives des résultats et des réflexions développées au cours de ce travail de recherche.

## 1.5. Références

Chocat, B., 1997. Le rôle possible de l'urbanisation dans l'aggravation du risque d'inondation : l'exemple de l'Yzeron à Lyon / The potential role of urbanization in increasing the risk of flooding : the example of the Yzeron in Lyon. *Rev. Géographie Lyon* 72, 273–280. <https://doi.org/10.3406/geoca.1997.4707>

Dotto, C.B.S., Kleidorfer, M., Deletic, A., Rauch, W., McCarthy, D.T., Fletcher, T.D., 2011. Performance and sensitivity analysis of stormwater models using a Bayesian approach and long-term high resolution data. *Environ. Model. Softw.* 26, 1225–1239. <https://doi.org/10.1016/j.envsoft.2011.03.013>

Fletcher, T.D., Andrieu, H., Hamel, P., 2013. Understanding, management and modelling of urban hydrology and its consequences for receiving waters: A state of the art. *Adv. Water Resour.*, 35th Year Anniversary Issue 51, 261–279. <https://doi.org/10.1016/j.advwatres.2012.09.001>

Freni, G., Mannina, G., Viviani, G., 2009. Urban runoff modelling uncertainty: Comparison among Bayesian and pseudo-Bayesian methods. *Environ. Model. Softw.* 24, 1100–1111. <https://doi.org/10.1016/j.envsoft.2009.03.003>

Hong, Y., 2016. Modélisation distribuée à base physique du transfert hydrologique des polluants routiers de l'échelle locale à l'échelle du quartier. École des Ponts ParisTech, France.

Kanso, A., 2004. Evaluation of urban stormwater quality models: a bayesian approach. Ecole des Ponts ParisTech.

Miller, J.D., Kim, H., Kjeldsen, T.R., Packman, J., Grebby, S., Dearden, R., 2014. Assessing the impact of urbanization on storm runoff in a peri-urban catchment using historical change in impervious cover. *J. Hydrol.* 515, 59–70. <https://doi.org/10.1016/j.jhydrol.2014.04.011>

Paul, M.J., Meyer, J.L., 2001. Streams in the Urban Landscape. *Annu. Rev. Ecol. Syst.* 32, 333–365. <https://doi.org/10.1146/annurev.ecolsys.32.081501.114040>

Sage, J., 2016. Concevoir et optimiser la gestion hydrologique du ruissellement pour une maîtrise à la source de la contamination des eaux pluviales urbaines. Paris Est.

Sartor, J.D., Boyd, G.B., Agardy, F.J., 1974. Water Pollution Aspects of Street Surface Contaminants. *J. Water Pollut. Control Fed.* 46, 458–467.

Schueler, T., 1994. THE COMPONENTS OF IMPERVIOUSNESS.





## Partie 2. Présentation des sites expérimentaux et de la base de données

Dans le cadre du projet Trafipollu, deux sites expérimentaux ont été équipés sur la commune du « Perreux-sur-Marne » située dans le département du Val-de-Marne en région Île-de-France. Le premier site correspond au bassin routier du boulevard d'Alsace Lorraine qui représente l'échelle locale et le deuxième est le bassin versant quartier qui représente la méso-échelle (Figure 2-1).

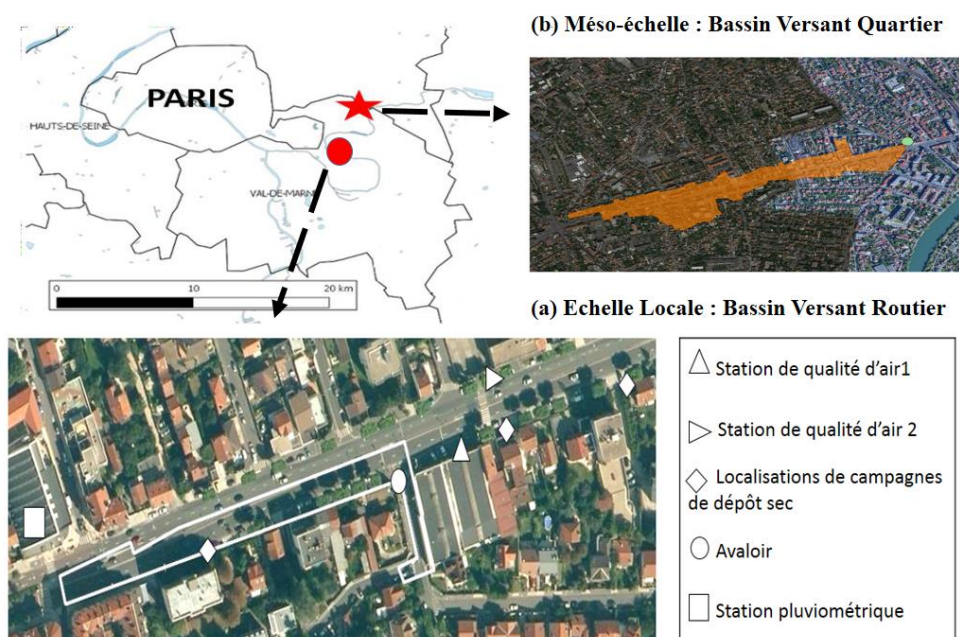


Figure 2-1 Les sites d'étude de la commune du "Perreux sur Marne". (a) Le bassin versant routier est délimité en blanc et représente l'échelle locale avec les localisations de toutes les stations expérimentales ; (b) Le bassin versant quartier délimité par la zone orange représente la méso-échelle. L'exutoire est représenté par le cercle vert. (Google Map@2016)

Dans cette partie, nous présentons successivement pour chacun des sites : leurs caractéristiques morphologiques, les équipements expérimentaux et les bases de données qui ont été acquises. Ces données ont servi comme données de calage et de validation des modèles hydrologiques et des modèles de qualité. Elles ont aussi été exploitées pour acquérir de nouvelles connaissances sur les processus d'accumulation et de lessivage.

## 2.1. Echelle locale : le bassin versant routier

### 2.1.1. Description du site

Le bassin versant routier a une superficie totale égale à 2661 m<sup>2</sup> (Figure 2-2). Il comprend un segment de trafic important (plus de 30 000 véhicules par jour) qui fait partie du boulevard d'Alsace Lorraine, et inclut les trottoirs et les zones de stationnement adjacentes. La voirie représente 65% de la surface totale, et le reste est réparti entre les trottoirs (30%), les caniveaux et les zones de stationnement (5%). L'eau qui s'écoule sur la partie supérieure du bassin est acheminée vers l'avaloir par l'intermédiaire des caniveaux qui sont situés entre la route et le trottoir. La pente moyenne du bassin versant est égale à 2.6%, avec une inclinaison plus importante en amont (partie Ouest).



Figure 2-2 Le bassin versant routier délimité en noir et les localisations de la station de pluviométrique et de l'avaloir (Google Map@2016)

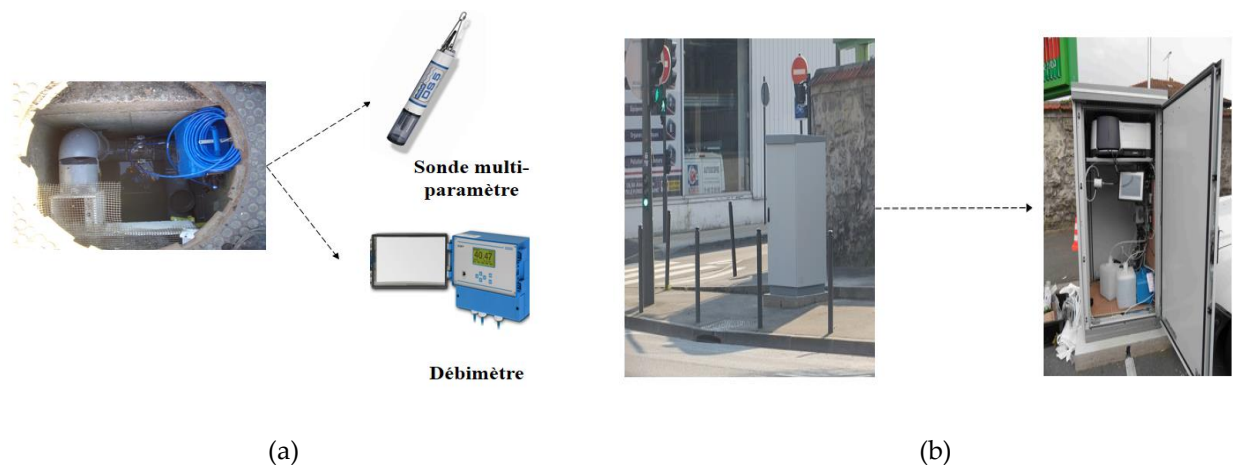
### 2.1.2. Mesures des paramètres quantitatifs et qualitatifs des eaux de ruissellement

Les dispositifs de mesure des paramètres de quantité (débit) et de qualité (turbidité, conductivité, pH et température) des eaux de ruissellement ont été situés à l'entrée de l'avaloir et ils enregistraient les mesures en continu à un pas de temps d'une minute pour la période d'avril 2014 jusqu'à septembre 2015 (Figure 2-3 (a)). Une grille métallique a été placée à l'entrée du collecteur pour collecter les macros déchets et empêcher l'obstruction de l'avaloir.

Le débit a été mesuré en utilisant un débitmètre « Nivus » qui utilise la méthode de corrélation croisée ultrasons pour calculer la vitesse d'écoulement pour différentes couches dans une conduite pleine, ce qui augmente la fiabilité des données. Les paramètres de qualité

ont été obtenus grâce à une sonde multiparamètres DS5 OTT (Figure 2-3 (a)). Pour économiser l'énergie et l'espace de stockage, le déclenchement de la sonde OTT a été asservi au débitmètre. Une fois que le débit est supérieur à 0,15 l/s (ce qui est considéré comme le seuil du déclenchement du débitmètre), les mesures de qualité sont lancées jusqu'à ce que le débit devienne inférieur à 0,13 l/s pendant plus de 15 minutes.

Un volume de 500 ml a été collecté tous les 300 l qui passaient dans le débitmètre, pour faire des analyses en laboratoire des métaux, des hydrocarbures aromatiques polycycliques (HAPs), du carbone organique dissous (COD), du carbone organique particulaire (COP) et des matières en suspension (MES) pour un total de 14 événements pluvieux. Pour chaque événement, le volume a été réparti dans deux flacons (un en verre et l'autre en plastique) d'une contenance de 20 l ; 250 ml ont été pompés dans chaque flacon, placé dans une armoire fermée sur le trottoir (Figure 2-3 (b)).



**Figure 2-3 Les équipements à l'avaloir pour mesurer des paramètres quantitatifs et qualitatifs des eaux de ruissellement. (a) Entrée de l'avaloir ; (b) L'armoire placée sur le trottoir dans laquelle elles sont placées les bouteilles de collectes des échantillons et la pompe**

### 2.1.3. Dépôts secs

Deux campagnes de mesure des dépôts secs ont été faites sur le bassin versant routier suite à une collaboration entre le LEE (IFSTTAR Nantes) et Le LEESU les 14/10/2014 et 07/07/2015 après successivement 2 et 37 jours de temps sec respectivement pour caractériser le stock des dépôts secs pour trois localisations (Figure 2-4 (a)) différentes et pour trois positions sur la chaussée, le caniveau et le trottoir (Figure 2-4 (b)).





Figure 2-4 (a) Les localisations où les campagnes de dépôts secs sont effectuées ; (b) Les trois positions de collecte des dépôts sur la localisation (1).

Trois campagnes similaires ont été faites ultérieurement sur le parking de l'École des Ponts à Champs sur Marne les 01/12/2016, 15/12/2016 et 10/02/2017 après 7, 2 et 1 jours de temps sec respectivement. Une surface de 2 m<sup>2</sup> (2mx1m) a été délimitée par des rubans puis nettoyée à la main pour enlever les macros déchets. Après avoir frotté la surface par des mouvements circulaires avec une brosse afin de mobiliser les particules piégées par la surface, les sédiments ont été aspirés dans des filtres en papier en parcourant de petites bandes pour couvrir toute la surface à une vitesse de 5 cm/s avec un aspirateur domestique « Rowenta RU 4022 ». Les échantillons ont été analysés ensuite dans le laboratoire pour déterminer leur masse

et leur contenu en HAPs et métaux après tamisage sur un tamis de 2mm. Les détails sur le protocole expérimental et les méthodes appliquées pour déterminer la composition des dépôts sont présentés dans (Bechet et al., 2015).

#### 2.1.4. Analyse granulométrique

Les distributions volumiques des dimensions des particules dans les échantillons d'eau et les échantillons de dépôt sec ont été déterminées à l'aide d'un diffractomètre laser pour la fraction inférieure à 2 mm (Malvern® Mastersizer 3000). La distribution de volume a été calculée en supposant que toutes les particules sont sphériques et diffusant de la même manière (théorie de Mie). Les indices de réfraction utilisés pour les mesures sont 1,33 pour la solution dispersante (eau) et 1,53 pour les particules sous forme de dispersion humide.

#### 2.1.5. Mesures des concentrations atmosphériques

Deux stations, dénommées 1 et 2, pour mesurer les concentrations des métaux et des HAPs dans l'air ont été installées sur le bassin versant routier (Figure 2-1). Les stations sont équipées par des préleveurs séquentiels LECKEL à faible volume (Figure 2-5). Les mesures de la qualité de l'air ont été effectuées par Airparif, qui est un organisme accrédité par le Ministère de l'Environnement pour le contrôle de la qualité de l'air à Paris.



**Figure 2-5 (a) Les préleveurs installés sur le bassin versant routier. (b) Le centre d'acquisition des données atmosphériques**

Les polluants ont été collectés à des débits de 2,3 m<sup>3</sup>/h sur des filtres à quartz, sur une période de 10 semaines du 1er avril au 9 juin 2014. Les métaux ont été échantillonnés sur une base hebdomadaire tandis que les HAPs ont été échantillonnés quotidiennement jusqu'au 21 avril, puis tous les trois jours. Dans l'ensemble, 10 échantillons de métaux ont été prélevés à la

station 1 et 11 à la station 2, tandis que 31 et 33 échantillons de HAPs ont été prélevés respectivement aux stations 1 et 2. Les métaux traces ont été analysés à l'aide de la spectrométrie de masse à plasma à couplage inductif (ICP-MS), tandis que les HAPs ont été déterminés par chromatographie en phase liquide à haute performance (HPLC) couplée à un test de fluorescence UV.

## 2.2. Méso-Echelle : le bassin versant quartier

### 2.2.1. Description du site

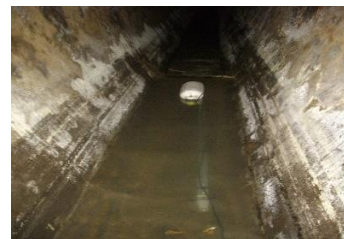
Le bassin versant étudié à la méso-échelle est le quartier du Perreux sur Marne (Figure 2-1). Ce bassin versant de 12 ha présente une pente moyenne de 2,6 %. Il s'agit d'un site résidentiel avec quelques commerces répartis le long du boulevard d'Alsace Lorraine qui le traverse. Les surfaces imperméables représentent près de 70% de la surface totale du bassin versant. Il est drainé par un réseau d'assainissement séparatif qui achemine le débit vers l'exutoire situé à la limite nord-est du bassin versant. Le flux est collecté de la surface par les regards, puis transporté dans les conduites principales.

### 2.2.2. Mesures des paramètres quantitatifs et qualitatifs des eaux à l'exutoire

Le débit dans la canalisation principale et les paramètres de qualité ont été mesurés par les mêmes instruments utilisés à l'échelle locale (Figure 2-6). Le débit dans une petite canalisation de diamètre égal à 30 cm qui arrive dans la canalisation principale a été mesuré par un débitmètre « Nivus » qui calcule la vitesse moyenne sur la colonne par effet Doppler. Les débits ont été mesurés à un pas de temps égal à 2 minutes et les paramètres de qualité ont été mesurés à un pas de temps égal à 1 minute. Les données ont été acquises sur la période de juin 2014 à septembre 2015.



(a)



(b)

**Figure 2-6 Les instrumentations à l'exutoire : (a) les débitmètres ; (b) la bouée flottante attachée à la sonde multiparamètre**



### 2.3. Station pluviométrique

La station pluviométrique a été installée sur la toiture de la piscine municipale à moins de 180 m de l'avaloir du bassin versant routier (Figure 2-7). Elle est constituée d'un pluviomètre dont le volume d'auget est de 10 ml, ce qui correspond à 0.1 mm de pluie et d'un disdromètre laser "THIES" qui a permis l'acquisition des distributions de la taille des gouttes de pluie. Le pluviomètre a été installé de juin 2014 à juillet 2015. Le disdromètre a été mis en place pour la période de février 2015 à septembre 2015.



Figure 2-7 Le disdromètre

### 2.4. L'expérimentation de lessivage

Une expérimentation dédiée à l'étude du lessivage a été faite sur les trottoirs du bassin versant routier « Trafipollu » présenté ci-dessus et sur le parking de l'Ecole des Ponts pour récupérer des échantillons de lessivage sous une pluie artificielle générée par un simulateur de pluie. Les tests ont été réalisés juste après les campagnes de dépôts secs pour toutes les dates à l'exception du 14 Octobre 2014. Six échantillons ont été obtenus et analysés pour déterminer la charge lessivée.

Le dispositif de lessivage a été conçu et construit au LEESU (Figure 2-8). Il permet non seulement la simulation des pluies artificielles mais aussi l'acquisition en continu des mesures instantanées de débit et de turbidité ce qui présente un aspect très innovant par rapport aux simulateurs de pluie traditionnels. Le dispositif présente aussi d'autres avantages d'ordre

économique et technique qui se résument respectivement par son coût modeste, sa structure légère qui favorise sa mobilité sur le terrain réel et sa manipulation par une seule personne et la simplicité de son emploi.

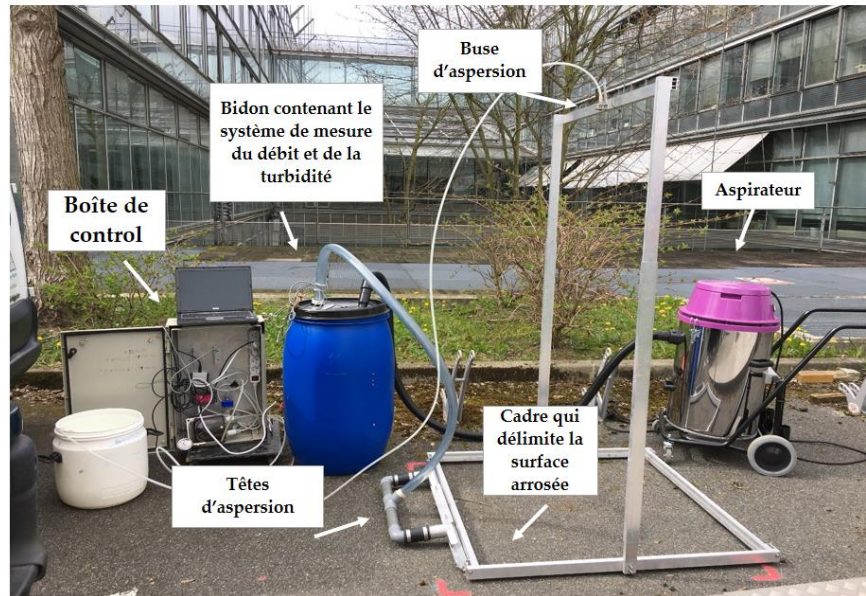


Figure 2-8 Le dispositif de lessivage qui comprend le simulateur de pluie et le système de mesure en continu du débit et de la turbidité

La fiabilité du dispositif a été évaluée par des essais préalables à son utilisation directe sur les sites. Les résultats ont mis en œuvre l'uniformité de l'aspersion de la surface avec un coefficient d'uniformité égale à 73% et qui s'élevait à 80% en excluant les extrémités. L'étanchéité et l'humidification totale de la surface ont aussi été vérifiées en comparant le volume d'eau initial utilisé pour l'aspersion et le volume final recueilli dans le bidon. Des tests préalables ont montré que les pertes étaient négligeables. Nous avons aussi vérifié que la distribution des tailles des gouttes générées par le simulateur était réaliste par rapport à celle d'une pluie naturelle ayant lieu dans la région parisienne, et ceci à l'aide du disdromètre.

## 2.5. Récapitulatif

Le tableau ci-dessous (Table 2-1) représente un récapitulatif des données qui sont acquises sur les bassins versants étudiés et qui sont exploitées dans le cadre de cette thèse.



**Table 2-1 Récapitulatif des données collectées et utilisées dans le cadre de cette thèse**

	<b>Données</b>	<b>Période de début</b>	<b>Période de fin</b>	<b>Paramètres analysés</b>	<b>Commentaire</b>
	Précipitation	Juin 2014	Juillet 2015	-	-
	Débit	Avril 2014	Septembre 2015	-	Pas de temps 1 minute
	Paramètre de qualité de l'eau (Turbidité-conductivité-pH-température)	Juin 2014	Septembre 2015	-	Pas de temps 1 minute
<b>Bassin versant routier</b>	Campagne de dépôt sec	14/10/2014 07/07/2014		Métaux lourds - HAPs -MES - Granulométrie	18 échantillons
	Prélèvements d'eau de ruissellement	Août 2014	Juillet 2015	Métaux lourds - HAPs - DCO - COD - MES - Granulométrie	14 échantillons
				Métaux	Pas de temps 7 jours
	Concentrations atmosphériques	1er Avril 2014	9 Juin 2014	HAPs	Pas de temps 1 jour jusqu'à 21 avril ensuite chaque 3 jours
	Expérimentation de lessivage	07/07/2014		MES - Granulométrie	9 échantillons
<b>Bassin versant quartier</b>	Débit principal	Juin 2014	Septembre 2015	-	Pas de temps 2 minutes
	Paramètre de qualité de l'eau (Turbidité-conductivité-pH-température)	Juin 2014	Septembre 2015	-	Pas de temps 1 minute
<b>Parking de l'ENPC</b>	Campagne de dépôt sec	01/12/2016 15/12/2016 10/02/2017		MES - Granulométrie	3 échantillons
	Expérimentation de lessivage	01/12/2016 15/12/2016 10/02/2017		MES	3 échantillons



## Partie 3. Etat de l'art

### 3.1. Le ruissellement en milieu urbain

Historiquement, la pollution engendrée par le ruissellement de surface était considérée comme une source de pollution relativement mineure. Cependant, à partir des années 1970, des campagnes de mesure ont été mises en place pour caractériser la contamination des eaux de ruissellement (Sartor and Boyd, 1972; Shaheen, 1975). De 1978 à 1983, le programme de mesures à grande échelle NURP (Nationwide Urban Runoff Program) (US EPA, 1983) a mis en évidence que les eaux de ruissellement véhiculent annuellement vers le milieu récepteur des contaminants à des niveaux comparables aux rejets de stations d'épuration, et des charges qui les excèdent largement lors de certains événements pluvieux (Desbordes et al., 1994). En France, plusieurs études ont été menées également pour quantifier la pollution des eaux pluviales et préciser ses caractéristiques à différentes échelles (Desbordes et al., 1980; Gromaire-Mertz et al., 1999; Lamprea, 2009; Percot, 2012; Zgheib et al., 2012).

Étant donné que la pollution des eaux de ruissellement entraîne une détérioration des milieux récepteurs, le suivi de l'évolution du développement urbain et l'identification des sources de polluant se révèlent d'une importance cruciale. Habituellement, les eaux de surface sont altérées par les contaminants qui viennent de sources ponctuelles et diffuses. Celles-ci incluent les activités de transport, les activités industrielles et commerciales, les activités de construction et de démolition, l'érosion du sol, et les retombées atmosphériques. Pour répondre adéquatement aux préoccupations relatives à la qualité des eaux de ruissellement, il est important de comprendre quels sont les polluants présents et quel est leur impact potentiel sur les environnements récepteurs. Les contaminants communs qui influent sur la qualité d'un milieu aquatique sont les particules en suspension, les métaux lourds et les hydrocarbures.

Dans cette partie, nous présentons les effets quantitatifs et qualitatifs de l'urbanisation sur le ruissellement en milieu urbain. Ensuite nous détaillons les sources qui sont responsables de la génération des polluants diffus dans le milieu urbain et présentons les principaux polluants concernés.

### 3.1.1. Effets de l'urbanisation

La transition démographique des zones rurales vers les zones urbaines a débuté depuis la moitié du XX<sup>ème</sup> siècle et ne cesse de croître. Aujourd'hui, plus de la moitié de la population dans le monde vit dans les zones urbaines et cette proportion atteindra 7 sur 10 en 2050 (OMS, 2010).

Les conséquences de l'expansion et de la densification des zones urbaines sur l'environnement et notamment sur l'eau sont profondes et d'une importance cruciale car c'est l'une des ressources les plus essentielles pour l'existence de l'être humain. Ces effets se reflètent sur le plan quantitatif notamment par l'augmentation des risques d'inondation et sur le plan qualitatif par la détérioration de la qualité des eaux de surface (Nelson and Booth, 2002; Schueler, 1994; Shuster et al., 2005; Tong, 1990).

La réalité de la dégradation accrue de la qualité des eaux de surface et les menaces qu'elle pose sur le milieu aquatique sont soulignées dans les textes réglementaires partout dans le monde. En Europe, une partie importante de la directive cadre sur l'eau DCE 2000/60/CEE, qui est entrée en vigueur le 22 Octobre 2000, est consacrée à lutter contre la contamination des eaux de surface. Elle impose les stratégies à adopter pour la maîtrise des rejets de polluants prioritaires prédéfinis, vers les milieux récepteurs, afin de protéger et d'améliorer la qualité écologique de l'eau. Deux directives filles qui détaillent des mesures complémentaires sont adoptées : la directive 2006/118/CE sur la protection des eaux souterraines et la directive 2008/105/CE sur les normes de qualité environnementale dans le domaine de l'eau.

#### 3.1.1.1. Effets hydrologiques

La pression exercée par l'urbanisation sur le cycle hydrologique est directement attribuée aux changements que subit la morphologie du bassin versant et qui incluent la diminution des surfaces vertes, l'expansion des surfaces imperméables et la modification du système de drainage des eaux de ruissellement.

Le remplacement de surfaces végétalisées par des surfaces imperméabilisées dans les villes a entraîné une forte diminution de l'évapotranspiration (Haase, 2009). Barron et al. (2013) ont noté que le flux d'évapotranspiration originaire des nappes d'eau souterraines à faible profondeur a été atténué de plus que 65% suite à l'augmentation des surfaces imperméables

dans le bassin versant étudié. La diminution de l'évapotranspiration entraîne une augmentation du volume ruisselé, et elle est aussi l'une des causes de l'apparition des « îlots de chaleur » (Bonan, 2008), puisque le refroidissement des surfaces est réduit ce qui conduit au stockage de la chaleur et au réchauffement de l'air urbain.

Les impacts de l'urbanisation sur le cycle hydrologique sont largement affectés par le pourcentage des surfaces imperméables (Brabec et al., 2002; Lee and Heaney, 2003). En fait, l'imperméabilisation des surfaces entraîne une diminution marquée de la capacité d'infiltration du sol (Arnold and Gibbons, 1996) ce qui se traduit par une réduction de la recharge des nappes phréatiques et une diminution des débits de base (Leopold, 1968; Simmons and Reynolds, 1982; Smakhtin, 2001). Schueler (1994) a montré que le volume ruisselé sur une zone imperméable peut être 16 fois plus important que le volume ruisselé sur la même surface ayant une couverture végétale.

L'imperméabilisation et l'amélioration des systèmes de drainage, en remplaçant le réseau hydrographique naturel par un réseau d'assainissement, accélèrent aussi la réponse hydrologique des bassins versants (Huang et al., 2008; Kang et al., 1998; Verbeiren et al., 2013). Une autre conséquence de cet aménagement des surfaces urbaines est l'accroissement des vitesses d'écoulement. Cela résulte en des débits de pointe très élevés dû à l'efficacité de transport hydraulique du système de drainage qui est favorisée par l'uniformisation des pentes (Chocat, 1997; Hall and Ellis, 1985; Hawley and Bledsoe, 2011; Schoonover et al., 2006; Zhao et al., 2016). Cette transformation que subit l'hydrogramme est associée avec une augmentation du risque d'inondation, comme l'eau véhiculée atteint les conditions d'inondation plus rapidement (Guo et al., 2008). Miller et al. (2014) ont trouvé que l'augmentation des surfaces imperméables sur un bassin versant péri-urbain à « Swindon » (UK) et la construction du réseau d'assainissement ont été accompagnés par une réduction de 50% de la durée caractéristique d'inondation et d'une augmentation de 400% du débit de pointe. Rose and Peters (2001) ont aussi remarqué que les débits de pointe dans les zones urbaines subissent une augmentation de 30 à 100% par comparaison aux zones moins urbaines.

### 3.1.1.2. Effets qualitatifs

L'urbanisation n'influence pas uniquement le régime hydrologique des bassins versants mais elle a également des impacts profonds sur la qualité des eaux et l'état des milieux récepteurs qui se manifestent par des changements physiques, chimiques et microbiologiques (Paul and Meyer, 2001; Yufen et al., 2008). Ces changements entraînent une augmentation de la demande en oxygène, de la conductivité, des matières en suspension, des nutriments, des métaux, et des hydrocarbures (Hatt et al., 2004; Horner et al., 1997; McMahon and Harned, 1998; Novotny, 1994), ainsi que des altérations de la température des milieux récepteurs (Miller et al., 2014).

Putro et al. (2016) ont comparé la demande en oxygène et la température pour quatre bassins versants en Grande Bretagne avec des degrés variables d'urbanisation. Les corrélations positives qu'ils ont calculées montrent que ces deux paramètres ont une tendance à augmenter avec l'intensité du développement urbain. Pareillement, Carle et al. (2005) ont trouvé que les concentrations en matières en suspension, azote, phosphore et bactéries coliformes fécales ont augmenté avec la densité de l'urbanisation en Caroline du nord aux Etats-Unis. Lind and Karro (1995) ont trouvé que les concentrations de zinc, plomb et cuivre dans les couches superficielles de sol qui se trouve à proximité des routes en Suède sont deux à huit fois plus grandes que celles trouvées dans les zones rurales. Line et al. (2002) ont rapporté que la contribution d'un bassin versant urbanisé à la charge de nutriments et de matière en suspension était 250% fois plus importante que celle d'un bassin versant rural.

Par ailleurs, les impacts qualitatifs de l'urbanisation sont beaucoup plus variables que les effets hydrologiques. Ils dépendent de facteurs multiples dont l'ancienneté et le type d'urbanisation (Strayer et al., 2003), la présence d'ouvrages de traitement des eaux usées, l'étendue des infrastructures de drainage des eaux pluviales (Paul and Meyer, 2001) et les pratiques de gestion appliquées (Jones et al., 2001; Miller et al., 2014).

L'augmentation des niveaux de pollution dans les zones urbaines est attribuée à la fois à des phénomènes de contamination ponctuelle et diffuse : rejets de stations de traitement des eaux usées mais aussi eaux de ruissellement qui entraînent les polluants provenant de sources diffuses (Miller et al., 2014; Paul and Meyer, 2001).

Malheureusement, le déversement des eaux usées non traitées dans les rivières et les océans demeure une pratique fréquente, où environ 25% des résidents urbains dans les pays moins développés n'ont pas accès à un assainissement adéquat (McGrane, 2016).

Dans les pays développés en revanche, les préoccupations primaires en termes de contrôle de la contamination se focalisent sur la contamination émergente liée aux micropolluants, en particulier les substances pharmaceutiques et à la contamination provenant des sources diffuses. Malgré les avancées dans les techniques adoptées dans les stations d'épuration pour réduire les charges de substances toxiques, certains polluants persistent après le traitement. Ceux-ci proviennent en particulier des rejets domestiques, des médicaments et des produits d'hygiène personnels (Li, 2014). Heberer (2002) a noté que plus de 80 substances provenant des médicaments et des produits pharmaceutiques sont détectées dans les milieux récepteurs à l'aval des stations d'épuration. Li (2014) a souligné la menace représentée par la persistance des substances pharmaceutiques dans le milieu aquatique sur les organismes vivants, comme elles sont susceptibles de subir des réactions imprévisibles avec les composés chimiques qui se trouvent dans l'environnement.

La pollution diffuse est une source majeure de contamination des milieux récepteurs dans les zones urbaines où les polluants accumulés sur les surfaces et ensuite charriés par les eaux de ruissellement peuvent dépasser ceux produits par les eaux usées domestiques après traitement (Bedient et al., 1978; Lee and Bang, 2000; Pitt and Field, 1977). La pollution diffuse est caractérisée par une très grande variabilité et une multitude de sources (Ellis and Mitchell, 2006), cependant les sources dominantes dans le milieu urbain sont les activités anthropiques et les surfaces imperméables (Goonetilleke et al., 2005; Schueler, 1994; Tsihrintzis and Hamid, 1997). Characklis and Wiesner (1997) ont noté des concentrations très élevées de carbone organique, fer et zinc qui sont attribués aux activités anthropiques. Arnold and Gibbons (1996) ont noté que l'augmentation des surfaces imperméables accélère la mobilisation des contaminants ce qui favorise l'entraînement des pathogènes, des nutriments et des substances toxiques (métaux et HAPs) et contribue ainsi à la pollution du ruissellement. Cependant, le lessivage des polluants accumulés sur les surfaces imperméables n'est pas la seule contribution des surfaces imperméables à la pollution. L'abrasion des chaussées est aussi une source importante de pollution des eaux de ruissellement (Thorpe and Harrison, 2008).

### 3.1.2. Pollution des eaux de ruissellement

#### 3.1.2.1. Sources de Polluants

##### 3.1.2.1.1. Dépôts atmosphériques

Les polluants qui se trouvent dans l'air peuvent rejoindre les surfaces urbaines via les mécanismes de dépôt secs qui surviennent pendant la durée de temps sec et de dépôt humides qui ont lieu pendant un événement pluvieux. Les particules se trouvent dans l'atmosphère sous différents états et leurs concentrations varient dans le temps et dans l'espace (Brinkmann, 1985). Elles sont influencées largement par les conditions météorologiques qui incluent l'humidité, la vitesse du vent et la pression atmosphérique (Lee et al., 2011; Tian et al., 2014).

Des conclusions variables sur le rôle que joue l'atmosphère en tant que source de la contamination des eaux de ruissellement sont rapportées dans la littérature. Sabin et al. (2005) ont investigué la contribution des retombées atmosphériques à la contamination des eaux de ruissellement en métaux sur un bassin versant urbain (5 ha) très imperméable à Los Angeles. Le site étudié est soumis à une faible densité de trafic (50 véhicules/jours) et se trouve dans une zone de climat semi-aride. Ils ont calculé des contributions potentielles très élevées de retombées atmosphériques totales (sèches+humides) à la contamination des eaux de ruissellement en substances métalliques qui varient entre 57 et 100%. Cette contribution est dominée par les retombées sèches qui ont compté jusqu'à 100% de la contribution totale pour certains métaux comme le nickel et le plomb. Cependant, Percot et al. (2016) ont rapporté des résultats totalement différents sur un bassin versant urbanisé (30 ha) situé à Nantes, France qui est constitué de 45% de surfaces imperméables et qui se trouve dans une zone de climat océanique. Ils ont conclu que la part atmosphérique dans la contamination métallique des eaux de ruissellement est mineure avec des pourcentages de contribution totale inférieurs à 36%. Ils ont aussi noté que la contribution des dépôts secs n'est pas significative comme elle n'a pas excédée le 10%. Gasperi et al. (2014) ont trouvé que 32% du nickel et 7% de l'arsenic dans les eaux de ruissellement proviennent de retombées atmosphériques sèches. Le même ordre de grandeur a été rapporté par (Percot et al., 2016) pour le nickel, cependant ils ont calculé une contribution moins significative pour l'arsenic à seulement 1%.

Cette variabilité de la contribution des dépôts atmosphériques à la contamination des eaux de ruissellement en métaux, observée dans la littérature, nécessite ainsi plus



d'investigation. Ceci est aussi vrai pour les HAPs où (Bressy et al., 2012) ont rapporté que jusqu'à 30% de la charge annuelle en HAPs véhiculée par l'eau de ruissellement sur un petit bassin versant urbain provient de l'atmosphère alors que les valeurs rapportées par (Motelay-Massei et al., 2006) ne dépassaient pas 18%.

#### **3.1.2.1.2. Trafic**

Les pressions exercées par le trafic routier sur la qualité des milieux urbains ne cessent d'augmenter à cause de l'expansion et du développement des infrastructures routières, des réseaux de transport et de l'augmentation du nombre de véhicules circulants. (Hoffman et al., 1985) ont rapporté que 50% des HAPs, plomb et zinc qui rejoignent la rivière de Pawtuxet en Rhode Island aux Etats-Unis provenaient du ruissellement sur l'autoroute adjacente à cette rivière. (Barrett Michael E. et al., 1998) ont montré que les charges de plusieurs polluants (MES, métaux, DCO, nutriments) sont corrélées avec l'intensité du trafic routier. Cependant, Kayhanian et al. (2003) ont montré que l'effet du volume journalier annuel de trafic sur les concentrations de polluant dans les eaux de ruissellement des autoroutes n'est significatif que lorsqu'il est considéré avec d'autres paramètres liés aux caractéristiques de l'événement pluvieux et à l'occupation du sol.

Les activités liées au transport affectent les niveaux des contaminants présents sur les voiries et les parkings. Les polluants qui y sont associés sont émis soit directement par les véhicules, soit indirectement via les processus d'abrasion des surfaces et la remise en suspension sous l'effet de la turbulence.

Les émissions directes des polluants dues à la circulation automobile incluent les émissions par l'échappement qui sont liées au fonctionnement du moteur, et les émissions non échappement qui proviennent de l'usure des pneus et des plaquettes de frein, de l'embrayage des véhicules ainsi que des fuites d'huile, de carburant et liquide de frein etc. (Fallah Shorshani, 2014). Les émissions par l'échappement sont une source importante des composés organiques qui incluent les HAPs, les alcanes et les acides carboxyliques, en plus de carbone organique (El Haddad et al., 2009; Riddle et al., 2007). Murakami et al. (2005) ont rapporté que les HAPs contenus dans le stock de sédiment collecté sur une route très fréquentée proviennent des émissions échappement diesel. Ils ont aussi noté que l'usure de pneus contribue aussi à la contamination en HAPs, ce qui était aussi noté par (Kwon and Castaldi,

2012). Cependant, les émissions non échappement ont tendance à agir comme source principale de métaux lourds. (Wählin et al., 2006) ont rapporté que l'usure des plaquettes de frein génère des concentrations élevées de Cr, Fe, Cu, Zn, Zr, Mo, Sn, Sb, Ba and Pb alors que l'usure des pneus et l'abrasion de la chaussée sont une source importante de Al, Si, K, Ca, Ti, Mn, Fe, Zn and Sr. (Duong and Lee, 2011) ont caractérisé le contenu en métaux lourds du stock de particules sur plusieurs routes soumises à des conditions de trafic variables. Ils ont trouvé que les principales sources de Ni étaient les émissions d'échappement des moteurs diesel et l'abrasion des freins et la corrosion des véhicules, alors que le cuivre provenait principalement de l'abrasion des freins et des gaz d'échappement de la combustion du carburant. Finalement, cette publication mentionne que la concentration de Zn observée est influencée par les émissions des véhicules et l'usure des pneus.

Les concentrations de polluant provenant de l'usure des pneus et des plaquettes de frein varient en fonction des conditions de trafic. Les zones situées à proximité de la route, comme les stationnements et les passages pour piétons, qui provoquent des freinages fréquents sont susceptibles de présenter des concentrations plus élevées de contaminants dans ces zones (Novotny et al., 1985). Cet effet a été observé par (Drapper et al., 2000) à côté des voies de sortie sur une route à Brisbane, Australie.

Les émissions indirectes du trafic ont aussi un impact significatif sur l'apport des polluants. L'usure de la surface d'une chaussée sous l'impact du trafic routier est une source importante de particules et d'hydrocarbures. En fait, lorsque les revêtements routiers en asphalte sont abrasés par les véhicules, ils relarguent des hydrocarbures et des métaux lourds (Thorpe and Harrison, 2008). (Murakami et al., 2005) ont signalé une grande contribution d'une chaussée dans une zone résidentielle au contenu en HAPs du stock des particules. La contribution des surfaces est cependant contrôlée par plusieurs facteurs et notamment le matériel du revêtement, l'âge et l'état de la chaussée (Brinkmann, 1985). (Sartor and Boyd, 1972) ont trouvé que les chaussées bitumées génèrent 80% des polluants de plus que les chaussées en béton. Ils ont aussi noté que les chaussées en bon état sont des sources faibles de contamination en comparaison avec les chaussées en mauvais état.

Les émissions indirectes incluent aussi le processus de re-suspension des particules. (Bukowiecki et al., 2010) ont souligné l'importance du processus de re-suspension sur

l'émission des particules où les particules émises sur une rue canyon et sur une autoroute et qui sont originaire de la re-suspension du stock constituait 38% et 56% respectivement. (Mancilla and Mendoza, 2012) ont aussi rapporté que 20-25% des émissions des particules fines PM<sub>2.5</sub> à Monterrey en Mexique provenait de la re-suspension du stock de la surface.

#### **3.1.2.1.3. Rejets industriels et commerciaux**

Les activités liées aux deux secteurs industriel et commercial contribuent énormément à la diffusion des polluants dans le milieu urbain (Bannerman et al., 1993). Stein et al. (2008) ont noté que les sites industriels étaient les sources les plus importantes des métaux dans les eaux de ruissellement surtout pour le cuivre, le zinc et le plomb. Des résultats similaires ont été rapportés par (Park and Stenstrom, 2008). Comme les surfaces des chaussées des zones industrielles ne sont pas nettoyées à la même fréquence que celles des zones résidentielles et commerciales, elles ont alors tendance à accumuler des stocks plus élevés de contaminants (Wanielista et al., 1977). Pour réduire les effets néfastes des rejets industriels sur les eaux dans le milieu urbain et atténuer de 75% les charges de polluants provenant des zones industrielles (Bannerman et al., 1993) ont suggéré que les outils de gestion (BMP) doivent traiter entre 40 et 53% des effluents industriels. Par contre, il suffit juste de traiter 14% des rejets des zones résidentielles pour avoir la même atténuation.

Les secteurs commerciaux sont aussi des contributeurs non négligeables à la pollution des eaux de ruissellement et ils constituent une source importante de HAPs et des métaux. (Herngren et al., 2006) ont constaté que les charges de métaux lourds les plus élevées coïncidaient avec les charges de sédiments les plus élevées qui sont observées dans les zones commerciales. Tiefenthaler et al. (2008) ont trouvé que plus de 70% des échantillons d'eau ruisselée qu'ils ont collectés dans une zone commerciale contiennent des concentrations de zinc et de cuivre qui dépassent les normes établies dans l'état de Californie. Même si les zones commerciales contribuent à des concentrations de MES et de métaux plus importantes que celles sur les chaussées et les zones résidentielles (Ackerman and Schiff, 2003; Wang et al., 2013), elles demeurent moins émettrices de polluants que les zones fortement circulées (Wang et al., 2013). Ainsi, les concentrations de MES véhiculées par une chaussée caractérisée par un trafic de 1800 véhicules/heure sont 4 fois plus importantes que celles générées par les zones commerciales et pareillement, pour les concentrations de cuivre et de zinc qui sont moins

significatives dans la zone commerciale que sur la chaussée fortement circulée (Wang et al., 2013) .

Hall and Anderson (1988) ont étudié la toxicité des eaux de ruissellement provenant de différents types d'utilisation de sol et leur effet sur un organisme vivant dans le milieu récepteur ; ils rapportent que les eaux de ruissellement générées sur les sites commerciaux présentent les plus grands dangers. Les charges élevées de polluants qui s'accumulent sur les sites commerciaux tels que les centres commerciaux, les parkings, les stations de gaz, les centres de maintenance des véhicules proviennent de la densité de trafic importante sur ces sites ainsi que des activités qui y sont pratiquées (Parra et al., 2006).

#### **3.1.2.1.4. Construction**

Les activités de construction et de démolition dans les zones urbaines sont reconnues pour avoir le potentiel de contribuer à des quantités importantes de sédiments et de détritiques sur les surfaces surtout si les mesures de contrôles ne sont pas mises en place (Sonzogni et al., 1980). Les masses de sédiments provenant des sites de construction peuvent être jusqu'à 100 fois plus grandes que les sédiments provenant des sites ruraux (Wolman, 1967). Line et al. (2002) ont comparé les contributions de différents types d'occupation du sol à la contamination des eaux de ruissellement en se basant sur les données expérimentales acquises sur chacun des sites. Ils ont trouvé que les sites de construction constituent la source majeure de sédiments puisqu'ils véhiculent une quantité de sédiments qui est dix fois plus importante que celle générée par les autres occupations de sol. (Amato et al., 2011) ont identifié les émissions des sites de construction comme étant une des sources des substances minérales qui s'accumulent sur les surfaces urbaines. En plus, l'érosion des sites de construction constitue aussi une source de différentes substances toxiques telles que les pesticides, les solvants et les acides qui proviennent de la composition chimique des matériaux utilisés dans la construction et qui sont adsorbées par les particules (Marsh, 1993). Les effets de l'entraînement des sédiments par les eaux de ruissellement ne sont pas limités à l'échelle locale où ils ont un impact direct et concentré mais ils s'étendent à plus grande échelle pour affecter les milieux récepteurs à long terme (Dunne and Leopold, 1978; Goldman and Jackson, 1986).

### **3.1.2.1.5. Erosion du sol**

L'augmentation des taux d'érosion des sols en milieu urbain est liée aux travaux de construction et à la réduction du couvert végétal qui implique l'apparition des surfaces ouvertes et l'exposition des sols au vent et aux précipitations (Line et al., 1999). Sous l'effet de l'énergie cinétique des gouttes de pluie, les particules du sol vont se détacher et se décomposer en leurs composantes qui seront entraînées par le ruissellement. Ceci augmente la contamination en MES des eaux ruisselées qui peut dépasser les concentrations véhiculées dans les eaux sur les sites industriels (Stein et al., 2008). Ainsi, l'érosion des sols génère une quantité relativement importante de solides dans le ruissellement des eaux pluviales urbaines (Novotny et al., 1985).

### **3.1.2.2. Polluants primaires**

#### **3.1.2.2.1. Matières en suspension (MES)**

Les solides retrouvés dans l'eau peuvent être sous forme dissoute ou en suspension. La limite entre les phases dissoute et particulaire est fixée à  $0.45\mu\text{m}$ . Selon leur forme et leur gravité spécifique, les matières en suspension peuvent sédimenter. Les particules ayant un diamètre  $< 100\ \mu\text{m}$  demeurent plus longtemps en suspension dans l'eau que les particules ayant un diamètre  $> 100\ \mu\text{m}$  qui sont facilement sédimentables (Andral et al., 1999).

Les sources de MES comprennent l'usure des chaussées, les émissions des gaz d'échappement des véhicules, l'usure des véhicules, les chantiers de construction, le sel de voirie, la peinture routière, l'érosion du sol, les débris végétaux, la corrosion des matériaux et les dépôts atmosphériques (Lecoanet et al., 2003; Taylor and Owens, 2009; Thorpe and Harrison, 2008).

Les dépôts particuliers contribuent à de nombreux effets négatifs sur l'état biologique, chimique et physique du milieu récepteur (EPA, 1993). Les niveaux élevés de particules dans l'eau accroissent la turbidité, réduisent la pénétration de la lumière en profondeur dans la colonne d'eau et limitent la croissance des plantes aquatiques. Les solides qui séimentent contribuent aussi à la formation de dépôts de fond, ce qui peut altérer et éventuellement détruire l'habitat des poissons et des organismes. Les particules solides constituent également des éléments privilégiés pour l'accumulation et le stockage d'autres polluants toxiques, y

compris les hydrocarbures, les nutriments et les métaux (Pitt et al., 2005; Roger et al., 1998; Shinya et al., 2000; Sutherland, 2003).

Les métaux et les composés organiques s'attachent à la surface des particules en suspension dans l'eau via des processus d'adsorption, contrôlés par les caractéristiques de MES qui influencent la relation entre les solides et les fractions de divers polluants (Minton, 2002). Ces caractéristiques incluent la distribution de la granulométrie des particules, le contenu en matière organique et la teneur en minéraux.

Différentes études ont mis en évidence le fait que certains polluants étaient davantage adsorbés sur les particules fines. Cela est généralement attribuable à l'augmentation de la surface spécifique de sorption avec la diminution de la taille des grains (McKenzie et al., 2008; Sansalone et al., 1998). (Vaze and Chiew, 2004) ont rapporté que pratiquement toutes les particules de nutriments (phosphore et azote) dans les échantillons d'eaux de ruissellement collectés sur une surface urbaine sont adsorbées aux sédiments entre 11 et 150 $\mu$ m. Robertson and Taylor (2007) ont aussi signalé que les concentrations de plomb, de cuivre et de zinc dans le stock de sédiments sur les chaussées en Manchester en Grande Bretagne sont les plus élevées dans les fractions fines < 63 $\mu$ m. Pareillement, (Zhao et al., 2010) ont trouvé que les métaux sont associés aux particules < 44 $\mu$ m. (Herngren et al., 2010) ont rapporté que les concentrations les plus élevées en HAPs mesurées dans l'eau de ruissellement sont associées aux particules entre 0.45 et 150 $\mu$ m.

La présence de la matière organique dans les eaux de ruissellement est aussi un facteur qui joue un rôle important dans l'adsorption des polluants aux solides puisqu'elle favorise les réactions de complexation des métaux ainsi que des HAPs (Bradl, 2004; McCarthy and Jimenez, 1985). En fait, les solides et les polluants dissous ont des charges électriques qui s'attirent lorsqu'elles sont complémentaires. (Schlautman and Morgan, 1993) ont montré que les HAPs sont associés au composant organique des solides et en particulier à la fraction humique qui s'y trouve. La complexation des métaux par les ligands organiques a été aussi observée pour les métaux par (Liu and Gonzalez, 1999; Qu and Kelderman, 2001). D'autre part, la matière minérale argileuse qui se trouve en majorité dans la fraction fine favorise aussi l'adsorption des métaux (Piatina and Hering, 2000; Uddin, 2017).

### 3.1.2.2.2. Métaux

Les métaux lourds dans le milieu urbain se trouvent à des niveaux de concentrations anormalement élevés par rapport au fond géochimique (Alloway and Ayres, 1997). Ils sont libérés dans le milieu par des sources anthropiques vastes parmi lesquels nous citons les procédés industriels, l'usure des câbles de freins et des pneus des véhicules, le gaz d'échappement, la fuite de fluides de véhicules, les toitures métalliques. Dans une étude faite par (Brown and Peake, 2006) sur les sources des métaux lourds et des HAPs dans les eaux de ruissellement sur deux bassins versants ayant des pourcentages distincts d'urbanisation, l'activité industrielle est identifiée comme étant la source des teneurs élevées de cuivre et de plomb qui ont été mesurés dans le bassin versant urbain. Tandis que l'abondance des teneurs en zinc a été attribuée aux apports par le ruissellement sur les toitures de fer galvanisées au zinc. En fait, ce type de matériau entraîne des émissions importantes de quantités de zinc pendant les précipitations (Gromaire-Mertz et al., 1999; Sörme and Lagerkvist, 2002). L'usure des pneumatiques contribue aussi à l'émission du zinc (Davis et al., 2001) et d'autres métaux comme l'aluminium, le cobalt et le plomb (Sadiq et al., 1989). Cependant les flux d'émission provenant de l'abrasion des pneus peuvent être très variables avec des gammes de valeurs très étendues (Pagotto, 1999). La dégradation de la garniture des câbles de freins constitue une source non négligeable de Zn, Cu et Pb qui sont les métaux principaux présents dans la structure de cette garniture, surtout à proximité des feux de signalisation et de passages à niveau, où il y a des freinages fréquents (Pitt et al., 1995). Les métaux lourds liés aux émissions à l'échappement diffèrent selon le type de carburant utilisé. Une étude par (Pulles et al., 2012) sur les émissions des métaux lourds par les véhicules circulant en Europe, a montré que la combustion du pétrole dans les voitures génère des charges élevées de As, Cd et de Hg tandis que la combustion du diesel dans les camions entraîne des émissions élevées de Cr, Cu, Ni, Pb et Zn.

La présence des métaux lourds dans les eaux de ruissellement avec des concentrations élevées augmente leur toxicité et leur bioaccumulation dans les organismes aquatiques qui ne réussissent plus à les dégrader. Ils posent aussi beaucoup de danger sur la santé humaine surtout le Cd, Pb, As et Hg car ils sont à l'origine de plusieurs maladies comme les maladies cardiovasculaires, les maladies des os, le dysfonctionnement rénal et l'endommagement du système nerveux (Järup, 2003).

La répartition des métaux entre les phases dissoute et particulaire n'est pas la même pour tous les métaux. (Yousef et al., 1984) ont montré que 80% du Pb, Cr et Cd se trouvent sous forme particulaire tandis que 92,5% du Zn et 67,5% du Ni se trouvent en phase dissoute. Le Cu est réparti entre les deux phases avec 48% dans la phase particulaire et 52% dans la phase dissoute. Les répartitions obtenues par (Sansalone et al., 1996) étaient analogues aux résultats précédents pour le Zn et le Ni, mais ils ont trouvé que la proportion de Cu dissoute était plus grande et que la partition du Pb entre les deux phases était intermédiaire. (Berbee et al., 1999) ont rapporté que 75% des métaux (Pb, Cu, Cd, Cr, Zn, Ni) sont associés aux particules, ce qui est en contradiction avec les résultats de (Dassenakis et al., 1998) qui ont trouvé que le Cu, Pb, Ni, Cr and Zn sont plutôt dans la phase dissoute. La variabilité des répartitions obtenues d'une étude à une autre s'explique par différents éléments chimiques et physiques qui contrôlent la biodisponibilité du métal, tel que les paramètres physico-chimiques de milieu qui comprennent le pH et le potentiel d'oxydoréduction, l'état d'oxydation du métal, la nature de l'absorbant (charge dépendant du pH, type de complexes ligands, surface spécifique) (Alloway and Ayres, 1997; Morrison et al., 1990). Cela met en évidence le dynamisme de la séparation des métaux entre les phases dissoutes et particulaires et le fait qu'un métal au cours de son transport vers le milieu récepteur peut facilement passer d'un état à l'autre.

#### **3.1.2.2.3. Hydrocarbures aromatiques polycycliques (HAPs)**

Les hydrocarbures aromatiques polycycliques (HAPs) désignent les composés organiques qui contiennent du carbone et de l'hydrogène ; ils sont constitués de 2 à 6 cycles aromatiques qui diffèrent par leurs masses moléculaires. Les émissions de ces composés sont dues à la pyrolyse et à la combustion incomplète de matières organiques.

Les sources d'émission des HAPs dans l'environnement sont divisées en sources naturelles et sources anthropiques. Les éruptions volcaniques et les feux de forêt sont les deux processus de combustion naturelle qui sont à l'origine de la production des HAPs. Cependant, ces phénomènes se passent pendant des épisodes séparés et donc ils ne contribuent pas énormément au rejet chronique des HAPs. La pollution chronique en HAPs provient principalement des sources anthropiques dont la circulation automobile et les procédés industriels (Manoli and Samara, 1999). Les émissions des gaz d'échappement qui proviennent



de la combustion incomplète des carburants et les déversements des fluides des véhicules (huiles lubrifiantes, carburant) ainsi que les débris de l'usure des véhicules et des pneus constituent des sources importantes d'hydrocarbures dans le milieu urbain (Walker et al., 1999). (Bomboi and Hernández, 1991) ont mesuré les niveaux de HAPs dans les eaux de ruissellement à Madrid pour des bassins versants représentant des occupations de sol résidentielles, industrielles et commerciales. Les résultats qu'ils ont obtenus montrent que les résidus pétroliers provenant des véhicules et la combustion incomplète de carburant constituent une part importante de la production d'hydrocarbures des zones urbaines et industrielles contribuant à la pollution du ruissellement urbain à Madrid. En outre, l'utilisation de systèmes de chauffage et la présence importante de véhicules à l'automne et en hiver produisent des niveaux d'hydrocarbures plus élevés que ceux émis en printemps et en été. La hausse des niveaux de contamination en HAPs qui accompagne l'augmentation de l'utilisation des automobiles est confirmée par plusieurs études (Krein and Schorer, 2000; Van Metre et al., 2000; Zgheib et al., 2012).

Les HAPs ont tendance à s'adsorber sur les matrices solides. (Hoffman et al., 1984) ont noté que le pourcentage des hydrocarbures associés aux particules dans les eaux de ruissellement varie de 79 à 96%. Pareillement, (Datry et al., 2003) ont trouvé que la majorité des hydrocarbures est attachée aux particules et une très petite quantité se trouve en phase dissoute. Les HAPs sont des composés très peu solubles dans l'eau et leur caractère hydrophobe s'accroît lorsque la masse molaire augmente (Wu et al., 2013). Ce sont des polluants organiques persistants, peu dégradés dans l'environnement qui peuvent s'accumuler dans les tissus vivants. Les hydrocarbures sont toxiques et dangereux non seulement pour la qualité des milieux récepteurs (Kayhanian et al., 2006; Zgheib et al., 2012) mais aussi pour la santé de l'homme parce qu'ils sont extrêmement cancérigènes (Göbel et al., 2007; Petry et al., 1996).

### 3.2. Processus d'accumulation et de lessivage

Au début des années 1970, (Sartor and Boyd, 1972) et (Sartor et al., 1974) ont mis en évidence l'accumulation et le lessivage comme étant les deux processus majeurs de production et de mobilisation des contaminants dans le milieu urbain.

L'accumulation résulte des interactions entre tous les processus qui ont lieu pendant le temps sec. Elle résulte de l'équilibre qui s'établit entre les mécanismes de dépôt et de remise en suspension des particules.

Lors d'un événement pluvieux, le stock est mobilisé sous l'effet du lessivage. Le lessivage résulte de l'équilibre entre le détachement des particules sous l'action de la pluie et sous l'action du ruissellement, et leur dépôt. Le processus d'érosion est le moteur du transfert des polluants vers les points de rejet.

Dans cette partie, nous présentons des descriptions détaillées des processus d'accumulation et de lessivage sur les surfaces urbaines imperméables, les facteurs qui les influencent et les caractéristiques de la contamination qu'ils engendrent en terme de charge et de distribution des dimensions des particules.

### 3.2.1. Accumulation

C'est un fait établi que pendant les périodes de temps sec, les particules solides s'accumulent sur les surfaces des bassins versants urbains, pour former un stock de polluants prêt à être mobilisé lors des épisodes de pluie. L'activité humaine est le premier responsable de la formation de ce stock dans le milieu urbain.

Les facteurs qui déterminent le bilan massique des charges de polluants qui se trouvent sur la surface à un instant donné comprennent (Ball et al., 1998; Novotny et al., 1985; Pitt et al., 2005; Sartor et al., 1974):

- Le taux de dépôt des particules pendant le temps qui s'est écoulé entre deux événements pluvieux ou deux nettoyages de la surface. Il est contrôlé par les dépôts atmosphériques et les dépôts directs qui proviennent des automobiles, des résidents, des travaux de chantier, de la végétation ainsi que de la dégradation de la surface.
- Le taux de remise en suspension qui dépend des conditions météorologiques (vent et la pluie) et des activités humaines incluant la turbulence induite par le passage des véhicules, le nettoyage des chaussées et la biodégradation.

- Le stock permanent qui résulte du piégeage des particules dans les fissures de la surface qui ne sont mobilisées ni par le vent ni par la pluie ni par les procédés de nettoyage. Il est contrôlé par la texture et l'état du revêtement.

(Sartor and Boyd, 1972) ont mené les premières recherches sur le processus d'accumulation des particules sur les chaussées urbaines. Leur étude a été conduite entre les années 1969 et 1971 dans 12 villes des Etats –unis où des échantillons de poussières ont été prélevés pour mesurer les charges polluantes sur les rues pour des zones résidentielles, commerciales et industrielles. Ces auteurs indiquent que la charge de polluant accumulée sur la surface dépend de deux facteurs principaux : l'occupation de sol, et la durée écoulée depuis le dernier lessivage de la rue par la pluie ou le balayage. L'accumulation de la masse des solides tend à croître de façon exponentielle en fonction de la période de temps sec antérieure sans égard à l'occupation de sol, avec un taux de croissance plus rapide observé pour les zones industrielles que pour les zones commerciales et résidentielles. En outre, (Sartor et al., 1974) ont démontré que le taux d'accumulation augmente rapidement après le processus de lessivage et diminue graduellement à mesure que le temps sec augmente pour atteindre finalement une asymptote qui représente une charge constante.

Ce comportement de l'accumulation des particules est aussi observé dans plusieurs études postérieures (Ball et al., 1998; Wicke et al., 2012). (Egodawatta and Goonetilleke, 2007) ont étudié l'accumulation sur trois chaussées situées dans des zones résidentielles en Australie et ils ont détectés des taux d'accumulation entre 1 et 2 g/m<sup>2</sup>/jour au cours des deux premiers jours. Les taux d'accumulation se sont ensuite réduits et l'accumulation totale a assez vite atteint une asymptote. Pareillement, (Egodawatta et al., 2009) ont observé la même tendance pour l'accumulation sur des toitures en tôles ondulées et en béton, où au bout d'une semaine 80% du stock total des particules s'est déposé. Cependant, le taux d'accumulation pendant les premiers jours sur les toitures est très petit (0.4 g/m<sup>2</sup>/jour) en comparaison avec celui mesuré sur les chaussées. Ce résultat est lié à la différence des sources et des mécanismes de dépôt auxquels sont soumises les deux surfaces.

Cependant, l'effet de la durée de temps sec sur le processus d'accumulation est critiqué par d'autres chercheurs. (Sutherland and Jelen, 1996) ont remarqué que la corrélation entre le stock accumulé et la période de temps sec n'est pas réaliste, car leurs observations sur le terrain

montrent que les accumulations sont sensiblement plus élevées pendant la saison des pluies (caractérisée par des durées de temps sec courtes) que pendant la saison sèche. Les résultats de l'étude expérimentale faite par (Deletic and Maksimovic, 1998) à Belgrade, en Yougoslavie, et à Lund (Suède), sur des surfaces imperméables, révèlent que la durée de temps sec n'a qu'un effet mineur sur l'accumulation des polluants de surface des routes. Des observations similaires sont constatées par (Shinya et al., 2003) qui ont trouvé que la période de temps sec et le débit du trafic ne sont pas corrélés avec la charge polluante dans le ruissellement sauf pour l'azote. (Deletic and Orr, 2005) d'autre part ont trouvé que la période de temps sec précédant l'événement pluvieux a une influence très faible et négative sur le taux d'accumulation des particules fines près du bord du trottoir, à Aberdeen, en Ecosse.

Les résultats contradictoires obtenus dans différentes études sont dus aux différentes conditions géographiques et météorologiques. En fait les facteurs tels que le type de surface, la rugosité, la pente, l'occupation des sols (Duong and Lee, 2009; Zhao et al., 2011) et les conditions météorologiques (Ball et al., 1998; Novotny et al., 1985) ont une influence importante sur le taux de dépôt et le taux de remise en suspension et par suite sur la redistribution des charges polluantes et, par conséquent, le taux d'accumulation. (Deletic and Orr, 2005) ont trouvé que les charges de sédiments, ainsi que les concentrations de chlorure et de sulfate, sont les plus élevées durant les mois d'hiver, surtout en présence de la neige à la surface de la route à cause de l'utilisation des sels de déneigement des routes. (Egodawatta and Goonetilleke, 2007) ont mesuré les taux d'accumulation les plus élevés sur la chaussée située dans la zone résidentielle où la densité de la population et le volume de trafic sont élevés par rapport aux autres sites. De plus, le site le plus chargé est plus plat et ayant une texture de surface plus rugueuse. (Vaze and Chiew, 2002) ont noté que l'accumulation de polluants sur les revêtements routiers varie dans le sens longitudinal en fonction de la pente et de la présence de feux de circulation et de goulets d'étranglement. (Mahbub et al., 2011) et (Kayhanian et al., 2003) ont aussi souligné l'influence du trafic journalier moyen sur le taux d'accumulation des polluants.

En fait, le trafic joue un rôle très important dans la redistribution des polluants à l'intérieur d'un bassin versant en raison de la turbulence provoquée par la circulation des véhicules (Namdeo et al., 1999; Shaheen, 1975). La répartition des sédiments dans la rue mesurée par (Sartor and Boyd, 1972) indiquait qu'environ 90 % du stock se trouvait à environ

30 cm du bord de trottoir à l'intérieur du caniveau. Pareillement, (Deletic and Orr, 2005) ont mesuré la charge la plus élevée des sédiments à 0.25 m du bord du trottoir. Ces résultats font la lumière sur le rôle que joue la présence du trottoir comme barrière qui empêche le transport des sédiments de la surface et favorise leur piégeage et l'accumulation près des caniveaux (Viklander Maria, 1998). Cependant, cette répartition n'est pas systématique, comme cela a été observé à l'échelle locale du bassin versant routier étudié dans le cadre de Trafipollu (Figure 3-1).

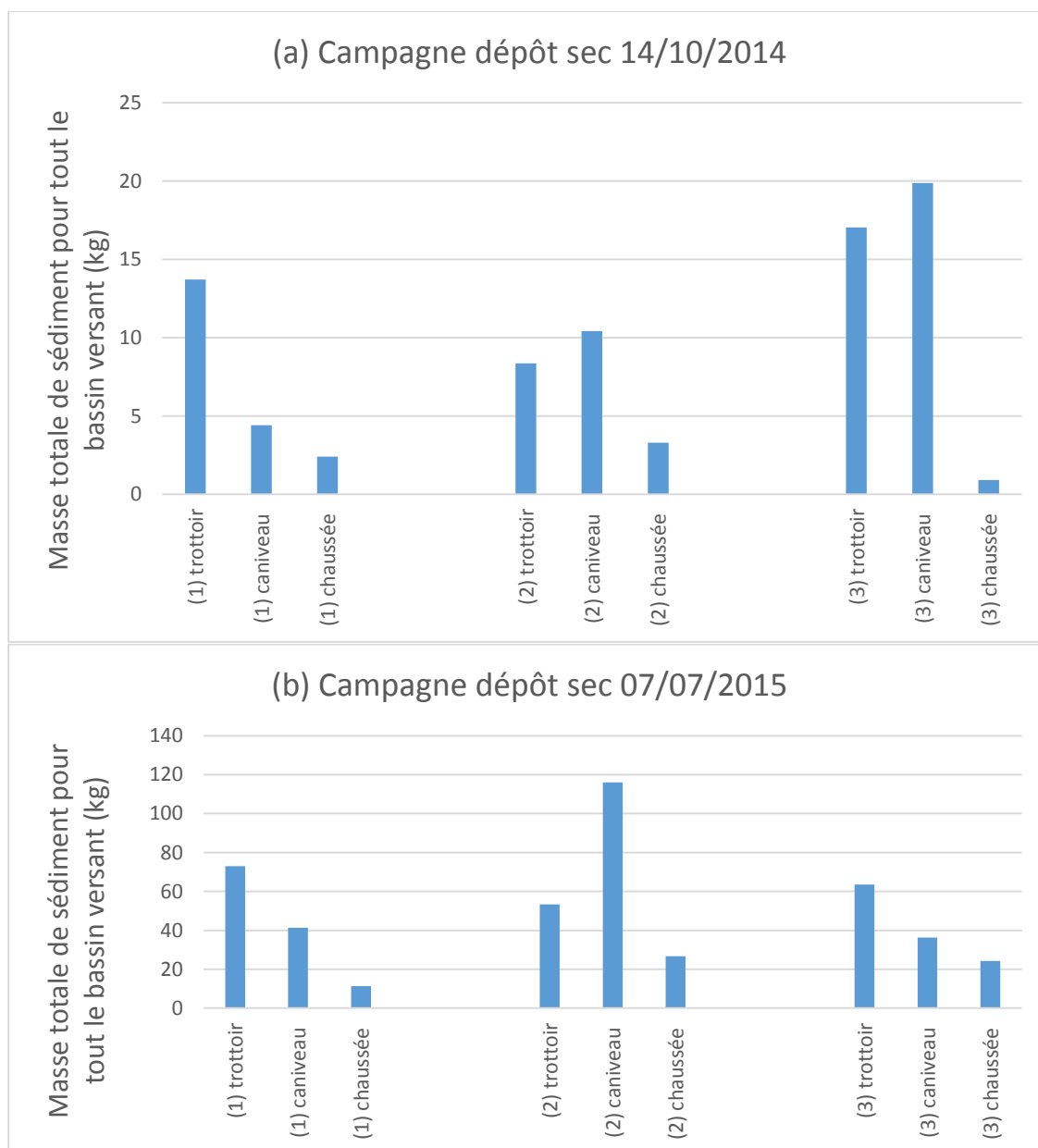


Figure 3-1 la masse totale de sédiment collecté pour les trois localisations (1), (2) et (3) (Figure 2-4) , sur le trottoir, le caniveau et la chaussée durant la campagne de dépôt sec du (a) 14/10/2014 et (b) 07/07/2015

Lors de la campagne du 14 octobre 2014, et pour deux localisations, les charges sédimentaires les plus élevées sont collectées dans le caniveau mais avec un écart très léger des charges collectées sur le trottoir. Lors de la deuxième campagne du 07 juillet 2015, ce sont les trottoirs qui accumulent le plus grand stock de sédiment suivis des caniveaux, à l'exception de la localisation 2 où les charges les plus élevées sont collectées dans le caniveau. Lors des deux campagnes, le stock accumulé sur les chaussées est minimal sur toutes les localisations. Ces résultats révèlent la variabilité importante de la répartition spatiale des particules même au sein d'un petit bassin versant et indique un rôle important des trottoirs dans la contamination des eaux de ruissellement qui mérite ainsi plus d'investigation.

La caractérisation du stock de sédiments sur la surface en termes de composition et de distribution granulométrique est très importante dans le cadre de la compréhension de la qualité des eaux dans le milieu urbain. Les distributions des dimensions des particules dans le stock de sédiment mesurées dans plusieurs études montrent une grande variabilité dans les fractions dominantes. Ceci est attribué au caractère dynamique du processus d'accumulation dont la redistribution est le responsable primaire (Egodawatta and Goonetilleke, 2007). Les échantillons de sédiments collectés par (Yuen et al., 2012) sur des chaussées urbaines pour un bassin versant résidentiel et un bassin versant industriel contiennent respectivement 25 et 24 % des particules dans la fraction de 250-500 $\mu\text{m}$ . Cependant, (Zhao et al., 2010) ont rapporté que pour les stocks mesurés sur trois occupations de sol distinctes, 50% des sédiments sont dans la partie fine dans la fraction 100-200 $\mu\text{m}$ . (Deletic and Orr, 2005) ont trouvé que 50% des particules à côté de la bordure du trottoir ont un diamètre < 400 $\mu\text{m}$  et 50% des particules échantillonnées à 3 mètres de la route ont un diamètre < 110  $\mu\text{m}$ . Malgré les différences dans la distribution des tailles des particules dans le stock de sédiment, les recherches montrent que le focus doit être dans tous les cas sur la fraction fine du stock car c'est la fraction sur laquelle les polluants toxiques vont s'adsorber (Deletic and Orr, 2005; Krein and Schorer, 2000; Sartor et al., 1974; Yuen et al., 2012). (Deletic and Orr, 2005) ont rapporté que les concentrations de Zn, Cu et Cd dans la fraction sédimentaire de 2-63  $\mu\text{m}$  sont huit à dix fois plus élevées que dans la fraction de 500  $\mu\text{m}$  alors que la concentration de Pb est environ 22 fois plus élevée. (Sartor et al., 1974) ont montré que malgré le fait que la fraction fine ne compte que pour 5.9% de la distribution des dimensions des particules, elle est la plus contaminée comme 50% des métaux et entre 1/3 et 1/2 des nutriments y sont associés.

Il faut noter que la fraction fine du stock des chaussées est susceptible d'augmenter sous l'effet du balayage traditionnel : (Vaze and Chiew, 2002), dans leur étude de l'effet du balayage des chaussées sur le stock de surface, ont noté que cette technique est efficace pour arracher les sédiments grossiers. Cependant, elle pourrait avoir un effet négatif qui se manifeste par le fait que sous l'action de la brosse, il y a une partie des particules fines qui va se libérer. (German and Svensson, 2002) ont montré que le balayage contribue à l'augmentation de la fraction fine ( $< 125 \mu\text{m}$ ) à laquelle les métaux sont associées ce qui augmente les risques des contaminations au cas où un événement pluvieux aura lieu juste après.

### 3.2.2. Lessivage

Le lessivage pendant un événement pluvieux est le processus par lequel les particules qui se sont accumulées durant le temps sec sur les surfaces urbaines sont entraînées vers les milieux récepteurs. Les particules retrouvées dans les eaux de ruissellement proviennent de deux sources qui sont les dépôts humides, processus par lequel les polluants solubles adsorbés sur les particules qui se trouvent en suspension dans l'atmosphère sont lessivés par les gouttes de pluie, et l'érosion du stock disponible sur la surface sous l'action des gouttes de pluie et des contraintes de cisaillement du ruissellement. L'érosion de surface est reconnue comme étant la source principale de contamination des eaux de ruissellement, puisqu'elle contribue à plus de 75% de la charge totale des polluants transportée par le ruissellement (Gromaire, 1998).

Etant donnée la complexité du processus de lessivage, les chercheurs ont mené des nombreuses études afin d'identifier les facteurs influençant principalement les quantités de polluants mobilisées. Ceux-ci incluent l'intensité des précipitations, la durée de l'événement pluvieux et le volume ruisselé (Egodawatta et al., 2007).

Dans l'étude qu'ils ont menée à Austin, Texas aux Etats-Unis (Charbeneau and Barrett, 1998) ont montré que la charge des matières en suspension entraînée par le lessivage peut s'expliquer en grande partie par le volume de ruissellement. Cette relation a aussi été mise en évidence par (Deletic and Maksimovic, 1998) qui ont calculé des coefficients de corrélation supérieurs à 0.85 entre le volume ruisselé et la charge en MES sur les deux bassins versants qu'ils ont étudié. Ils ont noté que l'intensité de la pluie influence aussi ces charges. (Wanielista and Yousef, 1993) ont trouvé qu'un événement pluvieux ayant une intensité plus élevée sur

une courte période est plus efficace à entraîner les particules de la surface qu'un événement ayant une faible intensité sur une longue période. Il est cependant difficile de déceler l'influence individuelle de chacune de ces variables explicatives parce qu'elles sont corrélées les unes aux autres, ainsi l'importance relative de chaque variable sur le taux de lessivage n'est pas très clair (Herngren et al., 2005). La durée de temps sec a été aussi identifiée dans certaines études comme un paramètre affectant le lessivage des polluants. (Chui, 1997) qui ont étudié la qualité de ruissellement sur deux bassins versants adjacents en Singapour, ont trouvé que les concentrations de MES et de COD sont largement influencées par la durée de temps sec, alors que les masses de ces polluants sont corrélées au volume ruisselé. (Neary et al., 2002) ont montré que la durée de temps sec et l'intensité de la pluie ont un effet sur le lessivage des particules sur des parkings à Cookeville, Tennessee aux Etats-Unis. Ceci a aussi été constaté par (Yaziz et al., 1989) pour les toitures. Par contre, (Hoffman et al., 1982) n'ont pas trouvé des effets significatifs de la durée de temps sec sur le lessivage. Cela montre que comme pour l'accumulation, les effets de cette variable sur le lessivage n'est pas très clair.

Les conditions météorologiques ne sont pas les seuls facteurs qui impactent l'entraînement des particules. (Berretta et al., 2007) ont trouvé que la dynamique du lessivage est influencée non seulement par les paramètres hydrologiques et notamment le temps de réponse du bassin versant mais aussi par les caractéristiques du bassin versant et la nature des polluants. (Chen and Adams, 2007) ont noté que les types et les conditions des chaussées, la taille des particules, le nettoyage des chaussées et la densité de la circulation influent le taux de transport des polluants.

L'érosion des particules pendant un événement pluvieux est gouvernée par deux mécanismes : le détachement et le transport (Rose, 1985).

Le détachement des particules s'effectue sous l'action des gouttes de pluie et du ruissellement. Le rôle que joue la pluie comme un agent érosif est bien connu (Ellison, 1945). L'énergie cinétique dissipée lors de l'impact des gouttes de pluie est à l'origine de la désagrégation et du détachement des particules qui sont présentes sur la surface lors d'un événement pluvieux. Les facteurs qui influencent l'érosivité de la pluie incluent l'intensité de la pluie, la taille des gouttes, leur vitesse et angle d'impact. Le détachement par les gouttes dépend aussi de la hauteur de la lame d'eau qui se forme sur la surface. Au-delà d'une hauteur



seuil, cette lame d'eau agit comme un agent protecteur qui réduit la fraction susceptible d'être détachée (Hairsine and Rose, 1992a; Proffitt et al., 1991). Le détachement des particules par le ruissellement s'effectue sous l'action de la contrainte de cisaillement qu'exerce l'écoulement sur la surface et de son énergie (Giménez and Govers, 2002; Hairsine and Rose, 1992a, 1992b). Il est lié à la pente et aux caractéristiques de l'écoulement qui sont la vitesse et la hauteur. La résistance des particules au détachement dépend de leur cohésion interne, cependant dans le contexte urbain, celle-ci est supposée nulle (Hong et al., 2016a). Les études qui ont investigué l'érosion des sédiments dans un contexte urbain ont mis en évidence la prépondérance du détachement par les gouttes de pluie stimulé par l'énergie cinétique des gouttes par rapport au détachement par ruissellement (Hong et al., 2016a; Mackay et al., 1999). Cependant, (Vaze and Chiew, 2003) ont souligné l'importance de la force de cisaillement provoquée par le ruissellement de surface pour détacher les particules et ils ont noté que l'effet des gouttes de pluie, très important au début de l'événement, se réduit progressivement au fur et à mesure de l'événement en raison de la diminution du stock mobilisable.

Après leur détachement, les particules sont entraînées principalement par le ruissellement. Un transfert local des particules peut avoir lieu sous l'impact de la goutte de pluie et qui est désigné par l'effet « splash » où les particules s'arrachent de la surface et se déposent immédiatement aux alentours directs du point d'impact. Cependant cet effet est souvent négligé et pas pris en compte comme agent de transport. L'entraînement peut être lié à la capacité de transport de l'écoulement (Foster, 1990), ou bien à la vitesse de sédimentation des particules qui sont détachées et mises en suspension dans la lame d'eau (Hairsine and Rose, 1992a, 1992b).

Durant un événement pluvieux, seule une fraction du stock est éliminée par le ruissellement (Hong et al., 2016a). L'étude expérimentale de (Vaze and Chiew, 2002) montre qu'un événement pluvieux significatif de 39,4 mm n'est capable d'entraîner que 35 % des polluants totaux. (H. Zhao et al., 2016) ont trouvé des résultats similaires, où la comparaison du stock avant et après deux événements pluvieux montre que 30% et 40% du stock est mobilisé par les événements ayant une hauteur précipitée égale à 2 et 23 mm respectivement. Les coefficients de lessivage qui correspondent au ratio entre la masse accumulée et la masse entraînée calculés par (Egodawatta et al., 2007) montrent qu'un événement pluvieux a une capacité à mobiliser une fraction des particules disponible et que cette fraction dépend de

l'intensité de pluie, où les coefficients de lessivage des événements peu intenses ne dépassent pas 40%.

L'analyse granulométrique de la fraction lessivée pour déterminer la distribution des tailles des particules dans le ruissellement révèle que la majorité des sédiments mobilisés lors d'un événement pluvieux appartiennent à la fraction fine. Cette analyse est très importante puisqu'elle aide à la sélection des outils de traitement appropriés pour l'enlèvement des sédiments de différentes tailles. (Hong et al., 2016a) ont trouvé que les particules fines  $< 50\mu\text{m}$  représentent plus de 90 % de la charge totale de MES véhiculée dans les eaux de ruissellement à l'avaloir d'un bassin versant routier. (H. Zhao et al., 2016) ont aussi noté la nature fine des particules dans les eaux de ruissellement où la contribution des particules  $< 105\mu\text{m}$  à la charge totale lessivée était 64 à 80 %. Les distributions des dimensions des particules mesurées par (Charters et al., 2015) dans le ruissellement de quatre surfaces urbaines distinctes sont les plus concentrés autour des tailles entre 60 et 100  $\mu\text{m}$ .

### 3.3. Modélisation

Les modèles développés pour étudier l'hydrologie en milieu urbain sont basés sur trois blocs :

- Bloc production : décrit la génération du ruissellement où la pluie est transformée en débit ruisselé en utilisant les modèles hydrologiques.
- Bloc pollution : décrit la génération des polluants pendant le temps sec et leur mobilisation dans l'écoulement en utilisant les modèles de qualité.
- Bloc transfert : décrit le transfert du débit et des polluants en utilisant les modèles de transfert.

Dans cette partie nous dressons un bilan sur les modèles hydrologiques et les modèles de qualité.

#### 3.3.1. Modélisation hydrologique et fonction de production

Les modèles hydrologiques sont développés dans le but d'évaluer les effets de l'urbanisation sur le cycle de l'eau, de compenser le manque de données fiables sur les bassins

versants non instrumentés et de faire des prévisions des crues et des scénarios de changement climatique (Salvadore et al., 2015).

Les modèles hydrologiques classiques utilisés en milieu urbain ont une fonction de production basée sur la représentation des pertes. Les pertes sont classées en deux catégories : les pertes initiales et les pertes continues. Les pertes initiales comprennent l'humidification de la surface, l'interception et le stockage dans les dépressions alors que les pertes continues comprennent l'évapotranspiration et l'infiltration (Ramier et al., 2010). Le principe de ces modèles repose sur l'idée de retirer à la pluie brute la valeur des pertes initiales en début d'événement pluvieux. . Dans un second temps, ces modèles appliquent soit un coefficient de ruissellement constant pour tenir compte des pertes continues, soit un coefficient de ruissellement qui varie dans le temps. Le ruissellement, ou pluie nette est déduit de cette approche. Ce concept de représentation des pertes est largement appliqué dans les logiciels de simulation du ruissellement tels que CANOE (INSAVALOR, 1997), STORM (US Army Corps of Engineers, 1977).

Cependant des modèles plus sophistiqués sont développés pour tenir compte de divers processus du cycle hydrologique dont le degré de complexité reflète l'objet de la modélisation. (Salvadore et al., 2015) ont classé les modèles selon l'objectif de leur application, et ils ont ainsi distingués les catégories suivantes :

- Variation de l'occupation du sol et de pourcentage d'imperméabilité
- Bilan hydrique conceptuel intégré
- Inondation et Conception des systèmes de protection contre les inondations et de drainage
- Sols urbains et eaux souterraines
- Climat urbain
- Modélisation intégrée à base physique

Les modèles hydrologiques peuvent aussi être classés selon leur discrétisation spatiale, leur discrétisation temporelle et la nature des variables (Zoppou, 2001). Le tableau ci-dessous résume les différents types de modèles hydrologiques (Table 3-1).

**Table 3-1 Typologie des modèles hydrologiques**

<b>Critère de classification</b>	<b>Type de modèle</b>	<b>Commentaire</b>
<b>Discretisation spatiale</b>	Global	Pas de variabilité spatiale
	Semi-distribué	Sous bassins versants
	Distribué	Maille Elément hydrologique
<b>Discretisation temporelle</b>	Continue	Simulations en continue pour plusieurs événement pluvieux
	évènementielle	Simulation pour un seul événement pluvieux
<b>Nature des variables</b>	Déterministe	valeurs uniques
	Stochastique	une distribution de probabilité

Même les modèles hydrologiques les plus simples donnent des estimations satisfaisantes des paramètres quantitatifs de l'eau de ruissellement en milieu urbain en revanche des modèles de qualité dont la performance n'est pas satisfaisante.

### 3.3.2. Modélisation de qualité

Les outils de modélisation de la qualité des eaux de ruissellement qui permettent d'estimer les masses et les flux de polluants rejetés sont développés depuis une quarantaine d'années. Les modèles proposés varient en fonction des approches adoptées, de leur complexité, de la masse de données nécessaire pour leur calage et validation et du temps de calcul qu'ils exigent (Merritt et al., 2003; Obropta and Kardos, 2007; Zoppou, 2001).

En termes de description des processus, les modèles de qualité sont classés en trois catégories qui présentent un degré croissant de complexité : empiriques, conceptuels et physiques. Les modèles empiriques n'incluent aucune notion sur les mécanismes qui contrôlent la génération des polluants. Ils sont développés à partir des régressions établies entre les masses et les concentrations mesurées sur un site spécifique et les caractéristiques du site et de la pluviométrie. Leur application est alors limitée au site pour lequel ils sont dérivés. Les modèles conceptuels sont basés sur la simulation des processus d'accumulation et de lessivage. Ils sont dérivés à l'issue des études expérimentales et tendent à simuler le comportement observé des polluants. Leurs formulations incluent des paramètres qui n'ont pas un sens physique et qui sont déterminés par calage. Les modèles physiques de qualité sont notamment basés sur la reproduction des mécanismes d'érosion et de transport pour la description de la mobilisation des sédiments, en partant du principe de la conservation de masse et en appliquant les lois d'advection-diffusion. Ils simulent le flux de sédiment qui sera

transporté dans la lame d'eau après le détachement et le dépôt. Le degré de complexité dans ces modèles est souvent élevé et les approches impliquées sont très sophistiquées.

Les modèles empiriques sont écartés dans cette étude vue la simplification excessive des processus. Dans les parties qui suivent, nous présentons une description et une discussion des modèles développés pour la simulation des processus d'accumulation et de mobilisation selon les approches conceptuelles et physiques.

### 3.3.2.1. Modélisation de l'accumulation

Des nombreux chercheurs ont formulé des relations fonctionnelles pour décrire l'accumulation des polluants qui résulte de deux processus de base : le dépôt et la disparition, en fonction de la durée de temps sec qui sépare deux événements pluvieux. L'accumulation des particules sur les surfaces évoluent avec le temps principalement suivant deux fonctions : exponentielle et puissance (Kang et al., 2006).

(Sartor et al., 1974) sont les premiers à proposer le modèle exponentiel qui décrit la relation entre la masse accumulée et le temps sec précédent. Par la suite, ce concept a été largement adopté pour la modélisation de l'accumulation des polluants dans de nombreuses études (Chen Jieyun and Adams Barry J., 2006; Novotny et al., 1985). Le modèle qu'ils ont proposé est donné par les équations suivantes (Sartor et al., 1974):

$$\frac{dM_a(t)}{dt} = K(M_{max} - M_a(t)) \quad (1)$$

$$M_a(DTS) = M_{max}[1 - e^{-KDTS}] + M_r e^{-KDTS} \quad (2)$$

Avec :  $M_a(t)$  est la masse des particules accumulée pendant la durée  $t$  (m) ;  $K$  est le paramètre d'accumulation ( $T^{-1}$ ) ;  $M_{max}$  est la masse maximale des particules déposée sur la surface (m) ;  $M_r$  est la masse résiduelle des particules de l'événement pluvieux précédent (m).

(Shaheen, 1975) ont proposé la même formulation exponentielle pour modéliser les dépôts prélevés sur une chaussée pour différentes périodes de temps sec mais sans tenir compte de la masse résiduelle. Leur formulation est basée sur l'hypothèse que le stock initial au début d'un événement pluvieux est nul, en supposant le lessivage totale des dépôts indépendamment des caractéristiques de la pluie. (Alley and Smith, 1981) ont repris la

formulation de (Sartor et al., 1974) et ils l'ont modifiée en ajoutant un paramètre supplémentaire. Les équations qu'ils ont proposées sont :

$$\frac{dM_a(t)}{dt} = D_{accu}S_{imp} - D_{ero}M_a(t) \quad (3)$$

$$M_a(DTS) = \frac{D_{accu}}{D_{ero}} S_{imp} [1 - e^{-D_{ero}DTS}] + M_r S_{imp} e^{-D_{ero}DTS} \quad (4)$$

Avec :  $M_a(DTS)$  est la masse des particules accumulées pendant la durée de temps sec DTS (Masse) ;  $D_{accu}$  est le taux d'accumulation (Masse.T<sup>-1</sup>) ;  $D_{ero}$  est le taux d'érosion (T<sup>-1</sup>) ;  $S_{imp}$  est la surface imperméable (L<sup>2</sup>) ;  $M_r$  est la masse résiduelle des particules de l'événement pluvieux précédent (Masse).

(Ball et al., 1998) ont établi plusieurs régressions entre la masse des polluants accumulée et la durée depuis le dernier événement de lessivage. Ils ont montré que les fonctions puissance et hyperbolique sont les plus appropriées pour déterminer le stock de sédiments. La fonction puissance décrit une tendance de la masse à augmenter avec le temps sec mais à un taux décroissant. Par contre, la fonction hyperbolique décrit une tendance asymptotique de la masse vers une valeur constante après une certaine durée, ce qui est plus en accord avec les résultats de (Sartor et al., 1974). La fonction puissance est aussi jugée la meilleure à représenter la relation entre la masse accumulée et la durée de temps sec selon l'étude menée par (Egodawatta et al., 2009). Elle est donnée par l'équation suivante :

$$M_a = aDTS^b \quad (5)$$

Avec :  $M_a$  est la masse accumulée pendant la durée DTS (Masse) ;  $DTS$  est la durée de temps sec ;  $a$  et  $b$  sont deux paramètres de à caler.

Les modèles qui simulent le processus d'accumulation s'appuient sur la durée de temps sec comme la variable explicative la plus importante, mais des chercheurs ont proposé des formulations qui incluent d'autres variables. (James and Shivalingaiyah, 1986), en se basant sur l'approche du bilan massique pour calculer la masse accumulée sur la surface. Ainsi, ils ont proposé une équation de flux massique dans laquelle ils ont calculé les masses déposées et éliminées en intégrant les sources de polluants anthropiques et naturelles. Les contributions des dépôts atmosphériques, des automobiles, de la dégradation des chaussées, ainsi que des sources naturelles ont tous été inclus dans leur modèle. Dans ce cas le processus d'accumulation est divisé en "accumulation positive" qui représente le dépôt et "accumulation

négative" qui représente les masses éliminées. Le taux d'accumulation réel disponible pour l'entraînement par le ruissellement est alors la différence entre les deux. Cependant, l'application de ce modèle n'est pas réaliste vu sa complexité et le fait qu'il intègre un très grand nombre de paramètres qui ne sont pas mesurés directement sur le site et qui nécessitent donc d'être calés.

### ➤ Discussion

Bien que des efforts soient faits pour quantifier les différentes composantes de l'accumulation, tous les modèles développés consistent en des formulations purement empiriques dans lesquelles l'accumulation est décrite en fonction de la période de temps sec. Cependant, s'appuyer sur la durée de temps sec comme la seule variable explicative qui domine les fractions de solides accumulées sur les surfaces n'est pas réaliste et son rôle dans le processus de production de pollution est remis en question (Charbeneau and Barrett, 1998). (Whipple Jr et al., 1977) ont critiqué fortement l'hypothèse de la dépendance entre la durée de temps sec et la masse accumulée des polluants, où les simulations de qualité qu'ils ont conduit ne concordent pas avec le postulat qui régit la relation entre les charges polluantes et le temps sec. Pareillement, (Bedient et al., 1978) ont considéré que l'effet de la durée de temps sec examiné sur les charges totales pour trois polluants sur deux sites différents est négligeable.

D'autre part, des larges incertitudes sont liées à l'estimation des paramètres d'accumulation dans ces modèles. (Kanso, 2004) ont trouvé que les paramètres d'accumulation  $D_{accu}$  et  $D_{ero}$  sont corrélés ce qui signifie que le modèle proposé par (Alley and Smith, 1981) est sur-paramétré. En plus des larges incertitudes sont liées à leurs valeurs estimées auxquelles le modèle n'est pas du tout sensible. (Dotto et al., 2011) sont arrivés aux mêmes conclusions pour le modèle asymptotique de (Sartor et al., 1974) où ils n'ont pas pu identifier des valeurs optimales pour les paramètres d'accumulation qui sont le stock maximal et le taux d'érosion.

Pour comprendre les raisons des lacunes des modèles usuels d'accumulation, il faut revoir comment les formulations sont dérivées. En fait, ces formulations doivent être calibrées pour chaque site. Les données à partir desquelles les modèles d'accumulation sont dérivés correspondent à des prélèvements « ponctuels » sur des positions précises qui ne sont pas soumises nécessairement aux mêmes conditions de turbulence que d'autres positions sur le

même bassin versant. Ainsi, elles ne peuvent pas être transposées sur une surface plus grande sans que cela n'engendre des problèmes de non-représentativité.

La variabilité du processus d'accumulation au sein du même bassin versant est très forte. L'étude de (Deletic and Orr, 2005) donne un bon exemple à ce sujet en montrant des différences significatives dans les charges accumulées en termes de quantité de stock et en termes de distribution des tailles de particules sur une distance inférieure à 10 mètres. (Wijesiri et al., 2015a) ont montré que la variabilité de l'accumulation pour la même occupation de sol est contrôlée par le comportement des particules, dépendant de leurs tailles. Ils ont trouvé que la fraction des particules ayant un diamètre  $< 150\mu\text{m}$  diminue pendant le temps sec alors que la fraction des particules ayant un diamètre  $> 150\mu\text{m}$  augmente. L'application du modèle puissance proposé par (Ball et al., 1998) pour simuler ces comportements n'est vérifiée que pour les particules  $> 150\mu\text{m}$ . La fraction fine a aussi une plus grande influence sur la variabilité du processus d'accumulation des polluants que la fraction grossière. Ces informations sont négligées dans les approches de modélisation de l'accumulation bien qu'elles doivent être prises en compte puisque le processus d'accumulation est un processus dynamique. Les particules qui sont accumulées sur les surfaces peuvent subir une redistribution en fonction de leur position, qui détermine à quel degré elles sont affectées par le trafic (Patra et al., 2008) et le balayage des chaussées (Vaze and Chiew, 2002) et en fonction des conditions météorologiques en temps sec et notamment du vent (Shao, 2008). Les processus de redistribution qui incluent la remise en suspension, l'agrégation, et la fragmentation, modifient la distribution des tailles des particules et par suite le comportement de ces particules pendant le temps sec et pendant le temps de pluie. De plus, dans la plupart des études de modélisation, il n'est généralement pas possible de mesurer directement l'accumulation des constituants de la qualité de l'eau sur un bassin hydrographique urbain. Par conséquent, l'accumulation des constituants et la charge initiale du bassin hydrographique sont déduites de la quantité qui est emportée par les eaux de ruissellement. Ceci implique que le stock modélisé est sous-estimé comme les particules entraînées sont en majorité des particules fines (Hong et al., 2016a).

La variabilité de l'accumulation dépend aussi de l'occupation de sol. Les concentrations des polluants rapportées par (Göbel et al., 2007) sont plus élevées pour les



chaussées et les parkings que pour les toitures à l'exception du cuivre et du zinc. (Egodawatta et al., 2009) ont aussi trouvé que les charges de particules recueillies sur les toitures sont significativement moindres par rapport à celles collectées sur les chaussées en plus elles ont plus fines. Ceci montre que l'application d'une seule formulation d'accumulation sans tenir compte de ces hétérogénéités va induire des erreurs dans l'estimation du stock et par suite dans les sorties des modèles à l'exutoire.

Pour tenir compte de toutes ces sources d'incertitude qui résultent de la variabilité du processus d'accumulation, (Charbeneau and Barrett, 1998) ont proposé de modéliser le stock initial comme une variable aléatoire logarithmique normalement distribuée. Les modèles probabilistes de la qualité des eaux de ruissellement qui sont développés tiennent compte partiellement de cette variabilité, en transformant les distributions probabilistes des précipitations en distributions de polluants (Chen and Adams, 2007; Osman Akan A., 1988). Dans certains modèles, l'accumulation n'est pas prise en compte en supposant qu'il existe un stock infini de polluant sur la surface (Escrig et al., 2011; Hong et al., 2016a).

### 3.3.2.2. Modélisation du lessivage

Les modèles les plus couramment utilisés pour calculer la charge transférée par le ruissellement sur les surfaces urbaines sont dérivés de la formulation de fonction exponentielle. Cette fonction estime la concentration décroissante de polluants accumulés durant le temps sec en fonction du temps qui s'est écoulé depuis le début de l'événement pluvieux. L'une des premières formulations de lessivage a été proposée par (Sartor et al., 1974) en se basant sur les résultats expérimentaux qu'ils ont obtenus. Leur formulation suppose que le taux de lessivage des particules est proportionnel au produit de la masse disponible des dépôts et l'intensité de pluie. Elle est donnée par les expressions suivantes :

$$\frac{dM_a(t)}{dt} = -K_w i(t) M_a(t) \quad (6)$$

$$M_{err}(t) = M_0 (1 - e^{-K_w i(t)t}) \quad (7)$$

Avec :  $M_a(t)$  est la masse de solides déposée à l'instant  $t$  (Masse);  $K_w$  est le coefficient de lessivage ;  $i(t)$  est l'intensité de pluie (mm.T-1) ;  $M_{err}(t)$  est la masse érodée par le ruissellement à l'instant  $t$  (Masse/m<sup>2</sup>) ;  $M_0$  est la masse de dépôt disponible initiale (Masse/ m<sup>2</sup>).

Différentes études ont adopté ce même concept mais ils ont introduit quelques ajustements sur sa formulation. (Alley and Smith, 1981) ont modifié ce modèle en supposant que le taux de ruissellement est plus important que l'intensité de pluie comme une variable explicative, ainsi ils ont simulé le lessivage avec la formulation suivante :

$$M_{err}(t) = M_0(1 - e^{-K_w r(t)t}) \quad (8)$$

Avec :  $r(t)$  est le taux de ruissellement ( $\text{mm.T}^{-1}$ ).

(Chen and Adams, 2006) ont considéré que les caractéristiques du ruissellement ont une plus grande influence sur le lessivage et du coup ils ont substitué l'intensité de pluie par le volume de ruissellement dans le modèle de (Sartor et al., 1974). (Barbé et al., 1996) se sont aussi basés sur le volume ruisselé pour calculer la masse lessivée selon une fonction puissance donnée par :

$$M_{err}(t) = k_w v(t)^\alpha \quad (9)$$

Avec :  $v(t)$  est le volume ruisselé à l'instant  $t$  ;  $\alpha$  est l'exposant de lessivage.

Le modèle de lessivage proposé par (Sartor et al., 1974) suppose que tous les dépôts sur la surface peuvent être lessivés si l'événement dure assez longtemps. Cependant, (Egodawatta et al., 2007) ont trouvé que ce principe n'est pas correct comme leurs résultats expérimentaux ont bien montré que seulement une fraction est entraînée par le ruissellement et que celle-ci dépend de l'intensité de la pluie. Par conséquent, ils ont introduit un coefficient de capacité dénoté  $C_F$  dont la valeur dépend de l'intensité de l'événement pluvieux et ils ont remplacé la masse lessivée par la « fraction lessivée »  $F_w$  qui est le rapport entre la masse lessivée et la masse disponible initiale. Le modèle qui en résulte est alors donné par :

$$F_w = \frac{M_{err}(t)}{M_0} = C_F(1 - e^{-K_w i(t)}) \quad (10)$$

En addition aux formulations exponentielle et puissance, le lessivage peut être modélisé avec de formulation de type « rating curve » qui permet d'estimer le transport des particules en fonction du taux de ruissellement. Ce modèle est implémenté dans SWMM (Rossman, 2010). Il intègre deux paramètres  $C_1$  et  $C_2$ , et il est donné par l'équation suivante :

$$M_{err}(t) = M_0 C_1 Q^{C_2} \quad (11)$$

Avec :  $C_1$  est le coefficient de lessivage ;  $C_2$  est l'exposant de lessivage ;  $Q$  est le taux de ruissellement ( $\text{mm.T}^{-1}$ ).

Bien que le modèle exponentiel soit le plus utilisé pour simuler le lessivage, et qui est incorporé dans plusieurs logiciels hydrologiques (SWMM, MUSIC, CANOE, FLUPOL, STORM...) certains chercheurs ont tenté de mettre au point des modèles physiques fondés sur la simulation des mécanismes d'érosion. (Akan A. Osman, 1987) ont développé un modèle d'érosion qui décrit le lessivage sous l'action de l'écoulement sur la surface où le taux de détachement des polluants est supposé proportionnel à la contrainte de cisaillement du ruissellement et à la masse de polluant initial disponible sur la surface. L'impact des gouttes de pluie dans ce modèle est négligé. (Tomanovic and Maksimovic, 1996) ont proposé un modèle d'érosion qui tient compte de l'énergie cinétique des gouttes de pluie en addition à la contrainte de cisaillement de ruissellement pour modéliser l'entraînement des dépôts, tout en supposant qu'aucune sédimentation ne peut se produire pendant le transport des solides vers les avaloirs. Dans une étude plus récente, (Shaw et al., 2006) ont développé un modèle d'érosion dans lequel les particules sont arrachées de la surface uniquement sous l'action des gouttes de pluie et transportées latéralement par le ruissellement tout en tenant compte de leur re-déposition. L'équation qui décrit le détachement des particules est proposée par (Lisle et al., 1998) alors que le mécanisme de dépôt est adapté de (Hairsine and Rose, 1991). Les équations de Hairsine-Rose sont aussi adaptées dans une étude récente par (Hong et al., 2016a) qui ont décrit en détail le mécanisme d'érosion en modélisant les deux processus d'érosion ainsi que le processus de dépôt.

### ➤ Discussion

Les formulations de lessivage qui sont utilisées dans la plupart des modèles existants sont des formulations conceptuelles basées sur la description exponentielle de la dynamique de transport des polluants par le ruissellement qui contiennent au moins un paramètre qui n'a pas de sens physique. Les limitations de ce modèle sont bien décrites par (Duncan, 1995). En fait, il explique que le modèle exponentiel basé sur l'intensité de la pluie comme variable explicative ne peut pas simuler les pics de concentrations qui peuvent apparaître à n'importe quel moment de l'événement pluvieux à part les pics qui apparaissent au début, ce qui a aussi été noté précédemment par (Alley, 1981). Ainsi, la proportionnalité entre l'intensité de pluie et les concentrations simulées n'est pas conservée ; même s'il y a une augmentation dans la masse de polluant véhiculée, la concentration simulée conservera un taux décroissant. Cela montre que l'effet de l'intensité de pluie n'est pas bien pris en compte dans cette formule. Pour

surmonter cette limitation, le taux de ruissellement a été utilisé comme la variable explicative dans une fonction puissance pour décrire le lessivage (Huber et al., 1988). Cependant, selon (Duncan, 1995) ces variables sont corrélées, ce qui fait qu'il est très difficile d'évaluer l'effet de chaque facteur.

Le lessivage dans les modèles conceptuels est souvent représenté comme étant « limité à la source » c.à.d que l'épuisement du stock disponible sur la surface entraîne la fin du lessivage. En se basant sur ce concept, si un événement pluvieux dure suffisamment sous une intensité convenable, il est capable à transporter la totalité du stock dont l'accumulation avant l'événement suivant repart de zéro (Alley, 1981; Rossman, 2010). Cependant, différentes études ont montré que seulement une fraction du stock est entraînée durant un événement pluvieux (Vaze and Chiew, 2002; Zhao et al., 2010) ce qui suggère que la masse dans ce cas n'est pas un facteur limitant pour le lessivage mais que c'est plutôt la capacité de transport du ruissellement. Néanmoins, (Sheng et al., 2008) ont montré que le lessivage « limité à la source » prédomine le lessivage « limité par le transport » à l'issue de la classification de 42 événements. Ils ont trouvé que les événements de premier flot sont « limités à la source » alors que les événements où la masse varie linéairement avec le volume ruisselé sont « limités par le transport ». Cela a été confirmé par (H. Zhao et al., 2016) qui ont traité cette question en caractérisant les stocks présents sur la surface et la masse lessivée. Ils ont trouvé notamment que le processus de lessivage en réalité n'est qu'une combinaison entre les deux facteurs qui dépendent de la durée et l'intensité de l'événement ainsi que la distribution de taille des particules présentes dans le stock. Ainsi ils ont montré que le lessivage des particules fines et pendant les longs événements est « limité à la source » alors que le lessivage des particules grossières et pendant les événements courts est « limité par le transport ». Ces points de vue contradictoires soulignent le fait que le concept de lessivage est très complexe et variable et que cela est mal représenté dans les modèles conceptuels actuels. La mauvaise compréhension des facteurs qui interviennent dans le processus de lessivage freine l'objectif de développer un modèle simple qui reproduit correctement ce qui se passe pendant un événement pluvieux.

Les lacunes des modèles conceptuels n'ont pas empêché leur diffusion, mais elles ont incité certains chercheurs à proposer des améliorations ou des alternatives.

Pour avoir de meilleures estimations des pollutogrammes et des charges mobilisées pendant un événement pluvieux, plusieurs chercheurs ont eu recours aux lois physiques pour décrire le lessivage. Ainsi le lessivage a été présenté comme étant le transport des particules qui se retrouvent dans l'écoulement suite à l'équilibre qui a lieu entre les particules qui se détachent sous les impacts des gouttes de pluie et la contrainte de cisaillement de l'écoulement et les particules qui se déposent sur la surface (Duncan, 1995). L'application de ce principe varie d'une étude à l'autre où certains indiquent que le détachement par l'énergie cinétique est la force motrice d'arrachement des particules (Shaw et al., 2006) alors que d'autres ne prennent en compte que le détachement par l'énergie de l'écoulement (Akan A. Osman, 1987). Le mécanisme de dépôt n'est pas aussi considéré dans certains modèles physiques (Deletic et al., 1997). Cela montre qu'il n'y a pas un accord général sur un modèle global pour décrire la physique du processus de lessivage. (Akan, 1987) ont même conclu qu'il n'est pas possible de parvenir à un modèle opérationnel exhaustif strictement basé sur la physique. Par exemple, le modèle d'érosion proposé par (Shaw et al., 2006) et par (Hong et al., 2016a) basé sur les équations de (Hairsine and Rose, 1991) contient un paramètre qui est le coefficient de détachement qui n'a pas de signification physique : il est déterminé soit par l'expérimentation soit par calage. Les prédictions obtenues par les modèles physiques quand elles sont confrontées aux mesures, elles ne sont pas très satisfaisantes. (Shaw et al., 2006) ont trouvé que leur modèle appliqué sur un canal expérimental sous-estime la masse érodée pour les faibles valeurs et surestime les valeurs plus élevées. La comparaison entre les pollutogrammes de MES mesurés et simulés pour un petit bassin urbain routier en se basant sur les critères de Nash et de RMSE par (Hong et al., 2016a) montre une performance limitée du modèle avec des déviations importantes des valeurs simulées par rapport aux valeurs mesurées. Ces résultats remettent en question la capacité des modèles physiques à substituer les modèles conceptuels pour avoir une meilleure estimation de la contamination en temps de pluie. La représentation du lessivage dans les modèles physiques est sans doute améliorée en terme de description des processus cependant l'application de ces modèles pour des cas réels étendus se révèle limitée. Premièrement, la mise en œuvre des modèles physiques nécessite une base de données énorme pour estimer leurs paramètres qui peuvent être mesurés directement sur le site ou bien calés et qui engendrent aussi des larges incertitudes (Merritt et al., 2003). En second temps, l'application d'équations physiques validées pour des surfaces élémentaires sur des bassins

versants plus larges manque de justification et a été mise en question (Merritt et al., 2003). Les coûts temporels et financiers pour utiliser les modèles physiques d'érosion présentent une limitation majeure pour leur application en dehors de l'objectif de recherche.

(Wijesiri et al., 2015b) ont proposé d'améliorer la modélisation conceptuelle du lessivage et ceci en tenant compte de la variabilité de lessivage qui est liée à la taille des particules. Ainsi, ils ont distingué la dynamique de lessivage des particules  $< 150\mu\text{m}$  et des particules  $> 150\mu\text{m}$  et ceci en attribuant à chaque classe de particule des valeurs différentes pour les paramètres du modèle de lessivage exponentiel. Cette méthodologie a réussi à prédire les masses totales lessivées pour les différents événements pluvieux qui ont été simulés. Cependant, une question se pose sur l'application de cette méthodologie à grande échelle, pour des événements pluvieux réels. La distinction de différents seuils selon lesquels les particules sont réparties dans les différentes classes de taille pour les événements réels n'est pas facile (Hong et al., 2016b) et la paramétrisation pour chaque fraction de particule entraînera une sur-paramétrisation et des incertitudes.

### 3.4. Conclusion

La contamination diffuse des eaux de ruissellement en milieu urbain par les substances toxiques représente une menace qui ne cesse de croître sur les écosystèmes. L'état actuel des connaissances sur les processus qui gouvernent la génération et le transfert de la pollution dans le ruissellement vers les milieux récepteurs est loin d'être suffisant. Les processus montrent une variabilité importante à différentes échelles et cela se reflète en une mauvaise performance des modèles de qualité des eaux urbaines qui souffrent des grosses lacunes en termes de prédiction des flux de polluants véhiculés vers les milieux récepteurs.

Il est ainsi nécessaire de définir une stratégie qui permet de répondre aux questions relatives à la compréhension des processus d'accumulation et de lessivage et à l'approche de modélisation à adopter tout en tenant compte de besoins, des données disponibles et des objectifs à atteindre.

### 3.5. Références

- Ackerman, D., Schiff, K., 2003. Modeling storm water mass emissions to the Southern California Bight. *J. Environ. Eng.* 129, 308–317.
- Akan, A.O., 1988. Derived Frequency Distribution for Storm Runoff Pollution. *J. Environ. Eng.* 114, 1344–1351. [https://doi.org/10.1061/\(ASCE\)0733-9372\(1988\)114:6\(1344\)](https://doi.org/10.1061/(ASCE)0733-9372(1988)114:6(1344))
- Akan, A.O., 1987. Pollutant Washoff by Overland Flow. *J. Environ. Eng.* 113, 811–823. [https://doi.org/10.1061/\(ASCE\)0733-9372\(1987\)113:4\(811\)](https://doi.org/10.1061/(ASCE)0733-9372(1987)113:4(811))
- Alley, W., Smith, P., 1981. Estimation of Accumulation Parameters for Urban Runoff Quality Modeling. *WATER Resour. Res.* 17, 1657–1664.
- Alley, W.M., 1981. Estimation of impervious-area Washoff Parameters. *Water Resour. Res.* 17, 1161–1166. <https://doi.org/10.1029/WR017i004p01161>
- Alloway, B., Ayres, D.C., 1997. *Chemical Principles of Environmental Pollution*, Second Edition. CRC Press.
- Amato, F., Pandolfi, M., Moreno, T., Furger, M., Pey, J., Alastuey, A., Bukowiecki, N., Prevot, A.S.H., Baltensperger, U., Querol, X., 2011. Sources and variability of inhalable road dust particles in three European cities. *Atmos. Environ.* 45, 6777–6787. <https://doi.org/10.1016/j.atmosenv.2011.06.003>
- Andral, M.C., Roger, S., Montréjaud-Vignoles, M., Herremans, L., 1999. Particle Size Distribution and Hydrodynamic Characteristics of Solid Matter Carried by Runoff from Motorways. *Water Environ. Res.* 71, 398–407. <https://doi.org/10.2307/25045232>
- Arnold, C.L., Gibbons, C.J., 1996. Impervious Surface Coverage: The Emergence of a Key Environmental Indicator. *J. Am. Plann. Assoc.* 62, 243–258. <https://doi.org/10.1080/01944369608975688>
- Ball, J.E., Jenks, R., Aubourg, D., 1998. An assessment of the availability of pollutant constituents on road surfaces. *Sci. Total Environ.* 209, 243–254. [https://doi.org/10.1016/S0048-9697\(98\)80115-0](https://doi.org/10.1016/S0048-9697(98)80115-0)
- Bannerman, R.T., Owens, D.W., Dodds, R.B., Hornewer, N.J., 1993. Sources of pollutants in Wisconsin stormwater. *Water Sci. Technol.* 28, 241–259.
- Barbé, D.E., Cruise, J.F., Mo, X., 1996. Modeling the Buildup and Washoff of Pollutants on Urban Watersheds1. *JAWRA J. Am. Water Resour. Assoc.* 32, 511–519. <https://doi.org/10.1111/j.1752-1688.1996.tb04049.x>
- Barrett Michael E., Irish Lyn B., Malina Joseph F., Charbeneau Randall J., 1998. Characterization of Highway Runoff in Austin, Texas, Area. *J. Environ. Eng.* 124, 131–137. [https://doi.org/10.1061/\(ASCE\)0733-9372\(1998\)124:2\(131\)](https://doi.org/10.1061/(ASCE)0733-9372(1998)124:2(131))
- Barron, O.V., Barr, A.D., Donn, M.J., 2013. Effect of urbanisation on the water balance of a catchment with shallow groundwater. *J. Hydrol.* 485, 162–176. <https://doi.org/10.1016/j.jhydrol.2012.04.027>

Bechet, B., Bonhomme, C., Lamprea, K., Campos, E., Jean Soro, L., Dubois, P., Lherm, D., 2015. Towards a modeling of traffic pollutant flux at local scale – Chemical analysis and micro-characterization of road dusts. Urban Proc. Environ. Symp.

Bedient, P.B., Characklis, W.G., Harned, D.A., 1978. Stormwater Analysis and Prediction in Houston. J. Environ. Eng. Div. 104, 1087–1100.

Berbee, R., Rijs, G., de Brouwer, R., van Velzen, L., 1999. Characterization and Treatment of Runoff from Highways in the Netherlands Paved with Impervious and Pervious Asphalt. Water Environ. Res. 71, 183–190. <https://doi.org/10.2175/106143098X121914>

Berretta, C., Gnecco, I., Lanza, L.G., Barbera, P.L., 2007. An investigation of wash-off controlling parameters at urban and commercial monitoring sites. Water Sci. Technol. 56, 77–84. <https://doi.org/10.2166/wst.2007.756>

Bomboi, M.T., Hernández, A., 1991. Hydrocarbons in urban runoff: Their contribution to the wastewaters. Water Res. 25, 557–565. [https://doi.org/10.1016/0043-1354\(91\)90128-D](https://doi.org/10.1016/0043-1354(91)90128-D)

Bonan, G.B., 2008. Ecological climatology: concepts and applications, 2nd ed. ed. Cambridge University Press, Cambridge ; New York.

Brabec, E., Schulte, S., Richards, P.L., 2002. Impervious Surfaces and Water Quality: A Review of Current Literature and Its Implications for Watershed Planning. CPL Bibliogr. 16, 499–514. <https://doi.org/10.1177/088541202400903563>

Bradl, H.B., 2004. Adsorption of heavy metal ions on soils and soils constituents. J. Colloid Interface Sci. 277, 1–18. <https://doi.org/10.1016/j.jcis.2004.04.005>

Bressy, A., Gromaire, M.-C., Lorgeoux, C., Saad, M., Leroy, F., Chebbo, G., 2012. Towards the determination of an optimal scale for stormwater quality management: Micropollutants in a small residential catchment. Water Res., Special Issue on Stormwater in urban areas 46, 6799–6810. <https://doi.org/10.1016/j.watres.2011.12.017>

Brinkmann, W.L.F., 1985. Urban stormwater pollutants: Sources and loadings. GeoJournal 11, 277–283. <https://doi.org/10.1007/BF00186341>

Brown, J.N., Peake, B.M., 2006. Sources of heavy metals and polycyclic aromatic hydrocarbons in urban stormwater runoff. Sci. Total Environ. 359, 145–155. <https://doi.org/10.1016/j.scitotenv.2005.05.016>

Bukowiecki, N., Lienemann, P., Hill, M., Furger, M., Richard, A., Amato, F., Prévôt, A.S.H., Baltensperger, U., Buchmann, B., Gehrig, R., 2010. PM10 emission factors for non-exhaust particles generated by road traffic in an urban street canyon and along a freeway in Switzerland. Atmos. Environ. 44, 2330–2340. <https://doi.org/10.1016/j.atmosenv.2010.03.039>

Burges Stephen J., Wigmosta Mark S., Meena Jack M., 1998. Hydrological Effects of Land-Use Change in a Zero-Order Catchment. J. Hydrol. Eng. 3, 86–97. [https://doi.org/10.1061/\(ASCE\)1084-0699\(1998\)3:2\(86\)](https://doi.org/10.1061/(ASCE)1084-0699(1998)3:2(86))

Carle, M.V., Halpin, P.N., Stow, C.A., 2005. Patterns of Watershed Urbanization and Impacts on Water Quality1. JAWRA J. Am. Water Resour. Assoc. 41, 693–708. <https://doi.org/10.1111/j.1752-1688.2005.tb03764.x>



Characklis, G.W., Wiesner, M.R., 1997. Particles, Metals, and Water Quality in Runoff from Large Urban Watershed. *J. Environ. Eng.* 123, 753–759. [https://doi.org/10.1061/\(ASCE\)0733-9372\(1997\)123:8\(753\)](https://doi.org/10.1061/(ASCE)0733-9372(1997)123:8(753))

Charbeneau, R.J., Barrett, M.E., 1998. Evaluation of methods for estimating stormwater pollutant loads. *Water Environ. Res.* 70, 1295–1302.

Charters, F.J., Cochrane, T.A., O’Sullivan, A.D., 2015. Particle size distribution variance in untreated urban runoff and its implication on treatment selection. *Water Res.* 85, 337–345. <https://doi.org/10.1016/j.watres.2015.08.029>

Chen, J., Adams, B.J., 2007. A derived probability distribution approach to stormwater quality modeling. *Adv. Water Resour.* 30, 80–100. <https://doi.org/10.1016/j.advwatres.2006.02.006>

Chen, J., Adams, B.J., 2006. A framework for urban storm water modeling and control analysis with analytical models: URBAN STORM WATER MODELING. *Water Resour. Res.* 42, n/a-n/a. <https://doi.org/10.1029/2005WR004540>

Chen Jieyun, Adams Barry J., 2006. Analytical Urban Storm Water Quality Models Based on Pollutant Buildup and Washoff Processes. *J. Environ. Eng.* 132, 1314–1330. [https://doi.org/10.1061/\(ASCE\)0733-9372\(2006\)132:10\(1314\)](https://doi.org/10.1061/(ASCE)0733-9372(2006)132:10(1314))

Chocat, B., 1997. Le rôle possible de l’urbanisation dans l’aggravation du risque d’inondation : l’exemple de l’Yseron à Lyon / The potential role of urbanization in increasing the risk of flooding : the example of the Yzeron in Lyon. *Rev. Géographie Lyon* 72, 273–280. <https://doi.org/10.3406/geoca.1997.4707>

Chui, P.C., 1997. Characteristics of Stormwater Quality from Two Urban Watersheds in Singapore. *Environ. Monit. Assess.* 44, 173–181. <https://doi.org/10.1023/A:1005776321684>

Dassenakis, M., Scoullou, M., Foufa, E., Krasakopoulou, E., Pavlidou, A., Kloukiniotou, M., 1998. Effects of multiple source pollution on a small Mediterranean river. *Appl. Geochem.* 13, 197–211. [https://doi.org/10.1016/S0883-2927\(97\)00065-6](https://doi.org/10.1016/S0883-2927(97)00065-6)

Datry, T., Malard, F., Vitry, L., Hervant, F., Gibert, J., 2003. Solute dynamics in the bed sediments of a stormwater infiltration basin. *J. Hydrol.* 273, 217–233. [https://doi.org/10.1016/S0022-1694\(02\)00388-8](https://doi.org/10.1016/S0022-1694(02)00388-8)

Davis, A.P., Shokouhian, M., Ni, S., 2001. Loading estimates of lead, copper, cadmium, and zinc in urban runoff from specific sources. *Chemosphere* 44, 997–1009. [https://doi.org/10.1016/S0045-6535\(00\)00561-0](https://doi.org/10.1016/S0045-6535(00)00561-0)

Deletic, A., Maksimovic, C., Ivetic, M., 1997. Modelling of storm wash-off of suspended solids from impervious surfaces. *J. Hydraul. Res.* 35, 99–118. <https://doi.org/10.1080/00221689709498646>

Deletic, A., Orr, D.W., 2005. Pollution Buildup on Road Surfaces. *J. Environ. Eng.* 131, 49–59. [https://doi.org/10.1061/\(ASCE\)0733-9372\(2005\)131:1\(49\)](https://doi.org/10.1061/(ASCE)0733-9372(2005)131:1(49))

Deletic, A.B., Maksimovic, C.T., 1998. Evaluation of Water Quality Factors in Storm Runoff from Paved Areas. *J. Environ. Eng.* 124, 869–879. [https://doi.org/10.1061/\(ASCE\)0733-9372\(1998\)124:9\(869\)](https://doi.org/10.1061/(ASCE)0733-9372(1998)124:9(869))

Desbordes, M., Deutsch, J.C., Hemain, J.C., 1980. Urban runoff pollution in France: a national programme. *Proc. Hels. Symp.* 29–36.

Desbordes, M.M., Bachoc, A., Tabuchi, J.P., Chebbo, G., Philippe, J.P., 1994. La pollution des rejets urbains par temps de pluie: quantité, origine et nature. *Houille Blanche* 21–33.

Dotto, C.B.S., Kleidorfer, M., Deletic, A., Rauch, W., McCarthy, D.T., Fletcher, T.D., 2011. Performance and sensitivity analysis of stormwater models using a Bayesian approach and long-term high resolution data. *Environ. Model. Softw.* 26, 1225–1239. <https://doi.org/10.1016/j.envsoft.2011.03.013>

Drapper, D., Tomlinson, R., Williams, P., 2000. Pollutant concentrations in road runoff: Southeast Queensland case study. *J. Environ. Eng.* 126, 313–320.

Duncan, H., 1995. A review of urban stormwater quality processes.

Dunne, T., Leopold, L.B., 1978. *Water in environmental planning*. Macmillan.

Duong, T.T.T., Lee, B.-K., 2011. Determining contamination level of heavy metals in road dust from busy traffic areas with different characteristics. *J. Environ. Manage.* 92, 554–562. <https://doi.org/10.1016/j.jenvman.2010.09.010>

Duong, T.T.T., Lee, B.-K., 2009. Partitioning and mobility behavior of metals in road dusts from national-scale industrial areas in Korea. *Atmos. Environ.* 43, 3502–3509. <https://doi.org/10.1016/j.atmosenv.2009.04.036>

Egodawatta, P., Goonetilleke, A., 2007. Characteristics of pollution build-up on residential road surfaces, in: Piasecki, M., Wang, S., Holz, K., Kawahara, M., Gonzalez, A., Beran, B. (Eds.), *7th International Conference on Hydrosience and Engineering*. Drexel University, Drexel University, Philadelphia.

Egodawatta, P., Thomas, E., Goonetilleke, A., 2009. Understanding the physical processes of pollutant build-up and wash-off on roof surfaces. *Sci. Total Environ.* 407, 1834–1841. <https://doi.org/10.1016/j.scitotenv.2008.12.027>

Egodawatta, P., Thomas, E., Goonetilleke, A., 2007. Mathematical interpretation of pollutant wash-off from urban road surfaces using simulated rainfall. *Water Res.* 41, 3025–3031. <https://doi.org/10.1016/j.watres.2007.03.037>

El Haddad, I., Marchand, N., Dron, J., Temime-Roussel, B., Quivet, E., Wortham, H., Jaffrezo, J.L., Baduel, C., Voisin, D., Besombes, J.L., Gille, G., 2009. Comprehensive primary particulate organic characterization of vehicular exhaust emissions in France. *Atmos. Environ.* 43, 6190–6198. <https://doi.org/10.1016/j.atmosenv.2009.09.001>

Ellis, J.B., Mitchell, G., 2006. Urban diffuse pollution: key data information approaches for the Water Framework Directive. *Water Environ. J.* 20, 19–26. <https://doi.org/10.1111/j.1747-6593.2006.00025.x>

Ellison, W.D., 1945. Some effects of raindrops and surface-flow on soil erosion and infiltration. *Eos Trans. Am. Geophys. Union* 26, 415–429.

EPA, 1993. Urban runoff pollution prevention and control planning., Handbook. U.S. Environmental Protection Agency, Cincinnati, OH.

Escrig, A., Amato, F., Pandolfi, M., Monfort, E., Querol, X., Celades, I., Sanf elix, V., Alastuey, A., Orza, J.A.G., 2011. Simple estimates of vehicle-induced resuspension rates. *J. Environ. Manage.* 92, 2855–2859. <https://doi.org/10.1016/j.jenvman.2011.06.042>

Fallah Shorshani, M., 2014. Mod elisation de l’impact du trafic routier sur la pollution de l’air et des eaux de ruissellement. Paris Est.

Foster, G.R., 1990. Process-based modelling of soil erosion by water on agricultural land., in: *Soil Erosion on Agricultural Land. Proceedings of a Workshop Sponsored by the British Geomorphological Research Group, Coventry, UK, January 1989.* John Wiley & Sons Ltd., pp. 429–445.

Gasperi, J., Sebastian, C., Ruban, V., Delamain, M., Percot, S., Wiest, L., Mirande, C., Caupos, E., Demare, D., Kessoo, M.D.K., Saad, M., Schwartz, J.J., Dubois, P., Fratta, C., Wolff, H., Moilleron, R., Chebbo, G., Cren, C., Millet, M., Barraud, S., Gromaire, M.C., 2014. Micropollutants in urban stormwater: occurrence, concentrations, and atmospheric contributions for a wide range of contaminants in three French catchments. *Environ. Sci. Pollut. Res.* 21, 5267–5281. <https://doi.org/10.1007/s11356-013-2396-0>

German, J., Svensson, G., 2002. Metal content and particle size distribution of street sediments and street sweeping waste. *Water Sci. Technol.* 46, 191–198.

Gim enez, R., Govers, G., 2002. Flow Detachment by Concentrated Flow on Smooth and Irregular Beds. *Soil Sci. Soc. Am. J.* 66, 1475–1483. <https://doi.org/10.2136/sssaj2002.1475>

G obel, P., Dierkes, C., Coldewey, W.G., 2007. Storm water runoff concentration matrix for urban areas. *J. Contam. Hydrol.* 91, 26–42. <https://doi.org/10.1016/j.jconhyd.2006.08.008>

Goldman, S.J., Jackson, K., 1986. EROSION AND SEDIMENT CONTROL HANDBOOK.

Goonetilleke, A., Thomas, E., Ginn, S., Gilbert, D., 2005. Understanding the role of land use in urban stormwater quality management. *J. Environ. Manage.* 74, 31–42. <https://doi.org/10.1016/j.jenvman.2004.08.006>

Gromaire, M.-C., 1998. La pollution des eaux pluviales urbaines en r seau d’assainissement unitaire. Caract ristiques et origines. Ecole des Ponts ParisTech, France.

Gromaire-Mertz, M.C., Garnaud, S., Gonzalez, A., Chebbo, G., 1999. Characterisation of urban runoff pollution in Paris. *Water Sci. Technol., Innovative Technologies in Urban Storm Drainage 1998 (Novatech ’98)* 39, 1–8. [https://doi.org/10.1016/S0273-1223\(99\)00002-5](https://doi.org/10.1016/S0273-1223(99)00002-5)

Guo, H., Hu, Q., Jiang, T., 2008. Annual and seasonal streamflow responses to climate and land-cover changes in the Poyang Lake basin, China. *J. Hydrol.* 355, 106–122. <https://doi.org/10.1016/j.jhydrol.2008.03.020>

Haase, D., 2009. Effects of urbanisation on the water balance – A long-term trajectory. *Environ. Impact Assess. Rev.* 29, 211–219. <https://doi.org/10.1016/j.eiar.2009.01.002>

Hairsine, P.B., Rose, C.W., 1992a. Modeling water erosion due to overland flow using physical principles: 1. Sheet flow. *Water Resour. Res.* 28, 237–243. <https://doi.org/10.1029/91WR02380>

Hairsine, P.B., Rose, C.W., 1992b. Modeling water erosion due to overland flow using physical principles: 2. Rill flow. *Water Resour. Res.* 28, 245–250. <https://doi.org/10.1029/91WR02381>

Hairsine, P.B., Rose, C.W., 1991. Rainfall detachment and deposition: sediment transport in the absence of flow-driven processes. *Soil Sci. Soc. Am. J.* 55, 320–324.

Hall, K.J., Anderson, B.C., 1988. The toxicity and chemical composition of urban stormwater runoff. *Can. J. Civ. Eng.* 15, 98–106. <https://doi.org/10.1139/188-011>

Hall, M.J., Ellis, J.B., 1985. Water quality problems of urban areas. *GeoJournal* 11, 265–275. <https://doi.org/10.1007/BF00186340>

Hatt, B.E., Fletcher, T.D., Walsh, C.J., Taylor, S.L., 2004. The influence of urban density and drainage infrastructure on the concentrations and loads of pollutants in small streams. *Environ. Manage.* 34, 112–124. <https://doi.org/10.1007/s00267-004-0221-8>

Hawley, R.J., Bledsoe, B.P., 2011. How do flow peaks and durations change in suburbanizing semi-arid watersheds? A southern California case study. *J. Hydrol.* 405, 69–82. <https://doi.org/10.1016/j.jhydrol.2011.05.011>

Heberer, T., 2002. Occurrence, fate, and removal of pharmaceutical residues in the aquatic environment: a review of recent research data. *Toxicol. Lett.* 131, 5–17. [https://doi.org/10.1016/S0378-4274\(02\)00041-3](https://doi.org/10.1016/S0378-4274(02)00041-3)

Herngren, L., Goonetilleke, A., Ayoko, G.A., 2006. Analysis of heavy metals in road-deposited sediments. *Anal. Chim. Acta* 571, 270–278. <https://doi.org/10.1016/j.aca.2006.04.064>

Herngren, L., Goonetilleke, A., Ayoko, G.A., 2005. Understanding heavy metal and suspended solids relationships in urban stormwater using simulated rainfall. *J. Environ. Manage.* 76, 149–158. <https://doi.org/10.1016/j.jenvman.2005.01.013>

Herngren, L., Goonetilleke, A., Ayoko, G.A., Mostert, M.M.M., 2010. Distribution of polycyclic aromatic hydrocarbons in urban stormwater in Queensland, Australia. *Environ. Pollut.* 158, 2848–2856. <https://doi.org/10.1016/j.envpol.2010.06.015>

Hoffman, E.J., Latimer, J.S., Hunt, C.D., Mills, G.L., Quinn, J.G., 1985. Stormwater runoff from highways. *Water. Air. Soil Pollut.* 25, 349–364. <https://doi.org/10.1007/BF00283788>

Hoffman, E.J., Latimer, J.S., Mills, G.L., Quinn, J.G., 1982. Petroleum Hydrocarbons in Urban Runoff from a Commercial Land Use Area. *J. Water Pollut. Control Fed.* 1517–1525.

Hoffman, E.J., Mills, G.L., Latimer, J.S., Quinn, J.G., 1984. Urban runoff as a source of polycyclic aromatic hydrocarbons to coastal waters. *Environ. Sci. Technol.* 18, 580–587. <https://doi.org/10.1021/es00126a003>

Hong, Y., Bonhomme, C., Le, M.-H., Chebbo, G., 2016a. A new approach of monitoring and physically-based modelling to investigate urban wash-off process on a road catchment near Paris. *Water Res.* 102, 96–108.

Hong, Y., Bonhomme, C., Le, M.-H., Chebbo, G., 2016b. New insights into the urban washoff process with detailed physical modelling. *Sci. Total Environ.* 573, 924–936. <https://doi.org/10.1016/j.scitotenv.2016.08.193>

Horner, R.R., Booth, D.B., Azous, A., May, C.W., 1997. Watershed Determinants of Ecosystem Functioning. Presented at the Effects of Watershed Development and Management on Aquatic Ecosystems, ASCE, pp. 251–274.

Huang, H., Cheng, S., Wen, J., Lee, J., 2008. Effect of growing watershed imperviousness on hydrograph parameters and peak discharge. *Hydrol. Process.* 22, 2075–2085. <https://doi.org/10.1002/hyp.6807>

Huber, W.C., Dickinson, R.E., Barnwell Jr, T.O., Branch, A., 1988. Storm water management model, version 4. US Environmental Protection Agency, Environmental Research Laboratory.

INSAVALOR, S.I., 1997. Software of Urban Hydrology, design and evaluation of sewer system, simulation of rainfall, water flow, and water quality.

James, W., Shivalingaiah, B., 1986. Continuous Mass-Balance of Pollutant Build-Up Processes, in: *Urban Runoff Pollution*, NATO ASI Series. Springer, Berlin, Heidelberg, pp. 243–271. [https://doi.org/10.1007/978-3-642-70889-3\\_9](https://doi.org/10.1007/978-3-642-70889-3_9)

Järup, L., 2003. Hazards of heavy metal contamination. *Br. Med. Bull.* 68, 167–182.

Jones, K.B., Neale, A.C., Nash, M.S., Remortel, R.D.V., Wickham, J.D., Riitters, K.H., O'Neill, R.V., 2001. Predicting nutrient and sediment loadings to streams from landscape metrics: A multiple watershed study from the United States Mid-Atlantic Region. *Landsc. Ecol.* 16, 301–312. <https://doi.org/10.1023/A:1011175013278>

Kang, I.S., Park, J.I., Singh, V.P., 1998. Effect of urbanization on runoff characteristics of the On-Cheon Stream watershed in Pusan, Korea. *Hydrol. Process.* 12, 351–363. [https://doi.org/10.1002/\(SICI\)1099-1085\(199802\)12:2<351::AID-HYP569>3.0.CO;2-O](https://doi.org/10.1002/(SICI)1099-1085(199802)12:2<351::AID-HYP569>3.0.CO;2-O)

Kang, J.-H., Kayhanian, M., Stenstrom, M.K., 2006. Implications of a kinematic wave model for first flush treatment design. *Water Res.* 40, 3820–3830. <https://doi.org/10.1016/j.watres.2006.09.007>

Kanso, A., 2004. Evaluation of urban stormwater quality models: a bayesian approach. Ecole des Ponts ParisTech.

Kayhanian, M., Singh, A., Suverkropp, C., Borroum, S., 2003. Impact of annual average daily traffic on highway runoff pollutant concentrations. *J. Environ. Eng.* 129, 975–990.

Kayhanian, M., Suverkropp, C., Ruby, A., Tsay, K., 2006. Characterization and prediction of highway runoff constituent event mean concentration. *J. Environ. Manage.* 85, 279–295. <https://doi.org/10.1016/j.jenvman.2006.09.024>

Krein, A., Schorer, M., 2000. Road runoff pollution by polycyclic aromatic hydrocarbons and its contribution to river sediments. *Water Res.* 34, 4110–4115. [https://doi.org/10.1016/S0043-1354\(00\)00156-1](https://doi.org/10.1016/S0043-1354(00)00156-1)

Kwon, E.E., Castaldi, M.J., 2012. Mechanistic understanding of polycyclic aromatic hydrocarbons (PAHs) from the thermal degradation of tires under various oxygen concentration atmospheres. *Environ. Sci. Technol.* 46, 12921–12926. <https://doi.org/10.1021/es303852e>

Lamprea, D.K., 2009. Caractérisation et origine des métaux traces, hydrocarbures aromatiques polycycliques et pesticides transportés par les retombées atmosphériques et les eaux de ruissellement dans les bassins versants séparatifs péri-urbains (phdthesis). Ecole Centrale de Nantes (ECN).

Lecoanet, H., Leveque, F., Ambrosi, J.-P., 2003. Combination of magnetic parameters: an efficient way to discriminate soil-contamination sources (south France). *Environ. Pollut.* 122, 229–234.

Lee, J.G., Heaney, J.P., 2003. Estimation of Urban Imperviousness and its Impacts on Storm Water Systems. *J. Water Resour. Plan. Manag.* 129, 419–426. [https://doi.org/10.1061/\(ASCE\)0733-9496\(2003\)129:5\(419\)](https://doi.org/10.1061/(ASCE)0733-9496(2003)129:5(419))

Lee, J.H., Bang, K.W., 2000. Characterization of urban stormwater runoff. *Water Res.* 34, 1773–1780. [https://doi.org/10.1016/S0043-1354\(99\)00325-5](https://doi.org/10.1016/S0043-1354(99)00325-5)

Lee, S., Ho, C.-H., Choi, Y.-S., 2011. High-PM10 concentration episodes in Seoul, Korea: Background sources and related meteorological conditions. *Atmos. Environ.* 45, 7240–7247. <https://doi.org/10.1016/j.atmosenv.2011.08.071>

Leopold, L.B., 1968. Hydrology for urban land planning: A guidebook on the hydrologic effects of urban land use.

Li, W.C., 2014. Occurrence, sources, and fate of pharmaceuticals in aquatic environment and soil. *Environ. Pollut.* 187, 193–201. <https://doi.org/10.1016/j.envpol.2014.01.015>

Lind, B.B., Karro, E., 1995. Stormwater infiltration and accumulation of heavy metals in roadside green areas in Göteborg, Sweden. *Ecol. Eng.* 5, 533–539. [https://doi.org/10.1016/0925-8574\(95\)00010-0](https://doi.org/10.1016/0925-8574(95)00010-0)

Line, D.E., Jennings, G.D., McLaughlin, R.A., Osmond, D.L., Harman, W.A., Lombardo, L.A., Tweedy, K.L., Spooner, J., 1999. Nonpoint Sources. *Water Environ. Res.* 71, 1054–1069. <https://doi.org/10.2307/25045282>

Line, D.E., White, N.M., Osmond, D.L., Jennings, G.D., Mojonier, C.B., 2002. Pollutant Export from Various Land Uses in the Upper Neuse River Basin. *Water Environ. Res.* 74, 100–108. <https://doi.org/10.2307/25045577>

Lisle, I.G., Rose, C.W., Hogarth, W.L., Hairsine, P.B., Sander, G.C., Parlange, J.-Y., 1998. Stochastic sediment transport in soil erosion. *J. Hydrol.* 204, 217–230. [https://doi.org/10.1016/S0022-1694\(97\)00123-6](https://doi.org/10.1016/S0022-1694(97)00123-6)

Liu, A., Gonzalez, R.D., 1999. Adsorption/Desorption in a System Consisting of Humic Acid, Heavy Metals, and Clay Minerals. *J. Colloid Interface Sci.* 218, 225–232. <https://doi.org/10.1006/jcis.1999.6419>

Liu, J.-S., Guo, L.-C., Luo, X.-L., Chen, F.-R., Zeng, E.Y., 2014. Impact of anthropogenic activities on urban stream water quality: a case study in Guangzhou, China. *Environ. Sci. Pollut. Res.* 21, 13412–13419. <https://doi.org/10.1007/s11356-014-3237-5>

Mackay, S., Australia, U.W.R.A. of, Water, S., Ensight, A.W.T., 1999. Sediment, nutrient and heavy metal characteristics of urban stormwater runoff (Article; Article/Report). Melbourne : Urban Water Research Association of Australia.

Mahbub, P., Goonetilleke, A., Ayoko, G.A., Egodawatta, P., Yigitcanlar, T., 2011. Analysis of build-up of heavy metals and volatile organics on urban roads in gold coast, Australia. *Water Sci. Technol.* 63, 2077–2085. <https://doi.org/10.2166/wst.2011.151>

Mancilla, Y., Mendoza, A., 2012. A tunnel study to characterize PM 2.5 emissions from gasoline-powered vehicles in Monterrey, Mexico. *Atmos. Environ.* 59, 449–460.

Manoli, E., Samara, C., 1999. Polycyclic aromatic hydrocarbons in natural waters: sources, occurrence and analysis. *TrAC Trends Anal. Chem.* 18, 417–428. [https://doi.org/10.1016/S0165-9936\(99\)00111-9](https://doi.org/10.1016/S0165-9936(99)00111-9)

Marsh, J.M., 1993. Assessment of nonpoint source pollution in stormwater runoff in Louisville, (Jefferson County) Kentucky, USA. *Arch. Environ. Contam. Toxicol.* 25, 446–455. <https://doi.org/10.1007/BF00214333>

McCarthy, J.F., Jimenez, B.D., 1985. Reduction in bioavailability to bluegills of polycyclic aromatic hydrocarbons bound to dissolved humic material. *Environ. Toxicol. Chem.* 4, 511–521.

McGrane, S.J., 2016. Impacts of urbanisation on hydrological and water quality dynamics, and urban water management: a review. *Hydrol. Sci. J.* 61, 2295–2311. <https://doi.org/10.1080/02626667.2015.1128084>

McKenzie, E.R., Wong, C.M., Green, P.G., Kayhanian, M., Young, T.M., 2008. Size Dependent Elemental Composition of Road-Associated Particles. *Sci. Total Environ.* 398, 145–153. <https://doi.org/10.1016/j.scitotenv.2008.02.052>

McMahon, G., Harned, D.A., 1998. Effect of Environmental Setting on Sediment, Nitrogen, and Phosphorus Concentrations in Albemarle-Pamlico Drainage Basin, North Carolina and Virginia, USA. *Environ. Manage.* 22, 887–903. <https://doi.org/10.1007/s002679900156>

Merritt, W.S., Letcher, R.A., Jakeman, A.J., 2003. A review of erosion and sediment transport models. *Environ. Model. Softw., The Modelling of Hydrologic Systems* 18, 761–799. [https://doi.org/10.1016/S1364-8152\(03\)00078-1](https://doi.org/10.1016/S1364-8152(03)00078-1)

Miller, J.D., Kim, H., Kjeldsen, T.R., Packman, J., Grebby, S., Dearden, R., 2014. Assessing the impact of urbanization on storm runoff in a peri-urban catchment using historical change in impervious cover. *J. Hydrol.* 515, 59–70. <https://doi.org/10.1016/j.jhydrol.2014.04.011>

Minton, G.R., 2002. Stormwater Treatment: Biological, Chemical, and Engineering Principles. Resource Planning Associates.

Morrison, G.M.P., Revitt, D.M., Ellis, J.B., 1990. Metal speciation in separate stormwater systems. *Water Sci. Technol.* 22, 53–60.

Motelay-Massei, A., Garban, B., Tiphagne-larcher, K., Chevreuril, M., Ollivon, D., 2006. Mass balance for polycyclic aromatic hydrocarbons in the urban watershed of Le Havre (France): Transport and fate of PAHs from the atmosphere to the outlet. *Water Res.* 40, 1995–2006. <https://doi.org/10.1016/j.watres.2006.03.015>

Murakami, M., Nakajima, F., Furumai, H., 2005. Size- and density-distributions and sources of polycyclic aromatic hydrocarbons in urban road dust. *Chemosphere* 61, 783–791. <https://doi.org/10.1016/j.chemosphere.2005.04.003>

Namdeo, A.K., Colls, J.J., Baker, C.J., 1999. Dispersion and re-suspension of fine and coarse particulates in an urban street canyon. *Sci. Total Environ.* 235, 3–13. [https://doi.org/10.1016/S0048-9697\(99\)00185-0](https://doi.org/10.1016/S0048-9697(99)00185-0)

Neary, V.S., Neel, T.C., Dewey, J.B., 2002. Pollutant Washoff and Loading from Parking Lots in Cookeville, Tennessee. *Glob. Solut. Urban Drain., Proceedings.* [https://doi.org/10.1061/40644\(2002\)220](https://doi.org/10.1061/40644(2002)220)

Nelson, E.J., Booth, D.B., 2002. Sediment sources in an urbanizing, mixed land-use watershed. *J. Hydrol.* 264, 51–68.

Novotny, V., 1994. *Water Quality: Prevention, Identification and Management of Diffuse Pollution.* Van Nostrand-Reinhold Publishers, New York.

Novotny, V., Sung, H.-M., Bannerman, R., Baum, K., 1985. Estimating nonpoint pollution from small urban watersheds. *J. Water Pollut. Control Fed.* 339–348.

Obropta, C.C., Kardos, J.S., 2007. Review of Urban Stormwater Quality Models: Deterministic, Stochastic, and Hybrid Approaches1: Review of Urban Stormwater Quality Models: Deterministic, Stochastic, and Hybrid Approaches. *JAWRA J. Am. Water Resour. Assoc.* 43, 1508–1523. <https://doi.org/10.1111/j.1752-1688.2007.00124.x>

OMS, 2010. *La face cachée des villes: mettre au jour et vaincre les inégalités en santé en milieu urbain.* Organisation mondiale de la Santé, Genève.

Pagotto, C., 1999. *Etude sur l'émission et le transfert dans les eaux et les sols des éléments traces métalliques et des hydrocarbures en domaine routier.* Poitiers.

Park, M.-H., Stenstrom, M.K., 2008. Comparison of pollutant loading estimation using different land uses and stormwater characteristics in Ballona Creek Watershed. *Water Sci. Technol. J. Int. Assoc. Water Pollut. Res.* 57, 1349–1354. <https://doi.org/10.2166/wst.2008.259>

Parra, R., Jiménez, P., Baldasano, J.M., 2006. Development of the high spatial resolution EMICAT2000 emission model for air pollutants from the north-eastern Iberian Peninsula (Catalonia, Spain). *Environ. Pollut. Barking Essex* 1987 140, 200–219. <https://doi.org/10.1016/j.envpol.2005.07.021>

Patra, A., Colvile, R., Arnold, S., Bowen, E., Shallcross, D., Martin, D., Price, C., Tate, J., ApSimon, H., Robins, A., 2008. On street observations of particulate matter movement and dispersion due to traffic on an urban road. *Atmos. Environ., Fifth International Conference on Urban Air Quality* 42, 3911–3926. <https://doi.org/10.1016/j.atmosenv.2006.10.070>



Paul, M.J., Meyer, J.L., 2001. Streams in the Urban Landscape. *Annu. Rev. Ecol. Syst.* 32, 333–365. <https://doi.org/10.1146/annurev.ecolsys.32.081501.114040>

Percot, S., 2012. Contribution des retombées atmosphériques aux flux de polluants issus d'un petit bassin versant urbain: Cas du Pin Sec à Nantes. *ÉCOLE CENTRALE DE NANTES*.

Percot, S., Ruban, V., Roupsard, P., Maro, D., Millet, M., 2016. A New Method for Assessing the Contribution of Atmospheric Deposition to the Stormwater Runoff Metal Load in a Small Urban Catchment. *Water. Air. Soil Pollut.* 227, 180. <https://doi.org/10.1007/s11270-016-2794-2>

Petry, T., Schmid, P., Schlatter, C., 1996. The use of toxic equivalency factors in assessing occupational and environmental health risk associated with exposure to airborne mixtures of polycyclic aromatic hydrocarbons (PAHs). *Chemosphere* 32, 639–648. [https://doi.org/10.1016/0045-6535\(95\)00348-7](https://doi.org/10.1016/0045-6535(95)00348-7)

Piatina, T.B., Hering, J.G., 2000. Direct Quantification of Metal-Organic Interactions by Size-Exclusion Chromatography (SEC) and Inductively Coupled Plasma Mass Spectrometry (ICP-MS). *J. Environ. Qual.* 29, 1839–1845. <https://doi.org/10.2134/jeq2000.00472425002900060015x>

Pitt, R., Field, R., 1977. Water-Quality Effects From Urban Runoff. *J. Am. Water Works Assoc.* 69, 432–436. <https://doi.org/10.2307/41269016>

Pitt, R., Field, R., Lalor, M., Brown, M., 1995. Urban stormwater toxic pollutants: assessment, sources, and treatability. *Water Environ. Res.* 67, 260–275.

Pitt, R.E., Williamson, D., Voorhees, J., Clark, S., 2005. Review of Historical Street Dust and Dirt Accumulation and Washoff Data. *J. Water Manag. Model.* <https://doi.org/10.14796/JWMM.R223-12>

Proffitt, A.P.B., Rose, C.W., Hairsine, P.B., 1991. Rainfall detachment and deposition: Experiments with low slopes and significant water depths. *Soil Sci. Soc. Am. J.* 55, 325–332.

Pulles, T., Denier van der Gon, H., Appelman, W., Verheul, M., 2012. Emission factors for heavy metals from diesel and petrol used in European vehicles. *Atmos. Environ.* 61, 641–651. <https://doi.org/10.1016/j.atmosenv.2012.07.022>

Putro, B., Kjeldsen, T.R., Hutchins, M.G., Miller, J., 2016. An empirical investigation of climate and land-use effects on water quantity and quality in two urbanising catchments in the southern United Kingdom. *Sci. Total Environ.* 548–549, 164–172. <https://doi.org/10.1016/j.scitotenv.2015.12.132>

Qu, W., Kelderman, P., 2001. Heavy metal contents in the Delft canal sediments and suspended solids of the River Rhine: multivariate analysis for source tracing. *Chemosphere* 45, 919–925.

Ramier, D., Berthier, E., Andrieu, H., 2010. The hydrological behaviour of urban streets: long-term observations and modelling of runoff losses and rainfall-runoff transformation. *Hydrol. Process.* 25, 2161–2178. <https://doi.org/10.1002/hyp.7968>

Riddle, S.G., Robert, M.A., Jakober, C.A., Hannigan, M.P., Kleeman, M.J., 2007. Size Distribution of Trace Organic Species Emitted from Light-Duty Gasoline Vehicles. *Environ. Sci. Technol.* 41, 7464–7471. <https://doi.org/10.1021/es070153n>

Robertson, D.J., Taylor, K.G., 2007. Temporal Variability of Metal Contamination in Urban Road-deposited Sediment in Manchester, UK: Implications for Urban Pollution Monitoring. *Water. Air. Soil Pollut.* 186, 209–220. <https://doi.org/10.1007/s11270-007-9478-x>

Roger, S., Montrejaud-Vignoles, M., Andral, M.C., Herremans, L., Fortune, J.P., 1998. Mineral, physical and chemical analysis of the solid matter carried by motorway runoff water. *Water Res.* 32, 1119–1125. [https://doi.org/10.1016/S0043-1354\(97\)00262-5](https://doi.org/10.1016/S0043-1354(97)00262-5)

Rose, C.W., 1985. Developments in soil erosion and deposition models. *Adv. Soil Sci.* 2, 1–63.

Rose, S., Peters, N.E., 2001. Effects of urbanization on streamflow in the Atlanta area (Georgia, USA): a comparative hydrological approach. *Hydrol. Process.* 15, 1441–1457. <https://doi.org/10.1002/hyp.218>

Rossman, L.A., 2010. Storm water management model user's manual, version 5.0. National Risk Management Research Laboratory, Office of Research and Development, US Environmental Protection Agency Cincinnati.

Sabin, L.D., Lim, J.H., Stolzenbach, K.D., Schiff, K.C., 2005. Contribution of trace metals from atmospheric deposition to stormwater runoff in a small impervious urban catchment. *Water Res.* 39, 3929–3937. <https://doi.org/10.1016/j.watres.2005.07.003>

Sadiq, M., Alam, I., El-Mubarek, A., Al-Mohdhar, H.M. (King F.U. of P. and M., 1989. Preliminary Evaluation of Metal Pollution from Wear of Auto Tires. *Bull. Environ. Contam. Toxicol. USA* 42:5. <https://doi.org/10.1007/BF01700397>

Salvadore, E., Bronders, J., Batelaan, O., 2015. Hydrological modelling of urbanized catchments: A review and future directions. *J. Hydrol.* 529, 62–81. <https://doi.org/10.1016/j.jhydrol.2015.06.028>

Sansalone, J.J., Buchberger, S.G., Al-Abed, S.R., 1996. Fractionation of heavy metals in pavement runoff. *Sci. Total Environ., Highway and Urban Pollution* 189, 371–378. [https://doi.org/10.1016/0048-9697\(96\)05233-3](https://doi.org/10.1016/0048-9697(96)05233-3)

Sansalone, J.J., Koran, J.M., Smithson, J.A., Buchberger, S.G., 1998. Physical characteristics of urban roadway solids transported during rain events. *J. Environ. Eng.* 124, 427–440.

Sartor, J.D., Boyd, G.B., 1972. *Water Pollution Aspects of Street Surface Contaminants*. U.S. Government Printing Office.

Sartor, J.D., Boyd, G.B., Agardy, F.J., 1974. *Water Pollution Aspects of Street Surface Contaminants*. *J. Water Pollut. Control Fed.* 46, 458–467.

Schlautman, M.A., Morgan, J.J., 1993. Effects of aqueous chemistry on the binding of polycyclic aromatic hydrocarbons by dissolved humic materials. *Environ. Sci. Technol.* 27, 961–969. <https://doi.org/10.1021/es00042a020>

Schoonover, J.E., Lockaby, B.G., Helms, B.S., 2006. Impacts of land cover on stream hydrology in the West Georgia Piedmont, USA. *J. Environ. Qual.* 35, 2123–2131. <https://doi.org/10.2134/jeq2006.0113>

Schueler, T., 1994. THE COMPONENTS OF IMPERVIOUSNESS.

Shaheen, D.G., 1975. Contributions of urban roadway usage to water pollution. Office of Research and Development, US Environmental Protection Agency.

Shao, Y., 2008. Physics and modelling of wind erosion. Springer Science & Business Media.

Shaw, S.B., Walter, M.T., Steenhuis, T.S., 2006. A physical model of particulate wash-off from rough impervious surfaces. *J. Hydrol.* 327, 618–626. <https://doi.org/10.1016/j.jhydrol.2006.01.024>

Sheng, Y., Ying, G., Sansalone, J., 2008. Differentiation of transport for particulate and dissolved water chemistry load indices in rainfall–runoff from urban source area watersheds. *J. Hydrol.* 361, 144–158. <https://doi.org/10.1016/j.jhydrol.2008.07.039>

Shinya, M., Tsuchinaga, T., Kitano, M., Yamada, Y., Ishikawa, M., 2000. Characterization of heavy metals and polycyclic aromatic hydrocarbons in urban highway runoff. *Water Sci. Technol.* 42, 201–208.

Shinya, M., Tsuruho, K., Konishi, T., Ishikawa, M., 2003. Evaluation of factors influencing diffusion of pollutant loads in urban highway runoff. *Water Sci. Technol. J. Int. Assoc. Water Pollut. Res.* 47, 227–232.

Shuster, W.D., Bonta, J., Thurston, H., Warnemuende, E., Smith, D.R., 2005. Impacts of impervious surface on watershed hydrology: A review. *Urban Water J.* 2, 263–275. <https://doi.org/10.1080/15730620500386529>

Simmons, D.L., Reynolds, R.J., 1982. Effects of Urbanization on Base Flow of Selected South-Shore Streams, Long Island, New York. *JAWRA J. Am. Water Resour. Assoc.* 18, 797–805. <https://doi.org/10.1111/j.1752-1688.1982.tb00075.x>

Smakhtin, V.U., 2001. Low flow hydrology: a review. *J. Hydrol.* 240, 147–186. [https://doi.org/10.1016/S0022-1694\(00\)00340-1](https://doi.org/10.1016/S0022-1694(00)00340-1)

Sonzogni, W.C., Chesters, G., Coote, D.R., Jeffs, D.N., Konrad, J.C., Ostry, R.C., Robinson, J.B., 1980. Pollution from land runoff. *Environ. Sci. Technol.* 14, 148–153. <https://doi.org/10.1021/es60162a003>

Sörme, L., Lagerkvist, R., 2002. Sources of heavy metals in urban wastewater in Stockholm. *Sci. Total Environ.* 298, 131–145. [https://doi.org/10.1016/S0048-9697\(02\)00197-3](https://doi.org/10.1016/S0048-9697(02)00197-3)

Stein, E.D., Tiefenthaler, L.L., Schiff, K.C., 2008. Comparison of stormwater pollutant loading by land use type. *South. Calif. Coast. Water Res. Proj.* 2008 Annu. Rep. 15–27.

Strayer, D.L., Beighley, R.E., Thompson, L.C., Brooks, S., Nilsson, C., Pinay, G., Naiman, R.J., 2003. Effects of Land Cover on Stream Ecosystems: Roles of Empirical Models and Scaling Issues. *Ecosystems* 6, 407–423. <https://doi.org/10.1007/PL00021506>

Sutherland, R., Jelen, S.L., 1996. Sophisticated Stormwater Quality Modeling is Worth the Effort. *J. Water Manag. Model.* <https://doi.org/10.14796/JWMM.R191-01>

Sutherland, R.A., 2003. Lead in grain size fractions of road-deposited sediment. *Environ. Pollut.* 121, 229–237. [https://doi.org/10.1016/S0269-7491\(02\)00219-1](https://doi.org/10.1016/S0269-7491(02)00219-1)

Taylor, K.G., Owens, P.N., 2009. Sediments in urban river basins: a review of sediment–contaminant dynamics in an environmental system conditioned by human activities. *J. Soils Sediments* 9, 281–303. <https://doi.org/10.1007/s11368-009-0103-z>

Thorpe, A., Harrison, R.M., 2008. Sources and properties of non-exhaust particulate matter from road traffic: a review. *Sci. Total Environ.* 400, 270–282. <https://doi.org/10.1016/j.scitotenv.2008.06.007>

Tian, G., Qiao, Z., Xu, X., 2014. Characteristics of particulate matter (PM<sub>10</sub>) and its relationship with meteorological factors during 2001–2012 in Beijing. *Environ. Pollut.* 192, 266–274. <https://doi.org/10.1016/j.envpol.2014.04.036>

Tiefenthaler, L.L., Stein, E.D., Schiff, K.C., 2008. Watershed and land use-based sources of trace metals in urban storm water. *Environ. Toxicol. Chem.* 27, 277–287. <https://doi.org/10.1897/07-126R.1>

Tomanovic, A., Maksimovic, C., 1996. Improved modelling of suspended solids discharge from asphalt surface during storm event. *Water Sci. Technol., Diffuse Pollution '95* 33, 363–369. [https://doi.org/10.1016/0273-1223\(96\)00253-3](https://doi.org/10.1016/0273-1223(96)00253-3)

Tong, S.T.Y., 1990. The hydrologic effects of urban land use: A case study of the little Miami River Basin. *Landsc. Urban Plan.* 19, 99–105. [https://doi.org/10.1016/0169-2046\(90\)90037-3](https://doi.org/10.1016/0169-2046(90)90037-3)

Tsihrintzis, V.A., Hamid, R., 1997. Modeling and management of urban stormwater runoff quality: a review. *Water Resour. Manag.* 11, 136–164.

Uddin, M.K., 2017. A review on the adsorption of heavy metals by clay minerals, with special focus on the past decade. *Chem. Eng. J.* 308, 438–462. <https://doi.org/10.1016/j.cej.2016.09.029>

US Army Corps of Engineers, 1977. STORM: Storage, treatment, overflow, runoff model – User's manual, 723-S8-L7520, Hydrologic Engineering Center, Davis, California, U.S.A.

US EPA, 1983. Results of the Nationwide Urban Runoff Program.

Van Metre, P.C., Mahler, B.J., Furlong, E.T., 2000. Urban Sprawl Leaves Its PAH Signature. *Environ. Sci. Technol.* 34, 4064–4070. <https://doi.org/10.1021/es991007n>

Vaze, J., Chiew, F.H., 2002. Experimental study of pollutant accumulation on an urban road surface. *Urban Water* 4, 379–389.

Vaze, J., Chiew, F.H.S., 2004. Nutrient Loads Associated with Different Sediment Sizes in Urban Stormwater and Surface Pollutants. *J. Environ. Eng.* 130, 391–396. [https://doi.org/10.1061/\(ASCE\)0733-9372\(2004\)130:4\(391\)](https://doi.org/10.1061/(ASCE)0733-9372(2004)130:4(391))

Vaze, J., Chiew, F.H.S., 2003. Study of pollutant washoff from small impervious experimental plots. *Water Resour. Res.* 39, 1160. <https://doi.org/10.1029/2002WR001786>

Verbeiren, B., Van De Voorde, T., Canters, F., Binard, M., Cornet, Y., Batelaan, O., 2013. Assessing urbanisation effects on rainfall-runoff using a remote sensing supported modelling strategy. *Int. J. Appl. Earth Obs. Geoinformation* 21, 92–102. <https://doi.org/10.1016/j.jag.2012.08.011>

Viklander Maria, 1998. Particle Size Distribution and Metal Content in Street Sediments. *J. Environ. Eng.* 124, 761–766. [https://doi.org/10.1061/\(ASCE\)0733-9372\(1998\)124:8\(761\)](https://doi.org/10.1061/(ASCE)0733-9372(1998)124:8(761))

Wählín, P., Berkowicz, R., Palmgren, F., 2006. Characterisation of traffic-generated particulate matter in Copenhagen. *Atmos. Environ.* 40, 2151–2159. <https://doi.org/10.1016/j.atmosenv.2005.11.049>

Walker, W.J., McNutt, R.P., Maslanka, C.K., 1999. The potential contribution of urban runoff to surface sediments of the Passaic River: sources and chemical characteristics. *Chemosphere* 38, 363–377.

Wang, S., He, Q., Ai, H., Wang, Z., Zhang, Q., 2013. Pollutant concentrations and pollution loads in stormwater runoff from different land uses in Chongqing. *J. Environ. Sci.* 25, 502–510. [https://doi.org/10.1016/S1001-0742\(11\)61032-2](https://doi.org/10.1016/S1001-0742(11)61032-2)

Wanielista, M.P., Yousef, Y.A., 1993. *Stormwater Management*. John Wiley & Sons.

Wanielista, M.P., Yousef, Y.A., McLellon, W.M., 1977. Nonpoint Source Effects on Water Quality. *J. Water Pollut. Control Fed.* 49, 441–451. <https://doi.org/10.2307/25039287>

Whipple Jr, W., Hunter, J.V., Yu, S.L., 1977. Effects of storm frequency on pollution from urban runoff. *J. Water Pollut. Control Fed.* 2243–2248.

Wicke, D., Cochrane, T.A., O'Sullivan, A., 2012. Build-up dynamics of heavy metals deposited on impermeable urban surfaces. *J. Environ. Manage.* 113, 347–354. <https://doi.org/10.1016/j.jenvman.2012.09.005>

Wijesiri, B., Egodawatta, P., McGree, J., Goonetilleke, A., 2015a. Process variability of pollutant build-up on urban road surfaces. *Sci. Total Environ.* 518–519, 434–40. <https://doi.org/10.1016/j.scitotenv.2015.03.014>

Wijesiri, B., Egodawatta, P., McGree, J., Goonetilleke, A., 2015b. Influence of pollutant build-up on variability in wash-off from urban road surfaces. *Sci. Total Environ.* 527–528, 344–350. <https://doi.org/10.1016/j.scitotenv.2015.04.093>

Wolman, M.G., 1967. A cycle of sedimentation and erosion in urban river channels. *Geogr. Ann. Ser. Phys. Geogr.* 385–395.

Wu, G., Kechavarzi, C., Li, X., Sui, H., Pollard, S.J.T., Coulon, F., 2013. Influence of mature compost amendment on total and bioavailable polycyclic aromatic hydrocarbons in contaminated soils. *Chemosphere* 90, 2240–2246. <https://doi.org/10.1016/j.chemosphere.2012.10.003>

Yaziz, M.I., Gunting, H., Sapari, N., Ghazali, A.W., 1989. Variations in rainwater quality from roof catchments. *Water Res.* 23, 761–765. [https://doi.org/10.1016/0043-1354\(89\)90211-X](https://doi.org/10.1016/0043-1354(89)90211-X)

Yousef, Y.A., Wanielista, M.P., Hvitved-Jacobsen, T., Harper, H.H., 1984. Fate of heavy metals in stormwater runoff from highway bridges. *Sci. Total Environ., Highway Pollution* 33, 233–244. [https://doi.org/10.1016/0048-9697\(84\)90397-8](https://doi.org/10.1016/0048-9697(84)90397-8)

Yuen, J.Q., Olin, P.H., Lim, H.S., Benner, S.G., Sutherland, R.A., Ziegler, A.D., 2012. Accumulation of potentially toxic elements in road deposited sediments in residential and light industrial neighborhoods of Singapore. *J. Environ. Manage.* 101, 151–163. <https://doi.org/10.1016/j.jenvman.2011.11.017>

Zgheib, S., Moilleron, R., Chebbo, G., 2012. Priority pollutants in urban stormwater: Part 1 – Case of separate storm sewers. *Water Res., Special Issue on Stormwater in urban areas* 46, 6683–6692. <https://doi.org/10.1016/j.watres.2011.12.012>

Zhao, G., Gao, H., Cuo, L., 2016. Effects of Urbanization and Climate Change on Peak Flows over the San Antonio River Basin, Texas. *J. Hydrometeorol.* 17, 2371–2389. <https://doi.org/10.1175/JHM-D-15-0216.1>

Zhao, H., Chen, X., Hao, S., Jiang, Y., Zhao, J., Zou, C., Xie, W., 2016. Is the wash-off process of road-deposited sediment source limited or transport limited? *Sci. Total Environ.* 563–564, 62–70. <https://doi.org/10.1016/j.scitotenv.2016.04.123>

Zhao, H., Li, X., Wang, X., 2011. Heavy Metal Contents of Road-Deposited Sediment along the Urban–Rural Gradient around Beijing and its Potential Contribution to Runoff Pollution. *Environ. Sci. Technol.* 45, 7120–7127. <https://doi.org/10.1021/es2003233>

Zhao, H., Li, X., Wang, X., Tian, D., 2010. Grain size distribution of road-deposited sediment and its contribution to heavy metal pollution in urban runoff in Beijing, China. *J. Hazard. Mater.* 183, 203–210. <https://doi.org/10.1016/j.jhazmat.2010.07.012>

Zoppou, C., 2001. Review of urban storm water models. *Environ. Model. Softw.* 16, 195–231.



## Partie 4. Compréhension des processus de production et de mobilisation des contaminants à l'échelle locale : modélisation et études expérimentales

L'échec des modèles conceptuels de qualité de l'eau à reproduire les pollutogrammes et à donner une bonne estimation des flux à l'exutoire des bassins versants urbain est souvent lié à deux raisons principales (Kanso, 2004) :

- La quantité et la qualité des données utilisées pour le calage et la validation
- Le manque des connaissances sur les processus mis en jeu

Cependant, les campagnes expérimentales menées dans le cadre du projet Trafipollu à l'échelle locale permettent de surmonter ces limites en mettant à notre disposition des bases de données très riches. Ainsi, dans cette partie nous présentons la stratégie que nous avons développée pour approfondir les connaissances sur les processus d'accumulation et de lessivage à l'échelle locale du bassin versant routier. La stratégie s'appuie à la fois sur (1) un travail de modélisation des dynamiques d'émissions de MES à l'exutoire de la chaussée en exploitant les mesures en continu de la quantité et de la qualité comme données d'entrée aux modèle et de confrontation aux simulations respectivement ; (2) l'évaluation de la contribution des dépôts secs atmosphériques à la contamination des eaux de ruissellement pour évaluer la pertinence de coupler les modèles atmosphériques aux modèles de la qualité des eaux de ruissellement, en exploitant les données des concentrations des HAPs et des métaux dans l'atmosphère, les poussières de la surface et l'eau de ruissellement ; et (3) la compréhension du lien entre l'accumulation et le lessivage en exploitant les données de dépôts secs et les données issues des expérimentations de lessivage réalisées en conditions contrôlées à l'aide d'un simulateur de pluie sur les surfaces urbaine en temps réel. La synthèse de ces travaux et les principales conclusions obtenues ainsi que le bilan des messages principaux de cette partie sont présentés dans les sections suivantes. Les chapitres 1, 2 et 3 correspondent aux articles suivants :

- *"Evaluation of the Performance and the Predictive Capacity of Build-Up and Wash-Off Models on Different Temporal Scales"* (2016, *Water*, 8,(8),312).



- *“Contribution of atmospheric dry deposition to stormwater loads for PAHs and trace metals in a small and highly trafficked urban road catchment” (2017, Environmental Science and Pollution Research, doi:10.1007/s11356-017-0238-1).*
- *“Investigation of the wash-off process using an innovative portable rainfall simulator allowing continuous monitoring of flow and turbidity at the urban surface outlet” (2017, Science of the Total Environment, 609, 17-26).*

Le chapitre 4 correspond au bilan des messages principaux dans cette partie.

### ➤ **Chapitre 1**

Grâce à la disponibilité d’une base de données riche de mesures en continu de débit et de turbidité à l’exutoire du bassin versant routier, la capacité des modèles conceptuels d’accumulation et de lessivage à simuler et à prédire correctement la variabilité temporelle des concentrations en MES est évaluée. Les modèles sont calés avec un algorithme de type Monte Carlo par chaîne de Markov (Hasting, 1970) qui permet aussi de quantifier les incertitudes liées aux valeurs estimées des paramètres.

Un travail similaire a été fait antérieurement sur une petite chaussée urbaine (800 m<sup>2</sup>), moyennement fréquentée (8000 véhicules/jours) située dans la commune de Sucy en Brie (94) (Sage et al., 2015). Dans cette étude, les données de débit et de turbidité acquises en continu sur une période de 11 mois ont été utilisées pour la mise en œuvre des modèles d’accumulation-lessivage qui sont calés et validés sur différentes périodes afin de simuler les flux et la dynamique des concentrations de MES. Les résultats obtenus soulignent que sur des longues périodes, l’accumulation décrite en fonction de la durée de temps sec est assez imprévisible. Si cela explique en partie le pouvoir prédictif limité du modèle conceptuel d’accumulation-lessivage à simuler la dynamique d’émission de MES, le modèle de lessivage aussi contribue à la faiblesse du pouvoir prédictif, car il ne réussit pas à reproduire systématiquement les fluctuations des concentrations mesurées. En termes de flux, le modèle aboutit à des meilleurs résultats qui pourraient cependant être obtenus à l’aide des modèles simples de concentration moyenne et qui sont actionnés principalement par la bonne estimation des volumes ruisselés.

Ces résultats nous ont poussés à réfléchir à une méthodologie d'analyse plus approfondie et détaillée qui nous permet d'avoir une meilleure compréhension de la variabilité de la performance du modèle d'accumulation-lessivage. Cela est aussi motivé par la qualité des données acquises sur le bassin versant d'Alsace Lorraine. Nous avons en effet été confrontés à plusieurs problèmes techniques dans le dispositif de mesures du débit mis en place sur le site de Sucy en Brie (système à augets basculants), ce qui a généré des périodes d'absence de mesure pour des semaines entières. En plus, la forte variabilité des mesures de turbidité a entravé le calage du modèle sur toute la période de mesure.

La méthodologie de recherche ainsi développée et appliquée sur le bassin versant routier consiste à évaluer dans un premier temps le modèle de lessivage exponentiel en réalisant des calages à l'échelle événementielle, et les modèles d'accumulation exponentielle et puissance en réalisant des calages en continu sur des périodes courtes de 3, 6 ou 9 événements pluvieux successifs. Dans un second temps, le pouvoir prédictif à court terme du modèle accumulation-lessivage est évalué à l'échelle inter-événementielle et à l'échelle intra-événementielle avec une approche d'assimilation de données.

Les résultats montrent que la performance du modèle de lessivage dépend du type d'évènement vis à vis de la dynamique du transport polluant. Le meilleur ajustement entre les concentrations de MES simulées et mesurées est enregistré pour les événements de type « premier flot ». L'analyse des jeux de paramètres optimaux du modèle de lessivage montrent que le calage tend parfois vers des valeurs extrêmes qui n'ont aucun sens physique et qui ne sont pas comparables entre les événements. En ce qui concerne l'accumulation, les résultats obtenus sont en accord avec ceux obtenus sur Sucy. Les stocks estimés par les modèles d'accumulation ne sont valides que pour des courtes périodes n'incluant pas plus que trois événements pluvieux consécutifs. La pertinence des formulations d'accumulation basées sur la durée de temps sec est encore une fois remise en cause, où elles se révèlent incapables de représenter la variabilité de ce processus à long terme. Le pouvoir prédictif inter-événement à court terme du modèle d'accumulation-lessivage est très pauvre et les dynamiques d'érosion pour chaque événement pluvieux ne peuvent pas être décrites par le même jeu de paramètres. La tentative d'estimer la masse disponible au début de l'évènement pluvieux à partir d'un certain nombre de mesure est faite en se basant sur une technique d'assimilation de donnée. Les résultats obtenus n'étaient pas acceptables que pour un nombre très limité d'évènements

qui sont tous des événements de « premier flot ». En addition, cette approche ne peut pas être appliquée sur des courts événements car sa validation nécessite d'avoir des mesures au moins pour les 20 premières minutes.

## ➤ Chapitre 2

Dans les modèles conceptuels d'accumulation, l'estimation du stock est faite sans distinction des particules qui proviennent de différentes sources incluant les apports atmosphériques. Cependant, nous pensons que sur un bassin versant soumis à une densité de trafic très importante et qui se trouve à proximité directe des voies de circulation (tel que le bassin d'Alsace Lorraine), il pourrait être approprié d'intégrer explicitement les dépôts atmosphériques comme source d'approvisionnement du stock sur la surface. Ceci est possible en couplant les modèles de qualité de l'air avec les modèles qualité de l'eau.

Pour étudier la pertinence d'une telle approche, le rôle potentiel que jouent les dépôts secs atmosphériques dans la contamination des eaux de ruissellement est évalué. Les données expérimentales sur les concentrations atmosphériques, sur les dépôts secs collectés sur la surface de la chaussée et sur les concentrations calculées dans les échantillons d'eau de ruissellement sont comparées en termes de granulométrie et de charges polluantes (HAPs et métaux). Les dépôts sont calculés en se basant sur la définition actuelle de la « contamination atmosphérique », qui correspond aux concentrations de polluants mesurées à une hauteur d'environ 2 mètres par rapport à la surface du sol.

Comme les périodes des campagnes de mesures de la qualité de l'air et de la qualité de l'eau n'étaient pas coïncidentes, il était nécessaire de reconstruire les données de qualité de l'air sur la période de l'étude. Les données de qualité de l'air mesurées à partir de stations permanentes d'observations d'Airparif ont été utilisées pour faire la reconstruction.

Les résultats obtenus suggèrent que l'hypothèse sur la pertinence du couplage des modèles de qualité de l'air (au moins ceux basés sur la définition actuelle de la contamination atmosphérique), avec les modèles de qualité de l'eau doit être révisée : les pourcentages de contributions potentielles des dépôts secs atmosphériques à la contamination des eaux de ruissellement simulés par cette approche sont très faibles. Pour les HAPs, la contribution potentielle moyenne des dépôts atmosphériques aux charges mesurées dans les eaux de

ruissellement ne dépasse pas 11% alors qu'elle est bien inférieure pour les métaux et n'excède pas 4%. Les contributions les plus élevées sont bien notées pour les événements ayant la plus longue durée de temps sec qui est aussi responsable de la variabilité des dépôts atmosphériques calculés. Cependant, aucune corrélation n'est calculée entre la durée de temps sec et les charges de contaminants dans les eaux de ruissellement ce qui fait la lumière encore une fois sur l'inaptitude de la prise en compte de l'accumulation qui dépend uniquement de la durée de temps sec comme donnée d'entrée aux modèles de lessivage. Les particules fines représentent la fraction la plus susceptible d'être mobilisée pendant l'événement pluvieux comme le montre la comparaison des distributions granulométriques des dépôts sur la chaussée et des échantillons d'eau.

Etablir le lien entre la contamination de l'atmosphère et la qualité de l'eau nécessite alors une révision et une extension de la définition de ce qui est considéré comme pollution atmosphérique pour inclure les émissions directes du trafic. Ainsi, les particules générées par les sources locales provenant des émissions directes (l'abrasion des pneus, l'abrasion de la surface et la remise en suspension sous l'effet de la turbulence) doivent être prises en compte lors de l'évaluation de la contamination atmosphérique. Ceci est possible en déployant des dispositifs de mesure à la surface des voiries.

### ➤ **Chapitre 3**

Pour avoir une meilleure compréhension des mécanismes de lessivage et de la relation qui existe entre le stock accumulé et le stock mobilisable, les stocks de dépôts secs présents sur la surface sont collectés et comparés, en termes de masse et de granulométrie, à la charge mesurée dans des échantillons d'eau. Les échantillons eau sont obtenus en lessivant deux surfaces distinctes grâce à un simulateur de pluie. Le simulateur de pluie réalisé présente deux innovations principales : il est caractérisé par son poids léger qui facilite sa portabilité sur les sites réels et il permet d'avoir des mesures en ligne du débit et de la turbidité pendant toute la durée de l'événement pluvieux.

Les expérimentations de lessivage et de collecte de dépôt sont ainsi effectuées sur deux types de surface représentées par un trottoir et par un parking. Pour chaque expérimentation de lessivage 20 litres d'eau sont utilisés pour arroser la surface pendant 10 minutes.

Les pollutogrammes observés sur les trottoirs montrent que même avec un débit constant, la charge de contaminant la plus élevée est véhiculée par la première fraction du volume ruisselé, signalant l'occurrence d'un « premier flot ». Ceci n'est pas systématique pour les pollutogrammes observés sur le parking qui montraient plutôt une distribution uniforme à l'exception d'une seule fois. Ces résultats remettent en question la capacité de la formulation classique de lessivage, basée sur le taux de ruissellement ou l'intensité de pluie comme variable indépendante, à reproduire ce comportement.

La comparaison des charges accumulées et mobilisées sur les deux surfaces révèle le caractère sélectif du mécanisme de lessivage. En moyenne, seulement 17% et 6% des particules présentes sur les trottoirs et le parking respectivement ont été lessivées. L'analyse granulométrique montre en outre que le détachement des particules fines est le plus favorable avec 75% des particules mobilisées sur les trottoirs dont le diamètre est inférieur à 100 $\mu$ m. Les charges mobilisées sur les trottoirs sont aussi plus élevées que celles véhiculées sur le parking. Ceci est en partie lié à la texture plus lisse de la surface du trottoir sur laquelle les forces de frottement sont plus faibles. Les résultats montrent aussi qu'une partie des particules même les plus fines peut demeurer sur la surface à la fin de l'événement pluvieux, ce qui insiste sur la nécessité de considérer la masse résiduelle fine lors de la modélisation en continue.

## Chapitre 1. Evaluation of the Performance and the Predictive Capacity of Build-Up and Wash-Off Models on Different Temporal Scales

**Abstract:** Stormwater quality modeling has arisen as a promising tool to develop mitigation strategies. The aim of this paper is to assess the build-up and wash-off processes and investigate the capacity of several water quality models to accurately simulate and predict the temporal variability of suspended solids concentrations in runoff, based on a long-term data set. A Markov Chain Monte-Carlo (MCMC) technique is applied to calibrate the models and analyze the parameter's uncertainty. The short-term predictive capacity of the models is assessed based on inter- and intra-event approaches. Results suggest that the performance of the wash-off model is related to the dynamic of pollutant transport where the best fit is recorded for first flush events. Assessment of SWMM (StormWater Management Model) exponential build-up model reveals that better performance is obtained on short periods and that build-up models relying only on the antecedent dry weather period as an explanatory variable, cannot predict satisfactorily the accumulated mass on the surface. The predictive inter-event capacity of SWMM exponential model proves its inability to predict the pollutograph while the intra-event approach based on data assimilation proves its efficiency for first flush events only. This method is very interesting for management practices because of its simplicity and easy implementation.

**Keywords:** urban stormwater; concentrations; suspended solids; modeling; build-up; wash-off; data assimilation; MCMC; water quality.

### 1. Introduction

Growing urbanization increases stormwater runoff on impervious surfaces and pollutant loads leading to a tremendous ecological footprint [1]. Nonpoint source pollution discharged during rainfall events into receiving water bodies carries a high load of contaminants, including microorganisms, PAHs (Polycyclic aromatic hydrocarbon), metals and other anthropogenic contaminants, mainly adsorbed onto suspended solids in runoff [2–4]. Pollutants accumulate on urban catchments during dry weather periods and are mostly generated by anthropogenic activities but also by atmospheric deposition and re-suspension of the surrounding soil [5–8]. These pollutants are washed off by storm events where the particles are eroded and detached by rainfall drops and transported by runoff into the

drainage network [9,10]. Several dynamics of pollutant transport exist and attempt to explain the variations in pollutant concentrations through the stages of runoff [11]. The fluctuations of the pressure exerted thus on ecosystems must be quantified including the accurate knowledge of the underlying processes of generation and transport of pollutants, in order to preserve the receiving environments from deterioration as well as meeting the legislative requirements imposed by the European Water Framework Directive [12]. Mitigation strategies include continuous monitoring of experimental sites. However, the high expenses involved in this approach bring to light the necessity to find a more appropriate alternative that can be transposed on unmonitored catchments. Hence, mathematical models have arisen as a promising tool to predict and simulate runoff quantity and quality since the 1970s [13,14].

Water quality models simulate pollutant loads based either on statistical regression equations or on conceptual and physical ones, replicating the processes of build-up and wash-off. Regression models rely on simple statistical methods that relate pollutant concentrations and loads to explanatory variables such as rainfall, runoff and catchment characteristics [15,16]. Even though regression equations are of interest for estimating total pollutant loads on the event and annual scale, they are not very reliable when they are applied at a small time step [16] and can hardly be transferred from a catchment to another since they are calibrated using a data set specific to one particular catchment. Process based models consist mainly of replicating the deposition of pollutants on surfaces between two storm events and their removal and transport by the rain [10,14,17]. Both conceptual and physical approaches have been developed and tested in order to achieve the best simulation of the pollutograph at the outlet of catchments.

Physical approaches developed for modeling the wash-off process usually consider the replication of the erosion of accumulated sediments on the surface, driven by the rainfall impact and the overland flow, as well as their deposition [18]. Shaw et al. [9] proposed in their study a saltation mechanistic wash-off model that describes the detachment of pollutant loads by raindrop while Massoudieh et al. [19] simulated pollutant concentrations using a wash-off model that includes the detachment and reattachment processes. In a recent study, Hong et al. [20] developed a physical model that considers both rainfall impact and overland flow as the driving mechanism of sediment erosion and suggested that raindrop is the major actor in detaching sediments of the urban surface. Physical approaches are very useful to have an in

depth insight into the corresponding process, however, the implementation of physically based models is not always possible especially if they are destined for operational use because they require the availability of large data sets that answer to the detailed description of the system. The large number of parameters also implicated in the model structure require an extensive calibration, thus it is time consuming. These reasons among others orient more toward the application of conceptual approaches. Conceptual build-up models are usually formulated as a function of antecedent dry weather period and are represented either by linear, power, exponential or the Michaelis–Menton equations [17,21–23]. As for wash-off, it is mathematically modeled as an exponential decrease of initial available pollutant mass on the surface, function of rainfall intensity, runoff volume or runoff rate [22]. Recent studies shows that these models can successfully replicate pollutant loads [24–26] but not the temporal variability of pollutant concentrations [13,19,27]. An in depth investigation based on a reliable and significant data set might be the answer to better understand the issue of accurate concentration estimates: the still unconquered holy grail of this field.

Therefore, the main purpose of this research is to evaluate the build-up and wash-off processes and investigate the capacity of commonly used water quality models to accurately simulate total suspended solids concentrations (TSS) and reproduce their temporal variability in runoff, based on a long-term, continuous data set. First, a wash-off model is evaluated and its performance is discussed with respect to different dynamics of pollutant transport to identify whether its applicability is specific to a certain type of events. Then two build-up models are evaluated in order to test their ability of replicating the accumulation of pollutants on urban surfaces in realistic conditions. Model calibration is performed based on the “Markov Chain Monte Carlo” technique, which enables the assessment of uncertainty associated with the model parameters. Finally, the short term predictive capacity of the models is investigated first at the inter-event scale, to test the period length during which the characteristics of a calibrated model remain valid, then at the intra-event scale where a new methodology is developed based on data assimilation, where the observations of the ongoing event are used for calibrating the available pollutant mass for erosion.



## 2. Materials and Methods

### 2.1. Experimental Site and Monitoring Equipment

The studied catchment is a 2661 m<sup>2</sup> road surface with its adjacent sidewalks, pavements and parking zones located in the residential French district “Le Perreux sur Marne”. The area carries high traffic loads (~30,000 vehicles per day) and is drained by a separate stormwater system. The catchment is characterized by an imperviousness equal to 70%, a runoff length of 167 m and an average slope of 2.6% (Figure 1).



**Figure 1.** The studied catchment delimited in bold black line. In the image we see the location of the sewer inlet station and the meteorological station installed at 180 m from the sewer inlet and 15 m of the extremity of the catchment (Photo taken from Google Map@2016)

From April 2014 to September 2015, monitoring systems were installed in the studied experimental site to monitor and sample rainfall and road runoff. In this research, data collected from June 2014 to April 2015 is exploited.

Precipitation data are collected from a meteorological station installed at 180 m from the road sewer inlet and at 15 m from the catchment’s extremity; 10 ml tipping bucket rain gauge is used for rainfall measurements, which corresponds to a resolution of 0.1 mm of precipitation height. The station was not installed directly on the road catchment to avoid its deterioration by the pedestrians and the surrounding activities and also to reduce the risk of technical problems that will induce significant errors in the measurements.

The monitoring devices of flow and water quality parameters for road runoff are located in the sewer inlet into the drainage system and recorded measurements at 1 min time step. For flow measurement, a Nivus flow meter, based on cross correlation method and providing high accurate ultrasonic flow measurements is used. As for quality aspects, turbidity (NTU), conductivity, pH and temperature are monitored with a DS5 OTT multi-

parameter probe. For reasons of power and storage savings, the setting off probe was triggered by the flow meter. Once the flow is higher than 0.15 L/s (which is considered as the limit of measurement of the flow meter) the quality measurements are launched until the flow becomes lower than 0.13 L/s for more than 15 min. Systematic volume of 500 mL are also collected for further laboratory analysis of metals, PAHs, DOC (Dissolved organic carbon), POC (Particulate organic carbon) and TSS for some rainfall events. For each event, the volume is pumped into two bottles (one made of glass and one made of plastic) of 20 L capacity; 250 mL are pumped into each one placed in a closed box on the sidewalk by a peristaltic pump (Watson-Marlow, Falmouth, Cornwall, UK), for each 300 L passing through the system. This volume was determined for covering 100% of most rainfall events, being thus representative of the total load during the rainfall event.

Linear relationship between turbidity and Total Suspended Solids is established in order to convert turbidity measurements into TSS concentrations. The TSS–turbidity relationship is calculated using measurements of turbidity obtained from nine samples. TSS concentrations are quantified by filtration, using 0.45 µm filters composed of glass fibers. Distinction between the metallic and the organic content of sediments is not considered. Thus the linear regression function adjusted over nine storm events, with a correlation factor  $R^2 = 0.98$ , is given by:

$$[\text{TSS}] = 0.9006 \times T \quad (1)$$

Where: [TSS] = the concentration of Total Suspended Solids in mg/l; T = Turbidity in NTU.

## 2.2. Data set

Overall, 246 rainfall events are recorded for the period between June 2014 and April 2015. Rainfall events are defined as uninterrupted measurement periods, during which the maximum time between bucket tips is 30 min. The precision of the rain gauge is 0.1 mm. The review of the collected meteorological data indicates extensive variability of rainfall characteristics (Table 1).

**Table 1. Statistics of the 246 recorded storm events**

	Rainfall depth (mm)	Duration (mins)	ADWP (jj HH:MM:SS)	Maximum 1 minute intensity (mm/h)	Maximum 5 minutes intensity (mm/h)	Maximum intensity (mm/h)	Average intensity (mm/h)
<b>Max</b>	21.3	641.1	21 05:28:19	131	100.2	360	53.9
<b>Min</b>	0.2	0.8	00 00:30:14	0.2	0.2	0.2	0.4
<b>Median</b>	0.7	34.78	00 06:47:05	3.03	2.31	2.94	1.36
<b>Mean</b>	2.128	75.2	01 06:14:24	9.19	6.61	14.09	3.25

Most storm events are short, as 50% of the events did not last for more than 35 min. The total rainfall depth varies from 0.2 to 21.3 mm, while maximum rainfall intensities varies between 0.2 mm/h and 360 mm/h. It is noteworthy that the median value of the antecedent dry weather period is 6 h indicating short time interval separating rainfall events; hence, the occurrence of successive storms. Fifty-four storms did not generate runoff, and precipitations in this case fulfilled initial losses.

Runoff data on the corresponding period are recorded for 187 events and were missing for five events due to technical problems, while turbidity measurements are recorded for 106 events on which water quality characteristics (event mean concentrations and loads) are assessed.

### 2.3. Data validation

#### 2.3.1. Turbidity

A crucial point in urban stormwater modeling is the quality of the data set used, since it is reflected in the quality of the results. Raw measurements obtained directly from site monitoring cannot be used before undergoing a validation procedure in order to eliminate non reliable measurements and interpolating when possible missing data points [28,29]. Automatic pre-validation is first developed to highlight wrong and doubtful data by associating a mark that reflects the validity of each measurement of turbidity, followed by a final manual validation. The technique is inspired by the work of Mourad and Bertrand-Krajewski [29] and the software EVOHE [30] but modified to fit this study case since turbidity measurements are obtained using one turbidimeter at the inlet of the drainage network.

The automatic pre-validation consists of several steps. First, initial marks are given to all turbidity measurements based on the sensor measurement range as follows:

- if the measurement is between the minimum and the maximum values given by the turbidity sensors, which are 0 and 3000, respectively;
- if the measurement is equal to the saturated value 3000;
- if the measurement is negative or equal to zero or recorded during intervention on site for maintenance operations.

Negative and zero values of turbidity are then interpolated and re-flagged 1 if they are recorded intra-event for three consecutive minutes or less. Finally, the values that exceeded the 99.5th percentile of global signal's gradient are considered as abnormal and marked 4. These measurements indicate sudden and irregular change in the signal that cannot be related to any physical process. All data that have a valid flag (i.e., equal to 1) at the end of the process are kept for the analysis. Others are checked for final validation manually by comparing rainfall, flow and turbidity graphs. If the saturated values or the values due to a high gradient, marked initially as 2 and 4, are coincident with a high rainfall intensity and high flow they are finally re-marked as 1 and taken as valid measurements. All data whose flag are different than 1 at the end of the manual validation were reflagged 2.

The above procedure generates a validated data set and is efficient in detecting the wrong and doubtful data that may induce errors in modeling results. In fact, these errors are noticed when comparing the Nash–Sutcliffe coefficients when calibrating on several events before and after the manual validation. False turbidity peaks that were kept after the automatic validation for the events of 14 and 15 November 2014, for example, clearly affected the calibration of the model. The Nash–Sutcliffe efficiencies obtained then were 0.03 and 0.55 respectively and they were highly improved after the removal of the mistaken turbidity values, Nash–Sutcliffe coefficients increased to 0.47 and 0.87, proving the sensibility of the model toward false measurements.

### **2.3.2. Hydrological modeling**

Flow measurements are validated by calculating the global runoff coefficient as well as the runoff coefficients for each event. Global runoff coefficient is equal to 0.73, calculated by taking into account the initial losses that correspond to 0.5 mm. The initial losses are defined as mean rainfall depths that never generated any runoff. Runoff coefficients for each event are variable and the initial loss is calculated for each event apart. This variability is noticed when

plotting the runoff depth function of rainfall depth (Appendix A, Figure A1). Precipitations with the same rainfall depth will result in different runoff depth, due to several factors including dry weather period, evaporation and depression storage. The events resulting in runoff coefficients greater than one are modeled in addition to the missing runoff data due to technical problems. A hydrological model consisting of a non-linear reservoir is calibrated and validated over 102 events using rainfall data of the rain gauge on site to substitute the lost records. The model replicates accurately the flow measurements with a Nash–Sutcliffe efficiency of 0.85.

**2.4. Intra-Event Dynamic of TSS Transport**

In order to distinguish the different dynamics of TSS transport during a rainfall event, dimensionless  $M(V)$  curves are plotted. Three typology of events (first flush, last flush and uniformly distributed) delimited by three zones A, B and C (Figure2) are defined based on a simplified classification of the  $M(V)$  curves inspired by the method proposed earlier by Bertrand-Krajewski et al. [11]. Simplifications are made since the definition of first flush given by these authors is very restrictive and given in the perspective of designing treatment facilities, while in our case a less restrictive definition is needed.

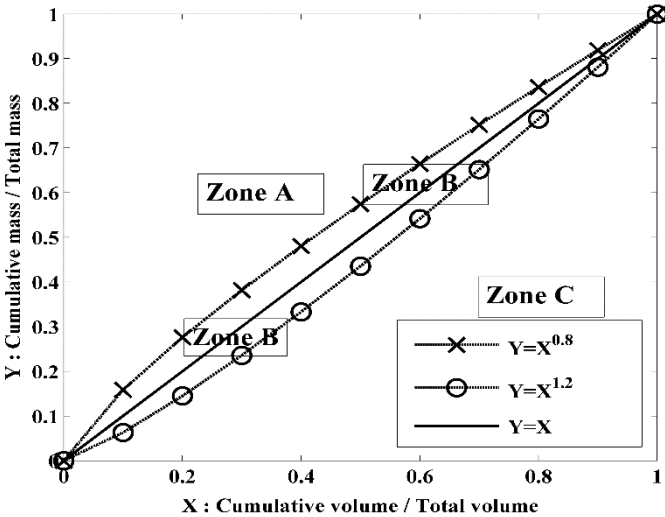


Figure 2. Definition of the  $M(V)$  curve zones

**2.5. Water quality modeling**

**2.5.1. The models**

Numerous modeling approaches for pollutant generation and transport exist and are detailed and compared in several reviews [1,31,32]. These reviews classify stormwater quality

models based on modeling approaches, process description, and spatial and temporal scales (Table2). In this study, we chose conceptual models to replicate the build-up and wash-off processes since they are easily implemented and simply applicable thus more attractive for practical applications. In addition, the diversity of the performance of these models emerging from past researches supports the need for further investigation of these formulations. Thus, we benefit from the extensive data set available on this site to test different models and contribute in the comprehension of build-up and wash-off processes.

**Table 2. General classification of stormwater quality models based on different criteria**

Criteria of classification	Model Type	Description
Variable description	Deterministic	Variables properties are well known and don't include any randomness. The same input will yield the same output.
	Stochastic	Variables have a probability distribution and its uncertainty is built into the model. The same input will yield different possible outputs.
Process description	Empirical	Relations between inputs and outputs are established from observations only without any intervention of physical laws
	Conceptual	Physical laws are applied in simple and simplified form
	Physically based	Logical structure based on physical laws governing the process
Spatial scale	Global (lumped)	Catchment is described as a whole entity
	Semi distributed	Catchment is divided into sub catchment
	Distributed	Catchment is divided into elementary unit using a grid
Temporal scale	Event	Individual events are simulated
	Continuous	Long period of time are simulated

We investigated two pollutant build-up models: the exponential build-up model of SWMM and a power function. The exponential build-up model describes an exponential growth of the build-up curve until it reaches asymptotically the upper limit which corresponds to the maximum pollutant load that can be accumulated on the surface. This limit is reached at the equilibrium state between deposition and removal of pollutant particle [17]. The remaining pollutant load from the previous rainfall event is also taken into account. The amount of build-up at the beginning of the rainfall event  $M_B$  (g/m<sup>2</sup>) is thus computed using the first order exponential equation:

$$M_B(i) = D_{ACCU}/D_{ERO} \times [1 - e^{(-D_{ERO} \times ADWP(i))}] + M_{RES} \cdot e^{(-D_{ERO} \times ADWP(i))} \quad (2)$$

where:  $M_{RES}$  = remaining pollutant load mass from the previous rainfall event ( $g/m^2$ );  $ADWP_{(i)}$  = antecedent dry weather period preceding the event  $i$  (day);  $D_{ACCU}$  = pollutant accumulation rate ( $g/m^2/day$ );  $D_{ERO}$  = pollutant erosion rate ( $/day$ )

The other model used to describe the accumulation process is based on the power function [21]. The pollutant load  $M_B$  ( $g/m^2$ ) present on the surface prior to a storm event is computed as follows:

$$M_B = a \cdot ADWP_{(i)}^b \quad (3)$$

where:  $a$  and  $b$  = build-up coefficients

This model assumes that the build-up process starts from zero and that the previous storm event erodes off all the pollutant present on the surface. Even though recent studies showed that a rainfall event washes away only a fraction of the pollutants available [10,33], this model gave the best results in replicating pollutant loads collected from experimental data [21,34].

Pollutant wash-off is simulated using the modified exponential model of SWMM [22] which considers the non-linear relation between the wash-off load and the runoff rate. This relation is taken into account by introducing the wash-off exponent  $C_2$ , which was initially set to be equal to one in the original SWMM version suggesting a linear dependency of the washed off fraction on the runoff rate. The eroded pollutant mass at time  $t$  during a storm event is calculated thus with the following equation:

$$M_{ERO}(t) = M_B(t) \cdot C_1 \cdot q(t)^{C_2} \cdot dt \quad (4)$$

$$M_B(t+dt) = M_B(t) - M_{ERO}(t) \quad (5)$$

where:  $M_{ERO}(t)$  = eroded pollutant mass at  $t$  during the time step  $dt$  ( $g/m^2$ );  $M_B(t)$  = the available pollutant mass for erosion at time  $t$  ( $g/m^2$ );  $q(t)$  = runoff rate ( $mm/h$ );  $dt$  = time step;  $C_1$  = wash-off coefficient;  $C_2$  = wash-off exponent.

### 2.5.2. Calibration

Application of water quality models requires estimation of build-up and wash-off parameters, as these models have very low performance if not calibrated [35].

The exponential build-up model integrates three parameters  $D_{ACCU}$ ,  $D_{ERO}$  and the initial pollutant load present on the surface  $M_{RES (t=0)}$ , whereas the power model integrates two parameters which are the build-up coefficients  $a$  and  $b$ . The exponential wash-off model requires the adjustment of two parameters  $C1$  and  $C2$ . These parameters are adjusted using an automatic calibration technique based on the Bayesian approach. This approach allows the assessment of parameters uncertainty by estimating their posterior probability distribution  $P(\theta/Y_{obs})$  given by Bayes' theorem and expressed as follow:

$$P(\theta/Y_{obs}) \propto L(\theta/Y_{obs}).P(\theta) \quad (6)$$

where:  $\theta$  = model parameter;  $Y_{obs}$  = the time series of observations;  $P(\theta)$  = prior probability distribution of the parameters;  $L(\theta/Y_{obs})$  = the likelihood function that describes the statistical characteristics of residuals between the observations and the model outputs.

The posterior probability is calculated based on the Metropolis-Hastings algorithm [36] of the Monte Carlo Markov Chain sampling technique.

The assumptions made in this study for the implementation of the Bayesian approach in the calibrations of build-up and wash-off models are the same as those made in the previous work of Kanso *et al.* [27].

At the end of calibration process we obtain not only the set of parameters for which we have the maximum likelihood, and that corresponds to the optimal set of parameters, but also the posterior probability distribution of the parameters that provides information on the uncertainty associated to these parameters and the likelihood probability vs. the parameters that allows the computation of model sensibility toward the parameters and the assessment of the uniqueness of the given optimum parameter set. The model performance is also assessed using the Nash–Sutcliffe coefficient [37].

Calibration is performed considering the period starting from November 2014 to April 2015. First, it is performed on single event scale to evaluate the wash-off process. The available mass at the beginning of the rainfall event in this case is considered as a parameter and is calibrated along with the wash-off coefficient and exponent. Overall, 42 events are included and the results are analyzed distinguishing the three typology of events in order to investigate if the performance of the wash-off model is related to the dynamic of pollutant transport by



runoff. Then calibration is performed on continuous periods consisting of three, six and nine successive events in order to evaluate the build-up process and check to which extent the build-up model can accurately predict the available mass between consecutive events. A total of 114 rainfall events are included. The configurations evaluated, couple the modified exponential SWMM build-up model, then the power build-up function with the SWMM wash-off model. A summary of the calibration procedure is presented in Table 3.

**Table 3. Calibration methodology of build-up and wash-off models**

	<b>Wash-off assessment</b>	<b>Build-up assessment</b>
<b>Number of events</b>	42	16 periods of 3 successive events each 8 periods of 6 successive events each 4 periods of 9 successive events each
<b>Model</b>	$M_{ERO}(t) = M_B(t) \cdot C1 \cdot q(t)^{C2} \cdot dt$	1. $M_B(i) = D_{ACCU}/D_{ERO} \times [1 - e^{(-D_{ERO} \times ADWP(i))}] + M_{RES} \cdot e^{(-D_{ERO} \times ADWP(i))}$ 2. $M_B(i) = a \cdot ADWP^{b(i)}$

**2.5.3. Prediction on short term**

The prediction capacity of the models on short term is also investigated to determine whether they can provide accurate predictions of the TSS concentrations over short periods of times. For that matter two approaches are investigated: inter-event and intra-event.

In the inter-event approach, 114 events are divided into periods of four events each; calibration is performed on the first two events and the models are validated on the third, and then on the third and fourth events simultaneously.

In the intra-event approach, observations are used along with the median value of wash-off parameters calibrated on first flush events to determine the available pollutant mass at the beginning of the storm. Then this mass is eroded by the storm and the Nash–Sutcliffe coefficient between the measured and the simulated TSS concentrations is calculated. The observations are included into the numerical model by a simple data assimilation technique. The number of points taken into account to calculate the available mass increase starting from two points up to considering the whole set of measurements. This allows identifying if the model can predict the total storm variation only if the first part of a storm is monitored. This method is applied on 38 events and a summary of the prediction methodology is presented in the table below (Table 4).

**Table 4. Prediction approaches: inter and intra event**

		Inter-event approach	Intra-event approach
<b>Number of events</b>		11 periods of 4 events each	38
<b>Model</b>	<b>Build-up</b>	$M_B(i) = D_{ACCU}/D_{ERO} \times [1 - e^{(-D_{ERO} \times ADWP(i))}] + M_{RES.} e^{(-D_{ERO} \times ADWP(i))}$ $M_B(i) = a.ADWP^{b(i)}$	-
	<b>Wash-off</b>	$M_{ERO}(t) = M_B(t).C1.q(t)^{C2}.dt$	
<b>Methodology</b>		-Calibration on the first two events of the period -Validation on the third event of the corresponding period -Validation on the third and the fourth events of the corresponding period	-Calculation of the available mass prior to the storm event using an a incremental number of observations -Simulation of the corresponding pollutograph

### 3. Results and discussion

#### 3.1. TSS concentrations and loads

Event mean concentration (EMC) is commonly used to evaluate the quality of runoff generated during a wet event and is considered as a surrogate indicator of runoff pollution [38,39]. From the EMC values summarized in Table 5, significant pollutant loads to receiving outlets are noticed. Median EMC of TSS obtained for this site is relatively much higher (320.97 mg/L) than those reported earlier in the literature. Gromaire [2] reported a median EMC of 97 mg/L calculated on six urban roads in “Le Marais” catchment while Gnecco et al. [40] calculated a median EMC equal to 119 mg/L in the experimental catchment of Villa Cambiosa in Italy.

The high EMC from the present study is explained mainly by the site’s characteristics related to high traffic density (~30,000 vehicles per day), since much lower concentrations (median EMC = 66 mg/L) yielded from road catchments that were less frequented [3].

Loads are expressed per unit of area and range from 0.0035 g/m<sup>2</sup> to 2.23 g/m<sup>2</sup>. The total annual load is equal to 89.23 g/m<sup>2</sup>.

**Table 5. Characteristics of TSS EMC and Loads for the monitored events**

	Maximum	Minimum	Mean	Median	Standard deviation
<b>EMC (mg/l)</b>	2174.37	35.39	452.09	320.97	432.42
<b>Load (g/m<sup>2</sup>)</b>	2.23	0.0035	0.51	0.27	0.56

To better understand the variability of EMC and loads of TSS between various storms and seasons, temporal variations are plotted (Figure3) and seasonal average EMC and total

loads are examined (Table 6). A seasonal trend is observed for EMC where the highest values are those recorded during the winter season. The average EMC calculated on winter (550 mg/L) is significantly higher than that on summer (228 mg/L) although the latter's events are heavier in terms of both precipitation depth and intensity than the former's. This highlights a dilution effect due to an increase in runoff volume (driven by depth) stronger than the increase in eroded mass (driven by intensity). Indeed, negative Pearson correlation calculated between the average seasonal EMC and the total rainfall depth collected for each season ( $R = -0.6$ ) support the occurrence of dilution. A similar pattern is not detected for loads whose values are at wide ranges. The seasonal trend disappears in winter and seasonal differences are not easily detected.

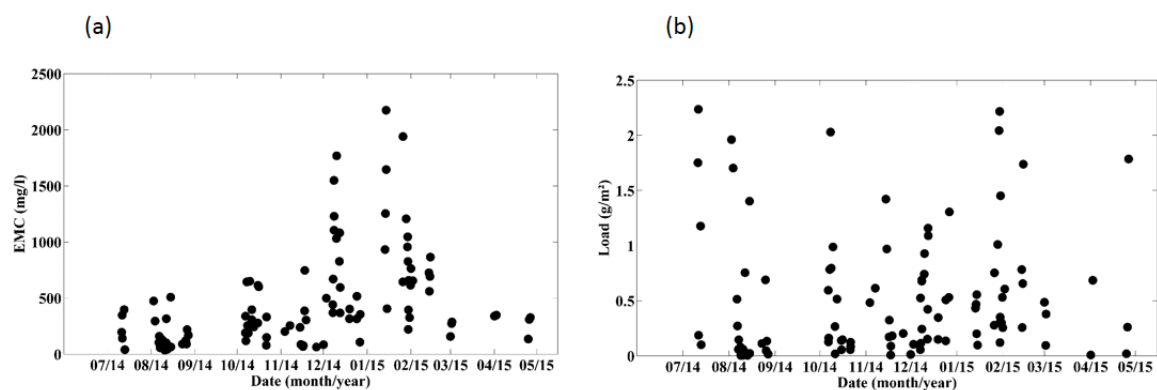


Figure 3. (a) Temporal variation of EMC (mg/L) for TSS from June 2014 to April 2015; and (b) temporal variation of load ( $\text{g/m}^2$ ) for TSS from June 2014 to April 2015

Table 6. Seasonal values of average EMC (mg/L) and total yields( $\text{g/m}^2$ ) and min-max values of maximum rainfall intensity (mm/h) and rainfall depth (mm) and total rainfall depth of storm events for each season.

Season	Autumn	Winter	Spring	Summer
<b>Beginning date</b>	06/10/2014 15:30	24/12/2014 15:30	01/04/2015 02:53	11/07/2014 02:16
<b>End date</b>	19/12/2014 13:53	02/03/2015 01:13	26/04/2015 12:56	27/08/2014 07:02
<b>Number of events</b>	42	29	5	30
<b>Average EMC (mg/l)</b>	270.35	550.82	326.43	228.37
<b>Total load (<math>\text{g/m}^2</math>)</b>	18.75	18.83	2.75	13.62
<b>Maximum intensity (mm/h) (min-max)</b>	0.54 - 72	0.71 - 72	4.23 - 120	1.77 - 180
<b>Rainfall depth (mm) (min-max)</b>	0.2 - 14.2	0.3 - 7.8	0.3 - 6.8	0.4 - 21.3
<b>Total rainfall depth (mm)</b>	131.3	43.7	11.3	129.2

Correlation coefficients are calculated between EMC and loads of TSS and rainfall characteristics to identify explanatory variables that may be used to predict EMC and loads. The rainfall characteristics are: antecedent dry weather period (ADWP), storm duration (Duration), average intensity (Imean), maximum intensity (Imax), maximum five-minute intensity (Imax 5) and precipitation amount (Hrain). Pearson correlation coefficients obtained are presented in Table 7.

**Table 7. Pearson correlation coefficients R between EMC and loads of TSS and rainfall characteristics**

	Pearson correlation coefficient R	
	[TSS]	TSS loads
<b>ADWP</b>	-0.048	0.14
<b>Duration</b>	-0.17	0.37
<b>Imean</b>	-0.19	0.12
<b>Imax</b>	-0.2	0.22
<b>Imax 5</b>	-0.18	0.28
<b>Hrain</b>	-0.26	0.52

No correlation is found between EMC and the antecedent dry weather period, which seems to have no effect on runoff quality ( $R = -0.048$ ). EMC is weakly negatively correlated with the rainfall depth ( $R = -0.26$ ) and the rainfall duration ( $R = -0.17$ ) suggesting the occurrence of dilution during long or heavy storm events.

As for loads, significant positive correlations are more common than for EMC. The strongest correlations are with the precipitation depth ( $R = 0.52$ ) and the storm duration ( $R = 0.37$ ). Positive correlations are also shown with maximum 5 min rainfall intensity and maximum intensity, but the coefficients are small, equal to 0.28 and 0.22, respectively. TSS loads are also positively correlated with the ADWP, however the correlation is weak as Pearson coefficient is low ( $R = 0.14$ ).

### 3.2. Dynamic of transport of TSS

Cumulative mass of TSS plotted against the corresponding cumulative runoff volume is presented in Figure 4. Overall, 17 events are classified as first flush while 22 events are uniformly distributed and three events are last flush.

Clear relationships between  $M(V)$  curves and the characteristics of rainfall events are not obvious. Rainfall depth and intensity have no direct influence on the distribution of  $M(V)$  curves, and neither on of the intensity peak.

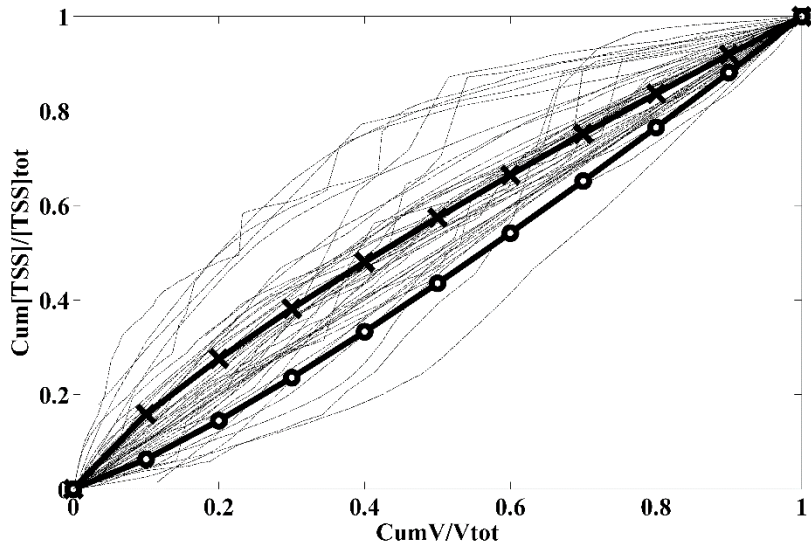


Figure 4.  $M(V)$  of TSS for 42 events from November 2014 to April 2015. The bold lines represent the upper (line with cross) and lower (line with circles) boundaries for the First Flush and Last Flush

### 3.3. Modeling

In this study we did not intend to replicate pollutant masses and our main concern was to replicate the dynamic of concentrations because several studies have shown that pollutant masses are easily predictable. A recent study by Sage et al. [25], who investigated the capacity of the commonly used accumulation/wash-off models on a similar road catchment, clearly demonstrated that load estimates are accurately replicated by the model with a Nash–Sutcliffe coefficient of 0.79. In addition, their results also show that loads are accurately estimated even with simple EMC models (Nash = 0.77). In fact, as the runoff volume is the main driver of event loads, respectable results are expected when the runoff volume is accurately predicted, therefore achieving high performance for modeling loads is easier than modeling pollutant concentrations and their dynamics which is much more complicated.

#### 3.3.1. Wash-off assessment

Figure 5 illustrates the variation of Nash–Sutcliffe coefficients obtained from calibrating on the whole data set. The best performance of the model is obtained when calibrating on first flush events, where Nash–Sutcliffe efficiency is higher than 0.45 for 14 out

of 17 events. This result suggests that SWWM wash-off model is more suitable for describing the fluctuation of TSS concentrations for first flush events.

For last flush and uniformly distributed events, agreement between measured and simulated TSS concentrations is poor and the model performance is unsatisfactory. Nash–Sutcliffe coefficients recorded when calibrating over uniformly distributed storms are lower than 0.15 for half of the events. Better results are obtained for last flush events; nevertheless, they are only assessed over three events and Nash–Sutcliffe coefficients are between 0.42 and 0.57.

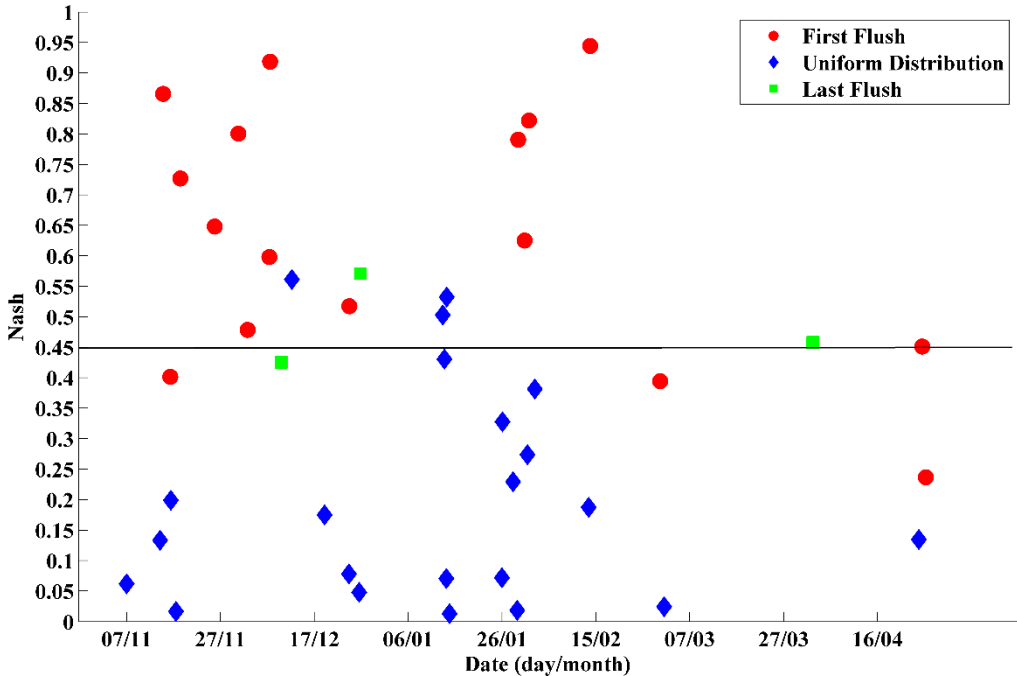
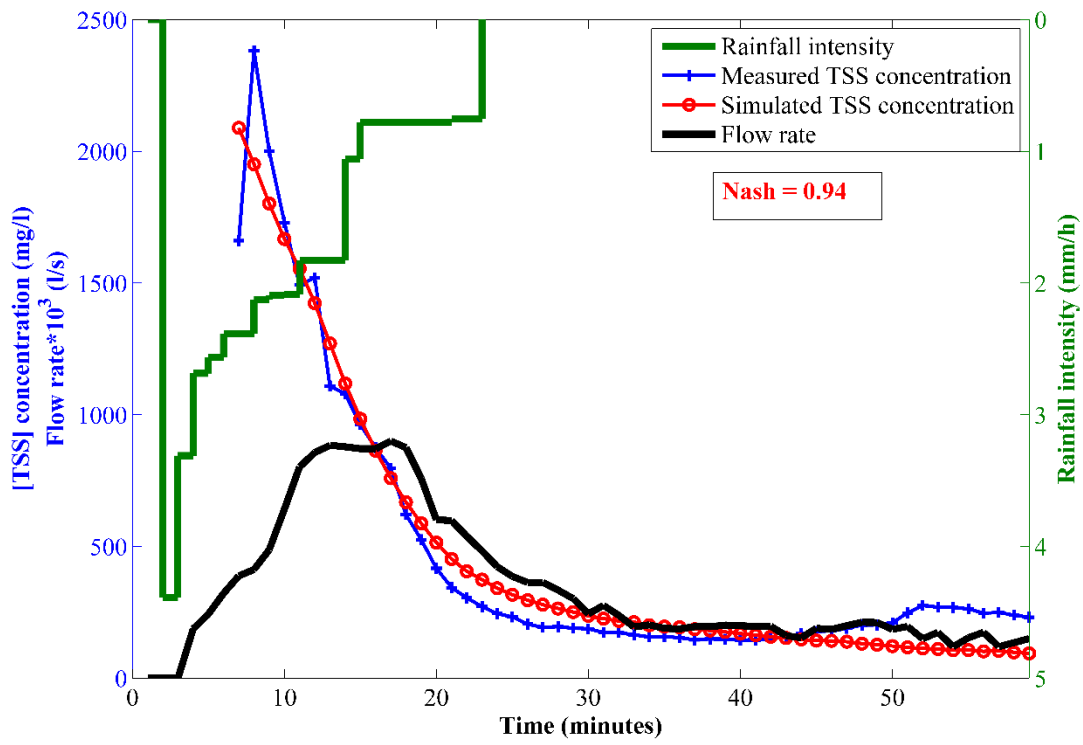
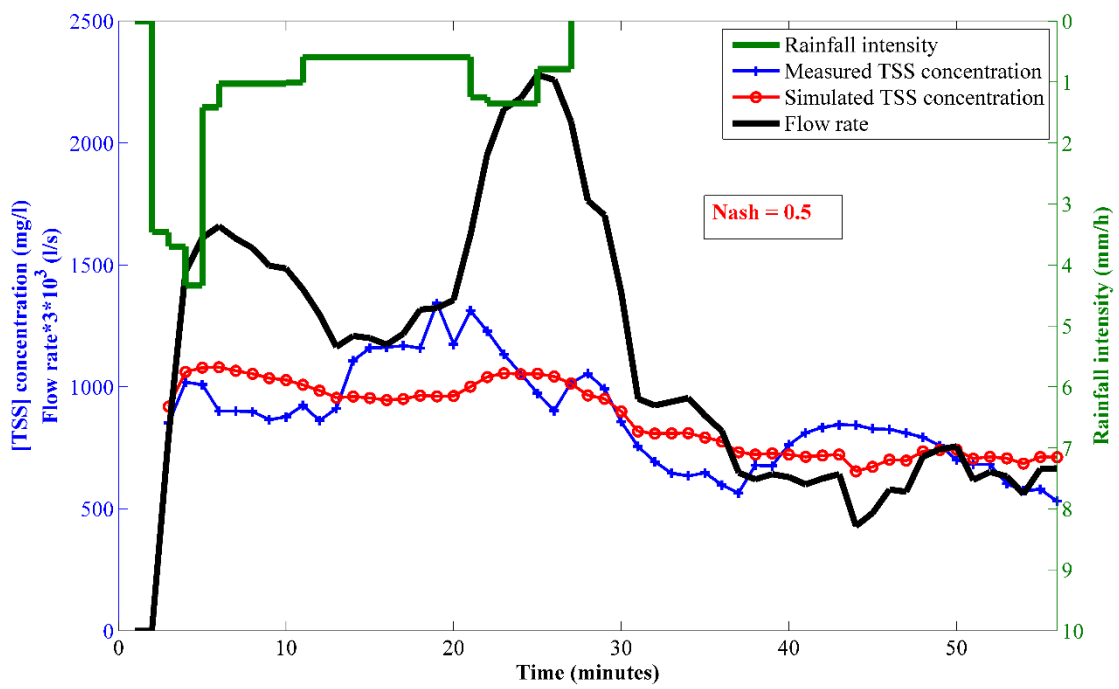


Figure 5. Variation of the Nash–Sutcliffe coefficients obtained when calibrating on first flush, uniformly distributed and last flush events

The pollutographs of three storm events are plotted in Figure 6. It is clearly shown that the simulated data fit very well with the measured data for the first flush event. The dynamic in this case is fully replicated by the model. However, for the other two events, the simulations cannot totally cope with the fluctuations of the concentrations, thus reflecting a lower performance of the model for uniformly distributed and last flush events.



(a)



(b)

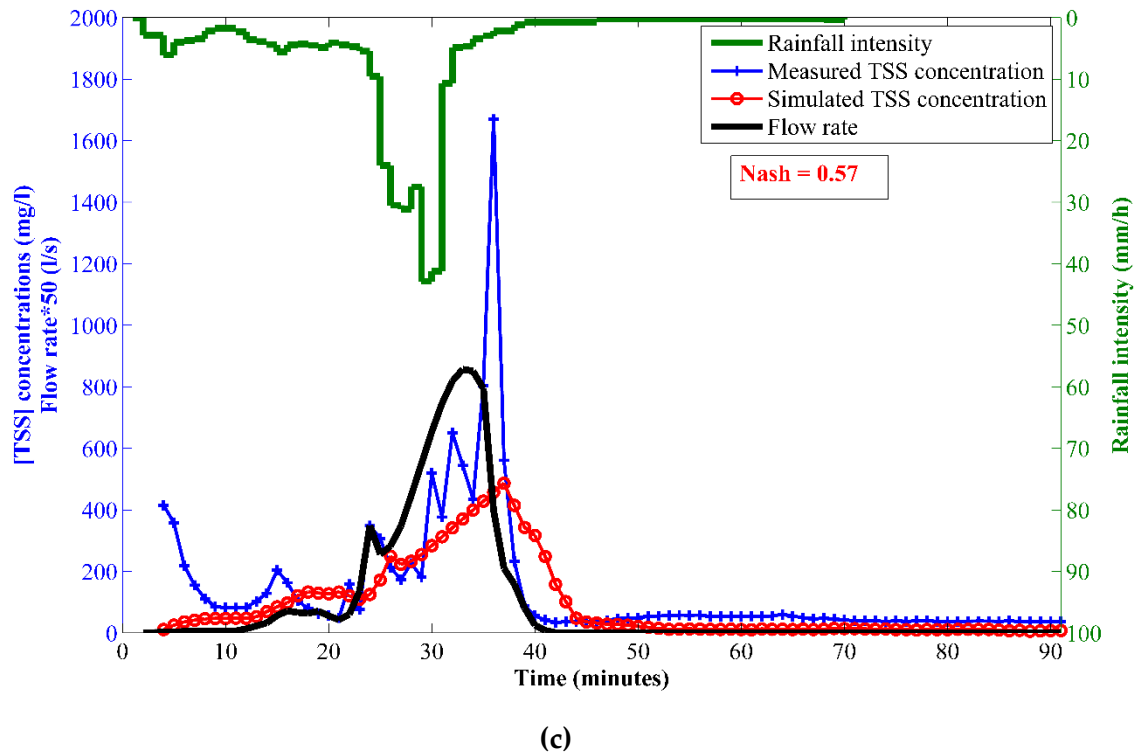


Figure 6. Calibration results for the rainfall events of: (a) 14 February 15 (First flush event); (b) 27 December 14 (Uniformly distributed event); and (c) 13 January 15 (Last flush event).

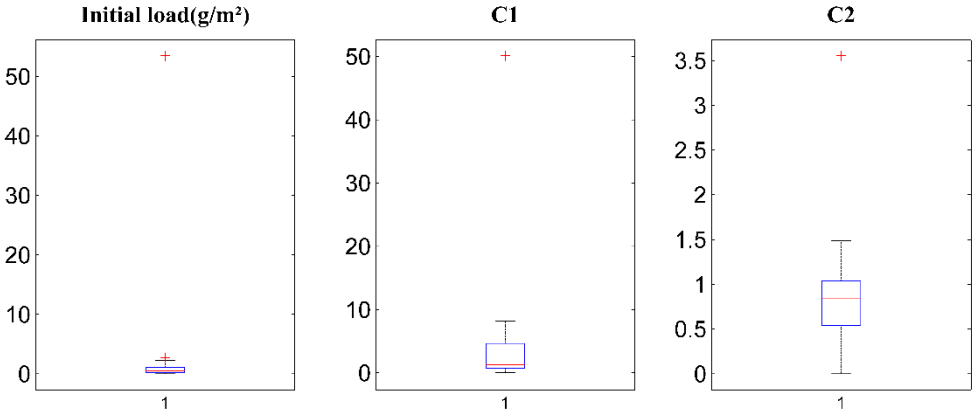
The best replication of TSS concentrations noticed only for first flush events could be attributed to a weakness in the model structure that is not adequate to replicate all types of events and require thus a re-adaptation in order to be not limited to a specific type of events. The re-adaptation could be the coupling of runoff rate with other variables, such as the rainfall intensity, which is proven to be an important explanatory variable of the wash-off process [16], or adding other parameters to the formulation that takes into account the impacts of factors such as the rainfall drop energy and the shear stress.

Since the model performance is not satisfying for all events, the assessment of the variability of optimal parameters as well as the correlations with rainfall characteristics and temperature are performed only on 19 events having a Nash–Sutcliffe coefficient higher than 0.45.

As we can see in Figure 7, showing the boxplots of the calibrated parameters, large variability is observed mainly for the initial load and the wash-off coefficient C1. The calibration on some events also tends to converge to optimum values that have no clear physical significance and that diverge extremely from the mean. The empirical based



formulation of SWMM wash-off model may be an explanatory factor of this result. In fact, the variability of the initial available mass prior to a storm event is also noticed on site where dust collection campaigns were carried over three distinct locations. The experimental protocol for dust collection is detailed in Becher et al. [41]. Dust was collected from the gutter, sidewalk and pavement. The highest mass was collected in the gutter with a mean value of 13.76 g/m<sup>2</sup> compared to 4.14 g/m<sup>2</sup> and 12.03 g/m<sup>2</sup> collected, respectively, on the pavement and on the sidewalk. Comparison of the mean observed and simulated values of available load on the surface shows that the simulations (3.53 g/m<sup>2</sup>) vary in the lower range of observations, which indicates the tendency of the model to underestimate pollutant loads. Moreover, this is confirmed by a significant negative Spearman correlation calculated between the initial load and C1 ( $R = -0.85$ ,  $p\text{-value} < 0.0001$ ). This correlation [42], which is a Pearson correlation calculated between the ranks of the corresponding variables and is not limited to a linear relation, shows that C1 and the initial load compensate each other which may also explain the difficulties encountered during calibration.



**Figure 7. Boxplots of optimal calibrated wash-off parameters. The central mark of each box is the median, the edges represent the 25th and 75th percentiles, and the whiskers extend to the maximum and minimum values that are not considered as outliers**

As for the wash-off exponent, the variability in C2 values suggests different patterns of erosion since the wash-off exponent is regarded as an indicator of the shape of the pollutograph [4]. For one event, C2 is calibrated to zero, suggesting linear variation between the washed pollutant mass and the available one for erosion. While for other events, calibrated C2 values are lower than 1 indicating a reduction in the flow rate and therefore slower rate of transport and decreasing of pollutant concentrations from initial values. A recent study by

Wijesisri et al. [43] shows that the wash-off of particles less than 150  $\mu\text{m}$  is associated with higher values of wash-off exponent and occurs faster than the wash-off of particles larger than 150  $\mu\text{m}$ . Subsequently, the variation of C2 values maybe also related to the difference in size distribution of the eroded particles.

Correlations for each parameter are summarized in Appendix A (Table A1) and significant correlations are presented in bold.

For the initial available mass, positive linear correlations are only calculated with maximum and average temperature ( $R_{T_{\text{max}}} = 0.509$ , p-value < 0.031;  $R_{T_{\text{mean}}} = 0.49$ , p-value < 0.038). No correlation exists with the antecedent dry weather period. This could be related to the fact that calibrated mass included other sources of supply such as the residual mass from the previous storm. Past research has shown that a storm event washes only a fraction of the available pollutants [10,33], therefore remaining loads are added to the ones that build-up during dry period between two rainfalls to give the total available mass for wash-off.

As for wash-off coefficient C1 and wash-off exponent C2, significant linear correlations are calculated with average intensity ( $R_{I_{\text{mean}}} = 0.78$ , p-value < 0.001) and maximum five-minute intensity ( $R_{I_{\text{max}}} = 0.84$ , p-value < 0.001). This finding is consistent with what we mentioned previously on rapid erosion of pollutants related to higher values of wash-off exponent. Accordingly, it is known that intense rainfalls generate drops with high kinetic energies; therefore, during intense storm events, particles are easily detached, eroded and transported by the flow. Alternatively, rainfalls characterized with low intensities generate a diluted runoff since the runoff transport capacity is weak.

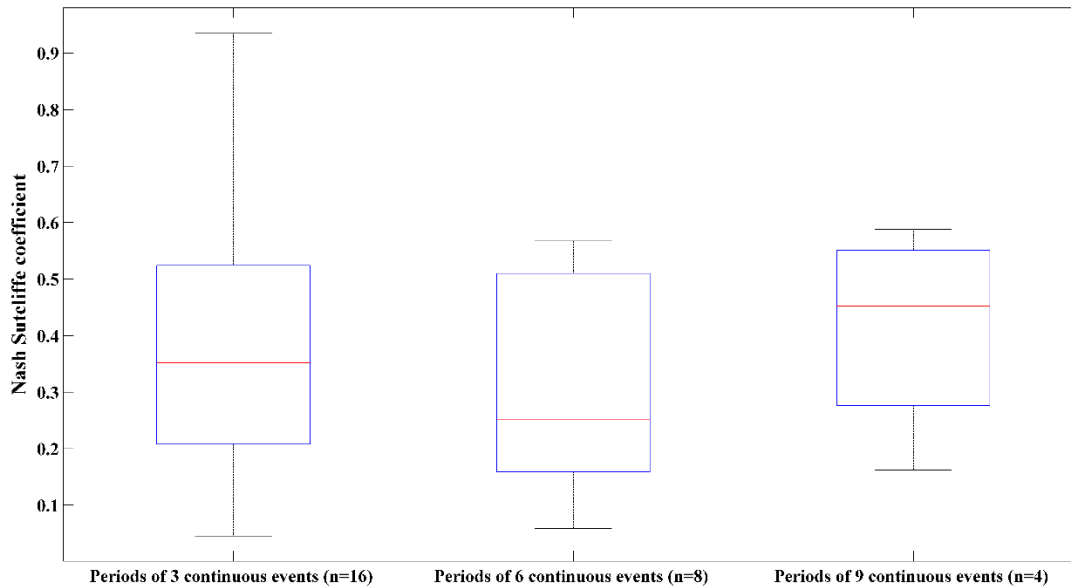
Negative Spearman correlations are calculated between C1 and the rainfall depths ( $R_{\text{rank},H_{\text{rain}}} = - 0.59$ , p-value = 0.008) and durations ( $R_{\text{rank},Duration} = - 0.64$ , p-value = 0.004) respectively; this is likely due to the formulation of the average rainfall intensity that includes the ratio of rainfall depth to rainfall duration.

### **3.3.2. Build-up assessment**

Calibration results obtained for the tested configurations are presented below.

- **Modified SWMM exponential build-up**

Calibrations over periods consisting of three, six and nine continuous events resulted in a wide range of Nash–Sutcliffe coefficients and parameters. Figure 8 shows the boxplot for the Nash–Sutcliffe coefficients obtained for the three periods of calibration.



**Figure 8. Boxplots of Nash–Sutcliffe coefficients obtained when calibrating over periods of three, six and nine continuous events. The central mark of each box is the median of the Nash coefficients; the edges represent the 25th and 75th percentiles, and the whiskers.**

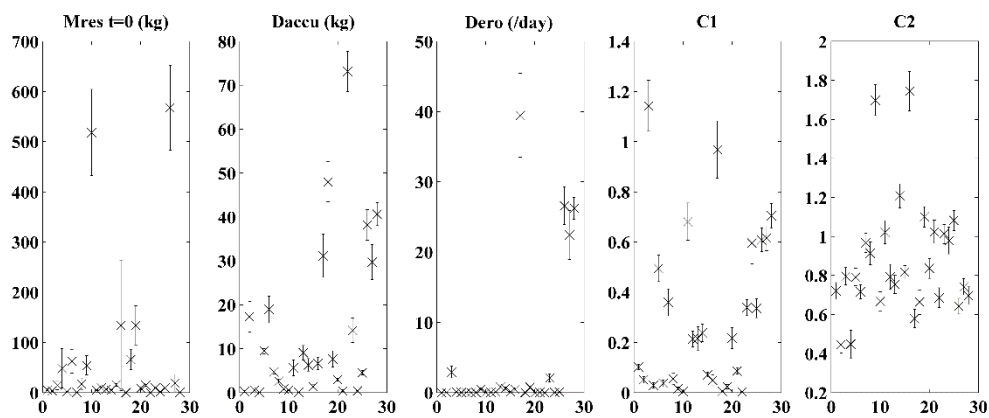
When calibrating over three events, Nash values vary between 0.045 and 0.93. Half of the periods have a Nash–Sutcliffe efficiency lower than 0.35, suggesting that the fit between the observations and the simulations of TSS concentrations is relatively poor.

Results obtained when calibrating over periods of six events are not more encouraging where the overall variation of Nash–Sutcliffe efficiency is between 0.058 and 0.55.

Calibration over periods of nine continuous events was not possible except for four periods due to missing data. Agreement between the measured and the simulated TSS concentrations is roughly reasonable for one period where the Nash–Sutcliffe coefficient is 0.58, while for the other periods it ranges from 0.16 to 0.51.

The behavior of the build-up model is not very obvious because of the large variability of the obtained Nash–Sutcliffe coefficients and the performance of the model is highly dependent on the calibration period. The variability is also noticed in the optimal sets of

calibrated parameters. As seen in Figure 9, the initial available load at the surface has a wide range of variability from zero up to 213.32 g/m<sup>2</sup>. This supports the high stochasticity influencing the accumulation process. The build-up parameters also are at wider ranges than the wash-off coefficients. The accumulation rate represented by the parameter  $D_{\text{accu}}$  varies between 0.0075 g/m<sup>2</sup> and 27.47 g/m<sup>2</sup>, and shows that pollutant accumulation on the surface can be significant for some events.  $D_{\text{ero}}$ , the pollutant removal rate during dry weather, is calibrated to zero for most of the events, which indicates that the equilibrium load represented by  $D_{\text{accu}}/D_{\text{ero}}$  tends to infinity, supporting the hypothesis of the presence of unlimited supply on the surface. As for wash-off coefficients, C1 has broader interval of variation than C2 who appears to be the best determined parameter since it fluctuates in the interval between 0.6 and 0.8 for the majority of the events. The uncertainty on the estimated parameters seems to be insignificant except for some events where the high dispersion of the calibrated parameter indicate that the model is not sensitive to the best calibrated set of parameters and that no optimum truly exist. This uncertainty will induce errors in the modeling outputs and justifies the low Nash–Sutcliffe efficiencies obtained in some cases.



**Figure 9. Standard deviation of the posterior probability of build-up and wash-off parameters**

To evaluate the suitability of the model for simulating the TSS concentrations over long term, we decided to calibrate the model over four successive incrementing length periods of three events increment and then compare the obtained Nash–Sutcliffe efficiencies.

As indicated in Figure 10 the model capacity to estimate the accumulated load between storm events has clearly declined after considering more than 3 events except for the first calibration period that started on the 14 November. For example, Nash coefficient has decreased from 0.93, to 0.54 and 0.58, respectively, when the calibration period starting the 16

November is extended to include six and nine consecutive events. The model performance is slightly different when comparing calibrations over six and nine events, with better Nash–Sutcliffe efficiency calculated over the periods consisting of six events except for the 16 November. This finding reveals the difficulties of calibrating the build-up model and the inefficiency of the model as it is to reproduce the inter-event variability and the complexity of the accumulation process over a long temporal scale.

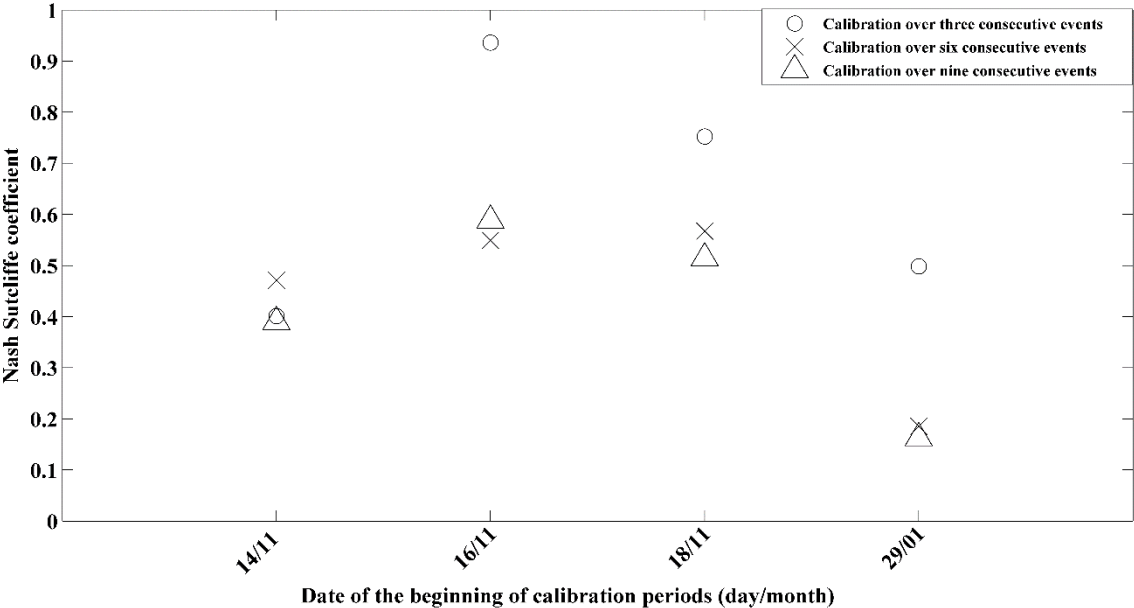


Figure 10. Nash coefficients calculated over four periods considering calibration over three, six and nine continuous.

Further investigation consisted on comparing the results obtained under the assumption of exponential build-up and the results obtained when the build-up model was omitted. Nash–Sutcliffe efficiencies are calculated in each case and the results are summarized in Figure 11.

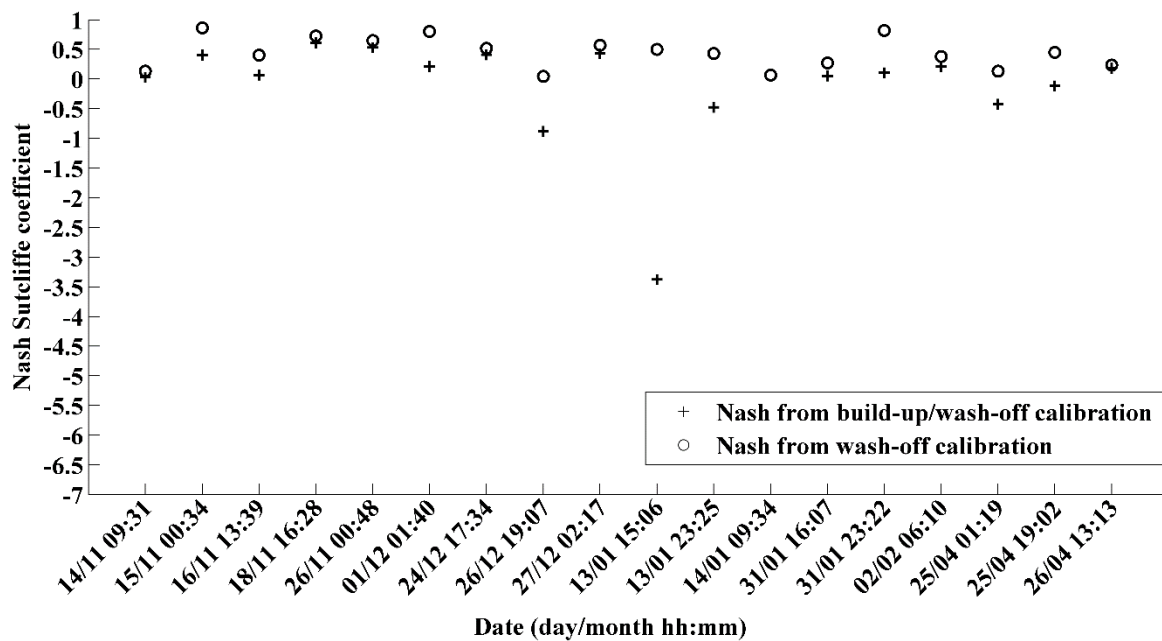


Figure 11. Comparison of the Nash coefficients calculated when calibrating the build-up and wash-off on periods of three successive events and the Nash coefficients calculated when calibrating only the wash-off.

The comparison shows that the model performance has decreased when the build-up model is introduced, suggesting that the initial TSS load predicted by the model is incorrect. Acceptable results were only obtained for the calibration period starting on the 18 November where the Nash–Sutcliffe coefficients calculated when calibrating the build-up (0.614 and 0.529) were slightly different from the Nash–Sutcliffe coefficients calculated when calibrating only the wash-off (0.727 and 0.648). However, for the rest of calibration periods, the ability to replicate TSS concentrations clearly decreased. This result indicates that the model performance is not significantly affected by modeling the pollutant build-up, which can be easily neglected without any consequences on the predictive capacity of the model.

- **Power build-up**

Calibration of the model is first performed over 16 periods of three consecutive events each. Same as for the exponential model, the model performance and the calibrated parameters are very distinct from one event to another as shown in Figure12.

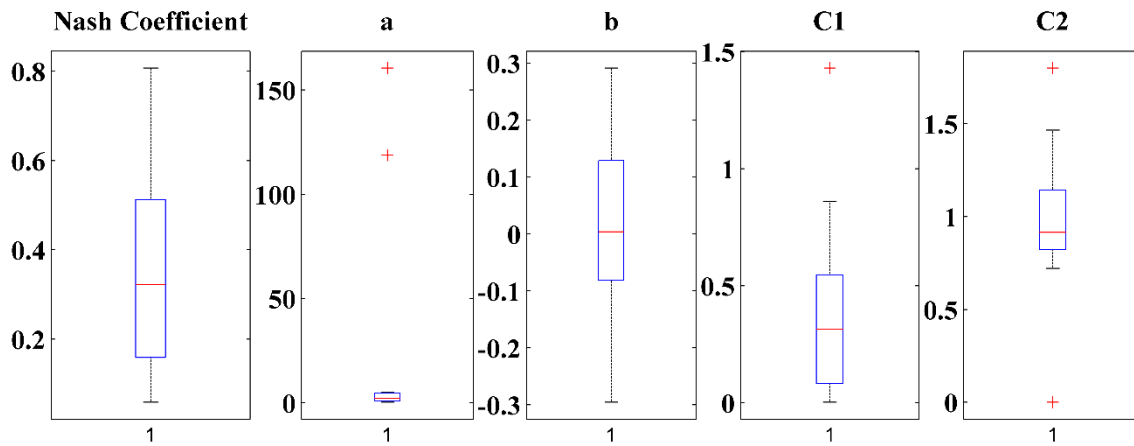


Figure 12. Boxplots of Nash–Sutcliffe coefficients, power build-up parameters and wash-off parameters obtained when calibrating over Periods of three continuous events

Nash–Sutcliffe coefficients range between 0.058 and 0.8 and the values associated with build-up parameters *a* and *b* are extremely variable. This is related mainly to the existing correlation between these parameters ( $R_{\text{Pearson}} = -0.56$ ,  $p\text{-value} = 0.023$ ), indicating that same results can be obtained combining different sets of *a* and *b*. The calibration of the parameter *b* results in negative and low values for most of the periods which proves that the model is completely dependent on the coefficient *a* to better fit the observations and that is not using the antecedent dry weather period as a predictive variable. Parameter *a* have the biggest weight in the calibration of the model and it compensates the effect of all other components. These results indicate that the structure of the model should be reviewed.

Comparison between the performances of the exponential and the power equations reveals that no specific model has the best performance for all periods (Figure 13). It seems that the exponential model outperforms the power model when calibrated on periods before 30 January and after that date the two models perform similarly in terms of simulating TSS concentrations.

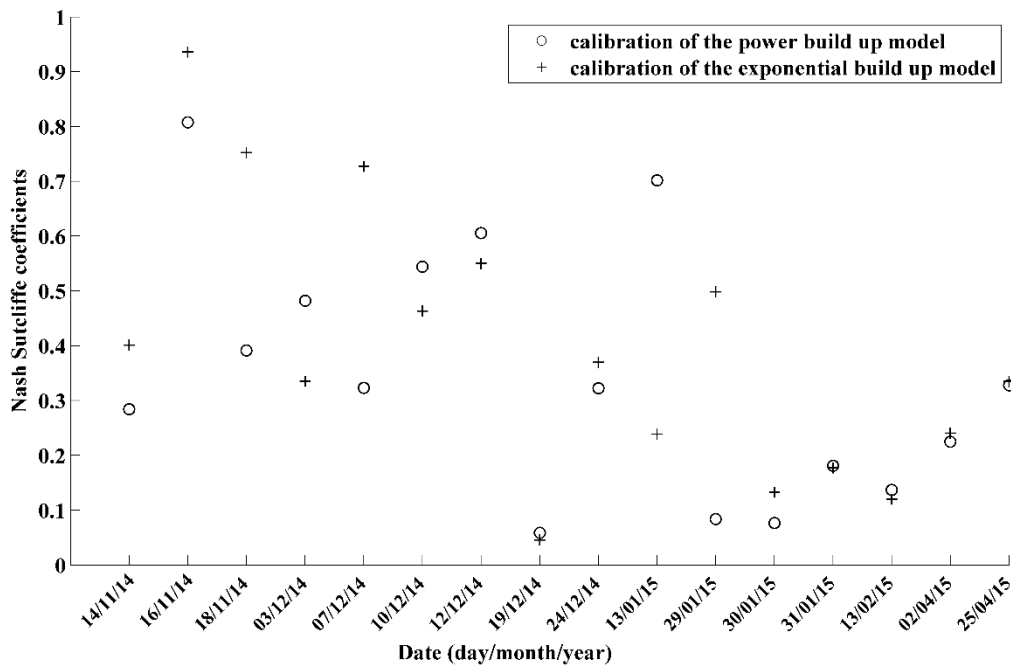


Figure 13. Comparison of the Nash–Sutcliffe coefficients calculated when calibrating the exponential build-up and the power build-up

The replication of the variability of the accumulation process under the assumption of dry weather period as being the main explanatory variable does not seem very accurate. The test of both SWMM and power models based on dry weather period and their unsatisfactory performance support this assumption.

Different sources of supply independent of dry weather period and resulting from random phenomenon such as leaf fall, and de-icing salt during fall and winter as well as animal wastes that occur between events are not taken into consideration in the models in their current formulation, which highly affect the stock of mass present of the surface and lead to a failure in its accurate estimate.

### 3.3.3.Short term predictive capacity

To assess the short term predictive capacity of water quality model that couples the exponential build-up and SWMM wash-off equations, two methodologies are tested and the obtained results are presented in the sections below.



- **Inter event**

The first approach consists of validating the model on the events immediately after the calibration period, making the assumption that the parameters remain valid during a given time after calibration. Only periods for which calibration was successful were considered. The results show that despite the efficient calibration of the model, its prediction capacity is very poor (Table8).

**Table 8. Nash Coefficients obtained from calibration and validation over the modelling period.**

<b>Beginning of the modelling period</b>	<b>Nash coefficient from calibration over the first two events</b>	<b>Nash coefficient from validation over the 3<sup>rd</sup> event</b>
2014-11-14	0.527	-0.5714
2014-11-17	0.787	-0.5981
2014-12-07	0.781	0.1643
2015-01-13	0.616	-0.5890
2015-01-30	0.629	-0.8874

The Nash–Sutcliffe coefficients reflect a very weak replication of the pollutograph and show that high errors are included in the predicted TSS concentrations, which do not seem to fit at all the observations and are very far from the ranges of variations of the measurements. The application of such models to predict pollutants from storm water runoff is thus largely limited and suggest that the characteristics of the calibrated parameters certainly cannot be kept or extended even to a limited number of events following immediately calibration period, making the assumption that calibrated parameters are not site specific rather event specific and that no unique set of parameters can replicate accurately the pollutographs for all considered periods.

- **Intra Event**

This approach consists in calculating the available pollutant mass at the beginning of the storm using the measurements recorded on the first time steps and the wash-off parameters calibrated from a previous knowledge of the studied site. The method is assessed over 38 single events. Four events are excluded because their calibration efficiency is very low. The 38 events consist of 17 first flush events, 18 with uniform distribution of pollutants and three last flush.

The calculated Nash–Sutcliffe Coefficients over the 38 events are presented in the Figures 14 and 15 below. The bar plots distinguish the results in function of the number of points considered for the calculation of the available initial load for erosion.

Validation results are mostly satisfactory when applying this method over first flush events. Three events are accurately predicted when using only the first two observations for calculating the available erodible load where Nash–Sutcliffe efficiencies were equal to 0.83, 0.57 and 0.46. Based on the first 30 points of observations, the model adequately predicted six events. This is an interesting result and could be helpful for the operational in the context of predicting the dynamic of the pollutants during a rainfall event only by knowing the dynamic at the beginning of the storm.

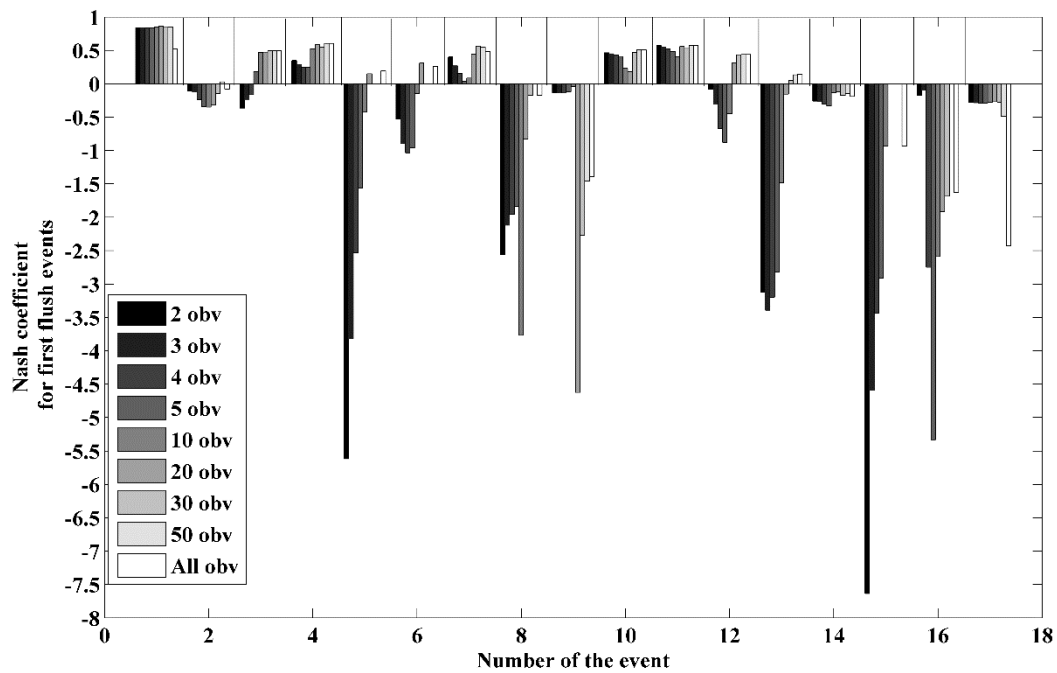


Figure 14. Bar plot of the Nash Sutcliffe coefficients calculated for first flush events.

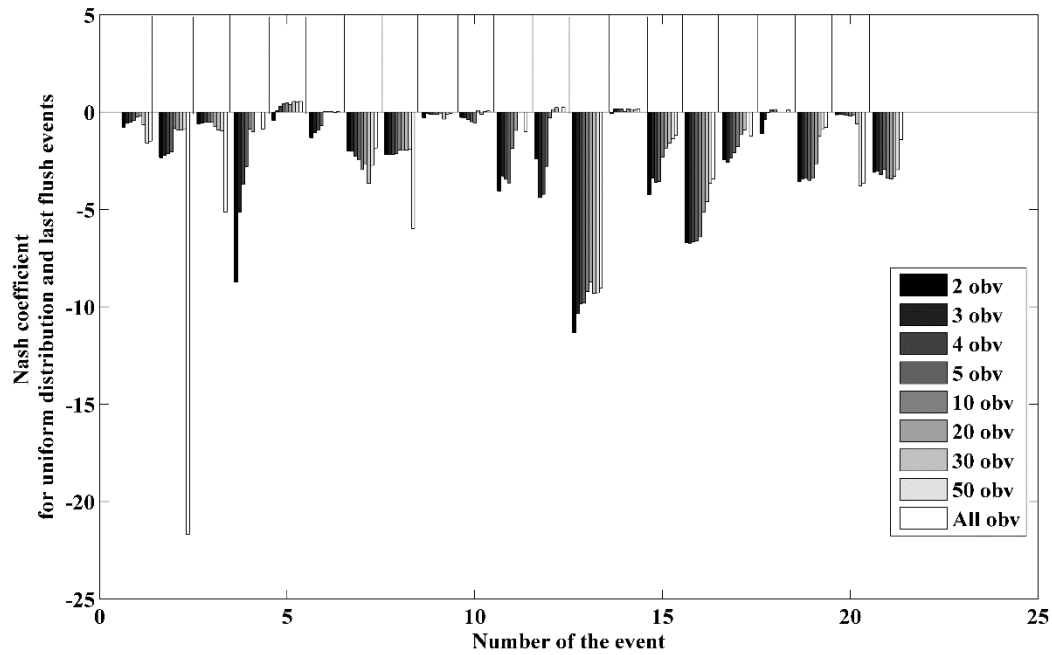


Figure 15. Bar plot of the Nash Sutcliffe coefficients calculated for uniformly distributed and last flush events.

As for the uniformly distributed events and the last flush events, the prediction of the model is not satisfying except for one uniform event where the pollutant concentrations are predicted with a Nash–Sutcliffe efficiency equal to 0.43, calculated when five points of the observations were included in the estimation of the available mass and it increased to 0.54 if the first 30 min of measurements were considered.

The intra-event approach based on data assimilation seems to be promising and deserves further investigation so it can be extended to give accurate prediction not only to first flush events.

The interest of this approach is that it may help planners and engineers to make accurate loading estimates based only on the first measurements and on the knowledge of the behavior of the catchment. Monitoring devices can be thus implemented to record the first points of observations, which can be transmitted automatically to a registration system and be integrated directly with numerical simulations.

#### 4. Conclusions and perspectives

This study presents a framework on modeling and assessing the TSS concentration generated during storm events on an urban road catchment. Qualitative characterization of

the studied site as well as calibration and prediction assessment of different water quality configurations are performed on a long-term database collected between June 2014 and April 2015. The results show that the performance of SWMM wash-off model depends on the dynamic of transport of pollutant during the event where the best fit between the observed and simulated TSS concentrations is recorded for first flush events. Assessment of SWMM exponential build-up model reveals that the model performs better on short periods suggesting the incapacity of the model to simulate the variation of the available mass for erosion for long periods. High variability involved in modeling the production of pollutants emerges from the large differences in the model's performance over distinct calibration periods. This behavior must be further investigated and stochastic approaches might hold the answers to better understand the accumulation process [43–45]. As for the predictive capacity of the model on the inter-event scale, the results clearly prove the inadequacy of the traditional build-up/wash-off model to predict the pollutograph using calibrated parameters, which seem to be event specific rather than site specific. The complexity of the accumulation and wash-off process, which is not very explicit in the model structure, and the absence of factors that play an important role in the generation of pollutants would have a significant fingerprint on the model outputs. On the intra-event scale, based on data assimilation, the model predicts half of the first flush events but is not able to predict last flush and the uniformly distributed events, which does not seem very surprising since these events were not satisfactorily calibrated. This method is very interesting for management practices because of its simplicity and its easy implementation; in addition, it also resolves the problem of missing data that occurs sometimes due to technical problems, making it possible to estimate the yield of a storm event even if not all points are recorded. Further investigation is indeed necessary to enhance this method and develop further the integration of data assimilation in the water quality modeling.

The complexity of the build-up and the wash-off processes and their limited knowledge in addition to the high variability in the modeling results highlighted in this study, rise the need for further in deep investigation of the mechanisms governing the generation and the transport of pollutant in urban catchments. For that matter, extensive site monitoring is recommended to better understand and assess from a physical point of view the implicated factors in the accumulation and erosion processes and the interactions within the system to have a precise and accurate estimation of the pollutograph generated during wet weather.

## Appendix A

Table A1. Pearson and Spearman Correlations and their corresponding p-values.

Initial available mass				
	R linear	p-value	R Spearman	p-value
Hrain	-0.052	0.836	0.101	0.689
Imax	0.086	0.734	-0.180	0.471
Imax 5	0.122	0.628	-0.015	0.954
Imean	-0.056	0.824	0.032	0.901
Duration	-0.106	0.675	0.120	0.632
ADWP	-0.083	0.742	-0.358	0.144
Tmax	0.509	0.031	0.106	0.674
Tmin	0.436	0.07	0.202	0.420
Tmean	0.491	0.038	0.16	0.525

C1				
	R linear	p-value	R Spearman	p-value
Hrain	-0.184	0.463	<b>-0.597</b>	<b>0.008</b>
Imax	-0.034	0.890	-0.275	0.267
Imax 5	0.009	0.971	-0.257	0.302
Imean	<b>0.779</b>	<b>&lt;0.001</b>	0.153	0.541
Duration	-0.283	0.256	<b>-0.645</b>	<b>0.004</b>
ADWP	0.212	0.398	0.279	0.260
Tmax	0.192	0.445	-0.240	0.336
Tmin	-0.051	0.838	-0.297	0.230
Tmean	0.097	0.701	-0.244	0.327

C2				
	R linear	p-value	R Spearman	p-value
Hrain	0.241	0.321	0.186	0.444
Imax	<b>0.649</b>	<b>0.002</b>	0.368	0.121
Imax 5	<b>0.846</b>	<b>&lt;0.001</b>	0.340	0.154
Imean	0.382	0.106	0.431	0.066
Duration	-0.114	0.642	-0.184	0.448
ADWP	-0.035	0.886	0.098	0.688
Tmax	0.237	0.327	0.136	0.578
Tmin	-0.055	0.823	-0.063	0.797
Tmean	0.067	0.785	0.053	0.827

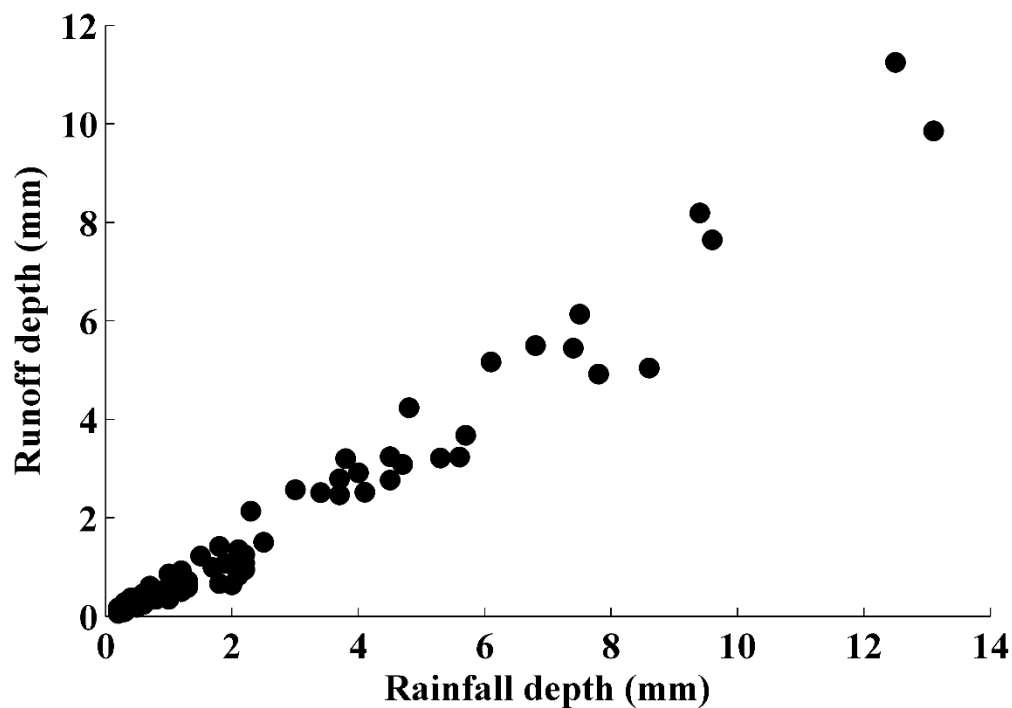


Figure A 1. Variation of runoff depth in function of rainfall depth for 106 events.

## 5. References

1. Elliott, A.; Trowsdale, S. A review of models for low impact urban stormwater drainage. *Environ. Model. Softw.* **2007**, *22*, 394–405.
2. Gromaire, M.-C. *La Pollution des Eaux Pluviales Urbaines en Réseau d'Assainissement Unitaire. Caractéristiques et Origines*; Ecole des Ponts ParisTech: Marne-la-Vallée, France, 1998.
3. Bressy, A. *Flux de Micropolluants Dans les Eaux de Ruissellement Urbaines: Effets de Différents Modes de Gestion à l'Amont*; Université Paris-Est: Paris, France, 2010.
4. Bai, S.; Li, J. Sediment Wash-Off from an Impervious Urban Land Surface. *J. Hydrol. Eng.* **2013**, *18*, 488–498.
5. Gunawardana, C.; Goonetilleke, A.; Egodawatta, P.; Dawes, L.; Kokot, S. Role of Solids in Heavy Metals Buildup on Urban Road Surfaces. *J. Environ. Eng.* **2012**, *138*, 490–498.
6. Hengren, L.; Goonetilleke, A.; Ayoko, G.A. Analysis of heavy metals in road-deposited sediments. *Anal. Chim. Acta* **2006**, *571*, 270–278.
7. Mahbub, P.; Goonetilleke, A.; Ayoko, G.A.; Egodawatta, P.; Yigitcanlar, T. Analysis of build-up of heavy metals and volatile organics on urban roads in gold coast, Australia. *Water Sci. Technol.* **2011**, *63*, 2077–2085.

8. Sabin, L.D.; Lim, J.H.; Stolzenbach, K.D.; Schiff, K.C. Contribution of trace metals from atmospheric deposition to stormwater runoff in a small impervious urban catchment. *Water Res.* **2005**, *39*, 3929–3937.
9. Shaw, S.B.; Walter, M.T.; Steenhuis, T.S. A physical model of particulate wash-off from rough impervious surfaces. *J. Hydrol.* **2006**, *327*, 618–626.
10. Vaze, J.; Chiew, F.H. Experimental study of pollutant accumulation on an urban road surface. *Urban Water* **2002**, *4*, 379–389.
11. Bertrand-Krajewski, J.-L.; Chebbo, G.; Saget, A. Distribution of pollutant mass vs volume in stormwater discharges and the first flush phenomenon. *Water Res.* **1998**, *32*, 2341–2356.
12. European Commission. Directive of the European Parliament and of the Council n 2000/60/EC establishing a framework for the community action in the field of water policy. *Off. J. Eur. Communities* **2000**, *327*, 1–72.
13. Dotto, C.B.S.; Kleidorfer, M.; Deletic, A.; Rauch, W.; McCarthy, D.T.; Fletcher, T.D. Performance and sensitivity analysis of stormwater models using a Bayesian approach and long-term high resolution data. *Environ. Model. Softw.* **2011**, *26*, 1225–1239.
14. Sartor, J.D.; Boyd, G.B.; Agardy, F.J. Water Pollution Aspects of Street Surface Contaminants. *J. Water Pollut. Control Fed.* **1974**, *46*, 458–467.
15. Francey, M.; Duncan, H.P.; Deletic, A.; Fletcher, T.D. Testing and Sensitivity of a Simple Method for Predicting Urban Pollutant Loads. *J. Environ. Eng.* **2011**, *137*, 782–789.
16. Vaze, J.; Chiew, F.H.S. Comparative evaluation of urban storm water quality models. *Water Resour. Res.* **2003**, *39*, 1280.
17. Alley, W.; Smith, P. Estimation of Accumulation Parameters for Urban Runoff Quality Modeling. *Water Resour. Res.* **1981**, *17*, 1657–1664.
18. Heng, B.C.P.; Sander, G.C.; Armstrong, A.; Quinton, J.N.; Chandler, J.H.; Scott, C.F. Modeling the dynamics of soil erosion and size-selective sediment transport over nonuniform topography in flume-scale experiments. *Water Resour. Res.* **2011**, *47*.
19. Massoudieh, A.; Abrishamchi, A.; Kayhanian, M. Mathematical modeling of first flush in highway storm runoff using genetic algorithm. *Sci. Total Environ.* **2008**, *398*, 107–121.
20. Hong, Y.; Bonhomme, C.; Le, M.-H.; Chebbo, G. A new approach of monitoring and physically-based modelling to investigate urban wash-off process on a road catchment near Paris. *Water Res.* **2016**, *102*, 96–108.
21. Ball, J.E.; Jenks, R.; Aubourg, D. An assessment of the availability of pollutant constituents on road surfaces. *Sci. Total Environ.* **1998**, *209*, 243–254.
22. Huber, W.C.; Dickinson, R.E.; Barnwell, T.O., Jr.; Branch, A. Storm Water Management Model, Version 4; U.S. Environmental Protection Agency, Environmental Research Laboratory: Athens, GA, USA, 1988.
23. Servat, E. Contribution à l'étude de la Pollution du Ruissellement Pluvial Urbain. Ph.D. Thesis, Université des Sciences et Techniques du Languedoc, Montpellier, France, 1987.

24. Dembélé, A.; Bertrand-Krajewski, J.-L.; Becouze, C.; Barillon, B.; Dauthuille, P. TSS, COD and Priority Pollutants in Stormwater—Event Fluxes Modelling Using Conceptual Approach, 2013. Available online: <http://hdl.handle.net/2042/51284> (accessed on 7 December 2015).
25. Sage, J.; Bonhomme, C.; Al Ali, S.; Gromaire, M.-C. Performance assessment of a commonly used “accumulation and wash-off” model from long-term continuous road runoff turbidity measurements. *Water Res.* **2015**, *78*, 47–59.
26. Wang, L.; Wei, J.; Huang, Y.; Wang, G.; Maqsood, I. Urban nonpoint source pollution buildup and washoff models for simulating storm runoff quality in the Los Angeles County. *Environ. Pollut.* **2011**, *159*, 1932–1940.
27. Kanso, A.; Tassin, B.; Chebbo, G. A benchmark methodology for managing uncertainties in urban runoff quality models. *Water Sci. Technol.* **2005**, *51*, 163–170.
28. Métadier, M.; Bertrand-Krajewski, J.-L. From mess to mass: A methodology for calculating storm event pollutant loads with their uncertainties, from continuous raw data time series. *Water Sci. Technol.* **2011**, *63*,
29. Mourad, M.; Bertrand-Krajewski, J.-L. A method for automatic validation of long time series of data in urban hydrology. *Water Sci. Technol.* **2002**, *45*, 263–270.
30. Becouze-Lareure, C.; Invernon, N. EVOHE-Logiciel de Suivi des Capteurs—Validation de Données-Auto-Surveillance des Systèmes d’Assainissement; INSA Lyon ALISON: Lyon, France, 2014.
31. Zoppou, C. Review of urban storm water models. *Environ. Model. Softw.* **2001**, *16*, 195–231.
32. Obropta, C.C.; Kardos, J.S. Review of Urban Stormwater Quality Models: Deterministic, Stochastic, and Hybrid Approaches JAWRA. *J. Am. Water Resour. Assoc.* **2007**, *43*, 1508–1523.
33. Egodawatta, P.; Thomas, E.; Goonetilleke, A. Mathematical interpretation of pollutant wash-off from urban road surfaces using simulated rainfall. *Water Res.* **2007**, *41*, 3025–3031.
34. Egodawatta, P. Translation of Small-Plot Scale Pollutant Build up and Wash off Measurements to Urban Catchment Scale. Ph.D. Thesis, Queensland University of Technology, Brisbane, Australia, 2007.
35. Bonhomme, C.; Petrucci, G. Spatial Representation in semi-distributed modelling of water quantity and quality. In International Conference on Urban Drainage, Kuching, Malaysia; ICUD: Kuching, Malaysia, 2014; p. 2488399.
36. Hasting, W.K. Monte carlo sampling methods using Markov chains and their applications. *Biometrika* **1970**, *57*, 97–109.
37. Nash, J.E.; Sutcliffe, J.V. River flow forecasting through conceptual models part I—A discussion of principles. *J. Hydrol.* **1970**, *10*, 282–290.



38. Lee, J.H.; Bang, K.W.; Ketchum, L.H.; Choe, J.S.; Yu, M.J. First flush analysis of urban storm runoff. *Sci. Total Environ.* **2001**, *293*, 163–175.
39. Maniquiz, M.C.; Lee, S.; Kim, L.-H. Multiple linear regression models of urban runoff pollutant load and event mean concentration considering rainfall variables. *J. Environ. Sci.* **2010**, *22*, 946–952.
40. Gnecco, I.; Berretta, C.; Lanza, L.G.; La Barbera, P. Storm water pollution in the urban environment of Genoa, Italy. *Atmos. Res.* **2005**, *77*, 60–73.
41. Bechet, B.; Bonhomme, C.; Lamprea, K.; Campos, E.; Jean Soro, L.; Dubois, P.; Lherm, D. Towards a Modeling of Traffic Pollutant Flux at Local Scale—Chemical Analysis and Micro-Characterization of Road Dusts. Available online: [http://hues.se/assets/Abstract\\_final\\_2015-05-27-final1.pdf](http://hues.se/assets/Abstract_final_2015-05-27-final1.pdf) (accessed on 22 March 2016).
42. Spearman, C. The Proof and Measurement of Association between Two Things. *Am. J. Psychol.* **1904**, *15*, 72–101.
43. Wijesiri, B.; Egodawatta, P.; McGree, J.; Goonetilleke, A. Influence of pollutant build-up on variability in wash-off from urban road surfaces. *Sci. Total Environ.* **2015**, *527–528*, 344–350.
44. Daly, E.; Bach, P.M.; Deletic, A. Stormwater pollutant runoff: A stochastic approach. *Adv. Water Resour.* **2014**, *74*, 148–155.
45. Wijesiri, B.; Egodawatta, P.; McGree, J.; Goonetilleke, A. Incorporating process variability into stormwater quality modelling. *Sci. Total Environ.* **2015**, *533*, 454–461.

## Chapitre 2. Contribution of atmospheric dry deposition to stormwater loads for PAHs and trace metals in a small and highly trafficked urban road catchment

**Abstract:** A deep understanding of pollutant build-up and wash-off is essential for accurate urban stormwater quality modeling and for the development of stormwater management practices, knowing the potential adverse impacts of runoff pollution on receiving waters. In the context of quantifying the contribution of airborne pollutants to the contamination of stormwater runoff, and assessing the need of developing an integrated AIR-WATER modeling chain, loads of polycyclic aromatic hydrocarbons (PAHs) and metal trace elements (MTEs) are calculated in atmospheric dry deposits, stormwater runoff and surface dust stock within a small yet highly trafficked urban road catchment (~30,000 vehicles per day) near Paris. Despite the important traffic load and according to the current definition of “atmospheric” source, atmospheric deposition did not account for more than 10% of the PAHs and trace metals loads in stormwater samples for the majority of the events, based on the ratio of deposition to stormwater. This result shows that atmospheric deposition is not a major source of pollutants in stormwater and thus linking the air and water compartment in a modeling chain to have more accurate estimates of pollutant loads in water might not be relevant. Comparison of road dust with water samples demonstrate that only the fine fraction of the available stock is eroded during a rainfall event. Even if the atmosphere mostly generates fine particles, the existence of other sources of fine particles to stormwater runoff is highlighted.

**Keywords:** Atmospheric deposition, Stormwater, Urban catchment, PAHs, Trace metal, Street dust.

### 1. Introduction

Significant amounts of polycyclic aromatic hydrocarbons (PAHs) and metal trace elements (MTEs) are released daily into the atmosphere of urban settings (Sabin et al. 2005), mainly through anthropogenic activities (Wang et al. 2011; Mijić et al. 2010; Bozlaker et al. 2008; Garban et al. 2002). These include road traffic, industrial activities as well as residential

heating, whose contribution significantly increases in winter (Weinbruch et al. 2014; Motelay-Massei et al. 2005; Terzi et Samara 2005; Rocher et al. 2004).

Pollutants accumulated on urban surfaces are generated from a wide variety of processes including atmospheric dry and wet deposition, direct exhaust emissions of vehicles, vehicle degradation (tire, brake...), leakage of oil and gasoline, deterioration of the road surface and re-deposition of soil particles under the effect of wind (Fallah shorshani et al. 2012; Gunawardena et al. 2015). After emission and deposition, pollutants are washed off from urban surfaces during rainfall events. Given the toxicity of PAHs and MTEs, urban stormwater pollution will have detrimental impacts on the receiving water environment (Lamprea and Ruban 2011; Joshi and Balasubramanian 2010; Egodawatta et al. 2007; Tasdemir et al. 2006).

The largest proportion of metals and PAHs exported to the receiving environment are bounded to the particulate matter and distributed over the particle size distribution (Kim and Sansalone 2008; Zhao and Li 2013). Particles originating from various sources have a heterogeneous composition, and knowing their granulometry is essential to give insights into their mobility and chemical retention capacity (Zhao et al. 2010). The focus has always been on the fine particles because of their sorption capacity (Herngren, et al. 2006; Padoan et al. 2017). They also contribute to air pollution through the mechanism of re-suspension (Amato et al. 2011; Pant and Harrison 2013). Particles  $< 10\mu\text{m}$  in street dust originates mainly from anthropogenic activities including brake and tire wear, motor exhaust and road wear (Amato et al. 2011). Atmospheric deposition also contributes to the fine content of street dust where Cao et al. (2011) reported that  $>70\%$  of atmospheric deposits have an aerodynamic diameter  $< 30\mu\text{m}$ . They also demonstrated that this fraction contained the highest fraction of toxic trace metals.

Nowadays, urban modeling evolves more and more toward integrated modeling, associating different research fields (Bach et al. 2014). Saagi et al. (2017) evaluated control strategies in urban wastewater systems based on a benchmark simulation model that simulates the dynamics of flow rates and pollutants within the catchment, the sewer network, the wastewater treatment plant and finally the river water system. In another study, integrated modeling have been developed to simulate the impact of traffic on both air and water quality, where traffic, emission, atmospheric dispersion and stormwater quality models were coupled

(Fallah Shorshani et al. 2015). This integrated modeling is now more recognized as an important tool to account for the complexity of the investigated processes such as the urban environmental pollution. In fact, some pollutants are present as air, water and soil pollutants. Therefore, an accurate urban stormwater quality modeling based on the deep understanding of pollutant build-up and wash-off, must assess the utility of incorporating the precise knowledge of these processes at the interface between air and water. However, the integration of air and water quality models needs to rely on solid experimental basis.

Today, commonly used water quality models are far from being reliable as the simulated pollutographs are poorly consistent with the measurements (Al Ali et al. 2016; Sage et al. 2015; Dotto et al. 2011). These results are supposed to be mainly due to the lack of knowledge of the accumulation process. This is reflected in the models by the non-exhaustive consideration of the various mechanisms of accumulation governing the build-up, as well as the difficulty to know exactly which amount of pollutant directly settle on the ground and which one is transported for a while through the atmosphere.

Among the build-up processes, atmospheric deposition in urban catchments is related to the intensity of traffic and human activities and it is particularly site-dependent (Sabin et al. 2005). It is therefore relevant to quantify the atmospheric deposition as a source of PAHs and MTEs loads in stormwater runoff, in order to determine whether accounting for atmospheric deposition explicitly as an entry to stormwater quality models might enhance the models outputs. Nonetheless, the lack of experimental atmospheric measurements collected directly on site at the same time as water data, amplify the challenges associated with the investigation of atmospheric deposition and the link with water pollution understanding (Gasperi et al. 2014; Murphy et al. 2014; Bressy 2010; Sakata et al. 2008; Sabin et al. 2005; Motelay-Massei et al. 2007; Fallah shorshani et al. 2012).

In the present study, we focus on assessing the link between water and air components by quantifying the contribution of atmospheric dry deposition to stormwater runoff pollution. Experimental data on atmospheric pollutant concentrations, road dusts and chemical loads in water samples are obtained at local scale within a highly trafficked road catchment near Paris. A methodology for the reconstruction of missing air quality data is developed and atmospheric dry depositions of PAHs and MTEs (As and Ni) are calculated and compared to

the chemical loads in stormwater and the dry stocks on the surface. The results should be helpful in developing a multi-scale modeling chain of traffic related pollution.

## 2. Materials and methods

### 2.1. Study site

The studied catchment is located in the residential French district “Le Perreux sur Marne” near Paris. It consists of a heavily trafficked (~30,000 vehicles per day) road surface with its adjacent sidewalks, pavements and parking zones of total surface equal to 2,661 m<sup>2</sup>. The area is drained by a separate stormwater sewer system and characterised by an imperviousness equal to 95% and an average slope of 2.6% (Fig. 1).



Fig. 1 The study site outlined by white bold line with the location of each measurement equipment (@Google,2016)

### 2.2. Instrumentation and sample analysis

#### 2.2.1. Air quality stations

Atmospheric experts and modelers define atmospheric particles as the particles measured in the air at about two meters' height of the ground. Therefore, a low volume sequential sampler LECKEL is installed at two sampling points (Air quality stations 1 and 2) at two meters' height of the ground (Fig. 1) in order to determine atmospheric concentrations of PAHs and MTEs. Atmospheric concentrations of eight PAHs (Benzo[a]anthracene (BaANT), chrysene (CHY), benzo[b]fluoranthene (BbFLT), benzo[k]fluoranthene (BkFLT), benzo[a]pyrene (BaPYR), benzo[g,h,i]perylene (BghiPL), indeno[1,2,3-c,d]pyrene (IcdPYR) and Benzo[e]pyrene (BePYR)) and eight MTEs (aluminium (Al), titanium (Ti), iron (Fe), nickel (Ni), copper (Cu), arsenic (As), cadmium (Cd) and barium (Ba)) are measured. Pollutants are collected at flow rates of 2.3 m<sup>3</sup>/h on quartz filters, over a 10 week-period starting on the 1<sup>st</sup> of

April until the 9<sup>th</sup> of June, 2014. The sampling period was limited due to financial considerations.

Trace metals are sampled on a weekly basis while PAHs are sampled daily until April 21<sup>th</sup> then every three days. Overall, ten samples of trace metals are collected at station 1 and eleven at station 2, while 31 and 33 samples of PAHs are collected respectively at station 1 and station 2. Trace metals are analyzed using inductively Coupled Plasma – Mass Spectrometry (ICP-MS), while PAHs are determined using high performance liquid chromatography (HPLC) coupled with UV fluorescence assay.

The air quality measurements are performed by Airparif, which is a non-profit organization accredited by the Ministry of Environment to monitor the air quality in Paris. These measurements are acquired within the Trafipollu project, which aims at developing modeling tools to characterize the traffic related pollutants at different urban scales. This project was accredited by the ANR which is the French National Agency for Research. At the same time with these experimental observations, Airparif continuously monitored air quality with permanent sampling stations (cf. Section 1.3), for which the pollutant analysis is identical to the one mentioned above. At AirParif stations, from March 2014 until December 2015, PAHs are collected every three days while MTEs are collected daily.

### **2.2.2. Meteorological station**

Rainfall data is collected at a meteorological station located only 5 meters away from the catchment limit, from April 2014 until September 2015. Measurements are obtained from a tipping bucket rain gauge, having a resolution of 0.1 mm. The rain gauge is installed at the rooftop of a building (Fig. 1). Rainfall events are identified as uninterrupted measurement periods during which the maximum time between bucket tips is 30 minutes. Defining a 30 minutes inter-event time was adequate in this study given both the characteristics of the local rainfall and of the studied catchment. Since the road catchment is very small (0.26 ha) and 95% impervious, its hydrological response to rainfall was very quick and the concentration time was small. The 30 minutes cut-off was longer than the time elapsed between the end of the rainfall and the end of the runoff. This was also confirmed by the absence of overlapping between any of the measured hydrographs.

### 2.2.3. Sewer inlet

Monitoring devices of flowrate and water quality parameters are located in the sewer inlet, at the entrance of the drainage system and recorded experimental continuous data at 1 minute time step. Runoff flowrate is measured using a Nivus flow meter, while water quality parameters are measured with a DS5 OTT multi-parameter probe. An automatic sampler is used to collect water samples in order to determine the chemical loads of PAHs and metals. The same metals and PAHs measured in the air were investigated in water samples. The water is pumped into two bottles placed in a cabinet at the side of the road using a peristaltic pump Watson-Marlow. One bottle is made of glass for PAHs analysis and the other is made of plastic "Polypropylene (PP)" for metal analysis. For each event, 250 ml of water is pumped into each bottle for each 300 L passing through the system. Samples were collected for ten events between August 26<sup>th</sup> 2014 and May 4<sup>th</sup> 2015. The runoff characteristics of the monitored events are presented in Table 1. The antecedent dry weather period (ADWP) is estimated from rain gauge and flowmeters records.

Analysis of trace metals is carried out by Inductively Coupled Plasma – Optical Emission Spectrometry (ICP-OES; Varian 720-ES). When the concentration is under the limit of quantification, the sample is analyzed by Inductively Coupled Plasma – Mass Spectrometry (ICP-MS; Varian 820-MS). Samples are analyzed for PAHs with a GC/MS (Focus DSQ, Thermo Fisher Scientific). Particle size distribution of the collected samples is performed using a laser diffractometer (Malvern® Mastersizer 3000) for the fraction below 2 mm, while volume distribution is calculated with the Mie light scattering theory. The Mastersizer operates over a particle size range from 10 nm to 3.5 mm. The refractive index used for the measurements are 1.33 for the dispersant solution (water) and 1.53 for the particles as wet dispersion.

**Table 1 Characteristics of monitored runoff events; ADWP=Antecedent Dry Weather Period; Vtot = total runoff volume; Qmax = maximum flowrate**

Event number	Start of runoff event (dd/mm/yyyy hh:mm)		ADWP (days)	Vtot (m <sup>3</sup> )	Runoff duration (h)	Qmax (L/s)
1	25/08/2014	12:15	2.4	13.17	11.4	2.39
2	08/10/2014	04:48	0.5	20.41	5	4.03
3	21/10/2014	12:05	4.5	5.74	6	7.60
4	16/11/2014	13:39	1.4	16.43	6.8	5.56
5	26/11/2014	00:48	7.3	8.83	6.7	3.03
6	02/02/2015	06:10	2.2	2.66	3.9	1.34
7	22/02/2015	21:38	1.3	34.49	10.2	6.36

8	26/04/2015	13:13	0.7	14.61	3.2	5.97
9	03/05/2015	06:22	0.3	15.70	3.5	2.52
10	05/05/2015	01:17	0.3	8.16	9.1	4.42

#### 2.2.4. Road dust

Samples of road dusts are collected on two surveys on the 14<sup>th</sup> of October 2014 and the 7<sup>th</sup> of July 2015 at three locations along the experimental catchment (Fig.1). The ADWP of the two surveys are respectively equal to 2 and 37 days. At each location, the sampling is performed at three different positions: on the sidewalk, in the gutter and on the road. A two-square meter surface is delimited and hand brushed before being dry-vacuumed to collect dusts, using a “Rowenta RU 4022” vacuum cleaner. The vacuum cleaner is characterized with a power equal to 1500 W and an air flux equal to 38 dm<sup>3</sup>/s. The details of the experiment are described in (Bechet et al. 2015). The metal content is determined after calcination at 450°C during 3 hours and mineralization of the samples using of a mixture of HF and HClO<sub>4</sub> acids (NF X 31-147). As for PAHs, they were extracted using Methylene chloride/Methanol (90/10, v/v). Loads of PAHs and trace metals, as well as the particle size distribution are determined using the same techniques as for water samples (Bechet et al. 2015).

#### 2.3. Air quality dataset reconstruction

Air and water quality were observed on the same territory but unfortunately, air and water quality measurement periods did not coincide perfectly, because administrative authorization could not be assigned at the same time. Therefore, a methodology is developed to calculate the atmospheric pollutant concentrations over the water sampling period. For that matter, data from three permanent stations (GEN, BPEST and PA18) of AirParif network are used (Fig. 2). GEN station is located in the northwestern suburb of Paris, while PA18 station is located in the 18<sup>th</sup> arrondissement of Paris and BPEST station is located on the eastern side of the highway surrounding the city of Paris (“boulevard périphérique”).

PAHs are measured at GEN and BPEST stations while MTEs are measured at PA18 station. The methodology consists of several steps. First, the time evolution of pollutant concentrations is compared at the experimental stations of the study site and at the permanent stations of AirParif. Then, Pearson correlations are calculated to choose the best representative



station of “Le Perreux” among AirParif stations. Finally, missing air quality data are extrapolated according to the derived linear regression equations.

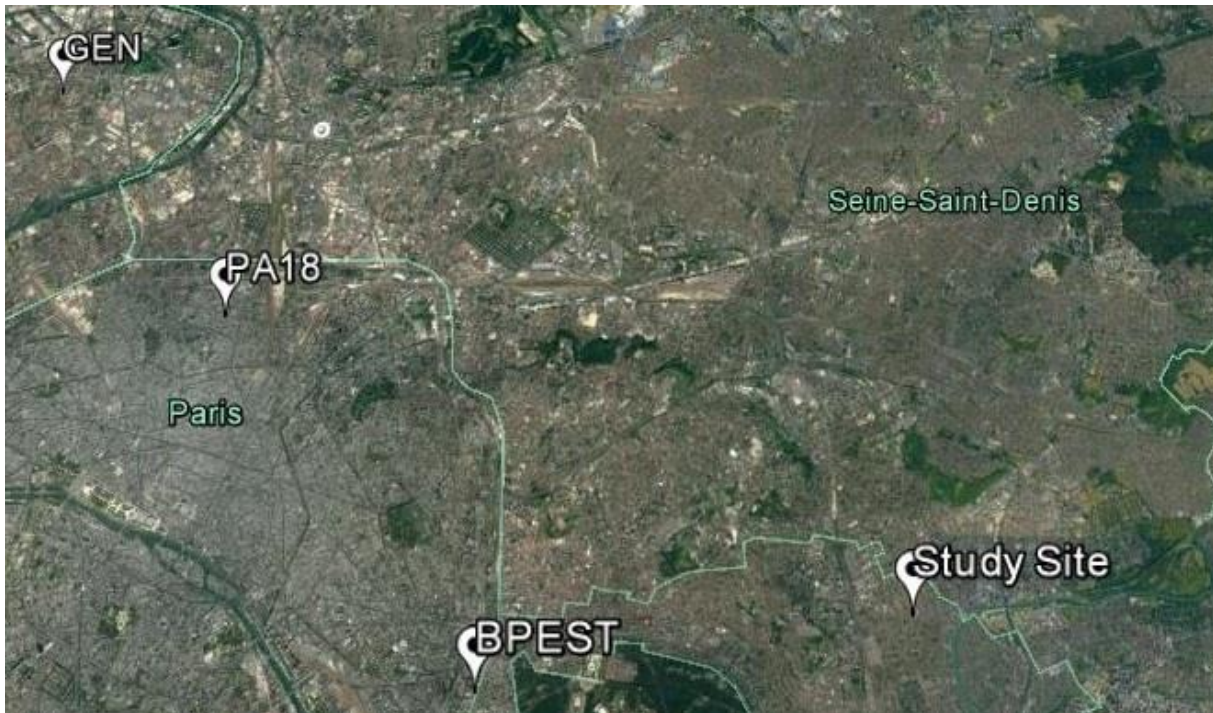


Fig. 2 The locations of AirParif permanent stations with respect to the location of the study site. The locations are represented with the white pins (@Google earth, 2016)

#### 2.4. Pollutant loads calculation

Pollutant loads are calculated for the ten rainfall events collected, and are limited to the PAHs and trace metals that are in common between air and water quality European regulation. Thus, BaANT, CHY, BbFLT, BkFLT, BaPYR, BghiPL and IcdPYR among PAHs; and among metals: Ni and As are quantified in this study.

Deposition from the atmosphere is only calculated considering the deposited flux of pollutants during dry weather. In fact, wet and dry deposition fluxes might be equivalent, and in some cases, wet deposition might be even higher than the dry one (Percot et al. 2016). But, due to the occurrence of less rainfall events, dry weather periods are much longer under Parisian climate, which results in a dominant dry atmospheric deposition in comparison with the wet one (Gunawardena et al. 2013; Sabin et al. 2005). Therefore, wet deposition fluxes might be neglected.

Deposition mass loads are calculated on the entire catchment based on the following equations:

$$Dry\ deposition\ load = S \times ADWP \times Flux_{atm} \quad (1)$$

$$Flux_{atm} = [Pollutant]_{atm} \times Velocity_{dry\ deposition} \quad (2)$$

Where: *Dry deposition load* = the deposited mass (mg); *S* = surface of the catchment (m<sup>2</sup>); *ADWP* = antecedent dry weather period (days); *Flux<sub>atm</sub>* = atmospheric flux (mg/m<sup>2</sup>/day); *[Pollutant]<sub>atm</sub>* = pollutant concentration in the air (mg/m<sup>3</sup>); *Velocity<sub>dry deposition</sub>* = dry deposition velocity (m/day).

The dry deposition velocity is set to 0.001 m/s for both PAHs and trace metals, according to commonly used settling velocity for atmospheric deposits in atmospheric models and based on existing data of average deposition velocity (Slinn 1982; Roupsard et al., 2013). However, deposition velocity might vary as a non-linear pattern according to particle size (Tasdemir et al. 2006), but the consideration of a singular dry deposition velocity, as an approximate approach, is commonly used by atmospheric experts and modelers. It is also assumed that the deposition fluxes are homogeneous within the entire catchment.

The mass loads of PAHs and trace metals in stormwater are calculated by multiplying the representative concentration of pollutant of the collected water sample by the total volume of runoff during the storm (equation 3):

$$Water\ load = [Pollutant]_{water} \times Volume_{runoff} \quad (3)$$

Where : *Water load* = pollutant mass (mg); *[Pollutant]<sub>water</sub>* = total concentration of the pollutant (mg/l); *Volume<sub>runoff</sub>* = total volume of runoff (l).

As for road dust, the total mass of dry stock over the entire catchment is given by the following equation:

$$Stock = Mass_{road\ dust} \times [Pollutant]_{road\ dust} \times S_{entire\ catchment} / S_{road\ dust\ collection} \quad (4)$$

Where: *Stock* = accumulated pollutant mass on the surface (mg); *Mass<sub>road dust</sub>* = mass of the collected road dust (kg); *[Pollutant]<sub>road dust</sub>* = concentration of pollutants in the road dust (mg/kg); *S<sub>entire catchment</sub>* = surface of the entire catchment (2661 m<sup>2</sup>); *S<sub>road dust collection</sub>* = surface on which the dusts were collected (2 m<sup>2</sup>).

Annual fluxes of PAHs and MTEs from atmospheric deposits and stormwater runoff are also estimated by extrapolating the total mass of these pollutants measured during the sampling periods proportionally to the duration of antecedent dry weather period and runoff volume respectively, based on the following equations:

$$Annual\ flux_{atmospheric\ deposition} = \left( \frac{\sum M_i}{\sum ADWP_i} \right) \times \left( \frac{ADWP_{total}}{S_{entire\ catchment}} \right) \quad (5)$$

Where:  $Annual\ flux_{atmospheric\ deposition}$  = Annual flux of pollutant from atmospheric deposition (mg/m<sup>2</sup>/year);  $M_i$  = pollutant mass from atmospheric deposition corresponding to the event  $i$  (mg);  $ADWP_i$  = antecedent dry weather period of the event  $i$  (days);  $ADWP_{total}$  = antecedent dry weather period over the entire year (days/year);  $S_{entire\ catchment}$  = surface of the entire catchment (2661 m<sup>2</sup>).

$$Annual\ flux_{exported\ by\ runoff} = \left( \frac{\sum M_i}{\sum V_i} \right) \times \left( \frac{V_{total}}{S_{entire\ catchment}} \right) \quad (6)$$

Where:  $Annual\ flux_{exported\ by\ runoff}$  = Annual flux of pollutant exported by stormwater runoff (mg/m<sup>2</sup>/year);  $M_i$  = pollutant mass in stormwater runoff corresponding to the event  $i$  (mg);  $V_i$  = runoff volume of the event  $i$  (m<sup>3</sup>);  $V_{total}$  = total runoff volume over the entire year (m<sup>3</sup>/year);  $S_{entire\ catchment}$  = surface of the entire catchment (2661 m<sup>2</sup>).

### 3. Results

#### 3.1. PAHs

##### 3.1.1. Reconstruction of missing air concentrations

Air concentrations of total PAHs ( $\sum 7$  PAHs) follow a similar temporal evolution, regardless of the measuring station (Fig. 3). However, higher fluctuations in the measurements are observed at the GEN and BPEST stations. The highest concentrations are measured at the BPEST station where the daily mean total concentration of PAHs is equal to 1.35 ng/m<sup>3</sup> with a minimum of 0.36 and a maximum of 1.98 ng/m<sup>3</sup>. As for the GEN station, the daily mean total concentration measured is 1.015 ng/m<sup>3</sup>, higher than those measured at the study site with values of 0.88 and 0.74 ng/m<sup>3</sup> calculated at stations 1 and 2 respectively. The high concentration levels observed at BPEST station are mainly explained by its geographic location on the “boulevard Périphérique” of Paris (ring road), which is a very busy and highly trafficked boulevard. The other stations are located in residential districts subjected to lower

volume of traffic. For the period starting on 17th of May until 29th of May 2014, we observed a decline in the PAHs concentration at all stations except at BPEST. The decline is explained by the turning-off of residential heating, very well known as an important source of emission of PAHs in the air. While at BPEST station, PAHs concentrations remain high due to the important traffic emissions.

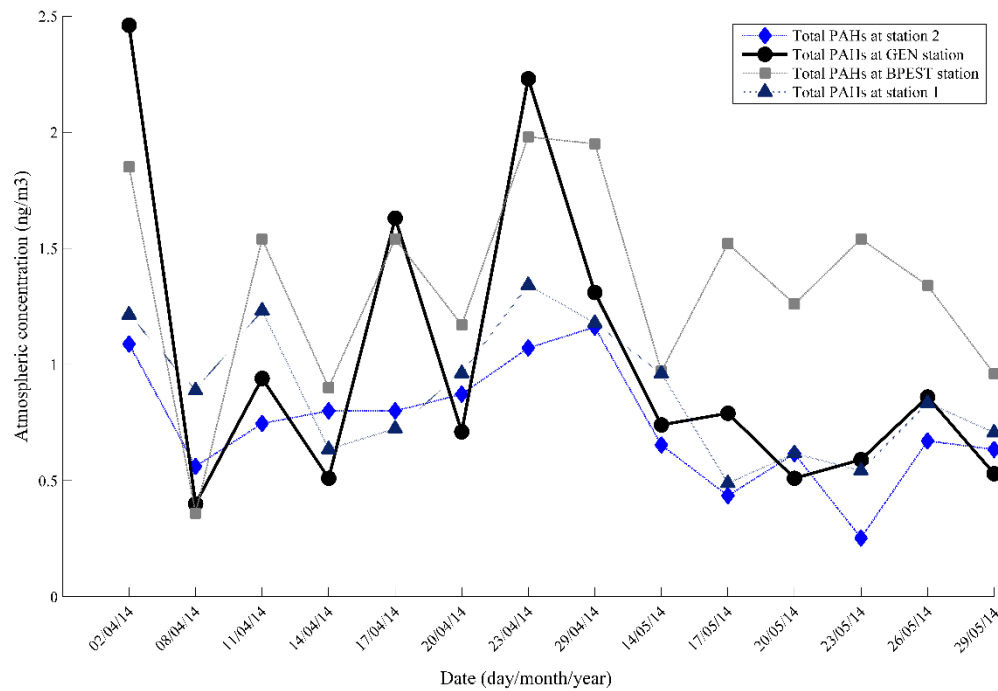
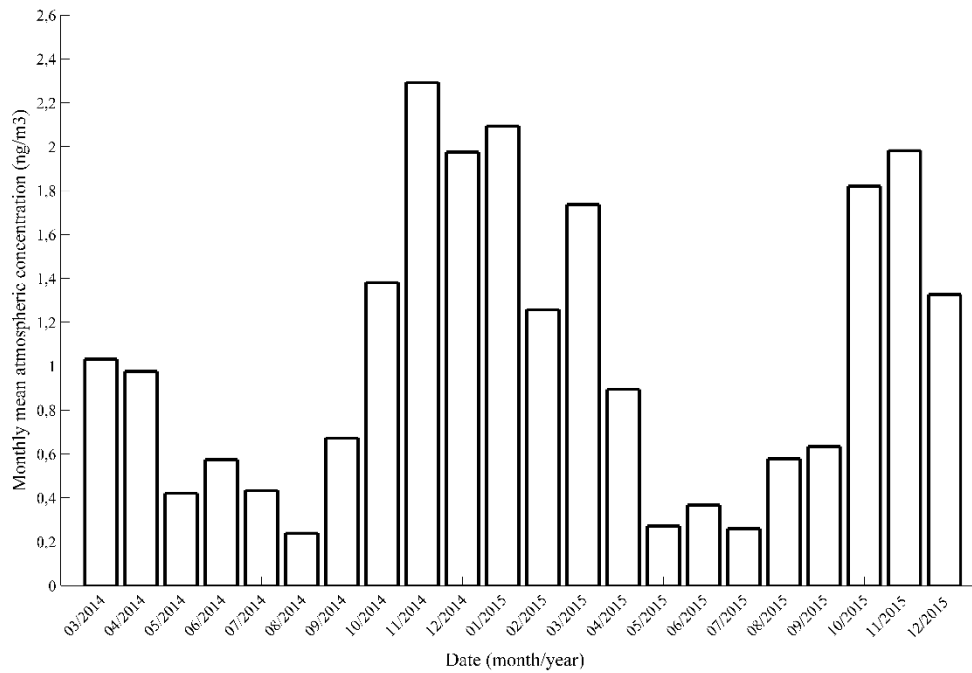


Fig. 3 Time series of total PAHs (ng/m<sup>3</sup>) measured at the study site and AirParif stations

Fig. 4 shows the time series of the monthly mean concentrations of  $\Sigma 6$  PAHs (the CHY is excluded, since it was not monitored in 2015) measured in the atmosphere at the GEN station. The figure shows clear seasonal fluctuations with the highest concentration levels recorded starting in late autumn and during winter. This finding is consistent with the literature, where higher concentrations were detected in winter for several urban catchments (Tasdemir and Esen 2007; Kim et al. 2013; Wang et al. 2011). Concentration peaks are usually associated with use of residential heating during the cold months, as well as with the limited dispersion of pollutants due to the occurrence of temperature inversions that trap the pollutants in the air (Amarillo and Carreras 2016). The existence of significant seasonal variability in the atmospheric concentrations, indeed explains the importance of extrapolating missing air quality data and not considering a constant value.



**Fig. 4 Time series of monthly mean atmospheric concentrations of total PAHs (ng/m3) at AirParif station GEN**

According to statistical analysis, the strongest correlation between the measurements of  $\Sigma 6$  PAHs (BaANT, BbFLT, BkFLT, BaPYR, BghiPL and IcdPYR) is calculated between station 1 at the study site, and the AirParif station GEN with a correlation coefficient equal to  $R = 0.8382$  ( $p$ -value = 0.002). Therefore, the GEN station is used to recover missing data of PAHs from the experimental station 1 on the Trafipollu site. The correlation between the measurements of BaPYR, IcdPYR and BghiPL at both stations was weak ( $R < 0.45$ ). Therefore, these PAHs are excluded from further analysis. As for BaANT, BbFLT and BkFLT the correlation between the measurements at station 1 and GEN station is high ( $R > 0.7$ ) which confirms that GEN station can be accurately used as a surrogate for station 1 missing values of these PAHs.

Thus, concentrations of BaANT, BbFLT and BkFLT at Trafipollu study site are calculated for the missing experimental periods using the following equations:

$$[PAH]_{station\ 1} = a + b \times [PAH]_{GEN\ station} \quad (7)$$

The corresponding values of the models coefficients  $a$  and  $b$  as well as their associated standard errors (SE) and the  $R$  value for each PAH are presented in Table 2:

**Table 2 Linear regression coefficients and their associated standard error (SE) for each PAH, as well as the R value of the linear regression**

PAH	A		b		R
	Value	SE	Value	SE	
BaANT	0.35	0.09	0.07	0.008	0.7
BbFLT	0.48	0.09	0.11	0.02	0.77
BkFLT	0.32	0.09	0.04	0.007	0.65

We considered the extrapolated values on a monthly basis to calculate deposition.

### 3.1.2. Contaminant loads

Monthly simulated mean values of atmospheric concentrations of PAH are used to calculate the atmospheric deposited masses on the entire catchment and its corresponding contribution to the chemical loads in stormwater.

Table 3 shows the atmospheric deposits, the stormwater loads and the percentage of potential contribution of atmospheric deposits to stormwater contamination for ten rainfall events for the three corresponding PAHs (BaANT, BbFLT and BkFLT).

**Table 3 Percentage of potential contribution of atmospheric deposits to stormwater contamination for ten rainfall event for BaANT, BbFLT and BkFLT.**

Pollutant	Event		Atmospheric deposit (mg)	Stormwater load (mg)	Percentage of potential contribution (%)
BaANT	25/08/2014	12:15	0.04	1.05	3.8
	08/10/2014	04:48	0.02	1.56	1.3
	21/10/2014	12:05	0.14	0.38	36.8
	16/11/2014	13:39	0.06	0.89	6.7
	26/11/2014	00:48	0.3	0.69	43.5
	02/02/2015	06:10	0.06	0.89	6.7
	22/02/2015	21:38	0.03	2.65	1.3
	26/04/2015	13:13	0.02	0.67	2.9
	03/05/2015	06:22	0.005	0.56	0.9
	05/05/2015	01:17	0.005	0.43	1.16
BbFLT	25/08/2014	12:15	0.08	2.37	3.4
	08/10/2014	04:48	0.03	3.61	0.8
	21/10/2014	12:05	0.27	0.65	41.5
	16/11/2014	13:39	0.11	1.52	7.2
	26/11/2014	00:48	0.59	0.83	71.1
	02/02/2015	06:10	0.11	3.23	3.4
	22/02/2015	21:38	0.07	6.71	1.04
	26/04/2015	13:13	0.03	2.87	1.04
	03/05/2015	06:22	0.01	1.99	0.5

	05/05/2015	01:17	0.01	1.47	0.7
	25/08/2014	12:15	0.03	0.87	3.4
	08/10/2014	04:48	0.01	1.19	0.8
	21/10/2014	12:05	0.08	0.23	34.8
	16/11/2014	13:39	0.04	0.55	7.3
<b>BkFLT</b>	26/11/2014	00:48	0.18	0.49	36.7
	02/02/2015	06:10	0.07	0.89	7.8
	22/02/2015	21:38	0.04	2.19	1.8
	26/04/2015	13:13	0.02	1.13	1.8
	03/05/2015	06:22	0.004	0.72	0.5
	05/05/2015	01:17	0.004	0.59	0.7

Over the studied period, deposition loads for each PAH are highly variable as they range within factors of 0.07 and 4.5 from their mean values, while water loads are also variable but to a lesser extent ranging within factors of 0.26 and 2.7 from their mean. PAH loads in stormwater are significantly higher than PAH loads in atmospheric deposits for all events. It is noteworthy that the calculated atmospheric deposits represent the “potential” deposited load during dry weather, which is assumed to be totally available for wash off by runoff. The assumption of total wash-off is mainly based on the characteristic of the atmospheric deposit particles that are mostly associated to fine particles. Wash-off of fine particles tends to be source limited (Zhao et al. 2016), suggesting a continuous decline of the sediments available for wash-off. A recent study by (Hong et al. 2016b) showed that the stock of fine particles rapidly decreases at the beginning of a rainfall event and that more than 90% of fine particles (< 7 $\mu$ m) are transferred to the outlet.

The potential contribution of estimated atmospheric deposits to stormwater contamination varies greatly (Table 3). It ranges between 0.9 and 43.5 % for BaANT; 0.5 and 71.1 % for BbFLT and 0.5 and 36.7% for BkFLT depending on the rainfall event. The mean value of the potential atmospheric contribution for all three PAHs is relatively low at 11%. The highest percentages of potential contribution are calculated for the third and fifth events that occurred on the 21<sup>th</sup> of October 2014 and the 26<sup>th</sup> of November 2014, which are characterized by the longest of dry periods; 4.5 and 7.3 days respectively. This suggests that the ADWP is an important explanatory factor of the variation of the potential atmospheric deposit contribution to water load. Multi-linear regression confirms this statement, where the *p-value* calculated for

ADWP for the three PAHs is < 0.001. However, this result could be expected as the calculation of the potential atmospheric deposition is directly driven by the length of the ADWP.

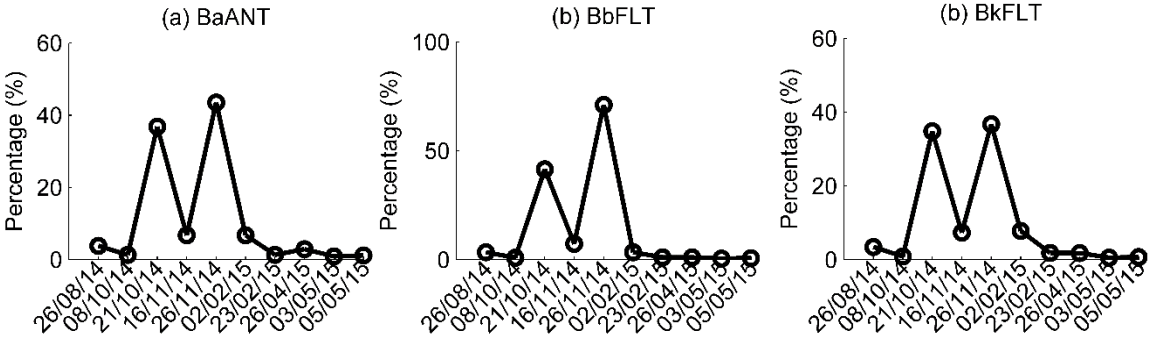


Fig. 5 Percentage of potential contribution of atmospheric deposit to stormwater load for (a) BaANT, (b) BbFLT and (c) BkFLT

We notice that the potential contribution of each PAH to stormwater contamination follows a similar pattern (Fig. 5). This result indicates a similar distribution behavior of the three PAHs between the air and water compartments.

Annual deposition fluxes are calculated for each PAH as well as for the  $\Sigma 3$  PAHs measured during the sampling periods throughout the year. Fig. 6 shows the annual fluxes of atmospheric deposition and loads exported by the runoff.

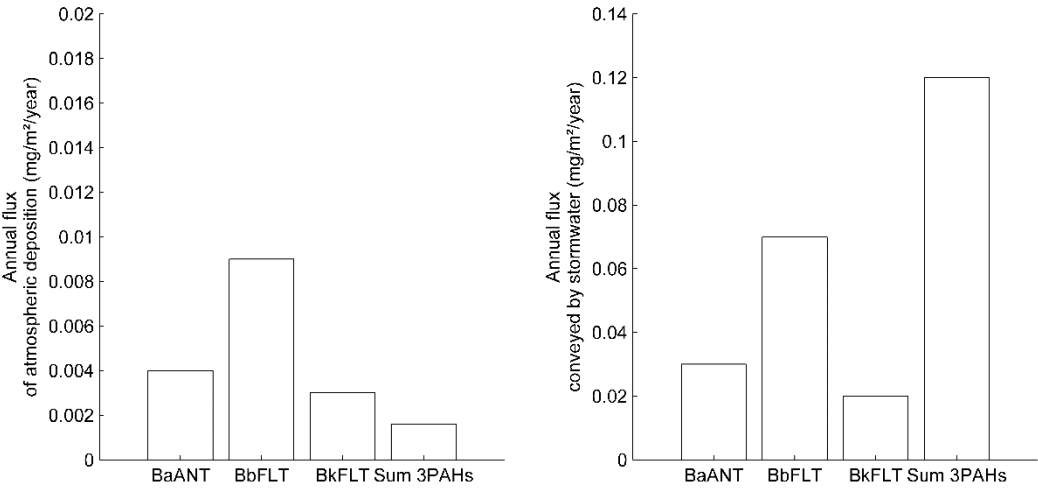


Fig. 6 Annual fluxes of atmospheric deposition and pollutants loads conveyed by stormwater

The calculations show that the atmospheric flux of BaANT, BbFLT and BkFLT is evaluated at 0.004, 0.009 and 0.003 mg/m<sup>2</sup>/year respectively, while the flux conveyed by

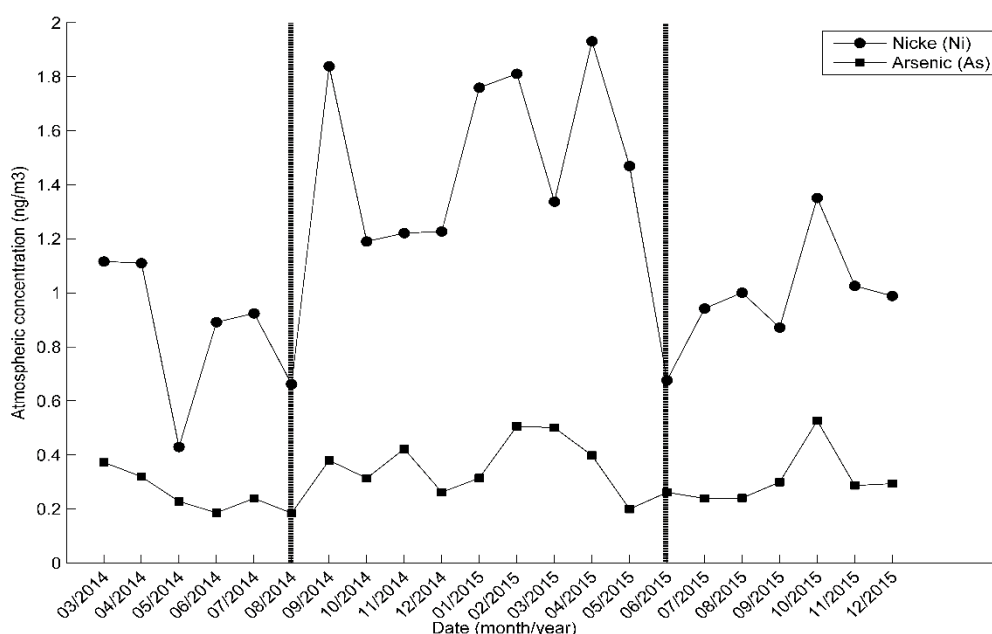


stormwater is 0.03, 0.07 and 0.02 mg/m<sup>2</sup>/year respectively. As for the total atmospheric flux of  $\Sigma$ 3 PAHs, it is evaluated at 0.016 mg/m<sup>2</sup>/year, with 0.12 mg/m<sup>2</sup>/year exported by runoff.

### 3.2. Trace metals

#### 3.2.1. Extrapolation of the missing air concentrations

The time variation of the monthly mean concentrations of trace metals measured at PA18 station from March 2014 to December 2015 is plotted in Fig. 7. The nickel (Ni) shows a higher variability than the other metals, which have relatively stable concentrations over time. Since we supposed that metal measurements at station 1 follow the same pattern as in station PA18, we assumed that the mean value of atmospheric trace metal concentrations calculated over the sampling period from 01/04/2014 to 09/06/2014 at station 1 is also representative of the metal concentration for the period of missing data. However, for the nickel, given its high variability, atmospheric concentrations are calculated over three distinct periods (delimited on Fig. 7 by the dashed line). For the first period, a mean atmospheric concentration calculated over the sampling period on site is considered, and for the others, atmospheric concentrations at station 1 are calculated from concentrations at station PA18 assuming these two values are related by the multiplying factor calculated during the first period.



**Fig. 7 Time series of monthly median concentration of trace metals measured at AirParif station PA18. The vertical bars represent the time limits between the three periods of different concentrations for Nickel**

### 3.2.2. Contaminant loads

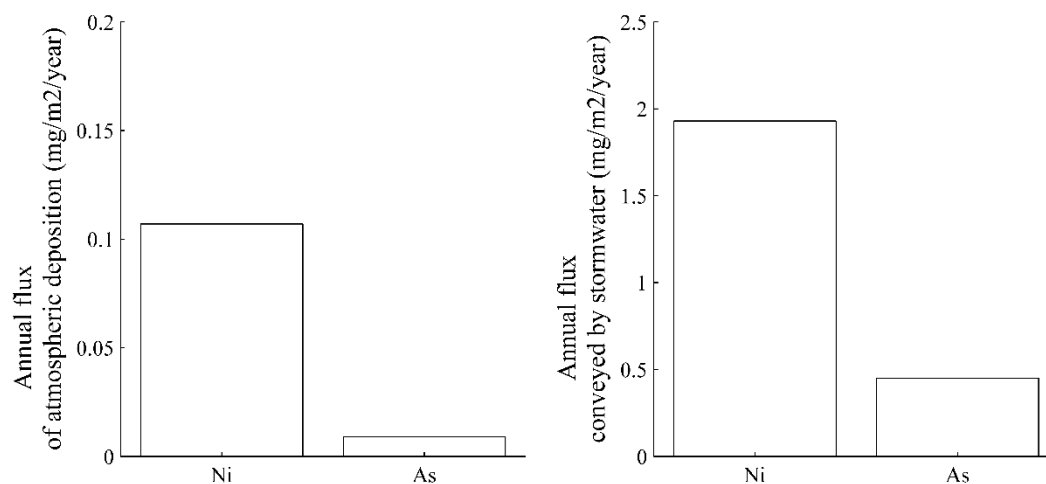
The calculation of atmospheric deposition and the potential contribution of atmospheric deposits to stormwater contamination of trace metals are presented in Table 4. The variability of atmospheric deposits for both metals is relatively lower than that of PAHs as it ranges between 0.18 and 2.75 from its mean value. Water loads vary almost in the same ranges within factors of 0.31 and 2.07 from their mean values for both metals.

**Table 4 Percentage of the potential contribution of atmospheric deposits to stormwater contamination for seven rainfall events for Nickel and Arsenic**

Event		Atmospheric deposit (mg)	Stormwater load (mg)	Percentage of potential contribution (%)
Ni	25/08/2014 12:15	1.16	49.75	2.33
	08/10/2014 04:48	0.43	113.93	0.38
	21/10/2014 12:05	3.89	22.71	17.12
	16/11/2014 13:39	1.21	52.8	2.29
	26/11/2014 00:48	6.31	57.94	10.89
	02/02/2015 06:10	1.9	64.18	2.96
	22/02/2015 21:38	1.12	152.56	0.74
As	25/08/2014 12:15	0.17	14.22	1.2
	08/10/2014 04:48	0.03	25.7	0.13
	21/10/2014 12:05	0.31	5.51	5.63
	16/11/2014 13:39	0.1	12.93	0.77
	26/11/2014 00:48	0.5	14.31	3.5
	02/02/2015 06:10	0.15	13.4	1.12
	22/02/2015 21:38	0.09	34.21	0.26

The potential contribution of estimated atmospheric deposits to stormwater contamination is relatively low as it varies between 0.38 and 17.12 % for nickel, and 0.13 and 5.63 % for arsenic. The highest percentages of potential contribution are calculated for the events having the longest length of antecedent dry periods, as for the PAHs. The potential atmospheric contribution for both metals is not very significant, as the corresponding mean value is equal to 3.52%. In fact, emissions of Ni and As mostly originate from fossil fuel combustion (Shi et al. 2012; Motelay-Massei et al. 2005) which is now reduced due to enhanced and cleaner industrial processes that reduced their emissions in order to protect the environment. An important decrease is registered for many trace metals, including Nickel whose emissions decreased by a factor of 16 in 14 years (Motelay-Massei et al. 2005).

Calculation of annual deposition fluxes for both metals are done as for PAHs and are presented in Fig. 8. The atmospheric flux of Ni is evaluated at 0.11 mg/m<sup>2</sup>/year while the flux exported by stormwater is 1.93 mg/m<sup>2</sup>/year. For As, both atmospheric flux and the flux in stormwater are lower, equal to 0.01 and 0.45 mg/m<sup>2</sup>/year respectively.



**Fig. 8 Annual fluxes of atmospheric deposition and loads conveyed by stormwater for nickel and arsenic**

### 3.3. Road dust

The potential contribution of atmospheric deposits to the stock on the road surface is presented for the two campaigns of dust collection in Table 5, as the ratio of pollutant mass from atmospheric deposition over the pollutant mass present on the road surface. Since the dust campaigns were performed on a non-coincident period with the sampling of atmospheric concentrations, missing atmospheric concentrations were calculated based on the same reconstruction methods developed in earlier sections 3.1.1 and 3.1.2. Then atmospheric deposits were calculated for the corresponding period of dust sampling. The comparison of atmospheric deposits and road dust will give a general idea of the quantities of pollutants present in both compartments, and it allows the assessment of the order of magnitude between the two variables.

**Table 5 Percentage of the potential contribution of atmospheric deposit to dry stock on the surface**

		Atmospheric deposit (mg)	Dry stock (mg)	Potential contribution (%)
14/10/2014 (ADWP=2 days)	BaANT	0.06	10.4	0.58
	BbFLT	0.12	14.56	0.82
	BkFLT	0.04	6.56	0.55
	Ni	1.73	502.7	0.34

	<b>As</b>	0.14	94.1	0.15
	<b>BaANT</b>	1.36	8.1	16.75
07/07/2015 (ADWP=37 days)	<b>BbFLT</b>	2.00	21.7	9.22
	<b>BkFLT</b>	1.05	7.06	14.82
	<b>Ni</b>	20.45	1614.2	1.27
	<b>As</b>	2.55	273.54	0.93

The potential contribution of atmospheric deposition to the street deposits is relatively low for both campaigns. It does not exceed 1 % and 18 % for all pollutants on the campaign of the 14<sup>th</sup> of October and the 7<sup>th</sup> of July respectively. Higher contributions are estimated for the second campaign since road dusts were collected after a longer period of dry weather, resulting thus in a higher calculated load of atmospheric deposits. The contribution of PAHs is more significant compared to that of trace metals, whose loads in stormwater samples are very important.

The low contribution percentages calculated show that atmospheric deposition is not a major source of PAHs and trace metals in dry stock on surfaces. Local sources such as soil erosion, vehicle emission, tire wear and street erosion would constitute a more important source for the build-up of pollutants on surfaces. In addition, the total mass of BaANT accumulated on the surface after two days of dry period (10.4 mg) is higher than the one accumulated after 37 days of dry weather (8.1 mg). Also, the collected masses of BKFLT in dust samples for both campaigns have almost the same magnitude. This result confirms previous findings on the need to reconsider the dry weather period as the only predictive variable in build-up models (Al Ali et al. 2016; Sage et al. 2015).

The comparison of pollutant loads in dry stocks and water samples shows that the mass of collected dry stocks is much higher than the mass of washed off particles calculated for several events for all pollutants (Table 6).

**Table 6 Mean values of ratios calculated between the mass of pollutant in stormwater samples (n=10 for PAHs and n=7 for metals) and the mass of pollutants in dry stock (%)**

	<b>BaANT</b>	<b>BbFLT</b>	<b>BkFLT</b>	<b>Ni</b>	<b>As</b>
<b>Ratio 14/10/2014 (%)</b>	9.39	17.34	13.49	14.60	18.26
<b>Ratio 07/07/2015 (%)</b>	12.06	11.64	12.53	4.55	6.28

The mean values of ratios calculated between the loads in stormwater and the loads in street deposits do not exceed 20% for all pollutants. This result confirms that during rainfall events only a small proportion of the available mass is washed away into the sewer inlets (Egodawatta, et al. 2007; Vaze and Chiew 2002).

Particle size distributions in stormwater samples and road dust samples are presented in Fig. 9. The analysis shows that 48% of particles mobilized by the runoff are fine (< 10µm) (Fig. 9 a) while only 7% of these particles are present in road dust (Fig. 9 b). This confirms that the fine particles are highly mobile compared to the coarse particles of surface buildup (Hong et al. 2016a). Moreover, the small proportion (7%) of particles smaller than 10 µm might suggest that the fine particles originate mainly from the atmosphere. However, given the low atmospheric contribution to stormwater loading, this indicates the existence of direct significant sources of fine particles, distinct from the atmospheric pathway.

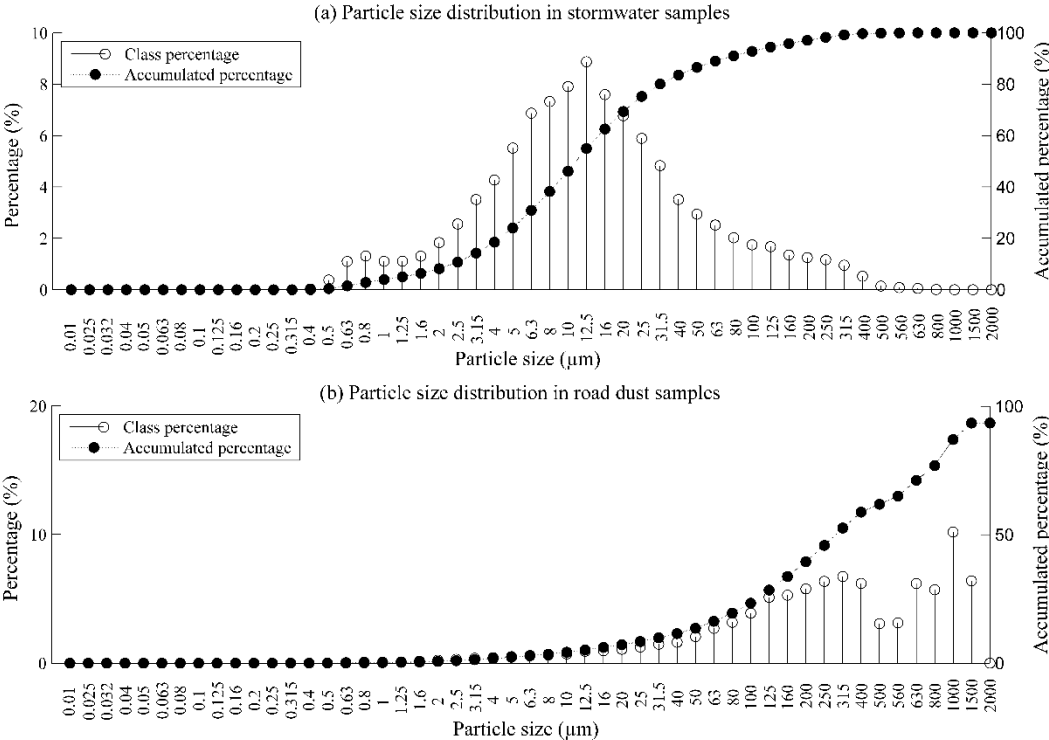


Fig. 9 Particle size distribution in stormwater samples (a) and in road dust (b)

#### 4. Discussion

The annual fluxes of atmospheric deposition for each PAH varied within the lower ranges stated by (Motelay-Massei et al. 2006), who calculated annual fluxes imported by bulk atmospheric deposition ranging between 0.005 and 0.009 mg/m<sup>2</sup>/year for BaANT; 0.008 and

0.016 mg/m<sup>2</sup>/year for BbFLT and finally 0.003 and 0.007 mg/m<sup>2</sup>/year for BkFLT. Comparison of the annual atmospheric deposition fluxes of total PAHs with the literature was not possible in our case, because in this study we considered only the sum of three PAHs and not total PAHs, as defined by the EPA (Keith 2015).

The magnitude of annual deposition fluxes of metals measured in the present study are lower than the fluxes calculated in previous papers. For example, Sabin et al. (2005) recorded a flux of 1.3 mg/m<sup>2</sup>/year on an urban catchment in Los Angeles for nickel. Sweet et al. (1998) calculated annual deposition fluxes ranging between 0.32 and 0.57 mg/m<sup>2</sup>/year for nickel, and 0.066 and 0.091 mg/m<sup>2</sup>/year for the arsenic three distinct locations.

The potential atmospheric contribution of PAHs to the contamination of stormwater is shown to be very low in this study, where mean values calculated for BaANT, BkFLT and BbFLT were respectively equal to 10.5, 9.5 and 13 %. Similar contributions for PAHs, based on concentrations, were estimated by Gasperi et al. (2014) where mean values of potential contributions were equal to 11% for both BaANT and BkFLT, and 14% for BbFLT. Bressy et al. (2012) found that atmospheric fallout didn't account for more than 30% of the annual load of PAHs exported by stormwater, while Motelay-Massei et al. (2006) stated even lower values ranging between 2 and 18 %. This result confirms previous findings on the dominance of "local" emissions as the primary source of PAH. Here we consider that local emissions are defined as emissions by traffic that do not reach the altitude of 2 meters above the ground and settle before being transported by the atmosphere. The study site is therefore, subjected to important direct emission loads that result in higher direct contribution to stormwater loads, for which the traffic is certainly strongly responsible. The asphalt abrasion due to the passage of cars, the tire abrasion and lubricating oil, may all contribute to the PAHs road deposit load.

Potential atmospheric contribution to metal loads in stormwater is also insignificant as the corresponding mean percentages are 5% for nickel and 1.8% for arsenic. Higher contributions were mentioned in previous works. For example, Gasperi et al. (2014) calculated a contribution of atmospheric fallout to the contamination of runoff equal to 32% and 7% for nickel and arsenic respectively, while Percot et al. (2016) attributed the same percentage for the contribution of nickel but lower value for arsenic (1%). Sabin et al. (2005) mentioned even higher values for the nickel ranging between 57 and 100%. The lower contributions calculated

in this study even on highly trafficked road (30000 vehicles/day) might be attributed to several factors such as the catchment size, the regional climate and the methodology for the estimation of deposition fluxes. This study is conducted on a very small road catchment not exceeding 0.27 ha, while other studies were conducted on larger urban catchments from 5 to 228 ha (Sabin et al. 2005; Gasperi et al. 2014; Percot et al. 2016) covering different types of urban surfaces including roofs, parking, gardens, pavements and subsequently wider ranges of activities resulting thus, in higher levels of contaminations and emissions. The meteorological factors including humidity, pressure and wind speed, also have an important influence on the levels of contribution since they highly control the concentrations of particulate matter (PM<sub>10</sub>) (Lee et al. 2011; Tian et al. 2014). This explains the extremely high contributions mentioned by Sabin et al. (2005), where in the semi-arid region, strong and very dry winds frequently occur. Differences in the material and devices used to collect the atmospheric fallout, and the subsequent analyses may induce divergence in the estimated atmospheric concentrations and deposition fluxes.

Atmospheric concentrations in this study were measured at a height of two meters of the ground, as in (Sabin et al. 2005), given the definition of atmospheric particles by the atmospheric experts and modelers. Therefore, air borne substances at lower heights and particles transported and settling near the ground, originating from vehicle emissions and the degradation of the road surface itself, are not taken into account leading thus to an underestimation of the atmospheric deposition, based on their current definition. To overcome this problem, samplers should be placed very close to the urban surface so that the measurements would cover a wider range of traffic emissions, including direct emissions not necessarily passing through the atmosphere before settling on the urban ground. However, this solution might not be easy due to the high risk of deterioration of the material on site. This study challenges our capacity to invent new measuring methodologies. A more accurate estimation of atmospheric deposition also would also include the quantification of the re-suspension process, which is induced by meteorological conditions and road traffic. Several researches reported its significance (Weinbruch et al. 2014) and relevance especially for road dust emission models such as the NORTRIP model (Norman et al. 2016). Taking into account these processes would result in a more accurate estimation of the percentage of the atmospheric contribution, in order to underlie our initial purpose to be able to integrate traffic,

air and water models to tackle the question of the pollution dispersion in the urban environment.

The analysis of road dust showed that the atmospheric deposition does not contribute significantly to the stock on the surface. This is coherent with what we mentioned previously on the traffic being a major source of contamination. However, this stock does not represent the mass susceptible to be mobilized by a rainfall event, which is clearly shown when comparing the mass of pollutants in stormwater samples and the mass of pollutants in dry stocks as well as the particle size distribution of pollutants in both stormwater samples and road dust. Fine particles are the most susceptible to be mobilized by the runoff during a rainfall event, which highlights the selectivity of the wash-off process. The dynamics of transport of the particles available on the surface prior to a storm event are thus dependent on the characteristics of the particles. Incorporating this knowledge in stormwater quality modeling by integrating a differential erosion rate depending on the particles size should be considered, to a better assessment of the mobilization of sediments from the surface (Hong et al. 2016b). Results also highlight the existence of important sources of fine particles other than the atmosphere, contributing to the high concentration of fine particles in stormwater.

## 5. Conclusion

The potential contribution of atmospheric dry deposits of PAHs and trace metals to stormwater loading was assessed on a highly trafficked urban road catchment. Results demonstrate that atmospheric deposits do not contribute significantly to pollutant loading in stormwater runoff, as mean contribution percentages of deposits to water loads didn't exceed 11 and 4 % for PAHs and metals respectively for the studied rainfall events. Therefore, taking explicitly the atmospheric deposits as an entry to water quality models and developing an integrated modeling chain between the two compartments might not be relevant. Further research must be conducted to account of the processes of re-suspension and aggregation of particles in the estimation of atmospheric deposition. The integration of the emission of all traffic related particles must be also reconsidered to propose new water quality models based not only on atmospheric accumulation processes but also on direct deposition processes especially with the results confirming the major role of traffic in the emission of contaminants.



The results also highlight the need of source characterization of the finest particles in stormwater, since they represent the highest fraction conveyed during a rainfall event.

## 6. References

Al Ali S, Bonhomme C, Chebbo G (2016) Evaluation of the Performance and the Predictive Capacity of Build-Up and Wash-Off Models on Different Temporal Scales. *Water* 8:312 doi:10.3390/w8080312.

Amarillo AC, Carreras H (2016) Quantifying the Influence of Meteorological Variables on Particle-Bound PAHs in Urban Environments. *Atmospheric Pollution Research* 7 (4): 597–602. doi:10.1016/j.apr.2016.02.006.

Amato F, Pandolfi M, Moreno T, Furger M, Pey J, Alastuey A, Bukowiecki N, Prevot ASH, Baltensperger U, Querol X (2011) Sources and variability of inhalable road dust particles in three European cities. *Atmos Environ* 45:6777–6787. doi: 10.1016/j.atmosenv.2011.06.003

Bach PM, Rauch W, Mikkelsen PS, McCarthy DT, Deletic A (2014) A critical review of integrated urban water modelling – Urban drainage and beyond. *Environ Model Softw* 54:88–107. doi: 10.1016/j.envsoft.2013.12.018

Bechet B, Bonhomme C, Lamprea K, Campos E, Jean Soro LJ, Dubois P, Lherm D (2015) Towards a Modeling of Traffic Pollutant Flux at Local Scale – Chemical Analysis and Micro-Characterization of Road Dusts. *Urban Proceedings of Environmental Symposium*, June.

Bozlaker A, Muezzinoglu A, Odabasi M (2008) Atmospheric concentrations, dry deposition and air–soil exchange of polycyclic aromatic hydrocarbons (PAHs) in an industrial region in Turkey. *J Hazard Mater* 153:1093–1102. doi:10.1016/j.jhazmat.2007.09.064.

Bressy A (2010) Flux de micropolluants dans les eaux de ruissellement urbaines. Effets de différents modes de gestion des eaux pluviales. LEESU Univ PARIS-EST. <https://hal-agroparistech.archives-ouvertes.fr/docs/00/58/23/79/PDF/TH2010PEST1051.pdf>.

Bressy, A., M. -C. Gromaire, C. Lorgeoux, M. Saad, F. Leroy, and G. Chebbo (2012) Towards the Determination of an Optimal Scale for Stormwater Quality Management: Micropollutants in a Small Residential Catchment. *Water Research*, Special Issue on Stormwater in urban areas, 46 (20): 6799–6810. doi:10.1016/j.watres.2011.12.017. doi:10.1016/j.watres.2011.12.017.

Cao Z, Yang Y, Lu J, Zhang C (2011) Atmospheric particle characterization, distribution, and deposition in Xi'an, Shaanxi Province, Central China. *Environ Pollut* 159:577–584. doi: 10.1016/j.envpol.2010.10.006

Dotto CBS, Kleidorfer M, Deletic A, Rauch W, McCarthy DT, Fletcher TD (2011) Performance and sensitivity analysis of stormwater models using a Bayesian approach and long-term high resolution data. *Environ Model Softw* 26:1225–1239. doi:10.1016/j.envsoft.2011.03.013.

Egodawatta P, Thomas E, Goonetilleke A (2007) Mathematical interpretation of pollutant wash-off from urban road surfaces using simulated rainfall. *Water Res* 41:3025–3031. doi:10.1016/j.watres.2007.03.037.

Egodawatta P, Ziyath AM, Goonetilleke A (2013) Characterising metal build-up on urban road surfaces. *Environ Pollut* 176:87–91. doi:10.1016/j.envpol.2013.01.021.

Fallah Shorshani M, André M, Bonhomme C, Seigneur C (2015) Modelling chain for the effect of road traffic on air and water quality: Techniques, current status and future prospects. *Environ Model Softw* 64:102–123. doi: 10.1016/j.envsoft.2014.11.020

Fallah shorshani M, André M, Bonhomme C, Seigneur C (2012) Coupling Traffic, Pollutant Emission, Air and Water Quality Models: Technical Review and Perspectives. *Procedia - Soc Behav Sci* 48:1794–1804. doi:10.1016/j.sbspro.2012.06.1154.

Garban B, Blanchoud H, Motelay-Massei A, Chevreuil M, Ollivon D (2002) Atmospheric bulk deposition of PAHs onto France: trends from urban to remote sites. *Atmos Environ* 36:5395–5403

Gasperi J, Sebastian C, Ruban V, Delamain M, Percot S, Wiest L, Mirande C, Caupos E, Demare D, Kessoo MDK, Saad M, Schwartz JJ, Dubois P, Fratta C, Wolff H, Moilleron R, Chebbo G, Cren C, Millet M, Barraud S, Gromaire MC (2014) Micropollutants in urban stormwater: occurrence, concentrations, and atmospheric contributions for a wide range of contaminants in three French catchments. *Environ Sci Pollut Res* 21:5267–5281. doi:10.1007/s11356-013-2396-0.

Gunawardena J, Egodawatta P, Ayoko GA, Goonetilleke A (2013) Atmospheric deposition as a source of heavy metals in urban stormwater. *Atmos Environ* 68:235–242. doi:10.1016/j.atmosenv.2012.11.062.

Gunawardena J, Ziyath AM, Egodawatta P, Ayoko GA, Goonetilleke A (2015) Sources and transport pathways of common heavy metals to urban road surfaces. *Ecol Eng* 77:98–102. doi:10.1016/j.ecoleng.2015.01.023.

Herngren L, Goonetilleke A, Ayoko GA (2006) Analysis of heavy metals in road-deposited sediments. *Anal Chim Acta* 571:270–278. doi: 10.1016/j.aca.2006.04.064

Hong Y, Bonhomme C, Le M-H, Chebbo G (2016a) A new approach of monitoring and physically-based modelling to investigate urban wash-off process on a road catchment near Paris. *Water Res* 102:96–108. doi:10.1016/j.watres.2016.06.027

Hong Y, Bonhomme C, Le M-H, Chebbo G (2016b) New insights into the urban washoff process with detailed physical modelling. *Sci Total Environ* 573:924–936. doi: 10.1016/j.scitotenv.2016.08.193

Joshi UM, Balasubramanian R (2010) Characteristics and environmental mobility of trace elements in urban runoff. *Chemosphere* 80:310–318. doi:10.1016/j.chemosphere.2010.03.059.

Keith LH (2015) The Source of U.S. EPA's Sixteen PAH Priority Pollutants. *Polycycl Aromat Compd* 35:147–160. doi: 10.1080/10406638.2014.892886

Kim J-Y, Sansalone JJ (2008) Event-based size distributions of particulate matter transported during urban rainfall-runoff events. *Water Res* 42:2756–2768. doi: 10.1016/j.watres.2008.02.005

Kim K-H, Jahan SA, Kabir E, Brown RJC (2013) A review of airborne polycyclic aromatic hydrocarbons (PAHs) and their human health effects. *Environ Int* 60:71–80. doi:10.1016/j.envint.2013.07.019.

Lamprea K, Ruban V (2011) Pollutant concentrations and fluxes in both stormwater and wastewater at the outlet of two urban watersheds in Nantes (France). *Urban Water J* 8:219–231. doi:10.1080/1573062X.2011.596211.

Lee S, Ho C-H, Choi Y-S (2011) High-PM10 concentration episodes in Seoul, Korea: Background sources and related meteorological conditions. *Atmos Environ* 45:7240–7247. doi:10.1016/j.atmosenv.2011.08.071.

Motelay-Massei A, Garban B, Tiphagne-larcher K, Chevreuril M, Ollivon D (2006) Mass balance for polycyclic aromatic hydrocarbons in the urban watershed of Le Havre (France): Transport and fate of PAHs from the atmosphere to the outlet. *Water Res* 40:1995–2006. doi:10.1016/j.watres.2006.03.015.

Motelay-Massei A, Ollivon D, Garban B, Tiphagne-Larcher K, Zimmerlin I, Chevreuril M (2007) PAHs in the bulk atmospheric deposition of the Seine river basin: Source identification and apportionment by ratios, multivariate statistical techniques and scanning electron microscopy. *Chemosphere* 67:312–321. doi:10.1016/j.chemosphere.2006.09.074.

Motelay-Massei A, Ollivon D, Tiphagne K, Garban B (2005) Atmospheric bulk deposition of trace metals to the Seine river Basin, France: concentrations, sources and evolution from 1988 to 2001 in Paris. *Water Air Soil Pollut* 164:119–135. doi:10.1007/s11270-005-1659-x

Murphy LU, O’Sullivan A, Cochrane TA (2014) Quantifying the Spatial Variability of Airborne Pollutants to Stormwater Runoff in different Land-Use Catchments. *Water Air Soil Pollut* 225. doi:10.1007/s11270-014-2016-8.

Norman M, Sundvor I, Denby BR, Johansson C, Gustafsson M, Blomqvist G, Janhäll S (2016) Modelling road dust emission abatement measures using the NORTRIP model: Vehicle speed and studded tyre reduction. *Atmos Environ* 134:96–108. doi:10.1016/j.atmosenv.2016.03.035.

Padoan E, Romè C, Ajmone-Marsan F (2017) Bioaccessibility and size distribution of metals in road dust and roadside soils along a peri-urban transect. *Sci Total Environ* 601–602:89–98. doi: 10.1016/j.scitotenv.2017.05.180

Pant P, Harrison RM (2013) Estimation of the contribution of road traffic emissions to particulate matter concentrations from field measurements: A review. *Atmos Environ* 77:78–97. doi: 10.1016/j.atmosenv.2013.04.028

Percot S, Ruban V, Roupsard P, Maro D, Millet M (2016) A New Method for Assessing the Contribution of Atmospheric Deposition to the Stormwater Runoff Metal Load in a Small Urban Catchment. *Water Air Soil Pollut* 227:180. doi:10.1007/s11270-016-2794-2.

Rocher V, Azimi S, Gasperi J, Beuvin L, Muller M, Moilleron R, Chebbo G (2004) Hydrocarbons and metals in atmospheric deposition and roof runoff in central Paris. *Water Air Soil Pollut* 159:67–86. doi:10.1023/B:WATE.0000049165.12410.98

Saagi R, Flores-Alsina X, Kroll S, Gernaey KV, Jeppsson U (2017) A model library for simulation and benchmarking of integrated urban wastewater systems. *Environ Model Softw* 93:282–295. doi: 10.1016/j.envsoft.2017.03.026

Roupsard, P, Amielh M, Maro D, Coppalle A, Branger H, Connan O, Laguionie P, Hébert D, Talbaut M. (2013) Measurement in a Wind Tunnel of Dry Deposition Velocities of Submicron Aerosol with Associated Turbulence onto Rough and Smooth Urban Surfaces. *Journal of Aerosol Science* 55: 12–24. doi:10.1016/j.jaerosci.2012.07.006.

Sabin LD, Lim JH, Stolzenbach KD, Schiff KC (2005) Contribution of trace metals from atmospheric deposition to stormwater runoff in a small impervious urban catchment. *Water Res* 39:3929–3937. doi:10.1016/j.watres.2005.07.003.

Sage J, Bonhomme C, Al Ali S, Gromaire M-C (2015) Performance assessment of a commonly used “accumulation and wash-off” model from long-term continuous road runoff turbidity measurements. *Water Res* 78:47–59. doi:10.1016/j.watres.2015.03.030.

Sakata M, Tani Y, Takagi T (2008) Wet and dry deposition fluxes of trace elements in Tokyo Bay. *Atmos Environ* 42:5913–5922. doi:10.1016/j.atmosenv.2008.03.027.

Shi G, Chen Z, Teng J, Bi C, Zhou D, Sun C, Li Y, Xu S (2012) Fluxes, variability and sources of cadmium, lead, arsenic and mercury in dry atmospheric depositions in urban, suburban and rural areas. *Environ Res* 113:28–32. doi:10.1016/j.envres.2012.01.001.

Slinn (1982) Predictions for particle deposition to vegetative canopies. *Atmos Environ* 16:1785–1794

Sweet CW, Weiss A, Vermette SJ (1998) Atmospheric Deposition of Trace Metals at Three Sites Near the Great Lakes. *Water Air Soil Pollut* 103:423–439. doi:10.1023/A:1004905832617.

Tasdemir Y, Esen F (2007) Dry deposition fluxes and deposition velocities of PAHs at an urban site in Turkey. *Atmos Environ* 41:1288–1301. doi:10.1016/j.atmosenv.2006.09.037.

Tasdemir Y, Kural C, Cindoruk SS, Vardar N (2006) Assessment of trace element concentrations and their estimated dry deposition fluxes in an urban atmosphere. *Atmospheric Res* 81:17–35. doi:10.1016/j.atmosres.2005.10.003.

Terzi E, Samara C (2005) Dry deposition of polycyclic aromatic hydrocarbons in urban and rural sites of Western Greece. *Atmos Environ* 39:6261–6270. doi:10.1016/j.atmosenv.2005.06.057.

Tian G, Qiao Z, Xu X (2014) Characteristics of particulate matter (PM<sub>10</sub>) and its relationship with meteorological factors during 2001–2012 in Beijing. *Environ Pollut* 192:266–274. doi:10.1016/j.envpol.2014.04.036.

Vaze J, Chiew FH (2002) Experimental study of pollutant accumulation on an urban road surface. *Urban Water* 4:379–389. doi:10.1016/S1462-0758(02)00027-4

Wang W, Simonich S, Giri B, Chang Y, Zhang Y, Jia Y, Tao S, Wang R, Wang B, Li W, Cao J, Lu X (2011) Atmospheric concentrations and air–soil gas exchange of polycyclic aromatic hydrocarbons (PAHs) in remote, rural village and urban areas of Beijing–Tianjin region, North China. *Sci Total Environ* 409:2942–2950. doi:10.1016/j.scitotenv.2011.04.021.

Weinbruch S, Worringen A, Ebert M, Scheuven D, Kandler K, Pfeffer U, Bruckmann P (2014) A quantitative estimation of the exhaust, abrasion and resuspension components of particulate traffic emissions using electron microscopy. *Atmos Environ* 99:175–182. doi:10.1016/j.atmosenv.2014.09.075.

Zhao H, Chen X, Hao S, Jiang Y, Zhao J, Zou C, Xie W (2016) Is the wash-off process of road-deposited sediment source limited or transport limited? *Sci Total Environ* 563–564:62–70. doi: 10.1016/j.scitotenv.2016.04.123

Zhao H, Li X (2013) Understanding the relationship between heavy metals in road-deposited sediments and washoff particles in urban stormwater using simulated rainfall. *J Hazard Mater* 246–247:267–276. doi: 10.1016/j.jhazmat.2012.12.035

Zhao H, Li X, Wang X, Tian D (2010) Grain size distribution of road-deposited sediment and its contribution to heavy metal pollution in urban runoff in Beijing, China. *J Hazard Mater* 183:203–210. doi: 10.1016/j.jhazmat.2010.07.012

## Chapitre 3. Investigation of the wash-off process using an innovative portable rainfall simulator allowing continuous monitoring of flow and turbidity at the urban surface outlet

**Abstract:** Development of appropriate models, based on an in-depth understanding of the wash-off process, is essential to accurately estimating pollutant loads transported by stormwater, thereby minimizing environmental contamination. To this end, we developed an innovative rainfall simulator, which simulated an intense rainfall (120mm/h) and permitted the acquisition of runoff samples as well as the in situ monitoring of continuous flow and turbidity dynamics. Relationships between deposited sediments and total suspended solids in simulated runoff were thus investigated on two different types of surfaces within the Paris region in terms of loads and particle size distribution. Results demonstrate the occurrence of first flush phenomenon on the sidewalks even under constant flow. Results also show that the highest fraction conveyed by runoff consisted of fine (<16 $\mu$ m) and medium-sized (<100 $\mu$ m) particles, whose detachment was more favorable from smooth surfaces than from rougher ones. In terms of stormwater quality modelling, results suggest that the integration of a wash-off fraction based on both particle size and rainfall intensity could be an entrance for a better prediction of stormwater pollution.

**Keywords:** Particle size distribution, Rainfall simulation, Sediments, Stormwater, Wash-off process.

### 1. Introduction

Modification of land surface due to urban expansion has led to a significant increase in impervious surfaces (Wilson and Weng, 2010). This has been accompanied by a rise in the volume of urban stormwater runoff (Chen et al., 2016) and pollutant loads. Pollutant wash-off from impervious surfaces in urban catchments, mainly roads and parking lots, is a major contributor to stormwater runoff contamination (Motelay-Massei et al., 2006; Revitt et al., 2014). During a rainfall event, pollutants deposited on the surface during the dry weather period will be mobilized in different forms and migrate into the sewer system. Pollutants transported within the particulate matter are recognized as the main source of contamination as toxic elements such as trace metals and polycyclic aromatic hydrocarbons as well as organic

matter are adsorbed on their surface and scattered over the particles in several size fractions (Kim and Sansalone, 2008; Sansalone et al., 1998; Zhao and Li, 2013). The most common indicator for particulate matter is the total suspended solids (TSS) (Rossi et al., 2013). The direct discharge of TSS into the receiving water bodies will pose a severe environmental risk if left untreated. The evaluation of such risk is primarily based on the understanding of build-up and wash-off processes (Deletic and Orr, 2005; Egodawatta et al., 2013; Vaze and Chiew, 2002), and in-depth investigation of relationships between sediment deposits and fractions transported by wash-off (Eckley and Branfireun, 2009; Zhao and Li, 2013). Furumai et al. (2002) showed that surface wash-off is highly dependent on the particle sizes that are present prior to a storm event, noting that more than half of the particulate load in runoff samples are associated with particles less than 20 $\mu$ m. In a recent study, Hong et al. (2016b) demonstrated that most fine particles (less than 15 $\mu$ m) are transported at the beginning of a rainfall event, while a number of coarser particles are transported later if the rainfall intensity is high enough, or if there is sufficient energy in the flow. These findings confirm that fine and coarse particles exhibit distinct transport behavior, revealing the need to not only compare particulate matter in terms of load, but also size distribution (Kim and Sansalone, 2008; Wijesiri et al., 2015; Zhao et al., 2010). Therefore, it is essential to incorporate this knowledge into stormwater quality models in order to enhance and elucidate the current description of the complex processes governing the generation and transport of pollutants. Obtaining new knowledge on these processes and their controlling factors requires an in-depth investigation in order to acquire the necessary data.

Several sampling techniques have been used to collect build-up and wash-off samples. Build-up samples are usually obtained either by spraying water on the surface and then collecting the effluent using a vacuum cleaner (Deletic and Orr, 2005) or by brushing the surface and dry vacuuming (Eckley and Branfireun, 2009; Vaze and Chiew, 2002). Both methods have high sampling efficiency and allow the collection of the fine particles that are dislodged under the pressure of water spray or the action of the brush. However, it should be noted that an accurate estimate of the available pollutant load on the surface alone is not sufficient in determining the level of contamination in the runoff. In fact, several studies have shown that the amount transported by stormwater runoff is minimal compared to the amount of stock present on the surface (Hong et al., 2016a; Pitt et al., 2005), suggesting that wash-off

sampling is a necessary complement to dust sampling in evaluating stormwater contamination.

Stormwater samples obtained from natural rainfall are usually collected at the catchment outlet, which is equipped with automatic samplers (Al Ali et al., 2016; Goonetilleke et al., 2005; Liu et al., 2013). Using these types of samples in order to understand and elucidate erosion and wash-off mechanisms is difficult given the high variability of rainfall characteristics and the random nature of rainfall events. To overcome these challenges, researchers resorted to artificial rainfall, where rainfall is generated under controlled conditions using rainfall simulators (Egodawatta et al., 2007; Hengren et al., 2005; Zhao and Li, 2013). Artificial rainfall conditions are favorable, since they allow for the simulation of different rainfall scenarios. This will help identify key explanatory factors that can be implemented in the mathematical replication of the wash-off process. By simulating rainfalls of different intensities and durations to investigate the wash-off of pollutants from urban road surfaces, Zhao and Li (2013) concluded that the wash-off fraction is proportional to both factors, as intense rainfall mobilized the highest fraction of loads. Based on similar results, Egodawatta et al. (2007) developed a new wash-off model by modifying the original exponential wash-off equation proposed by Sartor et al. (1974) and introducing a capacity factor that depends on rainfall intensity. These studies highlight the interest of using rainfall simulators to study wash-off; however, the results were analyzed only in terms of loads and their corresponding particle size distribution. Until now, no study has allowed for *in situ* analysis of the instantaneous hydrographs and pollutographs generated by the simulated runoff.

Another constraint of previous studies is the fact that rainfall simulators usually require more than one person to install and operate, adding time to the sampling process and making it impossible to perform several experiments on the same day at different locations. In addition, some simulators might not be used on real sites outside of the laboratory because of their sophisticated design. Therefore, the development of a portable field rainfall simulator seems adequate in addressing this issue. In fact, a number of studies have investigated wash-off using portable field rainfall simulators in natural catchments (Battany and Grismer, 2000).



In this paper, an innovative device consisting of a lightweight mobile rainfall simulator, equipped with a measuring system that allows for the continuous *in situ* monitoring of flow and turbidity, and thus the investigation of instantaneous hydrograph and pollutograph, was designed to study the transport dynamics of TSS from paved zones of two distinct surfaces. Dust and water samples were collected and compared in terms of loads and particle size distribution on both surfaces. Results are interpreted with the view of understanding the physical process of pollutant production and enhancing the current modelling approaches of stormwater wash-off.

## 2. Materials and methods

### 2.1. Study area

The research sites are located in two different districts situated in the eastern part of the Paris region. They were chosen to represent different surface types. The first site consisted of the sidewalks located at proximity of the highly trafficked (up to ~30,000 vehicles per day) boulevard “Alsace Lorraine” in the residential district of “Le Perreux sur Marne” in the department of “Val de Marne”. The surrounding area includes residential houses and small commercial shops. The sidewalks are characterized by a smooth surface.

The second research site was a parking lot in the University of “Ecole des Ponts Paristech”. The university is located in the district of “Champs sur Marne” within the department of “Seine et Marne”. The parking surface is made of coarse asphalt and is subjected to low traffic density.

The surfaces at both locations are presented in Fig. 1.

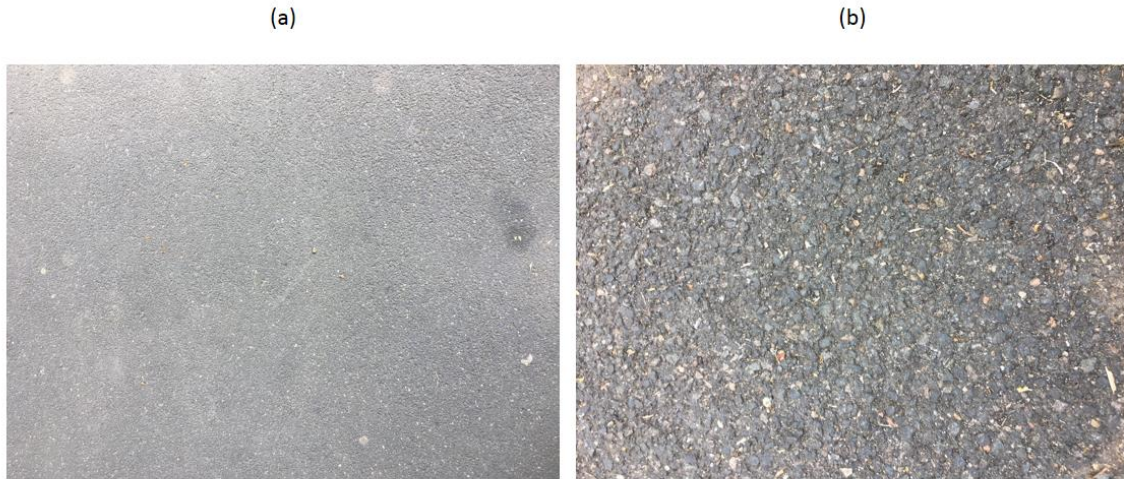


Fig. 1 (a) The sidewalk surface (b) The parking lot surface

## 2.2. Rainfall simulator, measuring system and experimental data

### 2.2.1. Design and conception

A specially designed portable field device consisting of a rainfall simulator and a measuring system that allows for continuous monitoring of flow and turbidity was used in this study. The device was designed to homogeneously spray an elementary area of 1 m<sup>2</sup>, with a one-year return period rainfall having a raindrop size distribution similar to the natural regional rainfall. Lightweight materials were used in the construction of the device so that it could be easily operated by one person and to reduce implementation time to less than an hour.

The simulator consisted of two aluminum frames: the first was a U-shape, where the nozzle spray and hollow parallelepipedic legs were attached; the other was a square plot frame (1mx1m) that delineated the plot boundary. The two frames were assembled by fitting the legs of the U-shaped frame into two parallelepipedic tubes fixed between two parallel outside borders of the plot frame, with an internal length equal to the external length of the legs of the U- shaped frame.

The U-shaped frame was equipped with a Fulljet standard spray nozzle (reference: 1/8HH-5) from Spraying Systems Company, which was attached to the middle of the frame and stood at 1.6 meters above the ground. At this height, the spray nozzle delivered a solid cone spray pattern, watering the plot area.

Water was driven to the nozzle using a peristaltic Watson Marlow pump. The motor was supplied with a voltage of 24 volts, allowing the pumping of the water from a 30-liter plastic tank that rested on the ground near the simulator. The tank was connected to the pump using a PVC TYGON tube, with an interior diameter of 12.7 mm and a thickness of 3.2 mm. Another PVC Watson Marlow tube with an interior diameter of 6.4 mm and a thickness of 2.4 mm, connected the nozzle to the pump, ensuring the flow of water. The pump was set to deliver a flow rate of 2000ml/min at the entry of the nozzle, with pressure equal to 1.5 bars.

To ensure that no leakage of sprayed water outside of the plot frame would occur, rubber joints were fixed using an aluminum blade screwed to all sides of the frame, and weights were placed on the top of the plot borders. A clear plastic sheet was also used to cover the frame to prevent the deviation of rainfall drops caused by the wind.

The water was then transported through two suction heads of 400 mm to a 100 liter “Manuttan” tank using an industrial vacuum “jet 60 RE”, which was connected to the tank through a hole. The water entered into a system consisting of funnels that acted as a flow straightener to tranquilize and stabilize the flux. The tank also contained a “Bamomatic” electromagnetic flow meter and an “Analite NEP 1610” turbidimeter that allowed the continuous measuring of both flow and turbidity. The functioning of the flow meter required that its electrodes maintained contact with water at all times, which is why a siphon, placed between the end of the funnel system and the entry of the flow meter, was filled with clean water prior to starting the simulation. A sediment catcher was also placed in the tank to trap big particles, which risk inducing false turbidity peaks. The turbidimeter and flow meter were connected to the acquisition unit that was placed in the control box along with the pump. A specific program operated the simulator by sending instructions to launch the pump at the specified flow rate. The equipments are represented in Fig. 2, and the scheme representing the functioning of the system is provided in appendix A (Fig.A.1).

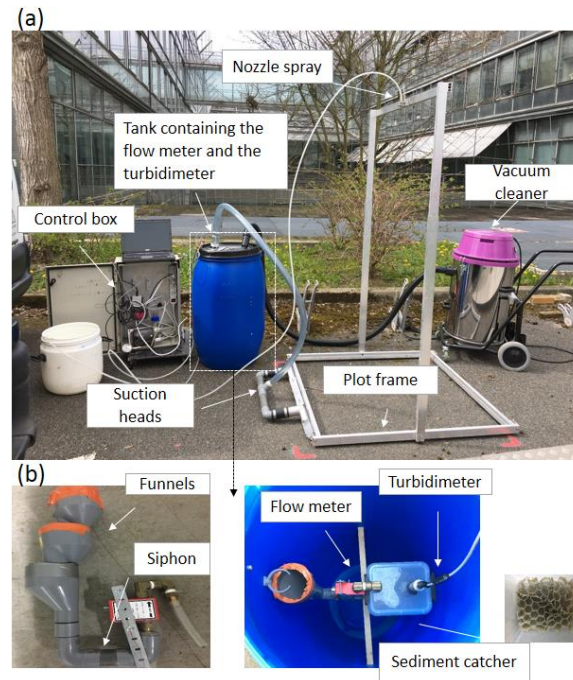


Fig. 2 (a) The equipment of the rainfall simulator, (b) the funnels and the measuring system

## 2.2.2. Sampling collection and laboratory analysis

- **Dry deposits samples**

Road deposits were collected using a domestic vacuum cleaner “Rowenta RU 4022” (Bechet et al., 2015). The vacuum is relatively powerful and consists of a highly compact 1500w motor. It delivers an air flux equal to 38 dm<sup>3</sup>/s. The use of domestic vacuum cleaners have shown high efficiency in collecting dust and mainly fine particles (Egodawatta, 2007; Zhao and Li, 2013). The samples were collected on both sites within an adhesive tape delimited rectangular frame plot of 2m<sup>2</sup> (2mx1m). First, the surface was scrubbed in a circular motion using a brush in order to dislodge and release the fine particles attached to the surface, therefore enhancing their collection. Then, the vacuum was passed over the entire area in small strips, with an aspiration velocity of approximately 5cm/s. The dust was collected in paper filters within the vacuum.

Three samples of dry deposits were collected on the sidewalks (one at each location) on June 7<sup>th</sup> 2015 after a dry weather period equal to 37 days. Three samples were also collected on the parking lot on the 1<sup>st</sup> and 15<sup>th</sup> of December 2016 and on the 10<sup>th</sup> of February 2017 after a dry weather period equal to seven, one and two days, respectively.

Samples collected on both the sidewalks and the parking lot, were taken to the laboratory for analysis. The dust samples were sieved into two fractions using a 2 mm sieve. Then, the sieved fraction was weighed to estimate the load and analyzed for particle size distribution using a laser diffractometer (Malvern® Mastersizer 3000) (Bechet et al., 2015). The (Malvern®Mastersizer 3000) reports the volume fraction for each size class. The volume distribution is calculated with the Mie light scattering theory, where all the particles are assumed to be spherical and diffuse in the same way. The refractive indexes used for the measurements are 1.33 for the dispersant solution (water) and 1.53 for the particles as wet dispersion. We also calculated the mass of particles in each size fraction. Since we didn't have any measurements for particles density for each size fraction, we assumed that all particles have the same density. Sediments usually are a mix of irregular particles with different shapes and densities. Nevertheless, for practical reasons and simplifications, all particles are assumed to be spherical and have the same density. These assumption are widely accepted and applied in mathematical models of sediment transport (Deletic, 2001; Hong et al., 2016a). However, when designing mitigation strategies for stormwater pollution, the density of the particles must be carefully chosen because it influences the estimation of the facility's efficiency (Zanders, 2005).

Dust samples collected at the parking lot were left for decantation (after adding pure water) the night preceding analysis in order to remove the high organic fraction, which resulted mainly from vegetation fragments originating from surrounding trees and vegetable foam on the surface.

- **Wash-off samples**

Wash-off samples were collected after ten minutes of simulated rainfall applied with a 120 mm/h intensity, at the same time and at the same locations as dust samples. For portability reasons, the duration of the simulation was short. To simulate a 10 minutes rainfall with a rainfall intensity of 120 mm/h we needed 20 liters of water. Simulating longer events will require using larger volume of water, whose transportation on site is not easy. Continuous measurements of flow and turbidity were recorded for the entire duration of the simulation, at a time step of 500 ms. At the end of the simulation, the contents of the tank were homogenized and the mean turbidity was measured. The samples were then transported to

the laboratory for analysis, and the volume of water recovered from the tank was calculated to check that there was no loss in the runoff volume. Then, after careful homogenization of the contents of the tank, three subsamples were taken to quantify the washed-off loads and the mean concentration of TSS by filtration, using 0.45µm glass fibers glass. The filters were weighed prior to the filtration to determine their initial mass. After filtration, the filters were placed in the oven at 60°C for 24 hours to dry. Then they were weighed again and the washed-off load was hence calculated as the difference between the initial mass and the mass after drying.

We did not perform any analysis on the filtrate to characterize the dissolved matter because in this study, we were mainly interested with the particulate matter. The interest in the particulate matter is based on its being the main vector of toxic pollutants such as PAHs and trace metals in stormwater runoff.

In addition, subsamples of two liters were taken at the end of the simulations on the sidewalks only to analyze the particle size distribution using the same technique as for dust samples.

The transport dynamics of TSS in the simulated runoff at both sites were also investigated, based on the analysis of the M(V) curves (Bertrand-Krajewski et al., 1998). M(V) curves were obtained by plotting the dimensionless cumulative TSS mass vs. the dimensionless cumulative runoff volume. In order to determine the mass of TSS, turbidity measurements must be converted into TSS concentrations. Therefore, TSS–turbidity linear relationships were established, and the TSS concentrations at each site were given by the following relationships, with a correlation factor  $R^2 > 0.97$ :

$$[TSS]_{sidewalk} = 6.1 \times T_{sidewalk} \quad (1)$$

$$[TSS]_{parking\ lot} = 6.38 \times T_{parking\ lot} \quad (2)$$

Where:  $[TSS]_{sidewalk}$  = the concentration of Total Suspended Solids at the sidewalks in mg/l;  $T_{sidewalk}$  = turbidity at the sidewalks in NTU;  $[TSS]_{parking\ lot}$  = the concentration of Total Suspended Solids at the parking lot in mg/l;  $T_{parking\ lot}$  = turbidity at the parking lot in NTU.

### 3. Results

#### 3.1. Rainfall simulator reliability

##### 3.1.1. Calibration

The uniformity analysis was carried out by exposing sixteen containers arranged in a 4x4 square frame within the area covered by the plot frame to a 10-minutes rainfall, with a rainfall intensity of 120mm/h. The containers were weighed before and after the rainfall, and the volume of water was determined by calculating the difference between both weights. The uniformity coefficient was then calculated based on the formula proposed by (Christiansen, 1942) :

$$CU = 1 - \frac{\sum X}{M \times N} \quad (3)$$

Where :  $CU$  = uniformity coefficient ;  $X$  = absolute value of the deviation from the mean of individual observations;  $M$  = the mean value of observations;  $N$  = number of observations.

The calculated uniformity coefficient was equal to 73%, similar results were obtained in previous studies (Iserloh et al., 2013; Lascelles et al., 2000). The spatial distribution of rainfall shows that the highest rainfall amount was collected in the central containers placed directly below the nozzle, while lower amounts reached the containers placed on the upper and lower ends of the plot. If we calculate the uniformity coefficient by excluding the upper and lower ends of the frame plot, the uniformity coefficient is higher and equal to 80%, which is in agreement with the “edge effect” resulting in a non-uniform spatial distribution across the plot (Loch et al., 2001). The spatial variability calculated for this rainfall simulator is still within the acceptable range to perform a successful rainfall simulation.

##### 3.1.2. Raindrop size distribution

The drop size distribution was obtained using a “THIES” laser precipitation monitor. The device allows for the acquisition of the particle spectrum, which is the distribution of the particles over the class bins. The precipitation monitor was placed on the ground in the center of the frame plot, and recorded measurements under an artificial 120mm/h rainfall during five minutes, at a pressure equal to 1.5 bars. Analysis of raindrop size distribution given by the disdrometer for the simulated rainfall showed that the drop sizes are small (Fig.A.2). The

maximum number of raindrops was attained within the 0.5-0.75 mm diameter range, which also corresponds to the central raindrop diameter measured for several natural rainfall events that occurred in the same region. The fall velocity of 85% of the measured drops was lower than 5m/s. The performance of the rainfall simulator is satisfying given that it accurately replicated the raindrop distribution of natural rainfall. Bigger raindrops in the simulated rainfall might have been expected since the simulated intensity was relatively high, however comparison with other small and portable rainfall simulators shows similarities concerning the obtained drop size distributions where the highest drop numbers are lower than 1 mm even under intense rainfall (Iserloh et al., 2013). Attaining distributions of higher raindrop diameters while maintaining high intensity range would require more sophisticated and complicated devices that do not have any restrictions on the design, which might reduce the simulator's portability and feasibility for direct *in situ* investigations.

### **3.1.3. Runoff coefficient**

The efficiency of the system in collecting runoff was evaluated by calculating the runoff coefficient, which corresponds to the ratio between the collected runoff volume and the precipitation volume, which was equal to 20 liters. Runoff coefficients calculated at both sites were higher than 0.83 for all simulations. The high value calculated for the runoff coefficient confirmed that the system collected most of the runoff generated during the simulation and ensured the total humidification of the surface.

### **3.2. Dynamics of TSS in runoff**

The TSS concentrations in simulated stormwater collected on the sidewalks, varied between 172.26 and 267.03 mg/l with a mean value equal to 226.69 mg/l. For comparison, the TSS concentrations calculated at the parking lot, were lower, as they varied between 88.31 and 252.4 mg/l with a mean value equal to 153.72 mg/l.

The TSS dynamics measured at both sites are presented in the Figure below (Fig. 3). It can be noted that the pollutographs measured at the parking lot showed distinctive patterns at each simulation. For the first and third simulations, the pollutographs presented two distinctive peaks. As displayed in Fig. 3 (a), the TSS concentration increased to reach 560 mg/l at the beginning of the runoff and then gradually decreased before reaching a peak value of 890 mg/l after eight minutes. For the second simulation (Fig. 3 (b)), a high peak of TSS



concentration was observed at the initial stage of runoff, before quickly decreasing to a stable period that lasted until the end of the event. The corresponding TSS concentration at the peak was equal to 865.1 mg/l, which is 30 times higher than the average TSS concentration recorded during the following stable period ( $91.38 \pm 63.8$  mg/l). The third simulation at the parking lot illustrated in Fig. 3 (c) also showed a high peak at the beginning of the runoff, with a TSS concentration equal to 325 mg/l, followed by a systematic decrease over time that was interrupted by a sudden increase at the seventh minute mark.

This inconsistency in TSS dynamics during the rainfall event was not observed at the sidewalk sites, where all pollutographs showed a quick increase in TSS concentration at the beginning of the event followed by a rapid decrease to a period of stabilization after three minutes. The peaks of TSS concentrations reached 979.6, 1115.1 and 1726.3 mg/l at the three sidewalk sites 1, 2 and 3 respectively (Fig. 3 (d), (e) and (f)), while the average TSS concentrations recorded during the corresponding stable period were respectively  $198.57 \pm 31.2$ ,  $50.94 \pm 28.07$  and  $185.73 \pm 136.07$  mg/l. To be noted that at sidewalk 3, near the end of the simulation, we observed an increase in the concentration of TSS that might be explained by the preceding increase of the flow. As we can see in Fig. 3 (c) and (f), the measured flow is not constant all the time. This variation can be explained by an instability of the funnel system that might have caused a loss in the volume passing through the flow meter, and resulting thus in the appearance of fluctuations in the measured hydrograph. The fraction of the sucked water that skipped the flow meter will drop directly to the bottom of the tank, in this case.

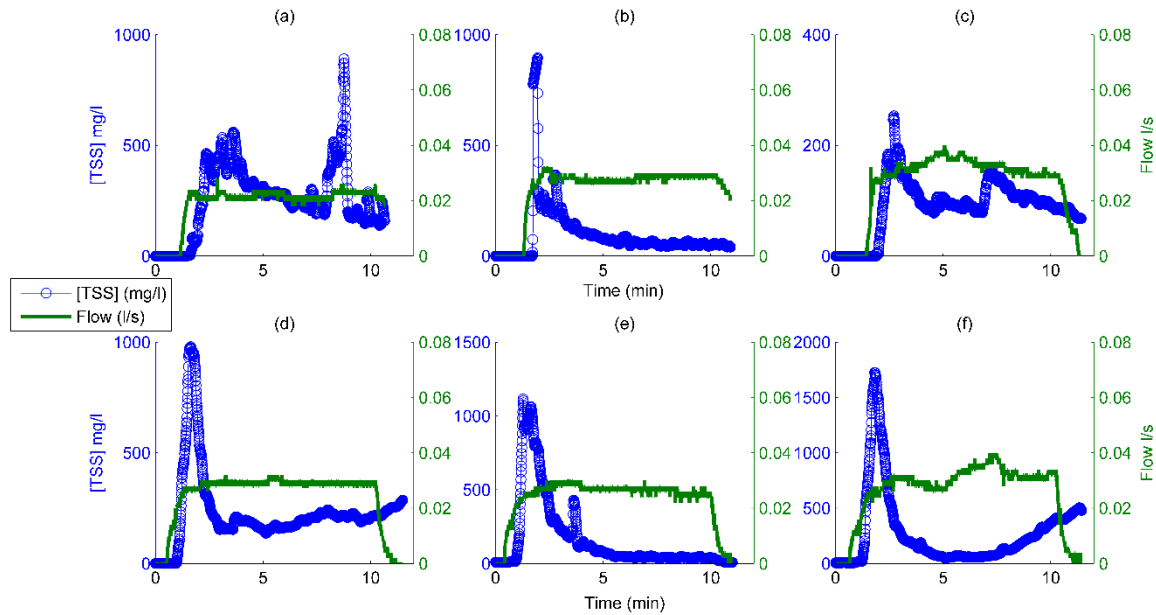


Fig. 3 TSS dynamics and hydrographs measured at the (a) parking lot on 01/12/2016 (b) parking lot on 15/12/2016 (c) parking lot on 10/02/2017 (d) sidewalk 1 (e) sidewalk 2 and (f) sidewalk 3

The M(V) curves obtained at the parking lot showed that the fraction of mass discharged by the volume at any time of the events is constant (Fig.A.3) except for the event recorded on December 15, 2016 where the occurrence of the first flush phenomenon is observed (Al Ali et al., 2016). On the other hand, the M(V) curves of the events recorded at the sidewalks, confirmed that the first volume of runoff always mobilized the highest load of contaminants where the initial 15% of runoff transported an average 50% of the TSS load.

### 3.3. TSS in runoff

#### 3.3.1. Washed-off loads

TSS loads collected in simulated wash-off samples at both the parking lot and the sidewalk sites are presented in Table 1. The analysis of wash-off data collected at the parking lot shows that there is very little variability in the TSS fraction mobilized for each simulation, which suggests that the amount of pollutant transported during the rainfall event is almost the same. The highest wash-off load accounting for 1.1 g/m<sup>2</sup> was calculated for the sample collected on December 1, 2016, while the wash-off loads measured at the other sampling dates were very close. As for the sidewalk sites, a higher wash-off load of TSS was measured at all locations in comparison to the ones measured at the parking lot. The results also highlight the existence of a spatial variability of TSS wash-off load, where maximum TSS loads equal to 5.18 g/m<sup>2</sup> are transported by the runoff at sidewalk 3, while minimum loads accounting for 2.86

g/m<sup>2</sup> are transported at sidewalk 2. The loads transported at sidewalk 1 were similar to the ones transported at sidewalk 3.

**Table 1 TSS loads measured in simulated wash-off samples at the parking lot and the sidewalks**

Date	Sampling location	Wash-off load (g/m <sup>2</sup> )	Mean	Standard deviation	
01/12/2016	Parking lot	1,10	0,89	0,19	
15/12/2016		0,83			
10/02/2017		0,73			
07/07/2015	Sidewalks	1	4,10	1,17	
		2			2,86
		3			5,18

### 3.3.2. Particle size distribution

The mass distribution of the washed-off TSS loads at the sidewalks shows that particles having a diameter of less than 100µm are the most abundant (Fig.A.4). Wash-off particles with less than 100µm accounted for 83% of the total wash-off load at sidewalk 3, and for 78 and 65 % respectively at sidewalks 1 and 2.

Particle size distribution was further analyzed by categorizing particles into three classes representing the finest (<16µm), medium-sized (16-100µm) and coarsest particles (>100µm) and the results are summarized in Table 2.

**Table 2 Cumulative masses and percentages of TSS loads in simulated wash-off samples collected at the sidewalks**

Particle size	< 16µm		16µm < - <100µm		> 100µm	
	Mass (g/m <sup>2</sup> )	Percentage (%)	Mass (g/m <sup>2</sup> )	Percentage (%)	Mass (g/m <sup>2</sup> )	Percentage (%)
Sidewalk 1	0,58	14	2,74	64	0,94	22
Sidewalk 2	0,34	12	1,53	53	0,98	35
Sidewalk 3	0,83	16	3,47	67	0,89	17

Particles transported in the finest fraction (less than 16µm) did not exceed 16% and had an equivalent mass varying between 0.34 and 0.83 g/m<sup>2</sup>. The majority of the particles transported at all sidewalks were in the medium-sized fraction, representing the highest percentage of mass, which ranged from 53 to 67%. Few coarse particles were also transported by the runoff. Even though the highest percentage of coarse particles was conveyed at sidewalk 2, it actually accounted for almost the same amount in terms of mass transported at the other locations. A comparison of the particle size distribution at the three locations

indicates similar distributions at both sidewalks 1 and 3, with slightly coarser yields from sidewalk 1 and finer yields from sidewalk 3. Whereas a more remarkable difference was seen at sidewalk 2, where the runoff mobilized lower loads of particles less than 100 $\mu$ m.

### 3.4. Dry stock

#### 3.4.1. Sediment load

Sediment loads calculated at the parking lot and the sidewalks are presented in Table 3. The amount of sediments collected at the parking lot varied proportionally to the antecedent dry weather period, where the highest amount of sediments were collected after seven days of dry weather. Comparison with the sediment load collected at the sidewalks after 37 days of dry weather, showed that almost the same amount of pollutant was present on the surface at sidewalks 2 and 3, while a higher amount was collected at sidewalk 1. This result is in agreement with the findings of Deletic and Orr (2005) concerning the influence of antecedent dry days on TSS stock. Sediments appear to gradually build-up and accumulate on the surface during dry weather, until reaching a steady state after several days. The build-up rate will then reduce, resulting in a low increase of stock on the surface regardless of the duration of the dry weather period. This shows that the impact of the antecedent dry weather period on the build-up is not negligible, but rather limited.

**Table 3 Sediment loads collected at the parking lot and the sidewalks**

Date	ADWP (days)	Sampling location	Sediment load (g/m <sup>2</sup> )	Mean	Standard deviation	
01/12/2016	7	Parking lot	20,45	16,6	4,96	
15/12/2016	1		11			
10/02/2017	2		18,35			
07/07/2015	37	Sidewalks	1	23,76	3,67	
			2			20,05
			3			23,85

#### 3.4.2. Particle size distribution

The particle size distribution of available sediments on the sidewalks showed an important fraction of coarse particles higher than 100 $\mu$ m, most remarkable at sidewalk 1 (Fig.A.5). Particles higher than 100 $\mu$ m accounted for 62% of the available sediments at

sidewalk 1, and for 40 and 34 % of the available sediments at sidewalk 2 and 3 respectively, representing thus double the load available in this fraction at the other locations (Table 4). Fine particles of less than 16 $\mu$ m were present in lower amounts, not exceeding 8% of the available sediments at all sidewalks, while the remaining sediments were present in the medium size fraction.

**Table 4 Cumulative masses and percentages of sediment loads in dust samples collected at the sidewalks and at the parking lot**

Particle size		< 16 $\mu$ m		16 $\mu$ m < - <100 $\mu$ m		> 100 $\mu$ m		
		Mass (g/m <sup>2</sup> )	Percentage (%)	Mass (g/m <sup>2</sup> )	Percentage (%)	Mass (g/m <sup>2</sup> )	Percentage (%)	
07/07/2015	Sidewalks	1	1,4	5	9,15	33	17	62
		2	1,2	5	11	55	8	40
		3	1,83	8	14	58	8	34
01/12/2016	Parking lot		0,6	3	2,75	14	17,1	83
15/12/2016			0,28	2,6	0,82	7,4	9,9	90
10/02/2017			0,72	4	2,95	16	14,68	80

The mass distribution of sediments in dust samples collected at the parking lot is shown in Fig. 4, and it clearly illustrates more remarkable dominance of the coarse fraction. In addition, the distribution seems to be bimodal as two distinct peaks emerge for all samples. The second peak is most likely due to the high fraction of vegetation fragments and tree leaves collected in the samples. Particles greater than 100 $\mu$ m accounted for more than 80% of the available sediments for the three sampling dates. The highest fraction of particles > 100 $\mu$ m was found in the sample of December 15<sup>th</sup>, where 90% of the available dust had a diameter higher than 100 $\mu$ m (Table 4). However, in terms of mass, samples collected on the other dates, conveyed higher loads within this coarse fraction. Fine particles of less than 16 $\mu$ m, were present in very low amounts as they did not account for more than 4% of the available sediments collected at the parking lot during the three campaigns, while the remaining particles were present in the medium size fraction. Comparison of the particle size distribution of the samples collected on the three dates, shows similar distributions, especially for the samples obtained on the first and third campaign.

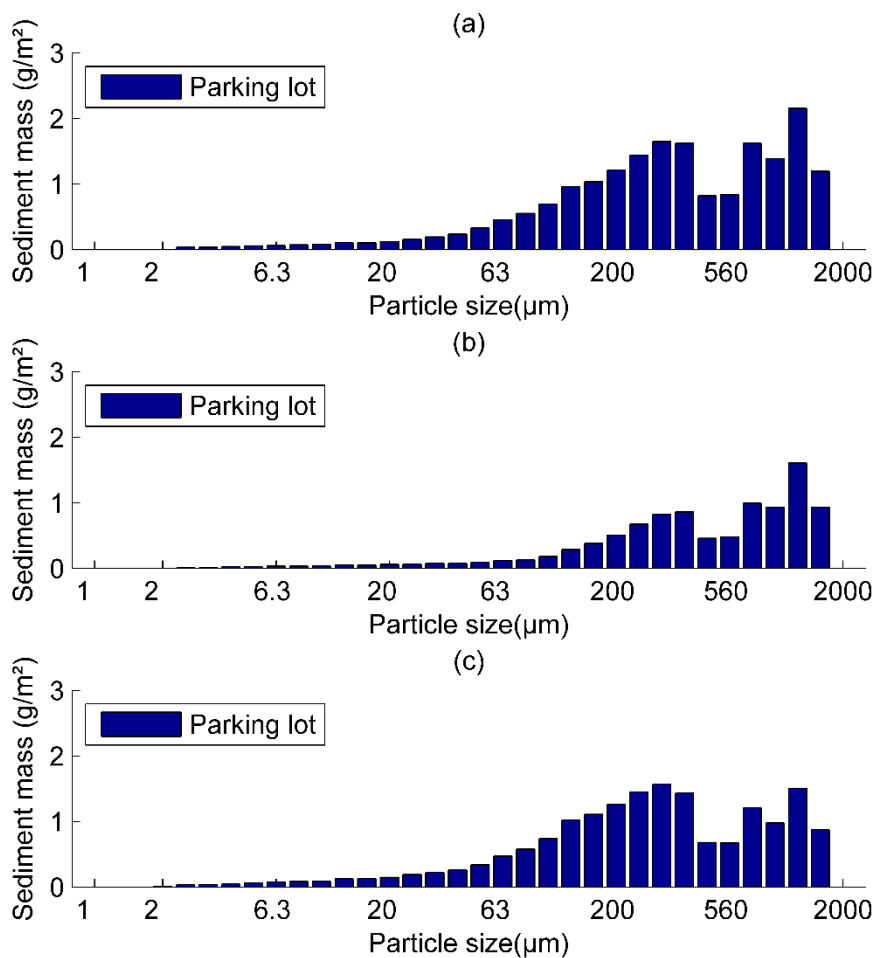


Fig. 4 Particle size distribution of sediments in dry dust collected at the parking lot on (a) 01/12/2016 (b) 15/12/2016 and (c) 10/02/2017

#### 4. Discussion

##### 4.1. Rainfall simulator

###### 4.1.1. Constraints on rainfall simulator design

When designing a rainfall simulator, one of the most substantial and critical characteristics of natural rainfall events that researchers tend to reproduce is the kinetic energy of the rainfall drops. Based on this, we intended to develop a rainfall simulator that simulates a rainfall having a drop size distribution similar to the one measured at the studied site for natural events. For this purpose, we chose a Fulljet standard spray nozzle from Spraying Systems Company, to generate the rainfall drops. This type of nozzles is usually used for irrigation purposes. The nozzle is easily transported and fixed, which is an important advantage for developing a lightweight mobile simulator that can be effortlessly handled by

one person on the site. To have a complete coverage of the plot surface, we decided to use a full cone nozzle having a spray angle around  $60^\circ$ . This type of nozzles provide a uniform spray distribution of drops. For this spray angle, the height at which the nozzle must be placed is 1.6 meters. This spraying angle was the most adequate since smaller angles would require higher fall heights that will reduce the mobility of the system, while higher angles will induce larger losses on the edges of the plot. Therefore, to have the appropriate rainfall drop distribution with the chosen nozzle at the specific height, the flow rate delivered by the pump is found to be equal to 2000 ml/min, corresponding to a rainfall intensity equal to 120 mm/h. Thus, the choice of this high intensity is the result of a compromise between the chosen nozzle, the frame's height and the pump. The high intensity will also compensate the effects of the low fall height.

Even though the simulated rainfall was very intense and had a short duration, the occurrence of natural rainfall events with the same characteristics in the Parisian region is not rare or uncommon. Several rainfall events recorded on the studied site had high intensity and lasted for a short time.

Currently a work is being conducted to enhance the simulator and extend its capabilities to simulate rainfall under different meteorological conditions (wider ranges of intensities, longer durations...), even though finding the accurate nozzle for variable intensities is not very easy. It should be also noted, that the spraying intensities should be high enough to obtain the instantaneous measurements of the flow. Otherwise, the water volume recovered in the tank would fail to produce continuous recording of the instantaneous flow, because the sucked water in this case will travel as a thin film through the measuring system.

#### **4.1.2. Flow driven detachment or raindrop detachment?**

After a certain time from the beginning of a natural rainfall event, the water height on the surface begins to rise. The energy carried by the flow will transport the particles present on the surface. If the energy is sufficient, particles under the turbulence created by the gravitational flow will begin to move, and will be flushed into the runoff. However, this phenomenon will not occur in our case study. Given the short duration of the simulated rainfall and the limitations at the boundaries, there will be no sufficient conditions for the flow sheet to be formed on the surface. The detachment of the particles is thus mainly driven by the

raindrop impact which was advanced as the main driving force for sediment transport from an urban surface in a recent study by Hong et al. (2016a). Achieving higher wash-off fractions using this rainfall simulator is rather controlled by the duration of the simulated rainfall than the potential shear stress of the flow. Recent study by (Zhao et al., 2016) showed that long rainfall events tend to be source limited while short events are transport limited, suggesting that during long rainfall events more significant loads will be transported.

#### **4.1.3. Vacuumed flow**

The use of the vacuum cleaner to collect the flow from the plot frame will result in the disturbance of the gravitational flow. The flow is sucked up at an accelerated speed from the surface into a pipe via two suction heads before reaching the tank. This will result in changing the characteristics of the overland flow and the creation of turbulence, which is very limited at proximity of the suction heads. The boundary conditions at the suction heads of the simulator resembles to the boundary conditions at the entry of a stormwater drain on the street, where at both edges the water height will drop to zero. The hole of the drain as well as the suction heads both function as a dam, preventing the gravitational flow from going any further. The manipulation of the impinging water when using the vacuum however might be higher. To minimize the effects of the vacuuming on the flow, we put the funnel system at the entry of the measuring system. The funnel system worked as a tranquilizer to help regain a steady state. The efficiency of the system was tested, by verifying that the total runoff volume and the total mass of TSS calculated from the recorded hydrographs and pollutographs respectively, were in accordance with the measurements undertaken in the laboratory. This shows that the effects of the turbulence on the flow and the mass were totally controlled.

#### **4.2. Comparison of sediments in dry stock and TSS loads in simulated wash-off**

Loads of sediments in dry stocks, whether on the parking lot or the sidewalks, were very high compared to the load transported by the runoff. Global wash-off factors at both sites, calculated as the ratio between the total wash-off load and the total accumulated load, are very low as their mean values at the sidewalks and at the parking lot were 17 and 6% respectively. However when assessing the wash-off fraction of particles in each size range (which is calculated as the ratio between the wash-off load and the dust load in the corresponding size fraction) we observe that for some of the particles in a specific size range, wash-off fractions can be higher than 50% (Fig. 5). This indicates that the wash-off is a selective process where



only a small fraction of the available particles on the surface is transported within the runoff, even under highly intense rainfall. Further investigation shows that this selectivity is related to the size of the particles, where more fine sediments reached the outlet than did the coarser. Half of the particles less than 100 $\mu\text{m}$  are washed-off by the rainfall while less than 10% of the coarser particles ( $>100\mu\text{m}$ ) were conveyed by the runoff. This was observed at all the sidewalks except for the sidewalk 2 for the coarser fraction, where wash-off factors increased gradually from 0.1 to 0.57 as the size of the particles increased from 250 $\mu\text{m}$  to 1000 $\mu\text{m}$ . This is explained by the removal of small gravels from the stock. Fine particles are easily removed from the surface since their detachment is quickly initiated at the beginning of the rainfall under the impact of the raindrop, becoming thus readily available for transport. While coarse particles, given that they have higher weight, are harder to be mobilized and if they are they will not travel far before they settle. It should be also noted that the short duration of the rainfall may have also been a reason for having such a small wash-off fraction (Zhao et al., 2016). For several events (Fig. ), the final stage of the recorded pollutographs shows that the runoff continues the mobilization of the particles. Therefore, if the duration of the event was longer, higher loads would have been washed-off and the calculated wash-off factors would have been higher. Wash-off factors reported by Zhao and Li (2013) for different particle sizes varied in the same ranges as the one calculated in this study.

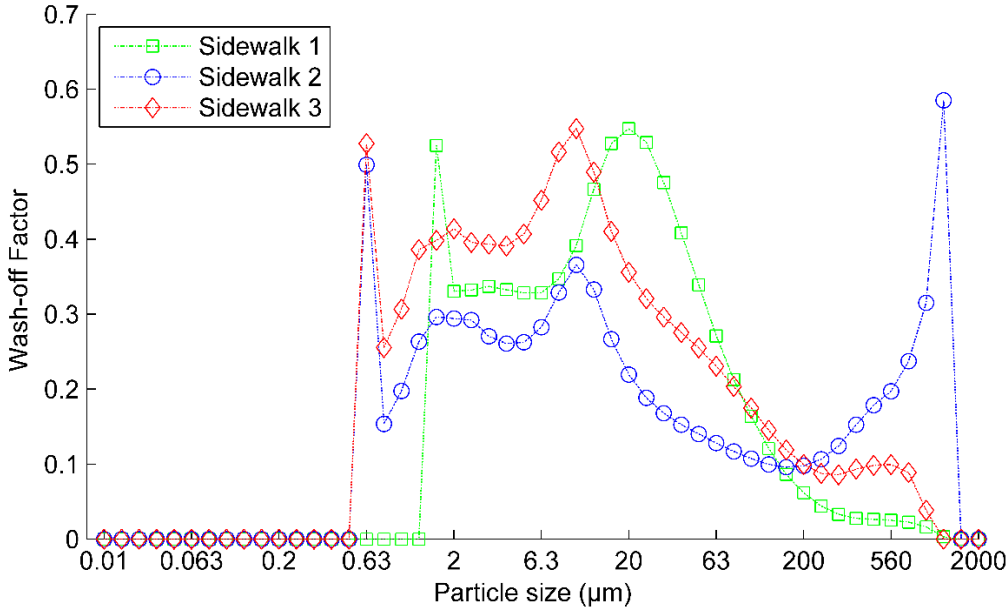


Fig. 5 Wash-off factor of specified particle size

The content of fine particles in TSS stock on the surface having the highest impact on stormwater contamination has also been demonstrated in other studies (Vaze and Chiew, 2003). Zhao and Li (2013) reported that 60-75 % of TSS in runoff were associated with particles of grain size less than 105 $\mu$ m, while sediments associated with the same size fraction in road deposits, did not account for more than 44% of the total mass. Similarly, Kim and Sansalone (2008) found that 25-80% of the particulate matter in runoff consisted of particles with a grain size of less than 75  $\mu$ m.

#### **4.3. Comparison of the loading from different surface type**

The smaller concentrations obtained at the parking lot suggest the mobilization of smaller loads from the parking lot compared to the sidewalk, and consequently, the existence of a higher stock of sediments on the sidewalks than on the parking lot. This was confirmed by comparing the loads of sediments in dry stocks on both surfaces. Comparison of wash-off loads clearly showed that the same rainfall event would transport higher loads of contaminants from the sidewalks than from the parking lot. Even if this is partially due to the availability of higher sediments on the sidewalks, it could also be explained by the difference of texture between both surfaces. The sidewalks usually have a smooth texture that prevents the trapping of particles and facilitates their mobilization by runoff, whereas the parking lot has a rougher texture, which increases the friction between the particles and the parking surface, eventually slowing down the motion of particles and reducing their ability to be carried by the flow. Therefore, under an intense rainfall, particles were more easily detached from the sidewalk than from the parking lot. In terms of particle size distribution, the analysis shows that the particles on the parking lot were much coarser than the one collected on the sidewalks. This was likely caused by the presence of a high fraction of vegetation debris in the samples collected on the parking lot. On the other hand, particles on the sidewalks were highly subjected to turbulence due to the movement of pedestrians, thereby causing the defragmentation of coarser particles into medium-sized particles. Whereas on the parking lot, the level of disturbance is lower, favoring thus the maintenance of the coarse structure of the particles.

#### **4.4. Perspectives on conceptual stormwater quality modeling**

This study highlights the important role of fine particles in the contamination of stormwater runoff and suggests that the focus should move towards the removal of fine

particles and consequently their accurate assessment. Until now, stormwater quality modeling has always relied on conceptual models that do not precisely represent the physical mechanisms governing the process of build-up and wash-off (Al Ali et al., 2016; Fletcher et al., 2013; Sage et al., 2015). Recent study by Al Ali et al. (2016) showed that the performance of conceptual SWMM stormwater quality models is related to the type of the event, where the best replication of the pollutant's dynamics was obtained when simulating first flush events.

Application of these formulations on the data set obtained in this study showed that the model failed at replicating all of the observations except for one event. The calculated Nash-Sutcliffe coefficient at sidewalk 2 was equal to 0.7 while for the rest of the simulations it did not exceed 0.4. This shows that even for a first flush event, under certain conditions, the ability of commonly used conceptual models is limited, and that their formulations based only on the flow or the intensity as entry variables, must be reconsidered.

Recent attempts to incorporate more knowledge into the conceptual modelling of wash-off have been made. For example, a recent study by Wijesiri et al. (2015) studied the influence of the particle size distribution of the build-up on the wash-off behavior using SWMM wash-off model, concluding that particles with grain size of  $>150\mu\text{m}$  and  $<150\mu\text{m}$  are mobilized differently, with a preference of mobilization of the finer fraction. In addition, more studies have investigated the wash-off mechanism based on size-selective erosion models using a physical approach (Deletic et al. 1997; Hong et al. 2016b).

Another important factor to consider when assessing the wash-off mechanism seems to be the rainfall intensity. High rainfall intensity is assigned with high kinetic energy. Studies have shown that kinetic energy transferred from raindrops to the impacted area can be derived from the rainfall intensity measurements (Brodie and Rosewell, 2007). Therefore, the simulated rainfall in this study have an important kinetic energy that will favorite the detachment and the entrainment of the sediments. This was also confirmed by comparing the simulated wash-off loads and the wash-off loads yielded from natural events on the same site that were presented in previous work (Hong et al., 2016a). The monitored rainfall events were characterized by low intensities, as maximum intensities for the corresponding events ranged between 2 and 32.72 mm/h. The transported loads of TSS in wash-off from natural events varied between 0.096 and 1.65 g/m<sup>2</sup> which is very low compared to the loads conveyed under

simulated rainfall on the sidewalks. Comparison with the parking lot showed that only 40% of the natural events transported almost equivalent loads as the ones transported from the parking lot under simulated rainfall. In terms of particle size distribution, samples collected under simulated rainfall contained higher fractions of coarse particles. Particles ( $>100\mu\text{m}$ ) accounted on average for 11% of the particles collected from natural samples, compared to 25% for simulated samples. This comparison clearly shows the impact of the rainfall intensity on the wash-off of sediments and demonstrate that the mobilization of coarser particles is fostered by high intensity rainfall.

Results also show the importance of considering the residual mass in continuous modelling, since the rainfall does not wash off the entire fine fraction in the stock. Vaze and Chiew (2002) showed that under the effect of low rainfall intensity, finer particles are not completely transported by the runoff. Instead, the remaining particles will attach to the surface where they will be readily available for wash-off by the next storm event. The results of this study also confirm this finding for intense rainfalls. As seen in Fig. 5, wash-off factors show that even under an intense rainfall, a non-negligible part of sediments in all size fractions will remain on the surface, even though it consists mainly of the coarser fraction. This result confirms that in this case, the wash-off is transport limited rather than source limited.

Based on the findings of this study, stormwater quality modelling might be enhanced by incorporating the control factors of sediment's transport identified as the particle size and the rainfall intensity as well as the texture of the surface in the mathematical formulation of wash-off models. A differential erosion rate based on the particle size and the rainfall intensity together can be added, along with a transfer time calculated, as a function of the distance from the source to the outlet and the velocity of the particle, might be blended to derive more appropriate conceptual stormwater quality models.

This approach might include a physical aspect translated by the distinction of the behavior of the sediments with respect to the flow, based on their size distribution, and on the other hand, a transfer time function that is relatively simple to implement.

## 5. Conclusion

In this study, an innovative device consisting of a rainfall simulator and a monitoring system that allows the continuous monitoring of flow and turbidity was used to generate a

simulated rainfall and therefore investigate the wash-off process. The device is innovative as it measures the instantaneous flow and turbidity and permits the analysis of continuous hydrographs and pollutographs *in situ*. The device also permits the acquisition of a big data set in a short time since it can be easily manipulated and handled by one individual. The device as it is designed permits the simulation of a rainfall with an intensity equal to 120 mm/h, it might benefit from further improvements to simulate different rainfall intensities, either by changing the nozzles or the flow with the pump. In this study, Wash-off samples from simulated rainfall, as well as dry dust samples were collected on three sidewalks near a highly trafficked boulevard and on a parking lot within the Paris region. The samples were analyzed for TSS loads and particle size distribution. Results show that efficient control strategies of stormwater contamination should focus on the removal of the fine fraction of available particles on the surface as they are the most likely to be mobilized and transported during a rainfall event. The detachment of the particles was mainly dependent on their size, the rainfall intensity as well as on the texture of the surface, where particles were easily transported from smoother surfaces compared to rougher surfaces. Even after an intense rainfall event, a fraction of fine particles will remain on the surface, which indicates the necessity to account for their residual mass in continuous modelling.

The results mainly showed that particles exhibit distinct wash-off behaviors based on their size range. Whether if the particle is fine or coarse, will have an important role in determining its mobility and probability to reach the outlet. This information is not currently integrated in conceptual stormwater quality models, where conceptual formulations do not account for the particles characteristics and transfer all the sediments on the surface in the same way without any differentiation. At the end, the comparison of the modelling results with the measurements at the outlet will not be accurate because what is being washed-off in reality is only a part of the available sediments and it consists mainly of fine particles. On the other hand, the wash-off fractions calculated reveal that even for the fine particles, an amount will remain on the surface, therefore adding a transfer time will also enhance quantifying what is finally the fraction that will reach the outlet.

These findings enhance the understanding of the main processes responsible for the transfer of contamination on urban catchment surfaces, and encourages the integration of a

new hypothesis in conceptual stormwater quality modelling, by integrating a wash-off fraction based on the particle size distribution and rainfall intensity.

Appendix A. Supplementary material

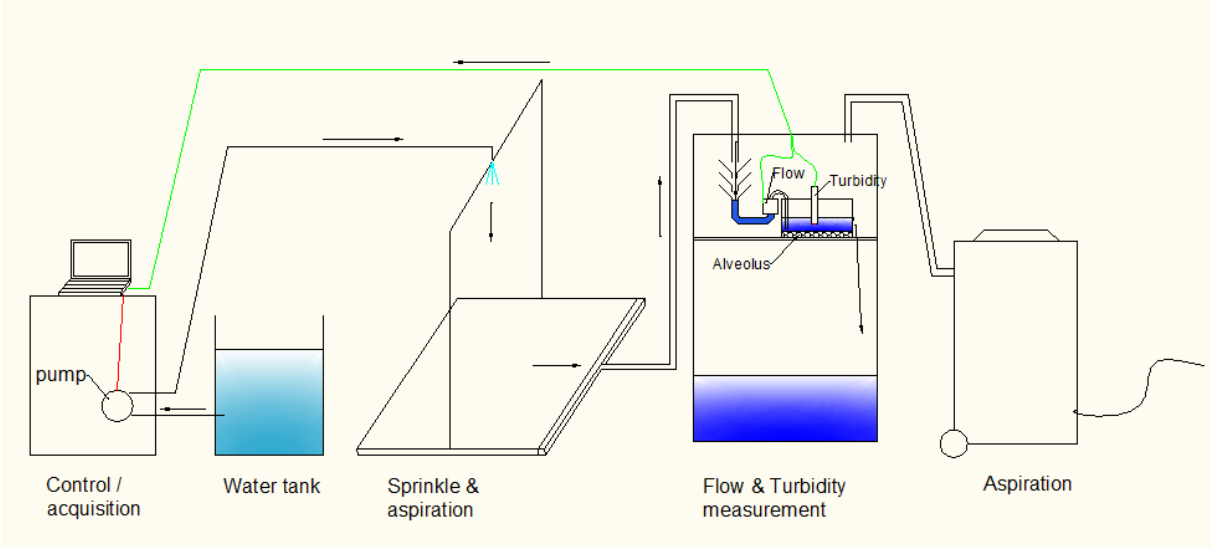


Fig.A.1 Representative scheme of the operational system of the rainfall simulator and the measuring unit

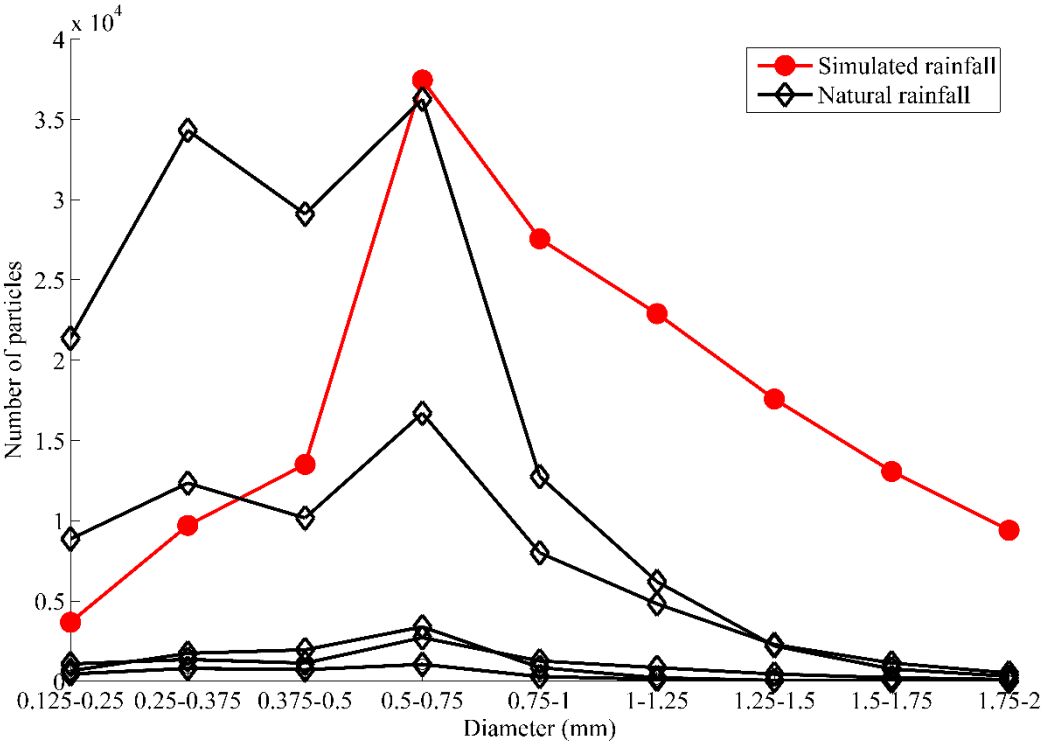


Fig.A.2 Raindrop size distribution represented as number of particles in each diameter range for simulated rainfall and several natural rainfalls that occurred in the same region

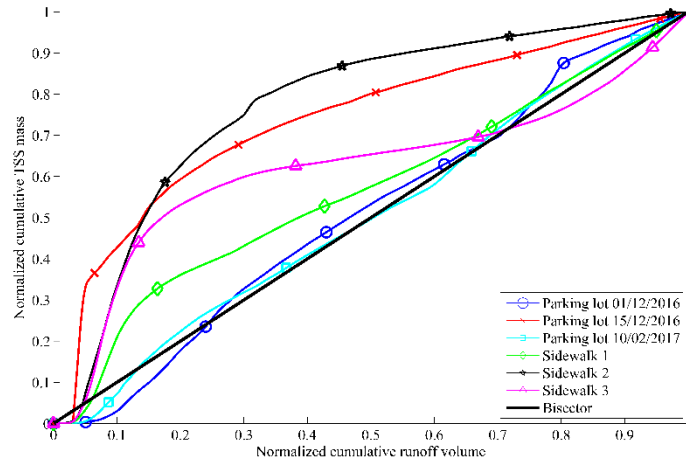


Fig.A.3 M(V) curves of TSS resulting from simulated rainfall at the sidewalks and at the parking lot

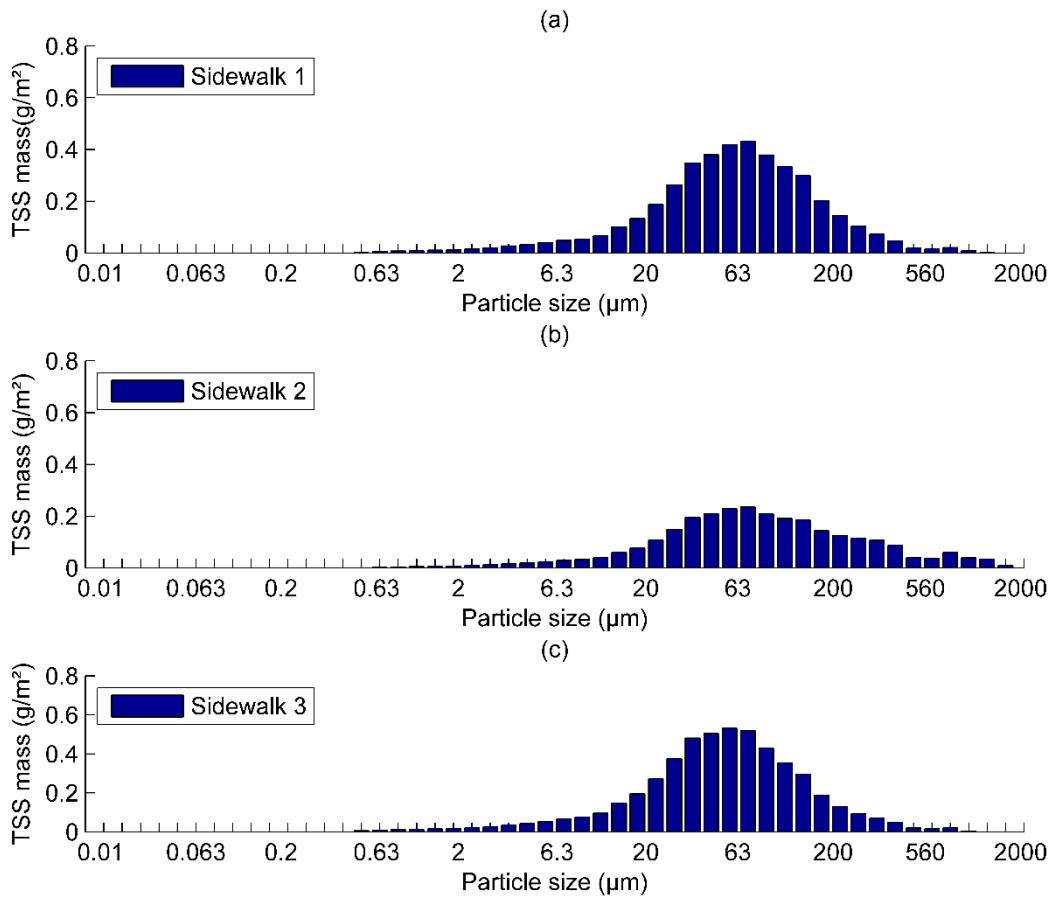


Fig.A.4 Mass distributions of TSS for simulated rainfall at (a) sidewalk 1 (b) sidewalk 2 and (c) sidewalk 3

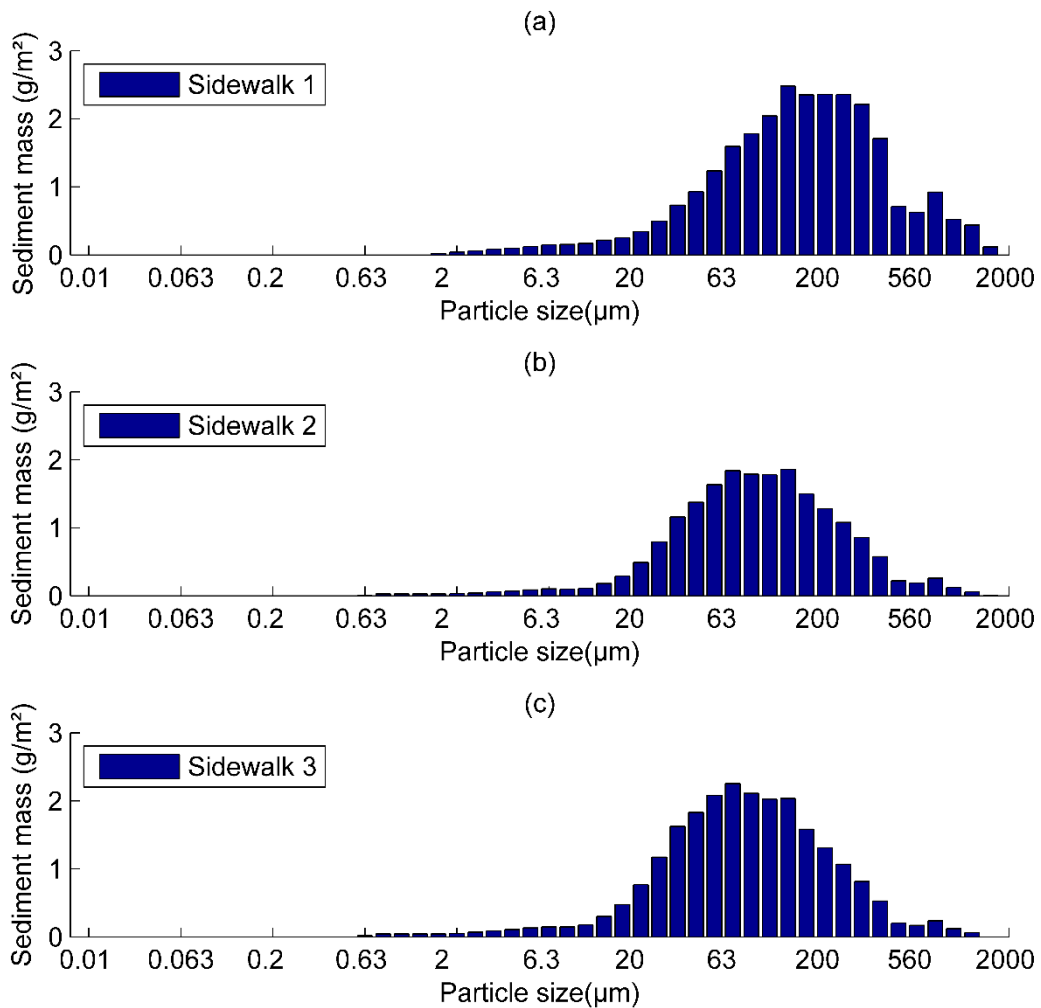


Fig.A.5 Particle size distribution of sediments in dry dust collected at (a) sidewalk 1 (b) sidewalk 2 and (c) sidewalk 3

## 6. References

Al Ali, S., Bonhomme, C., Chebbo, G., 2016. Evaluation of the Performance and the Predictive Capacity of Build-Up and Wash-Off Models on Different Temporal Scales. *Water* 8, 312. doi:10.3390/w8080312

Battany, M.C., Grismer, M.E., 2000. Development of a portable field rainfall simulator for use in hillside vineyard runo and erosion studies. *Hydrol Process* 14, 1119–1129.

Bechet, B., Bonhomme, C., Lamprea, K., Campos, E., Jean Soro, L., Dubois, P., Lherm, D., 2015. Towards a modeling of traffic pollutant flux at local scale – Chemical analysis and micro-characterization of road dusts. *Urban Proc. Environ. Symp.*



Bertrand-Krajewski, J.-L., Chebbo, G., Saget, A., 1998. Distribution of pollutant mass vs volume in stormwater discharges and the first flush phenomenon. *Water Res.* 32, 2341–2356. doi:10.1016/S0043-1354(97)00420-X

Brodie, I., Rosewell, C., 2007. Theoretical relationships between rainfall intensity and kinetic energy variants associated with stormwater particle washoff. *J. Hydrol.* 340, 40–47. doi:10.1016/j.jhydrol.2007.03.019

Chen, J., Theller, L., Gitau, M.W., Engel, B.A., Harbor, J.M., 2016. Urbanization impacts on surface runoff of the contiguous United States. *J. Environ. Manage.* 187, 470–481. doi:10.1016/j.jenvman.2016.11.017

Christiansen, J.E., 1942. *Irrigation by sprinkling*. Berkeley, Cal.: Agricultural Experiment Station.

Deletic, A., 2001. Modelling of water and sediment transport over grassed areas. *J. Hydrol.* 248, 168–182. doi:10.1016/S0022-1694(01)00403-6

Deletic, A., Maksimovic, C., Ivetic, M., 1997. Modelling of storm wash-off of suspended solids from impervious surfaces. *J. Hydraul. Res.* 35, 99–118. doi:10.1080/00221689709498646

Deletic, A., Orr, D.W., 2005. Pollution Buildup on Road Surfaces. *J. Environ. Eng.* 131, 49–59. doi:10.1061/(ASCE)0733-9372(2005)131:1(49)

Eckley, C.S., Branfireun, B., 2009. Simulated rain events on an urban roadway to understand the dynamics of mercury mobilization in stormwater runoff. *Water Res.* 43, 3635–3646. doi:10.1016/j.watres.2009.05.022

Egodawatta, P., 2007. Translation of small-plot scale pollutant build up and wash off measurements to urban catchment scale.

Egodawatta, P., Thomas, E., Goonetilleke, A., 2007. Mathematical interpretation of pollutant wash-off from urban road surfaces using simulated rainfall. *Water Res.* 41, 3025–3031. doi:10.1016/j.watres.2007.03.037

Egodawatta, P., Ziyath, A.M., Goonetilleke, A., 2013. Characterising metal build-up on urban road surfaces. *Environ. Pollut.* 176, 87–91. doi:10.1016/j.envpol.2013.01.021

Fletcher, T.D., Andrieu, H., Hamel, P., 2013. Understanding, management and modelling of urban hydrology and its consequences for receiving waters: A state of the art. *Adv. Water Resour.*, 35th Year Anniversary Issue 51, 261–279. doi:10.1016/j.advwatres.2012.09.001

Furumai, H., Balmer, H., Boller, M., 2002. Dynamic Behavior of Suspended Pollutants and Particle Size Distribution in Highway Runoff. *ResearchGate* 46, 413–8.

Goonetilleke, A., Thomas, E., Ginn, S., Gilbert, D., 2005. Understanding the role of land use in urban stormwater quality management. *J. Environ. Manage.* 74, 31–42. doi:10.1016/j.jenvman.2004.08.006

Herngren, L., Goonetilleke, A., Ayoko, G.A., 2005. Understanding heavy metal and suspended solids relationships in urban stormwater using simulated rainfall. *J. Environ. Manage.* 76, 149–158. doi:10.1016/j.jenvman.2005.01.013

Hong, Y., Bonhomme, C., Le, M.-H., Chebbo, G., 2016a. A new approach of monitoring and physically-based modelling to investigate urban wash-off process on a road catchment near Paris. *Water Res.* 102, 96–108. doi:10.1016/j.watres.2016.06.027

Hong, Y., Bonhomme, C., Le, M.-H., Chebbo, G., 2016b. New insights into the urban washoff process with detailed physical modelling. *Sci. Total Environ.* 573, 924–936. doi:10.1016/j.scitotenv.2016.08.193

Iserloh, T., Ries, J.B., Arnáez, J., Boix-Fayos, C., Butzen, V., Cerdà, A., Echeverría, M.T., Fernández-Gálvez, J., Fister, W., Geißler, C., Gómez, J.A., Gómez-Macpherson, H., Kuhn, N.J., Lázaro, R., León, F.J., Martínez-Mena, M., Martínez-Murillo, J.F., Marzen, M., Mingorance, M.D., Ortigosa, L., Peters, P., Regüés, D., Ruiz-Sinoga, J.D., Scholten, T., Seeger, M., Solé-Benet, A., Wengel, R., Wirtz, S., 2013. European small portable rainfall simulators: A comparison of rainfall characteristics. *CATENA* 110, 100–112. doi:10.1016/j.catena.2013.05.013

Kim, J.-Y., Sansalone, J.J., 2008. Event-based size distributions of particulate matter transported during urban rainfall-runoff events. *Water Res.* 42, 2756–2768. doi:10.1016/j.watres.2008.02.005

Lascelles, B., Favis-Mortlock, D.T., Parsons, A.J., Guerra, A.J., 2000. SPATIAL AND TEMPORAL VARIATION IN TWO RAINFALL SIMULATORS: IMPLICATIONS FOR SPATIALLY EXPLICIT RAINFALL SIMULATION EXPERIMENTS. *Earth Surf Process Landf.* 25, 709–721.

Liu, A., Egodawatta, P., Guan, Y., Goonetilleke, A., 2013. Influence of rainfall and catchment characteristics on urban stormwater quality. *Sci. Total Environ.* 444, 255–262. doi:10.1016/j.scitotenv.2012.11.053

Loch, R.J., Robotham, B.G., Zeller, L., Masterman, N., Orange, D.N., Bridge, B.J., Sheridan, G., Bourke, J.J., 2001. A multi-purpose rainfall simulator for field infiltration and erosion studies. *Soil Res.* 39, 599–610. doi:10.1071/SR00039

Motelay-Massei, A., Garban, B., Tiphagne-larcher, K., Chevreuril, M., Ollivon, D., 2006. Mass balance for polycyclic aromatic hydrocarbons in the urban watershed of Le Havre (France): Transport and fate of PAHs from the atmosphere to the outlet. *Water Res.* 40, 1995–2006. doi:10.1016/j.watres.2006.03.015

Pitt, R.E., Williamson, D., Voorhees, J., Clark, S., 2005. Review of Historical Street Dust and Dirt Accumulation and Washoff Data. *J. Water Manag. Model.* doi:10.14796/JWMM.R223-12

Revitt, D.M., Lundy, L., Coulon, F., Fairley, M., 2014. The sources, impact and management of car park runoff pollution: A review. *J. Environ. Manage.* 146, 552–567. doi:10.1016/j.jenvman.2014.05.041

Rossi, L., Chèvre, N., Fankhauser, R., Margot, J., Curdy, R., Babut, M., Barry, D.A., 2013. Sediment contamination assessment in urban areas based on total suspended solids. *Water Res.* 47, 339–350. doi:10.1016/j.watres.2012.10.011

Sage, J., Bonhomme, C., Al Ali, S., Gromaire, M.-C., 2015. Performance assessment of a commonly used “accumulation and wash-off” model from long-term continuous road runoff turbidity measurements. *Water Res.* 78, 47–59. doi:10.1016/j.watres.2015.03.030

Sansalone, J.J., Koran, J.M., Smithson, J.A., Buchberger, S.G., 1998. Physical characteristics of urban roadway solids transported during rain events. *J. Environ. Eng.* 124, 427–440.

Sartor, J.D., Boyd, G.B., Agardy, F.J., 1974. Water Pollution Aspects of Street Surface Contaminants. *J. Water Pollut. Control Fed.* 46, 458–467.

Vaze, J., Chiew, F.H., 2002. Experimental study of pollutant accumulation on an urban road surface. *Urban Water* 4, 379–389.

Vaze, J., Chiew, F.H.S., 2003. Study of pollutant washoff from small impervious experimental plots. *Water Resour. Res.* 39, 1160. doi:10.1029/2002WR001786

Wijesiri, B., Egodawatta, P., McGree, J., Goonetilleke, A., 2015. Influence of pollutant build-up on variability in wash-off from urban road surfaces. *Sci. Total Environ.* 527-528, 344–350. doi:10.1016/j.scitotenv.2015.04.093

Wilson, C., Weng, Q., 2010. Assessing Surface Water Quality and Its Relation with Urban Land Cover Changes in the Lake Calumet Area, Greater Chicago. *Environ. Manage.* 45, 1096–1111. doi:10.1007/s00267-010-9482-6

Zanders, J.M., 2005. Road sediment: characterization and implications for the performance of vegetated strips for treating road run-off. *Sci. Total Environ.* 339, 41–47. doi:10.1016/j.scitotenv.2004.07.023

Zhao, H., Chen, X., Hao, S., Jiang, Y., Zhao, J., Zou, C., Xie, W., 2016. Is the wash-off process of road-deposited sediment source limited or transport limited? *Sci. Total Environ.* 563–564, 62–70. doi:10.1016/j.scitotenv.2016.04.123

Zhao, H., Li, X., 2013. Understanding the relationship between heavy metals in road-deposited sediments and washoff particles in urban stormwater using simulated rainfall. *J. Hazard. Mater.* 246–247, 267–276. doi:10.1016/j.jhazmat.2012.12.035

Zhao, H., Li, X., Wang, X., Tian, D., 2010. Grain size distribution of road-deposited sediment and its contribution to heavy metal pollution in urban runoff in Beijing, China. *J. Hazard. Mater.* 183, 203–210. doi:10.1016/j.jhazmat.2010.07.012

## Chapitre 4. Bilan des messages principaux dans cette partie

Les modèles conceptuels d'accumulation-lessivage basés sur des formulations assez simplifiées des processus, qui n'intègrent que la durée de temps sec et le taux de ruissellement comme variables hydrologiques explicatives, ne fonctionnent pas correctement pour décrire les dynamiques d'émission de MES. Les modèles ne sont valides que pour des courtes durées au-delà desquelles ils ne sont plus capables de représenter les facteurs qui contrôlent la variabilité des mécanismes de contamination. Si le calage sur certaines périodes est une réussite, les jeux de paramètres optimaux changent d'une période à une autre ce qui met en évidence la difficulté de paramétrisation de ces modèles et le quasi impossibilité de définir un jeu de paramètre unique pour simuler les événements susceptibles de se reproduire en réalité. Une grande faille dans ces modèles paraît liée à l'accumulation qui est mal expliquée et qui entraîne des grosses erreurs pour les simulations en continu. La variabilité des paramètres liés à l'accumulation se révèle plus importante que celle des paramètres de lessivage. Cependant, le lessivage n'est pas facilement prédictible, car il dépend du stock mobilisable présent sur la surface (pour lequel l'atmosphère a une contribution mineure), de la taille des particules, du type de la surface...

Ainsi, même si nous avons réussi à élucider certains aspects des processus d'accumulation-lessivage, nous nous retrouvons face à une variabilité et une complexité importantes des facteurs qui contrôlent l'accumulation et le lessivage dont certains sont difficilement quantifiables et prévisibles tels que les apports parasites et les dépôts directs. Etant donnée l'insuffisance des approches traditionnelles à faire face à cette variabilité, une modélisation stochastique qui prend compte du caractère aléatoire de la génération des polluants en milieu urbain paraît inévitable et plus favorable qu'une modélisation déterministe.



## Partie 5. Modélisation de la production et du transfert de la contamination dans les eaux de ruissellement à l'échelle du quartier

Un modèle de qualité stochastique est intégré au modèle hydrologique spatialement distribué « URBS » (Urban Runoff Branching Structure) (Rodriguez et al., 2008) et appliqué pour simuler le transfert du débit et des MES à l'exutoire du bassin versant d'un quartier du « Perreux sur Marne ». L'approche stochastique permet de mieux représenter la variabilité spatiale et temporelle de la contamination au sein du bassin versant.

Le modèle hydrologique URBS a été choisi parce qu'il simule les processus par des lois physiques simples et il représente l'espace avec une discrétisation spatiale détaillée de haut niveau qui permet de considérer la contamination provenant de différentes sources (voirie, bâti).

D'autres approches de modélisation ont été aussi appliquées sur ce bassin versant pour simuler les paramètres quantitatifs et qualitatifs à l'exutoire. Ainsi, dans le cadre de la thèse de Yi Hong une approche très détaillée basée sur un modèle distribué à base physique a été développée et testée (Hong, 2016). Deux approches plus simples, qui utilisent le logiciel SWMM, l'une basée sur une description globale du bassin versant et l'autre sur une discrétisation en sous bassins versants ont été évaluées dans le cadre du stage de Master d'Edric Clayton (Clayton, 2017). Face à l'opportunité présentée par la disponibilité des résultats de différentes approches de modélisation sur le même bassin versant, nous avons comparé les différentes approches de modélisation en collaboration avec Yi Hong dans le cadre de son Post-doc au LEESU.

Les études à l'échelle du quartier sont présentées respectivement dans les chapitres 5 et 6 qui correspondent aux articles suivants :

- *“Accounting for the spatial-temporal variability of Pollutant processes in stormwater quality modelling based on stochastic approaches”*
- *“Benchmarking urban stormwater quality models of varying spatial discretization: lumped, sub-catchments based, urban hydrological element based and grid-based”*

Le bilan des principaux messages de cette partie est dressé dans le chapitre 7.

## ➤ Chapitre 5

Dans ce chapitre, le travail mené contribue à l'intégration d'un module qualité basé sur une approche stochastique au sein du modèle hydrologique distribué URBS, développé au laboratoire Eau et Environnement de l'IFSTTAR à Nantes (Rodriguez et al., 2008).

La représentation de l'espace urbain dans URBS est basée sur une description bidimensionnelle qui décrit le bassin versant comme un ensemble d'éléments hydrologiques urbains (EHUs) connectés au réseau hydrographique et qui est dérivée des données SIG. L'EHU comprend la parcelle cadastrale et la partie de la voirie adjacente. Dans chaque EHU, les surfaces sont découpées en trois occupations de sol : les bâtiments, les voiries (qui incluent aussi les allées et les parkings) et la surface naturelle. Une couverture végétale peut exister au-dessus des voiries et de la surface naturelle. Les caractéristiques d'un EHU sont : les superficies de chaque occupation de sol et de la couverture végétale, la pente, l'altitude, les coordonnées du centre de gravité et du point de connexion au réseau hydrographique.

Les processus hydrologiques sont simulés à l'échelle de l'EHU pour chacune des occupations de sol qui sont représentées par un même profil vertical décomposé en quatre réservoirs : les arbres, la surface du sol, la zone non saturée et la zone saturée du sol. Le même principe de modélisation est appliqué pour chacun des profils verticaux qui sont distingués par les valeurs affectées aux paramètres. Le débit produit par un profil vertical est calculé à partir des équations de bilan hydrologique qui s'appuient sur la représentation des processus d'infiltration, d'évaporation, du stockage en surface, d'évapotranspiration par les arbres, du ruissellement en surface, des échanges entre les zones non saturée et saturée, et d'infiltration de l'eau souterraine vers le réseau.

Le transfert de l'eau de chaque EHU vers l'exutoire est représenté au sein du réseau hydrographique premièrement par un temps de parcours. Cette fonction permet de déterminer le chemin de l'eau en surface qui relie le point de connexion de l'EHU au plus proche regard. Deuxièmement, l'eau est transférée dans les réseaux enterrés jusqu'à l'exutoire sous l'hypothèse d'un écoulement 1D et en appliquant l'équation de « Muskingum-Cunge » qui représente une approximation simple de l'équation de continuité.

Le module de modélisation conceptuelle de la qualité intégré au modèle hydrologique est basé sur une approche stochastique. Cette approche consiste de tirer au sort les concentrations moyennes de MES et les paramètres des équations de lessivage (qui sont utilisés pour dériver la dynamique de MES) au début de chaque événement pluvieux et pour chaque type d'occupation de sol. Les résultats obtenus à l'exutoire du bassin versant consistent en un faisceau de pollutogrammes qui permet la représentation des fluctuations des niveaux de contamination. Trois formulations de lessivage ont été testées pour dériver les concentrations instantanées de MES. La première est l'équation exponentielle de SWMM, la deuxième correspond à une relation d'homothétie entre le débit et la concentration et la troisième est l'équation des courbes masse/volume.

Les résultats montrent que la mise en œuvre du modèle SWMM dans un contexte stochastique permet de simuler des niveaux de concentrations acceptables à l'exutoire du bassin versant, ainsi que la tendance des fluctuations des concentrations de MES à l'intérieur d'un événement pluvieux. Ceci sans calage et avec peu de connaissance sur les paramètres. La prise en compte de la variabilité des processus à l'échelle de l'élément hydrologique et la distinction des émissions provenant de différents types de surface permet d'avoir une bonne représentation de la variabilité à l'exutoire. Cependant, l'approche développée montre des failles pour certains événements avec des simulations très éloignées des observations. Elle accorde aussi un degré de liberté très important au modélisateur. Ainsi, des recherches plus poussées devraient être menées pour améliorer cette approche, qui est d'un grand intérêt aux gestionnaires, et pour la positionner par rapport aux autres approches classiques de modélisation de la qualité.

## ➤ Chapitre 6

Dans ce chapitre, quatre approches de modélisation de la qualité, appliquées sur le bassin versant quartier pour six événements pluvieux, sont comparées selon différents critères en se basant sur des digrammes en radar. Cette comparaison permet de proposer une ligne directrice pour faciliter le choix de l'approche de modélisation optimale selon les données disponibles, les ressources humaines et informatiques, et les objectifs définis. Elle permet aussi de positionner l'approche de modélisation stochastique basée sur les EHU par rapport à d'autres approches de modélisation.



Le bassin versant quartier a été spatialement discrétisé comme (a) une entité globale, (b) des sous bassins versants en distinguant les occupations de sol (végétale, toiture, chaussée), (c) des éléments hydrologiques urbains (EHUs) et (d) une maille. Les concentrations de MES à l'exutoire pour les discrétisations globales et sous bassins versants ont été simulées en se basant sur les équations usuelles d'accumulation-lessivage (SWMM). A l'échelle de l'EHU, le modèle SWMM stochastique développé dans le chapitre 5 a été utilisé. Finalement, le modèle LISEM-SWMM basé sur les équations d'érosion a été utilisé pour les simulations de qualité à l'échelle de la cellule de la maille.

Chaque approche a été évaluée en fonction des six critères suivants : (i) la performance en calage, (ii) le pouvoir prédictif, (iii) la fiabilité de la simulation par rapport au changement du jeu de paramètre, (iv) la facilité de collecte des données d'entrées, (v) la vitesse des calculs et (vi) la complexité de la mise en œuvre.

Les résultats de comparaison montrent que les modèles globales et semi-distribué, basés sur les approches conceptuelles classiques de modélisation de la qualité, sont les plus faciles à mettre en œuvre et les plus rapides à implémenter. Ils donnent aussi les meilleurs ajustements entre les observations et les simulations avec des méthodes de calage automatique. Cependant, grosses incertitudes sont liées aux valeurs des paramètres de ces modèles et leur pouvoir prédictif est médiocre. D'autre part, les modèles basés sur l'approche stochastique appliquée sur les EHUs, et sur l'approche physique appliquée au niveau de chaque cellule de la maille, sont les plus puissants en termes de pouvoir prédictif et de fiabilité de la performance. Par contre, ils sont difficiles à implémenter et à optimiser et ils nécessitent l'acquisition des bases de données importantes pour leur mise en œuvre surtout l'approche physique distribuée.

Grâce à la méthodologie de comparaison développée, qui permet de visualiser clairement les points forts et les points faibles de chacun des modèles, les domaines d'application et les pistes d'amélioration possibles pour chaque type d'approche sont proposés.

## Chapitre 5. Accounting for the spatio-temporal variability of pollutant processes in stormwater quality modelling based on stochastic approaches

**Abstract:** Stormwater quality modelling remains until these days one of the most challenging issues in urban hydrology. The implicated processes in contaminant generation and transport are very complex and are associated with many uncertainties including the uncertainty arising from the processes variability. In this study, the spatio-temporal variability of the build-up/ wash-off processes on a heterogeneous urban catchment within the Parisian region is assessed based on three stochastic modelling approaches integrated in the physically based distributed hydrological model URBS. The results demonstrate that accounting for the processes variability at the elemental scale of a hydrological element is important to analyze the contamination recorded at the catchment outlet. The best simulations of the intra-event dynamics of TSS was obtained for the stochastic exponential SWMM model, as the model succeeded not only in simulating the general trend of TSS concentrations fluctuations but also in replicating multiple peaks observed in the pollutographs. The proposed approach is very interesting because it does not require extensive calibration and can be implemented with minimal prior knowledge. It may benefit from further enhancement to become a trustful tool for decision making.

**Keywords :** Stochastic approach, Process variability, Stormwater runoff, Modelling, Pollutant wash-off, TSS.

### 1. Introduction

Stormwater runoff is an important source of contamination in urban environments (Göbel et al., 2007; Kim and Sansalone, 2008; Lee and Bang, 2000). The design and implementation of management tools for stormwater quality control require the knowledge of stormwater quality loads and dynamics, which are commonly derived using mathematical models (Elliott and Trowsdale, 2007).

Multiple types of urban stormwater quality models exist in the literature with various degrees of complexity, ranging from generic empirical formulations to conceptual and physically-based models (Tsihrintzis and Hamid, 1997; Zoppou, 2001). The performance of these models have been questioned for a long time, as up to date no reliable model for

stormwater quality exists despite the extensive researches that have been conducted (Dotto et al., 2011). Conceptual models remain quite common for stormwater quality modeling as they are integrated in several softwares such as SWMM and Flupol (Bujon, 1988; Rossman, 2010), despite their limitations (Al Ali et al., 2016; Sage et al., 2015)

A key source of the poor performance of conceptual quality models are the uncertainties. The uncertainties arise from the input data, the aggregation of the contamination processes and from the considerable variability of the implicated mechanisms affecting stormwater quality (Chen et al., 2016; Dotto et al., 2011; Kanso et al., 2005; Wijesiri et al., 2016). Uncertainty analysis in stormwater quality modeling usually focuses on the uncertainty in relation with the model structure, parameters and input data, which are usually accounted for using Bayesian approaches such as Metropolis-Hastings algorithm and Generalized Likelihood Uncertainty Estimation (GLUE) (Dotto et al., 2011; Kanso et al., 2005; Lindblom et al., 2011). These approaches are subjected to several critics regarding the subjectivity granted to make the assumptions on the prior distributions of parameters and residuals (Freni and Mannina, 2010; Sage et al., 2017). They also do not account for all sources of uncertainties such as process variability.

The intrinsic variability of build-up and wash-off is dependent on many factors among which are the human activities, the land-use practices and the meteorological conditions, namely the rainfall intensity (Egodawatta et al., 2007; Liu et al., 2013; McCarthy et al., 2012). Human activities include unusual sediment inputs from construction works and the cleaning of the impervious surfaces (courtyards, roads...). Comparison of pollutant loads generated by different land use shows that the contaminants from roofs are different than those transported from roads and paved surfaces (Gromaire-Mertz et al., 1999; Lamprea, 2009). Even for the same land use the variability is extremely high. (Hong et al., 2016) found that within a small road catchment, the accumulated load varies with the position with respect to the road where the highest loads are collected in the gutter. This variability was also noted by (Deletic and Orr, 2005). Dynamic changes in pollutant behavior before and during the rainfall are continuously occurring, due to re-suspension, deposition and aggregation mechanisms.

In order to account for the randomness of the factors affecting the contaminant production processes, researches have used probabilistic and stochastic approaches.

For instance, (Akan, 1988) and (Chen and Adams, 2007) developed a probabilistic stormwater quality model that accounts for the impact of the variability of rainfall on stormwater loads. They integrated the probability distribution of rainfall depth and inter-event period into build-up and wash-off equations in order to derive the probability distribution of stormwater loads for each rainfall event. (Daly et al., 2014) also focused on the variability related to rainfall as they proposed a stochastic exponential decay model based on the assumption that the decay coefficient is subjected to random fluctuations dependent on the runoff depth and driven by a Gaussian noise. These approaches addressed mainly the temporal variability of the runoff pollution processes, whereas the spatial variability related to the catchment features was neglected. As such, the relationships between the pollutant loads, the models parameters and the land use were not identified. In addition, in the probabilistic approaches, the parameters of build-up and wash-off models were treated as constant values, ignoring thus any uncertainties related to them. An interesting stochastic approach for pollutant generation have been implemented in the software MUSIC (Wong et al., 2002). The approach consists of generating at each time step a pollutant concentration from a predefined lognormal distribution for each land use. Such approach will allow having a more realistic interpretation of the pollutant generated from each source.

The research undertaken in this study aims at integrating the spatial and temporal build-up/wash-off variability related to land use and rainfall characteristics into conceptual stormwater quality modeling to improve modeling results and to enhance the design of effective management practices. Accordingly, three simple and completely random stochastic approaches for stormwater quality modeling are developed and implemented within a hydrological model. To address the variability observed in the concentrations and loads of total suspended solids (TSS), we chose a spatially distributed model URBS (Urban Runoff Branching Structure model) (Rodriguez et al. 2008). This model, based on urban data banks, represents a detailed description of the morphology and the heterogeneity of the urban environment by splitting up a catchment into urban hydrological elements and distinguishing the different land uses within each element. A small urban catchment located in the east of Paris (France) and exposed to a high road traffic has been selected as a study case. Simulated pollutographs and total eroded mass for several rainfall events are confronted to the

measurements at the catchment outlet. The outcomes of each approach are compared and the spatial variability of TSS loads within the catchment is studied.

## 2. Materials and methods

### 2.1. Hydrological model URBS

Urban Runoff Branching Structure model (URBS) developed by the French institute of science and technology for transport, development and networks (IFSTTAR) in Nantes-France (Rodriguez et al. 2008) is selected for hydrologic modeling. This model provides a distributed representation of the catchment space and a physically based description of the hydrological dynamics in the surface and subsurface compartments. The choice of process-based distributed hydrological model is essential with respect to the investigation of contaminant transport, as the model incorporates the detailed description of the spatial variations of land use properties on the elemental scale of the cadastral parcel.

The catchment morphology is represented as a set of urban hydrological elements (UHE) connected to a hydrological network routing the flow toward the catchment outlet. The UHE include a cadastral parcel and its corresponding adjacent street segments (Fig. 1). The characteristics of the UHE are determined from common urban databanks and they consist of surface area, impervious fraction, vegetation fraction, slope, length, location of the connection point to the hydrological network, and the depth of the drainage network at this point. The hydrological network is composed of a series of street gutters and sewer conduits characterized by their length, slope and diameter (Rodriguez et al., 2008), connected to each other.

To account for the heterogeneity of land surface properties three vertical profiles are defined based on the distinction of land uses for each UHE including roofs, roads and natural soils. The hydrologic processes at the UHE scale are modeled for each vertical profile in four reservoirs representing the interception over the surface, the surface area, the vadose and the saturated zone. The entailed processes are the following : interception by trees over the surface area, water infiltration into the soil, surface runoff, evaporation of water intercepted at the ground surface, plant transpiration and drainage of soil water. Detailed description of the processes and their representative equations can be found in (Rodriguez et al., 2008).

The runoff generated by each UHE is drained first on the surface through a flow path relating the connection point to the first manhole of the sewer network, using a travel time function. Then the flow is transported in the sewer to the catchment outlet using the Muskingum-Cunge scheme. The processes representation in this model allows simulating separately, if necessary, the runoff deduced from each land use type.

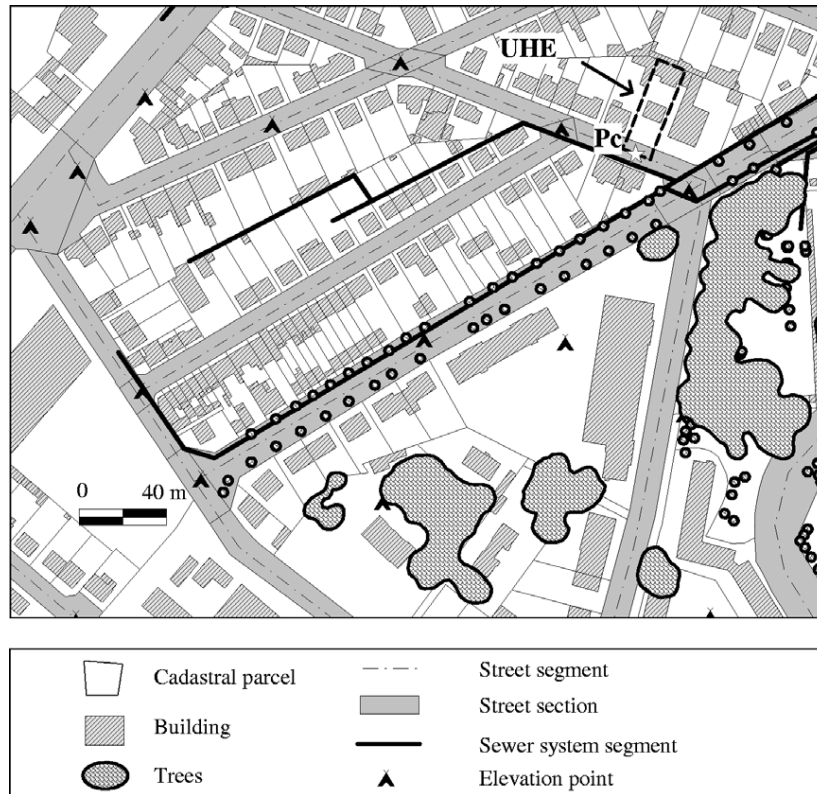


Fig. 1 Example of a cadastral map of an urban catchment in Nantes area (France). In the figure, an urban hydrological element (UHE) is delimited in dashed bold line, which is composed of a cadastral parcel and its adjacent street surface. The connection point to the hydrological network is also presented (Pc). This figure is adapted from (Rodriguez et al., 2008).

## 2.2. Stormwater quality modeling

### 2.2.1. Stochastic approach

While stormwater quantity runoff is well understood and often accurately replicated by hydrological models, feasible stormwater quality models are almost inexistent (Dotto et al., 2011). The variability of pollutant yielding in response to a storm event is not adequately represented in the common quality models. In this context, we developed a new methodology for quality modeling that incorporates the temporal and the spatial variability of pollutant generation and transport. The prediction of catchment stormwater quality is undertaken

under three stochastic approaches that account for the inter-event variability of pollutant load and the variability of pollutant load with respect to the land use. The stochastic approach assumes that the model inputs are purely random. Even though, the cause and effect of pollutant generation and transport, which are resumed by the build-up/wash-off processes, have been widely investigated, seldom however, the available information is sufficient to treat these processes in a rigorous deterministic way.

The concept of the proposed methods relies on spatio-temporal conceptualization of both the event mean concentration (EMC) of the corresponding pollutant and the parameters of the quality models destined to simulate the instantaneous variation of pollutant concentration. The EMC and the models parameters are described following the generic form  $\phi(p;ev;i;\Omega)$ .  $\phi$  represents the tempo-spatial variable quantity whose possible values are included in the sampling interval  $\Omega$  and that depends on the parcel  $p$ , the rainfall event  $ev$  and the land use  $i$ .  $\phi$  is a random variable chosen for each land use within every parcel at the beginning of a new rainfall event from the sampling interval with a uniform probability distribution.  $p$  is the indice of the UHE, while  $ev$  represents the rainfall events sample. The indice  $i$  comprises two components: the roof and the road. The sampling interval  $\Omega$  comprises the realizations of  $\phi$  within its lower and upper boundaries.

### 2.2.2. The models

Three quality models have been implemented. The first model is the commonly used exponential SWMM wash-off model (Rossman, 2010). For this model,  $\phi$  represents three variables which are the EMC and the model parameters  $C_1$  and  $C_2$ . After the selection of the values of EMC and the parameters, the initial available mass at the beginning of the rainfall event is calculated using equation (1):

$$M_{build-up}^{(initial)} = \frac{EMC \times V_{total}}{C_1 \times Q(t_1)^{C_2} \times dt + \sum_{n=2}^N C_1 \times Q(n)^{C_2} \times dt \times \prod_{j=1}^{n-1} (1 - C_1 \times Q(j)^{C_2} \times dt)} \quad (1)$$

Where :  $M_{build-up}^{(initial)}$  is the available mass at the beginning of the rainfall event (mg);  $EMC$  is the event mean concentration (mg/l);  $V_{total}$  is the total runoff volume for the corresponding rainfall event (liter);  $C_1$  and  $C_2$  are the wash-off parameters;  $Q(t_1)$  is the runoff

rate at the first time step of the rainfall event (mm/h);  $dt$  is the time step (minutes);  $N$  is the total time step of the rainfall event.

Then the eroded mass is calculated using equations (2) and (3):

$$M_{ero}(t) = C_1 \times Q(t)^{C_2} \times M_{build-up}(t) \times dt \quad (2)$$

$$M_{build-up}(t + dt) = M_{build-up}(t) - M_{ero}(t) \quad (3)$$

Where:  $M_{ero}(t)$  is the eroded mass at time  $t$  ( $g/m^2$ ) during the time step  $dt$ ;  $Q(t)$  is the runoff rate at time  $t$  expressed as water depth per time step (mm/h);  $M_{build-up}(t)$  is the available mass for erosion ( $g/m^2$ ) at time  $t$ ;  $C_1$  and  $C_2$  are the wash-off parameters.

The second model uses a homothetic relationship of ratio  $K$  between the concentrations of TSS and the runoff. For this model,  $\phi$  represents one variable: EMC. The EMC is first drawn from  $\Omega$  and the ratio  $K$  is then calculated as a function of the EMC and the instantaneous flow using equation (4):

$$K = EMC \times \frac{V_{total}}{\sum_{i=1}^N Q(i) \times dt} \quad (4)$$

Where:  $K$  is the homothety ratio ( $mg.s/l^2$ );  $EMC$  is the event mean concentration ( $mg/l$ );  $V_{total}$  is the total runoff volume for the corresponding rainfall event ( $l$ );  $Q(i)$  is the instantaneous flow at time  $i$  ( $l/s$ );  $dt$  is the time step;  $N$  is the total time step of the rainfall event.

The pollutograph is then obtained following equation (5):

$$C(t) = K \times Q(t) \quad (5)$$

The third model is based on the equations of  $M(V)$  curves.  $M(V)$  curves indicate the distribution of pollutant mass vs runoff volume (Bertrand-Krajewski et al., 1998). For this model,  $\phi$  integrates two variables : EMC and the model parameter  $b$  which is the exponent of the  $M(V)$  curve. Equation (6) is applied to simulate the pollutograph for this model:

$$\frac{\text{Cumulative eroded mass (t)}}{EMC \times V_{total}} = \left( \frac{\text{Cumulative runoff volume (t)}}{V_{total}} \right)^b \quad (6)$$



Where *Cumulative eroded mass* ( $t$ ) is the cumulative eroded mass at time  $t$  (mg); *EMC* is the event mean concentration (mg/l);  $V_{total}$  is the total runoff volume for the corresponding rainfall event (l); *Cumulative runoff volume* ( $t$ ) is the cumulative runoff volume at time  $t$  (liter);  $b$  is the M(V) curve coefficient.

The instantaneous eroded mass  $M_{eroded}(t)$  is then calculated by subtracting the cumulative eroded mass at time step  $t$  and the cumulative eroded mass at time  $t-1$ .

It is noteworthy that for all modelling approaches, the accumulated mass is supposed to be equal to the eroded mass and it is calculated by the means of the EMC. This assumption is very important as it accounts partially for the variability of the processes related to the particle size distribution, where all the fraction of build-up susceptible for entrainment and related to the fine particles is being transported by the runoff.

### **2.2.3. Boundaries of the sampling intervals**

Determining the boundaries of the sampling intervals for the EMC and for the models parameters is based on strong hypothesis. The values of the EMC are strongly related to the type of the land use while the wash-off parameters ranges are very wide and they are highly dependent on the calibration period; SWMM wash-off parameters have merely any physical meaning related to the characteristics of the studied catchment (Bonhomme and Petrucci, 2017). Even when the parameters are optimized, a large uncertainty is associated with their calibrated values (Kanso et al. 2005). This reveals important challenges in defining the sampling intervals for water quality parameters. The sampling intervals of the EMC for the roads are defined from the measurements collected at the inlet of the main boulevard within the catchment (Al Ali et al. 2016), and the one for roof surfaces are determined from data available in the literature (Göbel et al. 2007). The boundaries of the sampling intervals for SWMM wash-off parameters  $C_1$  and  $C_2$  correspond to the lowest and highest values obtained for the best cases investigated in an earlier study within the catchment (Al Ali et al. 2016). As for the M(V) curve coefficient  $b$ , the boundaries are selected as to replicate first flush and uniformly distributed events, since the occurrence of last flush events within the region was rare during the monitored period. The sampling intervals for the wash-off parameters are identical for all land uses while the EMC is distinguished for each land use. Except for the EMC for roofs, the sampling intervals for the wash-off parameters and the EMC for roads are

determined with respect to prior knowledge acquired on the site. This method encounters the difficulties for setting appropriate values for the sampling intervals.

The summary of modeling approaches and the corresponding inputs and parameters is shown in Table 2.

**Table 2 Summary of stormwater quality modeling approaches and the corresponding parameters**

<b>Stormwater quality approach</b>	<b>Water quality model</b>	$\phi$	<b>land use</b>	$\Omega$
<b>First approach (App-1)</b>	Exponential SWMM	EMC (mg/l)	Roof	[13 – 60]
			Road	[82 – 200]
		C1		[0.01 – 1.5]
		C2	Roof/Road	[0.8 – 1.9]
<b>Second approach (App-2)</b>	Homothetic hydrograph	EMC (mg/l)	Roof	[13 – 60]
			Road	[82 – 200]
<b>Third approach (App-3)</b>	M(V) curve	EMC (mg/l)	Roof	[13 – 60]
			Road	[82 – 200]
		b	Roof/Road	[0.5 – 1.2]

### 2.3. Catchment and data description

The studied catchment is located in the residential district of “Le Perreux sur Marne” in the eastern Paris suburb in the department of “Val de Marne” (Fig. 2). The catchment area is ~12 ha and has an average slope of 2.6%. The site consists mainly of residential houses and commercial shops distributed on both sides of the highly trafficked (> 30000 vehicles/day) boulevard “Alsace Lorraine” that crosses the catchment. Impervious surfaces account almost for 70% of the total catchment area. The catchment is drained via a separate sewer network that routes the flow to the outlet located at the North-Eastern edge of the catchment. The flow is collected from the surface via the manholes and then is transported into the main pipes.



Fig. 2 The studied catchment and the runoff branching network (including both street and sewer segments). The red point represents the outlet of the catchment.

Water quantity and quality data were collected at the catchment outlet. The outlet is equipped with a Nivus flowmeter that records the flow measurements at a 2-min time step. The water quality data including the measurements of turbidity is obtained using a multi-parameter probe DS5 OTT at a 1-min time step. The relationship between the turbidity and the concentration of TSS is established based on laboratory analysis conducted on several rainfall samples. The turbidity measurements are transformed into TSS concentrations using the following linear equation with a correlation factor  $R^2 > 0.98$ :

$$[TSS] = 0.9 \times Turbidity \quad (7)$$

Where:  $[TSS]$  is the Total suspended solids concentration (mg/l); Turbidity is the turbidity measurement in NTU.

The precipitation data was collected at a meteorological station installed on the rooftop of a building near the studied catchment. The station consisted of a tipping bucket rain gauge, which has a 0.1 mm resolution.

GIS data required for this study were obtained in collaboration with the “National Institute of Geographic and Forest Information” (IGN) France. An important dataset providing a detailed description of the parcels, buildings, vegetation and roads is available everywhere in France. The sewer network database was obtained from the local authority represented by the general council of the Val de Marne department. The GIS data were used to estimate the different morphological characteristics needed to describe the urban hydrological elements and to build the runoff branching network.

#### 2.4. Evaluation criterion of the model performance

The performance of both the hydrological and the water quality models was evaluated based on visual and statistical comparisons of the simulations and the measurements. A general overview of the models behavior in terms of dynamic replication of the hydrographs and pollutographs is first assessed by inspecting the graphical plots of flows and TSS concentrations. The goodness of fit is then assessed using multiple statistical criteria that estimate a normalized error between the simulated and observed variables (Table 3). The chosen mathematical efficiency criteria for models evaluations are the Nash Sutcliffe coefficient ( $C_{Nash}$ ), the determination factor ( $C_{R^2}$ ), and the Root mean square error ( $C_{RMSE}$ ).

**Table 3** Evaluation criteria of the performance of hydrological and water quality models. With:  $Sim_t$  is the simulated value at time  $t$ ;  $Obs_t$  is the observed value at time  $t$ ;  $\overline{Sim}$  is the average of the simulated values;  $\overline{Obs}$  is the average of the observed values;  $t_1$  is the beginning of the simulated event;  $t_n$  is the end of the simulated event;  $n$  is the total duration of the simulated event.

Statistical criterion	Equation	Applied for the evaluation of	
		Hydrological model	Water quality model
Nash Sutcliffe coefficient ( $C_{Nash}$ )	$C_{Nash} = 1 - \frac{\sum_{t_1}^{t_n} (Sim_t - Obs_t)^2}{\sum_{t_1}^{t_n} (Obs_t - \overline{Obs})^2}$	✓	–
Determination factor ( $C_{R^2}$ )	$C_{R^2} = \frac{(\sum_{t_1}^{t_n} (Sim_t - \overline{Sim})(Obs_t - \overline{Obs}))^2}{\sum_{t_1}^{t_n} (Sim_t - \overline{Sim})^2 \sum_{t_1}^{t_n} (Obs_t - \overline{Obs})^2}$	✓	✓
Root mean square error ( $C_{RMSE}$ )	$C_{RMSE} = \sqrt{\frac{\sum_{t_1}^{t_n} (Sim_t - Obs_t)^2}{n}}$	–	✓

Choosing the appropriate criteria for the evaluation of the goodness of fit is very critical and depends on the objectives of the modeler (Green and Stephenson, 1986). The purpose of the hydrological model is to give accurate estimates of the instantaneous flow rate and of the

total runoff volume, therefore the  $C_{Nash}$  and  $C_{R^2}$  were chosen for its evaluation. The Nash coefficient is widely used as an indicator of the overall fit of the hydrographs (Moriasi et al., 2007). On the other hand, the water quality modeling approach in this study aims at evaluating the variability of the processes on the pollutographs and not at fitting the measurements to the simulations. Therefore, the evaluation of the modeling performance in terms of Nash will not be appropriate. In this case, the use of the determination coefficient is important to assess if the variability follows the same trend as the measurements. Therefore the  $C_{R^2}$  is chosen to evaluate the water quality model. It was also coupled with the  $C_{RMSE}$  to have a general overview of the residuals between the measurements and the simulations.

## 2.5. Model application

Calibration of the hydrological model was carried out on 30 rainfall events that occurred between October 8<sup>th</sup> 2014 and January 1<sup>st</sup> 2015 (Table A.1). The events represented typical rainfalls occurring within this area with short duration and low intensities. The maximum rainfall intensities varied between 1.1 and 42.3 mm/h while the precipitation depth ranged between 2 and 22.1 mm. The duration of the events varied from 52 minutes to 12 hours while the average antecedent dry weather period was equal to 2.5 days. Validation of the hydrological model was carried on four rainfall events throughout the period from March 31 2015 to April 27 2015. The rainfall events had precipitation depths ranging between 2 and 6.7 mm. Their maximum rainfall intensities varied between 2.3 and 43.3 mm/h. The hydrological simulations were compared to the measurements in terms of runoff volume and instantaneous flow.

As for water quality modeling, nine rainfall events from the period between the 8<sup>th</sup> of October 2014 and January first 2015 were simulated for each approach and their characteristics are summarized in Table A.2. For each rainfall event, ten stochastic simulations were performed. The total washed-off load and the TSS dynamics were determined for each simulation, and the evaluation criteria were calculated. A statistical analysis to determine the minimum, maximum and mean values of the evaluation criteria was then carried.


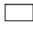


### 3. Results and discussion

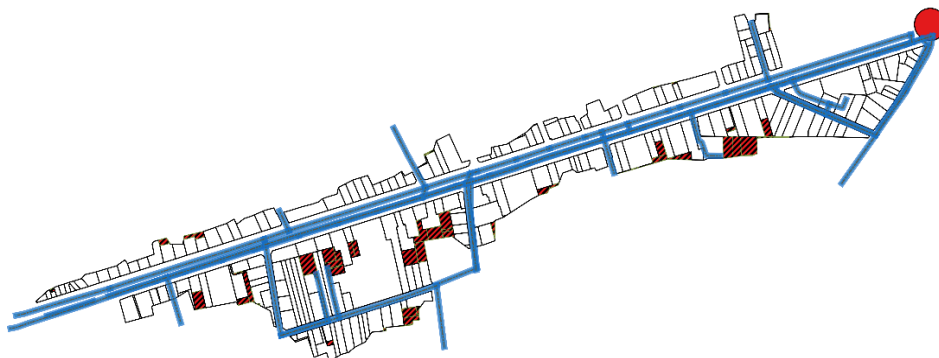
#### 3.1. Hydrological modeling

##### 3.1.1. Model implementation

The set-up of the input files was accomplished through the processing of the topographic and land uses data from the urban databanks using two free GIS softwares: QGIS and OrbisGIS. The data analysis shows that the catchment encompasses 274 cadastral parcels, which represent as many individual UHEs (Fig. 3). Among the 274 UHEs, 56 are not directly connected to an adjacent street as they represent an isolated parcel inside a block.

#### Legend

-  Internal parcel
-  Parcel
-  Runoff Branching Network
-  Catchment outlet



**Fig. 3** Cadastral parcels of "Le Perreux" catchment. White parcels represents the UHEs including a fraction of the adjacent street. Red dashed parcels represent isolated UHEs. The blue lines and the red circle represent respectively the segments of the hydrological network and the catchment outlet.

The roads account for 31% of the total area of the catchment, while roofs account for 26%. Half of the impervious surface consists of roads, 40% are roofs and the remaining fraction is the parking lots and the walkpaths. The hydrological network consists of 102 segments. 55



segments represent the street gutters and 47 represent the sewer pipes. The gutters are considered as small sized pipes having a 250 mm diameter. The major sewer pipes have a total length equal to 1165 m. They have an ellipsoidal form with a height of 2.3 m and a width equal to 1.3 m. Minor pipes have a total length of 446 m and they have a circular section of 0.3 m diameter.

The second step for model implementation is the estimation of the model parameters, which include 15 parameters for the water budget and two parameters for the transfer (Table A.3). Determining the parameters of physical models is not a straightforward task because the perfect physical model doesn't exist and some parameters need to be calibrated for the specific catchment (Bárdossy, 2007; Refsgaard, 1997). We distinguished the parameters that can be determined from field measurements and the ones that should be calibrated. The values of the parameters estimated from literature and used in (Rodriguez et al. 2008) for a similar urban catchment located in Nantes suburb (France) were kept the same. These included the values of tree interception parameters, the maximum reservoir capacities for impervious land uses, the groundwater drainage coefficient, the root depth and the representative position of the vadose zone. The hydraulic conductivity of the street and the natural soil were estimated based on field measurements for "Le Perreux" catchment. The other parameters corresponding to the hydrodynamic characteristics of the soil were calibrated.

Since UHE based models are not widely studied in the literature, the commonly applied strategy for their calibration is the simple artificial trial and error method. The parameters were continuously adjusted and the effects of parameter adjustments for each simulation were assessed quickly from simple graphical analyses and the value of the Nash Sutcliffe coefficient.

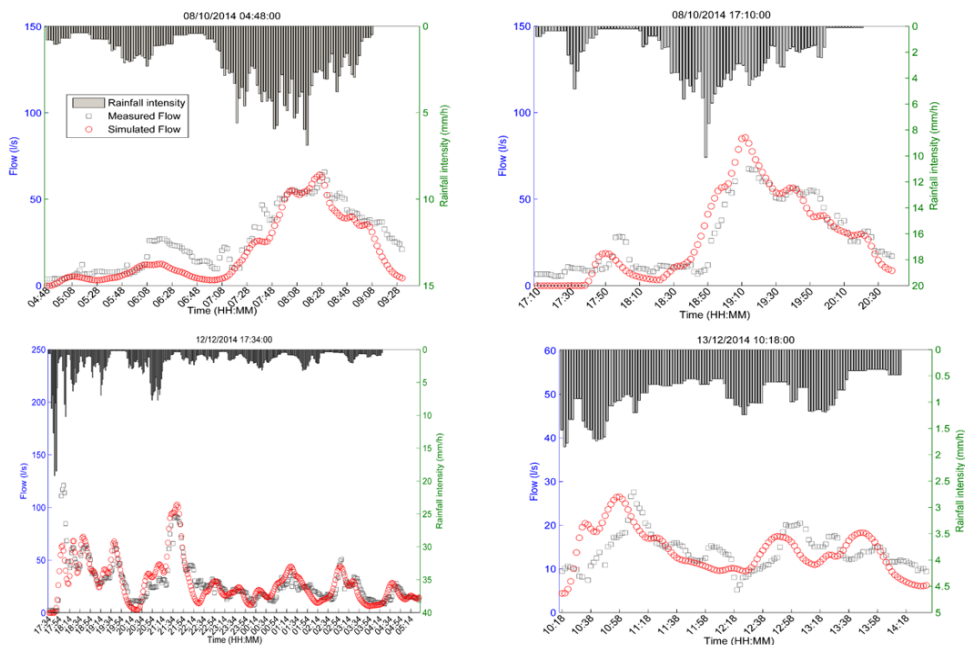
### **3.1.2. Water flow simulations**

The evaluation criteria for water flow simulations are summarized in (Table 4). The calibration results demonstrate a strong level of agreement between simulated runoff volumes and the observations with  $C_{Nash}$  and  $C_{R^2} \geq 0.9$ .

**Table 4 Evaluation criteria for simulations of event runoff volumes (V) and instantaneous flow (Q) for the calibration (n=30 events) and validation (n=4 events) periods**

	$C_{R^2}$	$C_{Nash}$
Calibration (8 October 2014 / January first 2015; n=30)		
V	0,93	0,9
Q	0,77	0,71
Validation (31 March 2015/ 27 April 2015 ; n=4)		
V	0.99	0.56
Q	0.91	0.58

The model had a satisfactory performance in calibration where it succeeded at replicating the instantaneous flow wherein the  $C_{Nash}$  and  $C_{R^2}$  were higher than 0.7. Visual inspection of the simulated and observed hydrographs showed that the model provided a good replication of the overall trend in runoff generation (Fig. 4). A minor time offset is noticed for the second event on the 8<sup>th</sup> of October and the event on the 13<sup>th</sup> of December. The measured peak flows are slightly ahead of the simulated peaks. This could be due to the simple routing scheme used to describe the transfer function. Using more robust numerical schemes based on Barre de St Venant equations might give better performance. However, this effect is in all cases small and doesn't appear for all events.



**Fig. 4 Water flow simulations for four events from the period from October 8 2014 to December 31 2014. The simulated flow at the outlet is represented by red circles. The measured flow is represented by grey squares. The rainfall intensity is plotted on the upper part of the figures.**



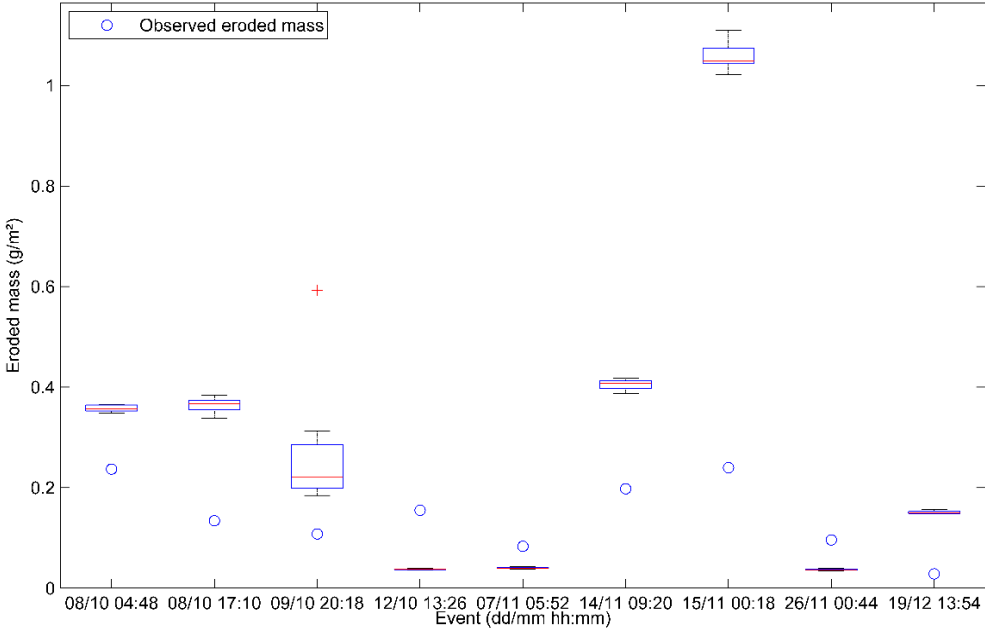
The model was also validated on four events throughout the period from March 31 2015 to April 27 2015. The results show that the dispersion of the observed runoff volumes and flow are accurately explained by the simulations. However, the  $C_{Nash}$  for both runoff volumes and instantaneous flow are slightly lower than the ones calculated for the calibration period with values equal to 0.57 and 0.58 respectively. This is attributed to the parameters which might be not very suitable to represent the hydrological processes for this period.

### **3.2. Water Quality modeling**

#### **3.2.1. TSS loads**

The simulated eroded masses for each event varied in the same ranges for all modeling approaches (Fig. 5) whose performances in terms of predicting the washed-off loads were the same. This was expected since the EMC for each simulated event for all models were generated from the same intervals. The result shows important deviations of the estimates of the TSS loads from the measurements for most of the events. The inter-event variability of the measured loads fluctuates in narrow ranges, whereas it varies in larger ranges for the simulations. The measurements demonstrate that the yield of TSS loads on the outlet of this catchment is limited and tends towards a stable value. However, the simulations show higher variability from an event to another where no systematic trend in the model estimates is observed. The models underestimated the measurements for 3 events and overestimated them for others. The highest deviation is observed for the event of the 15<sup>th</sup> of November 2014 where the modeling results suggested the probability of mobilizing higher loads of TSS. This is likely due to the high rainfall depth of this event, which suggests the shift of the sediments loading towards high values. The simulated washed-off loads are driven by the runoff volume, however in real cases the mobilized fraction of sediments during a rainfall event is mainly controlled by its particle size and the kinetic energy of the rainfall drop, which is represented by the rainfall intensity. Fine particles are the most susceptible for entrainment and intense rainfalls generate higher contaminant yields and enhance the mobilization of coarser particles (Al Ali et al., 2017; Hong et al., 2016). Introducing more explicitly the particle size into the model and accounting for the impact of the rainfall intensity in the sampling procedure, can improve the estimated TSS loads. Rainfall profiles can be dressed to classify the low and high intensity rainfalls and then higher EMC will be affected to the more intense events. Then, different classes of particle size can be introduced into the model, with new modeling

assumptions, such as: (i) total mobilization of fine particles could be assumed and (ii) a percentage representing the fraction susceptible of mobilization for coarser particles could be defined based on the rainfall intensity.



**Fig. 5** Boxplots of simulated wash-off load obtained with the three modelling approaches. The central red mark is the median, the edges are the 25<sup>th</sup> and the 75<sup>th</sup> percentiles and the whiskers extend to the extreme values that are not considered as outliers. The measured wash-off load is presented in blue circles.

The evaluation criteria obtained by comparing the simulated and the observed TSS loads are similar for the three models. The determination coefficients varied around 0.5 demonstrating a direct yet not very strong proportionality between the observed and the simulated TSS loads. The values of the RMSE coefficients showed that the discrepancy between the observations and the simulations for all models were low as they fluctuated around 0.3. The 3<sup>rd</sup> approach slightly performs better than both others.

**3.2.2. TSS dynamics**

The replicated dynamics of TSS by the models showed some promising results for several events. However, the modeling performance was not systematic for all rainfalls neither for all models as the results were dependent on both factors (Table 5). For some events, high values of determination coefficient are obtained while for others the variability of the

simulations and the observations may be very different. The RMSE coefficients were in acceptable ranges for the majority of the events, which means that the divergence of the simulations from the observations can be regarded as low. It should be also noted that the variability of the simulated pollutographs is generally low since the interval of variations of the RMSE coefficients is narrow.

**Table 5 Mean [Min-Max] Correlation and RMSE coefficients calculated between the observed and simulated TSS concentrations for three modeling approaches for each of the nine events. The grey cells represent the simulations for which the  $CR^2$  is higher than 0.5 or the CRMSE is lower than 50**

	$CR^2$			CRMSE		
	App-1	App-2	App-3	App-1	App-2	App-3
<b>08/10/2014</b> <b>04:48</b>	<b>0.22</b> [0.18 0.3]	<b>0.01</b> [0.002 0.018]	<b>0.47</b> [0.41 0.55]	<b>46</b> [37 – 42]	<b>41</b> [39 42]	<b>42</b> [41 43]
<b>08/10/2014</b> <b>17:10</b>	<b>0.8</b> [0.73 0.77]	<b>0.59</b> [0.57 0.6]	<b>0.2</b> [0.11 0.32]	<b>34</b> [28 -30]	<b>33</b> [31 35]	<b>37</b> [34 39]
<b>09/10/2014</b> <b>20:18</b>	<b>0.1</b> [4.53E-3 0.45]	<b>0.17</b> [0.12 0.21]	<b>0.06</b> [0.003 0.14]	<b>86</b> [39 321]	<b>45</b> [44 46]	<b>43</b> [42 – 45]
<b>12/10/2014</b> <b>13:26</b>	<b>0.1</b> [0.06 0.16]	<b>0.52</b> [0.49 0.54]	<b>0.02</b> [8.2E-5 0.08]	<b>235</b> [234 236]	<b>232</b> [231 234]	<b>236</b> [234 238]
<b>07/11/2014</b> <b>05:52</b>	<b>0.24</b> [0.22 0.26]	<b>0.06</b> [0.05 0.07]	<b>0.18</b> [0.15 0.2]	<b>57</b> [56 59]	<b>47</b> [46 50]	<b>47</b> [44 48]
<b>14/11/2014</b> <b>09:20</b>	<b>0.003</b> [0.11 0.013]	<b>0.07</b> [0.06 0.09]	<b>0.13</b> [0.1 0.17]	<b>69</b> [68 72]	<b>76</b> [75 77]	<b>63</b> [61 65]
<b>15/11/2014</b> <b>00:18</b>	<b>0.84</b> [0.83 0.85]	<b>0.09</b> [0.08 0.1]	<b>0.5</b> [0.43 0.62]	<b>99</b> [89 108]	<b>45</b> [43 47]	<b>36</b> [34 38]
<b>26/11/2014</b> <b>00:44</b>	<b>0.04</b> [0.03 0.07]	<b>0.33</b> [0.29 0.39]	<b>9.4E-4</b> [8.8E-6 0.003]	<b>92</b> [90 93]	<b>84</b> [83 86]	<b>92</b> [91 93]
<b>19/12/2014</b> <b>13:54</b>	<b>0.03</b> [0.0012 0.005]	<b>0.003</b> [0.0012 0.0047]	<b>0.017</b> [0.011 0.022]	<b>816,8</b> [816,4 817]	<b>821</b> [820 822]	<b>818,9</b> [818,8 819,1]

The pollutographs of the events for which the models had their best performance with respect to the  $CR^2$  are shown in Fig. 6. The visual assessment of the model outputs reveals an important strength of the applied approaches that is the replication of multiple peaks of TSS concentrations. This was a forgone result for the homothetic model, but not for the others. The observation of the pollutographs shows that the simulated beam does not frame the entire observations with a varying level of coverage depending on the model and on the rainfall. However, the width of the beam is narrow revealing small uncertainties associated with the simulated TSS concentrations. Accounting for the variability of pollutant generation and transport mechanisms at the elemental scale of the UHE lead to small uncertainties regarding the estimate at the outlet of the TSS concentrations dynamics. The stochastic representation of

the processes succeeded thus in assessing the spatial propagation of uncertainty throughout the catchment space that led to have acceptable prediction of the TSS wash-off.

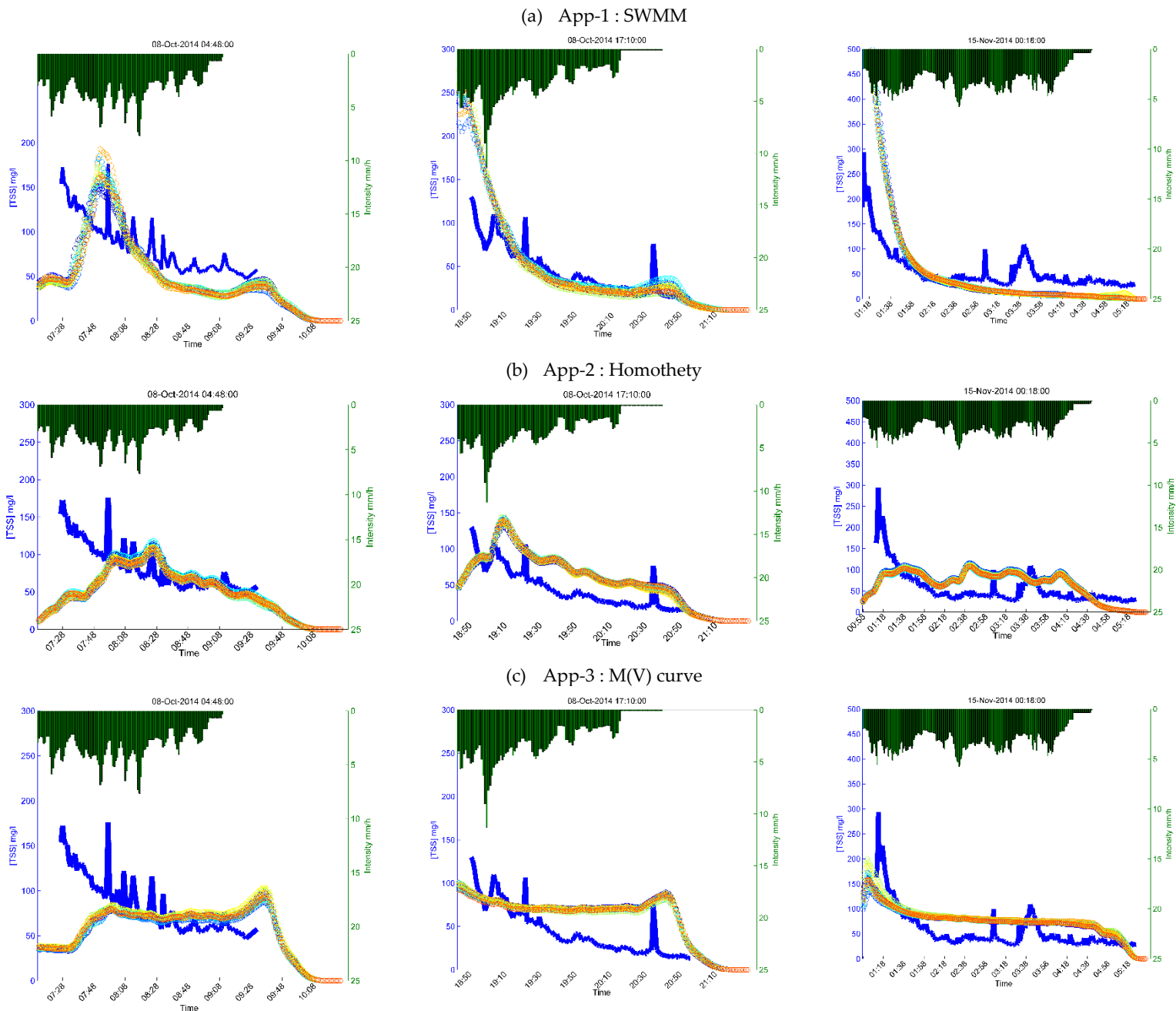


Fig. 6 Best performance events based on TSS concentrations using  $C_{R^2}$  and the  $C_{RMSE}$  criteria for two rainfall events on October 8<sup>th</sup>, and one on November 15<sup>th</sup> simulated with (a) App-1 – SWMM, (b) App-2 – Homothety and (c) App-3 – M(V) curve . The rainfall intensity is plotted on the upper part of the graphs

The stochastic SWMM approach had the best performance among the developed water quality models while the homothety and the M(V) curve approaches didn't perform accurately. All three approaches gave the same results with respect to the RMSE evaluation criteria where the calculated  $C_{RMSE}$  were all in the same ranges. However, the determination coefficients show

the incapability of the model to cope with the intra-event variability of TSS concentrations especially for App 2 and 3. Visual observation of the pollutographs shows that the simulated dynamics with the stochastic SWMM were in accordance with the general decreasing tendency of the TSS concentrations. However, the coverage of the pollutographs with respect to the simulations was variable. For the first event, the model failed at replicating the initial rise of the concentrations but it succeeded in replicating the second peak and the small rise at the end of the event. While for the two other events, the simulations replicated the occurrence of the highest peak at the beginning of the rainfall but the concentrations were overestimated since the beam was higher than the measurement. The decrease of the concentrations was accurately replicated then for the second event while it was underestimated for the steady phase recorded for the third event. The pollutographs simulated with the homothetic model did not succeed at replicating the initial peaks, but they copped better with the steady phase fluctuations with an underestimation for the first event and an overestimation recorded for the second and third. The M(V) curve model failed completely with respect to simulating the dynamics of TSS. The obtained pollutographs were constant during the majority of the event with the appearance of a small peak at the end of two of the events. The most acceptable simulation is for the event of November 15<sup>th</sup> as a small peak of TSS appears at the beginning of the pollutographs then it rapidly decreases into the constant phase.

The difference in the model behavior from an event to another is dependent on the EMC values and the wash-off parameters. The values of these variables are controlled by the probability distribution and the boundaries of the sampling space. The first implementation of this approach assumed that the water quality controlling variables are generated following a uniform probability distribution. Even though there is no straightforward justification to choose the appropriate probability distribution to fit the EMC, the lognormal distribution have been always privileged by researchers to describe the randomness of the EMC (Van Buren et al. 1997; Charbeneau and Barrett 1998). Assuming the log-normality of the EMC sample in the proposed stochastic approach incorporates more knowledge into the wash-off process, which will enhance the selection of the EMC. As for the boundaries of the sampling intervals, they were defined based on both the literature and the prior knowledge of the basin. The latter information however is not available for ungauged catchments, which let the modeler quite free in setting the interval limits. In this case, the sampling intervals must be enlarged to

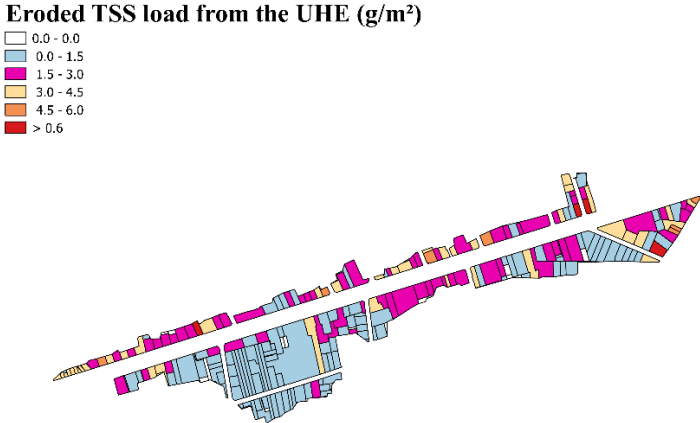
encounter most possibilities. This would require the generation of an important set of parameters which is not possible without the implementation of an automatic sampling technique. In this term, using a Monte Carlo for EMC and parameters iterations can be explored.

### 3.3. Spatial variability of TSS loads

The spatial variability of the simulated eroded TSS loads (mean value) using the first approach (App-1) for the UHE, the roads and the alleys, and the roofs is presented in Fig. 7 for the rainfall event on November 15<sup>th</sup> which had the best performance.

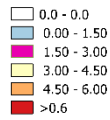
15/11/2014 00:18

(a)



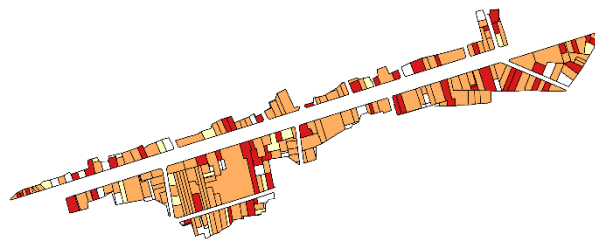
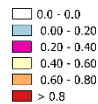
(b)

**Eroded TSS load from the roads and the alleys (g/m<sup>2</sup>)**



(c)

**Eroded TSS load from the roofs (g/m<sup>2</sup>)**



**Fig. 7 Spatial variability of mean TSS washed-off loads (g/m<sup>2</sup>) from the (a) UHE, (b) roads and alleys and (c) roofs for the rainfall event of November 15<sup>th</sup>**

The spatial patterns show distinct yielding of TSS loads for each UHE and for each land use within the UHE confirming the capacity of the stochastic approach in accounting for the variability within every element. The standard deviation of the loads calculated for the UHE is 35 g/m<sup>2</sup> while it is at 20 g/m<sup>2</sup> and 6 g/m<sup>2</sup> respectively for the roads and the roofs. At the UHE scale, higher loads yielded from the parcels connected to the boulevard. The loads generated by the roads ranged mostly between 1.5 and 3 g/m<sup>2</sup> regardless of the road fraction. However, assuming that all roads are subjected to the same traffic density, larger areas must have larger

contaminants yield and the areas closer to the traffic are also subjected to higher contamination than the isolated areas (Saeedi et al., 2009). As such, the distance of the cadastral parcel from the adjacent road and also the fraction of the adjacent road connected to the parcel should be incorporated in the sampling of the EMC in order to account more explicitly for the effect of traffic on pollutant generation. The relationship between these parameters and the EMC could be represented by accounting for an exponential decreasing function with the distance to the street.

#### 4. Conclusion

In this research, a stochastic approach for stormwater quality modeling is developed. The approach is integrated in the physically based distributed hydrological model (URBS), and accounts for the spatial and temporal variability of the governing processes of pollutant production and transport on an urban catchment and. The methodology adopted consisted of generating the EMC and the corresponding wash-off parameters at the beginning of each rainfall event and for each land use, using a uniform probability distribution. Three wash-off models were proposed based on SWMM exponential equations, a homothetic relation between the concentration of TSS and the flow and finally the M(V) relationship. The results demonstrate that incorporating the inherent variability of the build-up/wash-off processes when assessing the contamination of stormwater runoff is essential for better analysis of the outcomes of stormwater quality modeling. The stochastic approaches without any calibration and with little knowledge on the parameters gave fair estimates of the trend of the intra-event fluctuations of TSS concentrations and performed well for several events. The SWMM model had the best performance regarding the replication of the intra-event fluctuation of TSS dynamics.

The integration of stochastic components into stormwater quality modeling is important with respect to the inclusion of processes uncertainties; however, it is accompanied with a high degree of freedom granted to the modeler to make the choices of the boundaries conditions and to characterize the randomness of the parameters. Accordingly, the proposed approach requires deeper research to enhance its potentials as prediction tools for designing efficient mitigation tools which have low cost of implementation compared to other sophisticated approaches. Comparison of this approach with other stormwater quality models



including lumped, sub-catchment based and physically based models is currently being conducted.

## Appendix A

**Table A.1 Characteristics of the simulated rainfall events for the calibration period from October 2014 until January 2015. (ADWP is the antecedent dry weather period)**

	Duration (min)	ADWP (hours)	Rainfall depth (mm)	Maximum intensity (mm/h)
<b>Min</b>	52	0,8	2	1,1
<b>Max</b>	720	274,4	22,1	42,3
<b>Mean</b>	185,4	61,7	5,7	8,3
<b>Median</b>	124	37,2	3,8	5,3
<b>d10</b>	57,6	1,7	2,3	1,1
<b>d90</b>	347	175,1	11,9	15,2

**Table A.2 Characteristics of the nine rainfall events for which water quality modeling results were exploited**

Beginning Date	End Date	Duration (min)	ADWP (hours)	Precipitation height (mm)	Maximum intensity (mm/h)
08/10/2014 04:48	08/10/2014 09:34	288	11,8	9,1	6,89
08/10/2014 17:10	08/10/2014 20:40	212	8	7,47	10,1
09/10/2014 20:18	09/10/2014 21:10	54	24	4,63	42
12/10/2014 13:26	12/10/2014 15:22	118	64,5	3,54	6,9
07/11/2014 05:52	07/11/2014 07:54	124	76,5	3,77	6,71
14/11/2014 09:20	14/11/2014 13:08	230	170	7,42	7,95
15/11/2014 00:18	15/11/2014 04:42	266	11,4	12,83	5,54
26/11/2014 00:44	26/11/2014 02:34	112	221	3,4	4,99
19/12/2014 13:54	19/12/2014 16:04	132	52,7	3,39	12,2

**Table A.3 Values of physical and transfer parameters for hydrological modeling of “Le Perreux” catchment**

Parameter	unit	Description	Value
<b>S<sub>tree,min</sub></b>	mm	Minimum value of the tree interception	1
<b>a</b>	min <sup>-1</sup>	Drainage law coefficient for tree interception	0.04
<b>S<sub>max,soil</sub></b>	Mm	Maximum capacity of the surface reservoir for the natural soil	5
<b>S<sub>max,roof</sub></b>	Mm	Maximum capacity of the surface reservoir for the roof	0.5
<b>S<sub>max,street</sub></b>	Mm	Maximum capacity of the surface reservoir for the street	3.5
<b>K<sub>s,soil</sub></b>	m/s	Hydraulic conductivity at natural saturation for the natural soil	10 <sup>-5</sup>

$K_{s,street}$	m/s	Hydraulic conductivity at natural saturation for the street	$10^{-8}$
$M$	-	Scaling parameter of the hydraulic conductivity	5
$\theta_s$	-	Water content at natural saturation	0.43
$\psi_e$	-	Suction head at air entry	0.05
$Z_{root}$	M	Root depth	1.5
$\Lambda$	-	Ground water drainage coefficient	4
$\mu$	-	Ground water drainage exponent	4
$\alpha_v$	-	Representative position of the vadose zone	0.5
$B$	-	Retention curve exponent	5
$x$	-	Routing parameter of Muskingum	0.2
$\theta_{pipe}$	-	Pipe filling rate	2.51

## 5. References

- Akan, A.O., 1988. Derived Frequency Distribution for Storm Runoff Pollution. *J. Environ. Eng.* 114, 1344–1351. [https://doi.org/10.1061/\(ASCE\)0733-9372\(1988\)114:6\(1344\)](https://doi.org/10.1061/(ASCE)0733-9372(1988)114:6(1344))
- Al Ali, S., Bonhomme, C., Chebbo, G., 2016. Evaluation of the Performance and the Predictive Capacity of Build-Up and Wash-Off Models on Different Temporal Scales. *Water* 8, 312. <https://doi.org/10.3390/w8080312>
- Bárdossy, A., 2007. Calibration of hydrological model parameters for ungauged catchments. *Hydrol. Earth Syst. Sci. Discuss.* 11, 703–710.
- Bertrand-Krajewski, J.-L., Chebbo, G., Saget, A., 1998. Distribution of pollutant mass vs volume in stormwater discharges and the first flush phenomenon. *Water Res.* 32, 2341–2356. [https://doi.org/10.1016/S0043-1354\(97\)00420-X](https://doi.org/10.1016/S0043-1354(97)00420-X)
- Bonhomme, C., Petrucci, G., 2017. Should we trust build-up/wash-off water quality models at the scale of urban catchments? *Water Res.* 108, 422–431. <https://doi.org/10.1016/j.watres.2016.11.027>
- Bujon, G., 1988. Pr evision des d ebits et des flux polluants transit es par les r eseaux d' egouts par temps de pluie. Le mod ele FLUPOL. *Houille Blanche* 11–23. <https://doi.org/10.1051/lhb/1988001>
- Charbeneau, R.J., Barrett, M.E., 1998. Evaluation of methods for estimating stormwater pollutant loads. *Water Environ. Res.* 70, 1295–1302.
- Chen, J., Adams, B.J., 2007. A derived probability distribution approach to stormwater quality modeling. *Adv. Water Resour.* 30, 80–100. <https://doi.org/10.1016/j.advwatres.2006.02.006>
- Chen, L., Gong, Y., Shen, Z., 2016. Structural uncertainty in watershed phosphorus modeling: Toward a stochastic framework. *J. Hydrol.* 537, 36–44. <https://doi.org/10.1016/j.jhydrol.2016.03.039>
- Daly, E., Bach, P.M., Deletic, A., 2014. Stormwater pollutant runoff: A stochastic approach. *Adv. Water Resour.* 74, 148–155. <https://doi.org/10.1016/j.advwatres.2014.09.003>

Deletic, A.B., Orr, D.W., 2005. Pollution Buildup on Road Surfaces. *J. Environ. Eng.* 131, 49–59. [https://doi.org/10.1061/\(ASCE\)0733-9372\(2005\)131:1\(49\)](https://doi.org/10.1061/(ASCE)0733-9372(2005)131:1(49))

Dotto, C.B.S., Kleidorfer, M., Deletic, A., Rauch, W., McCarthy, D.T., Fletcher, T.D., 2011. Performance and sensitivity analysis of stormwater models using a Bayesian approach and long-term high resolution data. *Environ. Model. Softw.* 26, 1225–1239. <https://doi.org/10.1016/j.envsoft.2011.03.013>

Egodawatta, P., Thomas, E., Goonetilleke, A., 2007. Mathematical interpretation of pollutant wash-off from urban road surfaces using simulated rainfall. *Water Res.* 41, 3025–3031. <https://doi.org/10.1016/j.watres.2007.03.037>

Elliott, A., Trowsdale, S., 2007. A review of models for low impact urban stormwater drainage. *Environ. Model. Softw.* 22, 394–405. <https://doi.org/10.1016/j.envsoft.2005.12.005>

Freni, G., Mannina, G., 2010. Bayesian approach for uncertainty quantification in water quality modelling: The influence of prior distribution. *J. Hydrol.* 392, 31–39. <https://doi.org/10.1016/j.jhydrol.2010.07.043>

Göbel, P., Dierkes, C., Coldewey, W.G., 2007. Storm water runoff concentration matrix for urban areas. *J. Contam. Hydrol.* 91, 26–42. <https://doi.org/10.1016/j.jconhyd.2006.08.008>

Green, I.R.A., Stephenson, D., 1986. Criteria for comparison of single event models. *Hydrol. Sci. J.* 31, 395–411.

Gromaire-Mertz, M.C., Garnaud, S., Gonzalez, A., Chebbo, G., 1999. Characterisation of urban runoff pollution in Paris. *Water Sci. Technol.* 39, 1–8.

Hong, Y., Bonhomme, C., Le, M.-H., Chebbo, G., 2016. A new approach of monitoring and physically-based modelling to investigate urban wash-off process on a road catchment near Paris. *Water Res.* 102, 96–108. <https://doi.org/10.1016/j.watres.2016.06.027>

Kanso, A., Tassin, B., Chebbo, G., 2005. A benchmark methodology for managing uncertainties in urban runoff quality models. *Water Sci. Technol.* 51, 163–170.

Kim, J.-Y., Sansalone, J.J., 2008. Event-based size distributions of particulate matter transported during urban rainfall-runoff events. *Water Res.* 42, 2756–2768. <https://doi.org/10.1016/j.watres.2008.02.005>

Lamprea, D.K., 2009. Caractérisation et origine des métaux traces, hydrocarbures aromatiques polycycliques et pesticides transportés par les retombées atmosphériques et les eaux de ruissellement dans les bassins versants séparatifs péri-urbains (phdthesis). Ecole Centrale de Nantes (ECN).

Lee, J.H., Bang, K.W., 2000. Characterization of urban stormwater runoff. *Water Res.* 34, 1773–1780. [https://doi.org/10.1016/S0043-1354\(99\)00325-5](https://doi.org/10.1016/S0043-1354(99)00325-5)

Lindblom, E., Ahlman, S., Mikkelsen, P.S., 2011. Uncertainty-based calibration and prediction with a stormwater surface accumulation-washoff model based on coverage of sampled Zn, Cu, Pb and Cd field data. *Water Res.* 45, 3823–3835. <https://doi.org/10.1016/j.watres.2011.04.033>

Liu, A., Egodawatta, P., Guan, Y., Goonetilleke, A., 2013. Influence of rainfall and catchment characteristics on urban stormwater quality. *Sci. Total Environ.* 444, 255–262. <https://doi.org/10.1016/j.scitotenv.2012.11.053>

McCarthy, D.T., Hathaway, J.M., Hunt, W.F., Deletic, A., 2012. Intra-event variability of *Escherichia coli* and total suspended solids in urban stormwater runoff. *Water Res.* 46, 6661–6670. <https://doi.org/10.1016/j.watres.2012.01.006>

Moriasi, D.N., Arnold, J.G., Van Liew, M.W., Bingner, R.L., Harmel, R.D., Veith, T.L., 2007. Model evaluation guidelines for systematic quantification of accuracy in watershed simulations. *Trans. ASABE*.

Refsgaard, J.C., 1997. Parameterisation, calibration and validation of distributed hydrological models. *J. Hydrol.* 198, 69–97. [https://doi.org/10.1016/S0022-1694\(96\)03329-X](https://doi.org/10.1016/S0022-1694(96)03329-X)

Rodriguez, F., Andrieu, H., Morena, F., 2008. A distributed hydrological model for urbanized areas – Model development and application to case studies. *J. Hydrol.* 351, 268–287. <https://doi.org/10.1016/j.jhydrol.2007.12.007>

Rossman, L.A., 2010. Storm water management model user’s manual, version 5.0. National Risk Management Research Laboratory, Office of Research and Development, US Environmental Protection Agency Cincinnati.

Saeedi, M., Hosseinzadeh, M., Jamshidi, A., Pajooeshfar, S.P., 2009. Assessment of heavy metals contamination and leaching characteristics in highway side soils, Iran. *Environ. Monit. Assess.* 151, 231–241. <https://doi.org/10.1007/s10661-008-0264-z>

Sage, J., Bonhomme, C., Al Ali, S., Gromaire, M.-C., 2015. Performance assessment of a commonly used “accumulation and wash-off” model from long-term continuous road runoff turbidity measurements. *Water Res.* 78, 47–59. <https://doi.org/10.1016/j.watres.2015.03.030>

Sage, J., Bonhomme, C., Emmanuel, B., Gromaire, M.C., 2017. Assessing the Effect of Uncertainties in Pollutant Wash-Off Dynamics in Stormwater Source-Control Systems Modeling: Consequences of Using an Inappropriate Error Model. *J. Environ. Eng.* 143, 04016077. [https://doi.org/10.1061/\(ASCE\)EE.1943-7870.0001163](https://doi.org/10.1061/(ASCE)EE.1943-7870.0001163)

Tsihrintzis, V.A., Hamid, R., 1997. Modeling and management of urban stormwater runoff quality: a review. *Water Resour. Manag.* 11, 136–164.

Van Buren, M.A., Watt, W.E., Marsalek, J., 1997. Application of the log-normal and normal distributions to stormwater quality parameters. *Water Res.* 31, 95–104.

Wijesiri, B., Egodawatta, P., McGree, J., Goonetilleke, A., 2016. Understanding the uncertainty associated with particle-bound pollutant build-up and wash-off: A critical review. *Water Res.* 101, 582–596. <https://doi.org/10.1016/j.watres.2016.06.013>

Wong, T.H., Fletcher, T.D., Duncan, H.P., Coleman, J.R., Jenkins, G.A., 2002. A Model for Urban Stormwater Improvement: Conceptualization, in: *Global Solutions for Urban Drainage*. pp. 1–14.

Zoppou, C., 2001. Review of urban storm water models. *Environ. Model. Softw.* 16, 195–231.

## Chapitre 6. Benchmarking urban stormwater quality models of varying spatial discretization: A case study with lumped, sub-catchments based, urban hydrological element based and grid-based models

**Abstract:** In recent years, urban stormwater models have been increasingly used as a management tool by various researchers and practitioners. Various approaches for stormwater modelling exist, making it difficult to choose the appropriate approach to be applied. In order to make optimal use of the available data, human and computational resources, we proposed a radar chart method for quantitatively benchmarking urban stormwater quality models of varying spatial discretizations, including lumped, sub-catchments based, urban hydrological element (UHE) based and grid-based models. The models are applied to an urban catchment near Paris (Le Perreux sur Marne). Models are evaluated according to various characteristics, such as (i) optimized modelling performance, (ii) predictive power, (iii) simulation reliability, (iv) ease of data collection, (v) computational speed, and (vi) ease of implementation. The results have demonstrated that lumped and sub-catchment based models are generally easier and faster than the other approaches, and can achieve good simulation performance with limited calibration efforts; however, these types of model suffer significant uncertainty and low predictive ability. On the contrary, UHE and grid based models performs satisfactorily in the predictive power and simulation reliability; nevertheless, these models are not easy to execute, and difficult to achieve optimized parameters. Considering the advantages and drawbacks of different types of model, this paper tries to identify the suitable model for different application fields, as well as the future directions for practice issues.

**Keywords:** Urban stormwater quality modelling, Spatial discretization, SWMM, URBS, LISEM-SWMM, Radar chart.

### 1. Introduction

The expansion of urbanization has been accompanied by a big conversion towards impervious surfaces causing important changes in both the quantity and the quality of stormwater runoff that led mainly to increased flood risk and contaminants loads carried by the runoff (Fletcher et al., 2013; Nelson and Booth, 2002; Schueler, 1994). These negative

impacts have placed great emphasis on finding the adequate stormwater management tools to conserve the environment and the quality of life in the cities. In this context, the practitioners have been increasingly using urban stormwater models. Despite this rapid development in the field of urban stormwater modelling, the simulation of urban water quality is still challenging. So far, no ideal methodology exists for simulating stormwater quality at the urban catchment scale (Bonhomme and Petrucci, 2017; Rauch et al., 2005; Salvadore et al., 2015).

Depending on data availability, research/management objectives and study cases, urban hydrological models are commonly classified according to the following criteria.

- Relying on the relations between input and output variables, models can be identified as (i) determinist, (ii) stochastic and (iii) hybrid (Obropta and Kardos, 2007);
- Depending on the mathematical representation of physical processes, models are classified as (i) empirical (also known as black box), (ii) conceptual and (iii) physically-based (Refsgaard, 1990);
- Based on the simulation period, models are recognized as (i) event-based or (ii) continuous (Fletcher et al., 2013);
- According to the spatial discretization, models can be categorized as (i) lumped, (ii) semi-distributed using sub-catchments (sub-catchment based), (iii) urban hydrological element (UHE) based and (iv) grid based two-dimensional (Salvadore et al., 2015).

Among the above criteria, the implementation of water quantity/quality formulations is connected to the model spatial discretization and structuration. For instance, stochastic and empirical equations are often used within the lumped models, while determinist and physically-based equations are commonly applied within the grid based models. Therefore, it is essential to provide a benchmark of the different water quality models based on different spatial discretizations, in order to help researchers and practitioners to choose the appropriate type of model prior to operational applications, making optimal use of the available data and computational resources according to their objectives.

The reviews of (Fletcher et al., 2013; Salvadore et al., 2015; Zoppou, 2001) presented the general characteristics of urban hydrological models. Generally, lumped models, e.g. BASINS (Brun and Band, 2000), KAREN (Dotto et al., 2011), use spatially averaged information to represent the overall behavior of an urban catchment. Sub-catchment based models, e.g.

SWMM (Storm Water Management Model)(Rossman, 2010), InfoWORKS (Innovyze Ltd, 2011), consider sub-regions in the urban catchment as uniform with respect to the hydrological processes and landuse considerations. Grid-based models, e.g. MIKE-Flood (DHI, 2008), FullSWOF (Hong et al., 2016a, 2016b), perform calculation for each grid cell. While UHE based models, e.g. URBS (Rodriguez et al., 2008), CWB (Mackay and Last, 2010), are based on the identification of an object or a unit of calculation small enough to represent the urban heterogeneity regarding the urban hydrological processes.

Existing literature mainly focused on the water flow simulations by using models based on different spatial discretizations. For example, Petrucci and Bonhomme (2014) investigated the trade-off among complexity, calibration and input data using a sub-catchment based model. Leandro et al. (2016) assessed the trade-off between model performance and proper resolution scales using a grid-based model. However, the urban stormwater quality modelling is supported with far less case studies. To our knowledge, no study has been conducted yet aiming to present a complete comparison of the available urban stormwater quality models based on different spatial discretizations on the same studied catchment.

In order to propose a benchmark of using (a) lumped, (b) sub-catchment based, (c) UHE based and (d) grid based models for urban stormwater quality modelling, this paper compares four types of modelling approaches integrated within these types of discretization over an urban catchment near Paris (Le Perreux sur Marne). Models are evaluated according to various characteristics including (i) optimized modelling performance, (ii) predictive power, (iii) simulation reliability, (iv) ease of data collection, (v) computational speed, and (vi) ease of implementation. Although four specific models are used in this study over only a particular urban catchment, the tested modelling approaches and assumptions follow the common agreements in the field of urban stormwater quality modelling. Therefore, the suggested benchmark aims to serve as a preliminary guideline for researchers and practitioners to choose appropriate models in future studies.

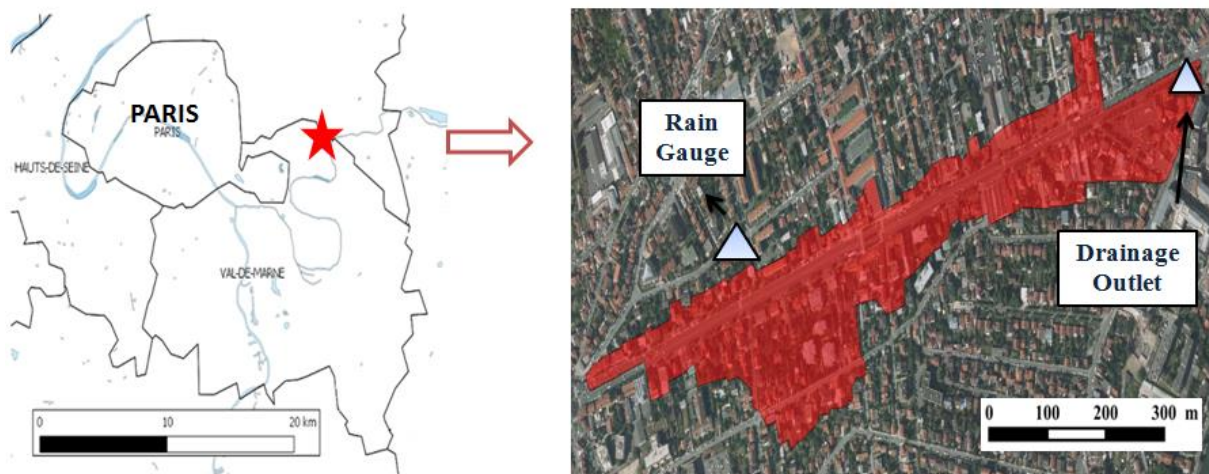
## 2. Study site and data availability

### 2.1. Study site description and monitoring at the catchment outlet

The study site is a residential area located in the eastern suburb of Paris (Le Perreux sur Marne, Val de Marne, France). The area is mainly residential with small commercial shops.

It is crossed by the highly trafficked boulevard “Alsace Lorraine” (more than 30,000 vehicles per day). The total area of this catchment is 12 ha and the impervious surfaces account for 70%. The Western section has a higher slope than the Eastern side, with an average slope of less than 2% (Fig. 1).

The catchment is drained with a separated sewer network. The sewage outlet is located at the North-Eastern edge of the catchment, where the flow is continuously monitored by a Nivus Flowmeter with 2 minutes time interval, and the turbidity is consistently measured by a multi-parameter probe (mini-probe OTT) at 1 minute time step. The turbidity measurements are transformed into total suspended solids (TSS) concentrations following the linear regression  $TSS \text{ (mg/l)} = 0.8533 \times \text{Turbidity (NTU)}$  ( $R^2 = 0.97$ ) derived based on laboratory analysis conducted on samplings from 16 studied rainfall events.



**Fig. 1** Study site at Eastern Paris (12 ha, Le Perreux sur Marne, France). The location of the rain gauge and the drainage outlet equipped with the flow and quality parameters monitoring devices are presented.

## 2.2. Rainfall events description

A tipping-bucket rain gauge is installed on the roof of a building close to the urban catchment (see Fig 1). The rain gauge has a resolution of 0.1 mm. Since the study area is quite small, rainfall is considered as homogeneous within the basin. The monitoring is performed between September 20, 2014 and April 27, 2015. In the work of (Hong et al., 2016a), 56 rainfall events were identified during this study period. More than 88% of the events have a rainfall depth less than 8 mm, nearly 89% of the events have a mean intensity smaller than 3 mm/h, and 87% of the events have a duration shorter than 7 h. These characteristics are typical of the



meteorological conditions of this Parisian metropolitan area, which is subjected to oceanic climate.

For calculation time convenience, only 6 typical rainfall events were selected for models assessment. These rainfall events can be considered as representative of some various hydrological situations on the catchment. The characteristics of the selected rainfall events are summarized in Table S1.

### 2.3. Spatially distributed information

In collaboration with the National Institute of Geography of France (IGN), the department council (Conseil Départemental de Val-de-Marne) and the municipality of “Le Perreux sur Marne”, the studied urban catchment has been well monitored and investigated to acquire the necessary detailed spatial information for models implementation.

#### 2.3.1. Sewer networks and inlet locations

Simulations using sub-catchment, UHE and grid based models require having the data on sewer networks and inlet locations. This precise information is derived from the combination of departmental networks (provided by Conseil Départemental de Val-de-Marne) and municipal sewer networks (provided by “Le Perreux”). The stormwater sewer system consists of 1156 metres departmental pipes (vertical ellipse, 2.3m × 1.3m) along the main street, and nearly 1000 metres municipal pipes (circular, 0.3m × 0.3m) used to connect manholes to the major pipes. In total, there are 35 manholes in the studied catchment (Fig. 2).

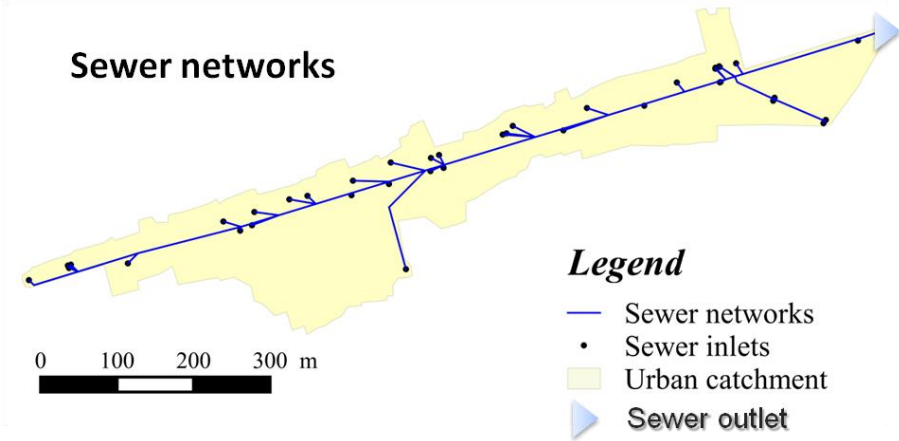


Fig. 2 Separate stormwater sewer networks in the studied urban catchment.

### 2.3.2. Topography

In France, the National Institute of Geographic and Forestry Information (IGN) provides the large-scale reference database (RGE®, <http://professionnels.ign.fr/rge>) that contains DEM (Digital Elevation Model) data of 25 m resolution for the whole country. Fig. 3a shows a part of this data on the study site. In collaboration with the IGN, a mobile mapping system (MMS) called Stereopolis (Paparoditis et al., 2012) has been applied over the study area in order to produce a 20 cm resolution topographic data of road and sidewalks (Fig. 3b). This data is used to generate the input data for UHE based and grid based models.

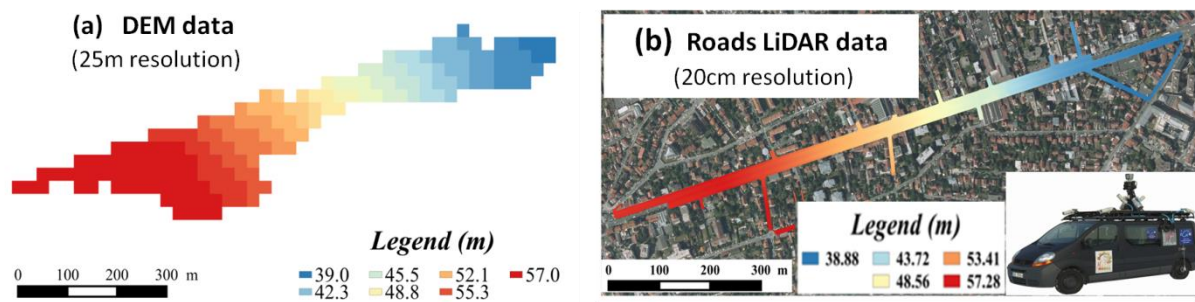


Fig. 3 Different sources of the topographic data. (a) DEM of 25 m resolution; (b) LiDAR data of 20cm resolution for roads and sidewalks.

### 2.3.3. Urban landuse

Landuse data is also necessary for the implementation of both UHE and grid based models. The detailed landuse data (Fig. 4) is identified by combining multiple data sources, such as aerial ortho-photos, LiDAR data and public accessible database. It includes the description of the impervious surfaces (roads, sidewalks, and parking lots) and the vegetation cover.

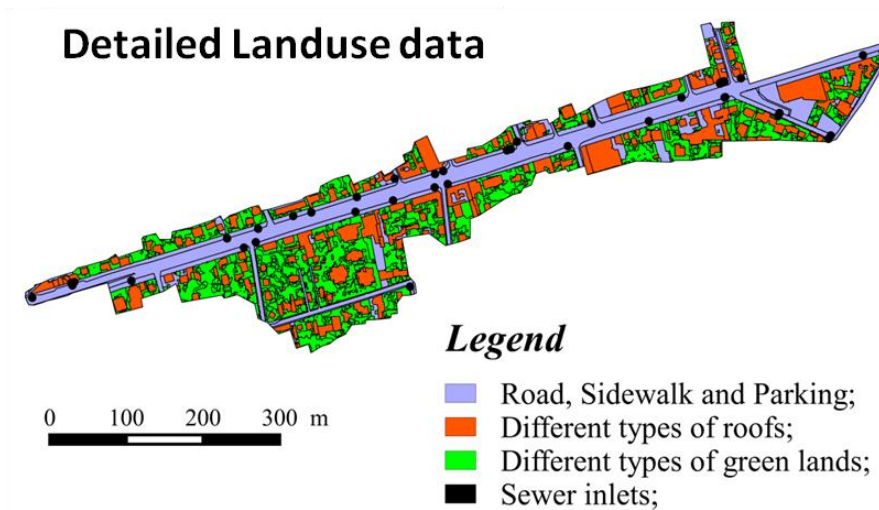


Fig. 4 Detailed landuse information derived by combining multiple data sources.

#### 2.3.4. Cadastral parcels

The cadastral map of the studied site is available in urban data banks provided by the IGN (Fig 5). It defines and delimits the locations and the boundaries of cadastral parcels for “Le Perreux” catchment. This information is essential for the implementation of the UHE based model.



Fig 5. The cadastral map of “Le Perreux” catchment.

### 3. Modelling approaches

Four distinct modelling approaches are investigated in this study and detailed in the sections below. One of the major obstacle for comparing multiple modelling approaches at the urban catchment scale is the difficulty of ensuring consistency between different types of models. In this study, this is encountered with respect to the modelling of the sewer network. To overcome this issue, the processes in sewer network such as deposition, erosion and reaction are neglected, since these mechanisms are not included in the lumped and UHE based models. Therefore, the sewer network compartment of the used models only calculates the transport of water flow and total suspended solids (TSS). Moreover, the same sewer network compartment is used in both the sub-catchment based and grid based models confirming thus the validity of the comparisons between these models based on different spatial discretizations.

#### 3.1. Lumped modelling

In this approach, the surface compartment of SWMM model (Rossman, 2010) is applied without considering any spatial variability within the catchment (Fig. S1). The entire catchment is thus conceptualized as a rectangular surface with a uniform slope and a pre-defined width that drains into a single outlet. The water flow is generated by modelling the catchment as a nonlinear reservoir.

The quality module in this approach is represented by the commonly used exponential build-up/wash-off models. The available mass for erosion at the beginning of the rainfall is computed using the following equation (Eq. 1), in which the build-up rate is represented as a decreasing order increasing rate:

$$M_{accu(i)} = C_1 \times (1 - e^{-C_2 \times ADWP(i)}) + M_{res(i-1)} \quad (1)$$

Where  $M_{accu(i)}$  is the accumulated mass available for wash-off at the beginning of the rainfall event (i);  $C_1$  and  $C_2$  are the build-up parameters;  $ADWP(i)$  is the antecedent dry weather period of the rainfall (i) ;  $M_{res(i-1)}$  is the remaining mass on the surface after the preceding rainfall event (i-1).

The washoff process is simulated using an exponential equation, where the eroded mass is proportional to the water flow and the remaining particles on the urban surface (Eq. 2 and 3).

$$w(t) = c_3 q(t)^{c_4} m_B(t) dt \quad (2)$$

$$m_B(t + dt) = M_{accu}(t) - w(t) \quad (3)$$

Where  $w$  is the eroded mass at a time-step;  $c_3, c_4$  are the washoff coefficients;  $q$  is the flow discharge at the catchment outlet;  $m_B$  is the remaining particles on the urban surface and  $dt$  is the times step.

In this approach, the hydrological and the water quality parameters are homogeneous over the entire urban catchment. One set of parameters is calibrated for the entire surface where no distinction between the processes over different land use is made.

### 3.2. Sub-catchment based modelling

In this approach, the spatial variability of the processes is accounted for through the discretization of the urban surface into sub-catchments (Fig. S1). The basin is divided into three parts that represents the downstream, upstream and center areas. Each part is also divided into three sub-catchments that represent three types of landuses (road, roof and vegetation). As a total, the whole catchment is represented by nine sub-catchments. . The water flow and quality processes are simulated at the scale of each sub-catchment based on the same principles as the lumped model, where a different set of parameters is calibrated for every sub-catchment.

The surface runoff and suspended solids generated from the sub-catchments flow into the sewer networks via junction nodes. Flow routing in pipes from one junction node to another is computed by the one-dimensional (1D) kinematic wave approximation of the Shallow Water (SW) equations. Water quality routing considers that the sewer pipes are represented as completely mixed reactors connected together at junction nodes. The concentration of TSS for a completely mixed reactor is calculated by the mass conservation equation (Eq. 4).

$$\frac{d(V c)}{dt} = C_{in} Q_{in} - c Q_{out} \quad (4)$$

Where  $V$  is the volume within the reactor,  $c$  is the concentration within the reactor,  $C_{in}$  is the concentration of any inflow to the reactor,  $Q_{in}$  is the volumetric flow rate leaving the reactor.

### **3.3. UHE based modelling**

The spatially distributed model Urban Runoff Branching Structure (URBS) is used in this study to represent the UHE based modelling approach (Rodriguez et al., 2008). The surface is divided into Urban Hydrological Elements (UHE), which encompass both cadastral parcels and their adjacent street. Each UHE includes three land use type: street, roof and uncovered soil. For each UHE, the areas of the entire parcel, the buildings, the adjacent street, the alleys, the parking lots and the vegetation are calculated. The coordinates of the center of gravity of the UHE and of the ends of the hydrological network segments are used to determine the connection point of the UHE to the sewer. In total, the studied urban catchment encompasses 274 UHEs, including 56 isolated parcels, which are not connected to the street (Fig. S2).

Water flow at each UHE outlet is simulated by modelling the hydrological processes such as interception, infiltration, surface runoff, evapotranspiration, and soil water drainage. The detailed description of the hydrological modelling principles applied in this approach can be found in (Rodriguez et al., 2008). One set of hydrological parameters is defined for the entire catchment. Water quality simulations are based on a stochastic implementation of the exponential washoff equation (Eq. 2) at the UHE scale, where the parameters are randomly selected for each UHE; the details of this selection are presented in the section (4.1.2).

Water flow and SS are first drained from the surface into the closest manhole of the sewer through a flow path using a travel time function. Then they are routed in the sewer networks to the outlet using the Muskingum-Cunge scheme.

### **3.4. Grid based two-dimensional (2D) modelling**

In this paper, LISEM-SWMM model (Hong et al., 2017) is used for the grid based 2D modelling. Within LISEM-SWMM, the catchment surface is divided into  $224 \times 85$  rectangular meshes. Grids are then categorized into several classes according to the landuse information. Different parameters are attributed to each grid point in accordance with the landuse type. Interception, infiltration, water runoff and pollutant transfer processes are calculated at the grid scale. Diffusive wave approximation of SW equations is applied for simulating the surface



runoff, which is able to represent the spatial and temporal variations of the water flow at the grid level.

As for the sediment transport on the urban surface, the detachment and deposition processes are simulated at steady state. Eq. 5 represents the calculations of the final concentration of the  $i$ -th class of particles in a grid-cell at the end of a time-step. Within each time-step, particles eroded by the rainfall splash detachment are firstly added to the concentration of suspended solids; the updated concentration is then compared with the transport capacity of the water flow, which is calculated by the (Hairsine and Rose, 1992) (H-R) equations. The flow-driven detachment takes place when the updated concentration falls below the transport capacity, while the deposition occurs when the transport capacity is exceeded.

$$\begin{cases} E_i = C_i + \frac{dt}{A h} (det_{splash,i} + det_{flow,i}); & \text{if } C_i + \frac{dt}{A h} det_{splash,i} < T_i, \\ E_i = C_i + \frac{dt}{A h} (det_{splash,i} - dep_i); & \text{if } C_i + \frac{dt}{A h} det_{splash,i} > T_i, \end{cases} \quad (5)$$

Where  $E_i$  is the final concentration of the  $i$ -th class of particles in a grid-cell at the end of a time-step ( $kg/m^3$ );  $C_i$  is the concentration of the  $i$ -th class of particles in a grid-cell at the beginning of a time-step ( $kg/m^3$ );  $dt$  is the time step (s);  $A$  is the surface area of a grid-cell ( $m^2$ );  $h$  is the water depth (m);  $det_{splash,i}$  is the rainfall splash detachment rate of the  $i$ -th class of particles ( $kg/s$ );  $det_{flow,i}$  is the flow detachment rate of the  $i$ -th class of particles ( $kg/s$ );  $dep_i$  is the deposition rate of the  $i$ -th class of particles ( $kg/s$ ).

In this approach, the simulation of flow routing and SS transport in sewer networks relies on the sewer network compartment of the SWMM model. Building roofs are represented as virtual sub-catchments connecting to their nearest sewer nodes. Interactions between the 2D surface component and the sewer network component is modelled through flow exchange at identified linking points, named "junction nodes". These "junction nodes" can receive water and pollutant flows from the virtual sub-basins and the gully-holes. The water flow in sewer networks is computed by the 1D kinematic wave approximation of the SW equations and solved by the finite-difference scheme. Otherwise, water quality routing within conduits assumes that the conduit behaves as a continuously stirred tank reactor (CSTR).

#### 4. Benchmarking different modelling approaches

The comparison of the above four modelling approaches is conducted with respect to different characteristics: (i) simulation performance, including (a) optimized simulation performance, (b) predictive power, and (c) simulation reliability; (ii) data requirement; (iii) demanded computational efforts; and (iv) complexity of model implementation. The simulation performance of each type of model are firstly compared for each rainfall event, and then they are averaged and associated with the rest of the aspects for the overall modelling performance comparisons. The radar chart graphical method is used to display the evaluation criteria for each modelling approach. This method is chosen to compare the models because it allows a simple and clear representation of the performance indicators, whereas the weakness and the strength of each approach are easily and directly spotted. Each characteristic of the simulation performance is compared using reversed scale two-dimensional radar charts of RSR (the standardized version of the Root Mean Square Error) and  $R^2$  obtained with each modelling approach for each rainfall event. The overall performance is assessed using also a two-dimensional radar chart of the performance score calculated for the comparison characteristics stated above for each model.

##### 4.1. Model performance evaluations

###### 4.1.1. RSR and $R^2$ objective functions

Following (Legates and McCabe, 1999; Moriasi et al., 2007), the standardized version of the RMSE (Root-Mean-Square-Error) (Eq. 6), calculated as the ratio of RMSE to the standard deviation of the observations (RSR), is used to calculate the bias between the simulated and observed TSS concentrations. In addition, since the RMSE-based coefficients underestimate the variability and the relative correlation between the measured and simulated signals (Hong et al., 2016a; Krause et al., 2005), the coefficient of determination  $R^2$  (square of the Pearson's product-moment correlation coefficient) (Eq. 7) is applied as a complement to evaluate the colinearity between simulated and measured data.

$$RSR = \frac{RMSE}{STDEV_{obs}} = \frac{\sqrt{\sum_{t=1}^n (Sim_t - Obs_t)^2}}{\sqrt{\sum_{t=1}^n (Obs_t - \overline{Obs})^2}} \quad (6)$$



$$R^2 = \left( \frac{\sum_{t=1}^n (Sim_t - \overline{Sim})(Obs_t - \overline{Obs})}{\sqrt{\sum_{t=1}^n (Sim_t - \overline{Sim})^2} \sqrt{\sum_{t=1}^n (Obs_t - \overline{Obs})^2}} \right)^2 \quad (7)$$

Where  $STDEV_{obs}$  is the standard deviation of the observed data,  $n$  is the total duration of the simulated rainfall duration,  $Sim_t$  and  $Obs_t$  are the simulated and observed TSS concentration at  $t^{th}$  minute,  $\overline{Sim}$  and  $\overline{Obs}$  are the averaged simulated and observed TSS concentration.

RSR incorporates the benefits of error index statistics and includes a scaling/normalization factor, so that the resulting values can be applied to various rainfall events. RSR varies from the optimal value of 0, which indicates zero RMSE and hence perfect model simulation, to large positive values. The lower RSR, the better is the model simulation performance.  $R^2$  can also be expressed as the squared ratio between the covariance and the multiplied standard deviations of the observed and simulated values. Therefore, it estimates the combined dispersion against the single dispersion of the observed and simulated series. The range of  $R^2$  lies between 0 and 1. A value of zero means no correlation at all whereas a value of 1 means that the dispersion of the simulation is equal to that of the observation.

#### 4.1.2. Model optimization methods and performance assessment

The optimized performance assessment for each rainfall event is evaluated by comparing the “best fitted” simulations determined based on the lowest RSR values or highest  $R^2$  results.

- **Optimization method for lumped and sub-catchment based models**

The lumped and sub-catchment based models are calibrated using the genetic algorithm for both water quantity and quality. The optimized parameters are obtained following a procedure that mimics the processes observed in the natural evolution. First, an initial random population is generated from the predefined samples which were adapted from (Bonhomme and Petrucci, 2017). The best members of the population survive to the next generation based on their goodness of fit estimated by the objective function, which is the Nash Sutcliffe. A crossover and a mutation are performed to create a new generation from the

chosen members. These processes are repeated for a certain number of iterations and the best parameter set is determined at the end. For water quantity calibration, 100 generations of 30 parameter sets are adapted while for water quality calibration, 200 generations of 20 parameter sets are adapted.

- **Optimization method for UHE based model**

A part of water quantity parameters is determined by direct field measurements, while the rest is calibrated using a trial and error method. The water quality model implemented in this approach was not calibrated to account for the random nature of the variables and the parameters. The variability of the wash-off is accounted for through the tempo-spatial conceptualization of the event mean concentration (EMC) of SS and the wash-off parameters  $C_3$  and  $C_4$ , which are represented as random uniformly distributed variables. The values of these variables are sampled for each UHE, at the beginning of the rainfall and for each land use from predefined intervals. The interval for the EMC values for the roads is defined from the analysis of samples collected at the inlet of the main boulevard in the catchment, while the interval for the roof is defined based on the literature (Al Ali et al., 2016; Göbel et al., 2007). Then the initial deposited particles can be calculated by using the chosen EMC and two washoff parameters with the following equation (Eq. 8):

$$M_{build-up\ initial} = \frac{EMC \times V_{total}}{C_3 \times Q(t_1)^{C_4} \times dt + \sum_{n=2}^N C_3 \times Q(n)^{C_4} \times dt \times \prod_{j=1}^{n-1} (1 - C_3 \times Q(j)^{C_4} \times dt)} \quad (8)$$

Where:  $M_{build-up\ initial}$  is the available mass of particles at the beginning of a rainfall event;  $EMC$  is the event mean concentration (mg/l);  $V_{total}$  is the total runoff volume for the corresponding rainfall event (l);  $C_3$  and  $C_4$  are the wash-off parameters;  $Q(t_1)$  is the runoff rate at the first time step of the rainfall event;  $dt$  is the time step;  $N$  is the total time step of the rainfall event.

The intervals of the wash-off parameters  $C_3$  and  $C_4$  are defined based on previous work within the catchment and they encompass the values corresponding for the best fit (Al Ali et al., 2016). The intervals are summarized in Table S2.

In summary, for one rainfall event at the scale of the entire urban catchment, 274×6 water quality parameters are sampled and the sampling process is then repeated for ten iterations.

- **Optimization method for grid based model**

Hydrological parameters for this approach are estimated based on a trial and error method. Water quality simulations using grid based model rely on the estimated initial dry deposits derived from the in-situ measurements (Hong et al., 2017). Only the cohesion coefficient (*coh*) can vary from one rainfall event to another. According to (Geotechdata.info, 2014), the typical values of *coh* for the non-cohesive solid vary from 9 - 16. Simulations are hence operated for each event with the *coh* equals to 9, 10, 11, ...,16. In total, 8 simulations are performed for each rainfall event.

#### **4.1.3. Predictive power**

The predictive power of different modelling approaches is evaluated for each rainfall event. For the lumped and sub-catchment based modelling approaches, the predictive power for one rainfall event is calculated by averaging the obtained RSR and  $r^2$  values, using the calibrated parameters on other events. While for the UHE and grid based modelling approaches, since 10 and 8 simulations were performed respectively for every rainfall event, the predictive power of these models can be considered as the mean RSR and the mean  $r^2$  of these simulated results.

#### **4.1.4. Simulation reliability**

According to the section 4.1.2, several simulations have been computed for the UHE based and the grid based models. The simulation diversity of these two types of model can be evaluated by calculating the difference between the highest and smallest RSR and  $R^2$ , respectively. As for the lumped and sub-catchment based models, the simulation diversity are estimated as the variations of RSR and  $R^2$  calculated by modelling one rainfall event using the optimized parameters of different rainfalls.

## **4.2. Ease of data collection**

The better ease of data collection implies the less data requirements to obtain a simulation. Therefore, the required input data and parameters are estimated for the four types

of studied modelling approaches. In order to quantitatively analyze the data requirements, we propose to count the necessary data for implementing the water quantity/quality modelling approaches. An outline of the total data requirements for each type of models is illustrated in Table. 1. In summary, the required data for general configurations mainly relies on the spatial discretizations, while required input water quantity/quality parameters mostly depend on the related conceptual or physical equations.

### 4.3. Computational speed

The computational speed of the models is assessed by considering the demanded computational time for simulating a rainfall event of a duration of 4 hours. Simulations are performed with a computer of 2.7 GHz Intel Core i7 processor and 16G RAM. The needed time for model optimizations (see section 4.1.2) is also taken into account. At the end, the estimated computational time for lumped model is 3 minutes, for sub-catchment based model it is 15 minutes, for UHE based model it is 30 min, and finally for grid based model it is 200 min.

### 4.4. Ease of implementation

For estimating the complexity of model implementation, we assessed the working time needed by an undergraduate student (master degree candidate) to apply the different modelling approaches for the studied urban catchment. Approximately, the student takes 1 week for setting up the lumped model, 2 weeks for the sub-catchment based model, 10 weeks for the UHE based model, and 8 weeks for the grid based model.

### 4.5. Standardization for overall modelling performance

In order to compare the overall performance of the different modelling approaches, a logarithmic function is proposed to grade the modelling performance with a score between 0 and 5 (Eq. 9). For each characteristic, the higher score indicates that the model performs better.

$$Score(Char_i, Mod_j) = 5 \times \frac{MAX(\{LOG[coef(Char_i, Mod_j)]: j = 1,2,3,4\}) - LOG[coef(Char_i, Mod_j)]}{MAX(\{LOG[coef(Char_i, Mod_j)]: j = 1,2,3,4\}) - MIN(\{LOG[coef(Char_i, Mod_j)]: j = 1,2,3,4\})} \quad (9)$$

Where  $Score(Char_i, Mod_j)$  is the score in  $i_{th}$  characteristic of the  $j_{th}$  type of model ( $j = 1,2,3,4$ );  $coef(Char_i, Mod_j)$  is the overall coefficient in  $i_{th}$  characteristic of the  $j_{th}$  type of model.

In this study,  $Coef(characteristic, model)$  for the characteristics such as optimized modelling performance, predictive power and simulation reliability are evaluated by averaging the calculated event-scale RSR of different rainfall events, respectively. While  $Coef(characteristic, model)$  for the other characteristics including ease of data collection, computational speed, and ease of implementation are described by the total data requirements, computational time, and working time for model configurations, respectively. For all these characteristics, the lower  $Coef(characteristic, model)$  implies the better modelling performance.

**Table 1. Data requirements for urban stormwater quality modelling based on different spatial discretizations**

	Required input data for general configurations						Required input parameters for water quantity/quality simulations						<b>Total data requirements</b>
	Surface configurations			Sewer network configurations			Parameters for water flow simulations				Parameters for water quality simulations		
	Spatial discretization units	Input data per unit	Sub-total	Sewer sections	Input data per section	Sub-total	Landuse groups	Input parameters per landuse group	Input parameters for sewer transport	Sub-total	Input parameters per landuse group	Sub-total	
<b>Lumped</b>	1 Catchment	Area; Slope; Width;	<b>3</b>	-	-	<b>0</b>	Lumped catchment;	Impermeability (1); Manning's (Imp & Perm); Rugosity (Imp & Perm); Green & Ampt (3);	-	<b>1x8</b>	Build-up & Washoff (4)	<b>1x4</b>	<b><u>15</u></b>
<b>Sub-catchment based</b>	9 Sub-catchment	Area; Slope; Width; Outlet node;	<b>9x4</b>	23 sewer sections	Begin node elevation; End node elevation; Length; Begin node coordinates (x, y); Shape; Geometry (horizontal & vertical);	<b>23x8</b>	Roofs; Roads; Vegetation;	Impermeability (1); Manning's (Imp & Perm); Rugosity (Imp & Perm); Green & Ampt (3);	Manning's (1)	<b>3x8+1</b>	Build-up & Washoff (4)	<b>3x4</b>	<b><u>257</u></b>
<b>UHE based</b>	274 Urban Hydrological Elements	Outlet coordinates (x,y); Topography; Gravity Coordinates (xg, yg); Total area; Area of different surface types (6);	<b>274x12</b>	103 sewer sections	Begin node elevation; End node elevation; Length; Begin node coordinates (x, y); Diameter	<b>103x6</b>	Roofs; Roads; Vegetation s;	Interception (2); Surface storage(1); Evapotranspiration (3); Darcy's infiltration (6); Travel time function (2);	Muskingum-Cunge (2)	<b>3x14+2</b>	Event MeanConcentration (1); Washoff (4);	<b>3x5</b>	<b><u>3965</u></b>
<b>Grid based</b>	224 x 85 grid cells (5m resolution)	Low-left side coordinates (x,y); Topography; Landuse;	<b>224x85x4</b>	61 sewer sections	Begin node elevation; End node elevation; Length; Begin node coordinates (x, y); Shape; Geometry (horizontal & vertical);	<b>61x8</b>	Roofs; Roads; Vegetation; Gully holes;	Interception (1); Surface storage (1); Manning's (1); Green & Ampt (3);	Manning's (1)	<b>4x6+1</b>	Initial deposits (2 particle classes); Rain splash (1); Flow erosion (1);	<b>4x4</b>	<b><u>76689</u></b>

## 5. Results and discussion

### 5.1. Calibration/validation of the water flow modelling

Accurate water quantity simulations are required for reliable water quality modelling. The simulations of the flow, regardless of the modelling approach, match well with the in-situ measurements at the catchment outlet, with Nash Sutcliffe coefficients higher than 0.7 (Bonhomme and Petrucci, 2017; Hong et al., 2017).

### 5.2. Water quality modelling performance

Since the TSS measurements are quite variable for different rainfall events, the optimized simulation performance, predictive power and simulation reliability of the studied modelling approaches are firstly assessed at the rainfall event scale.

#### 5.2.1. Optimized simulation performance

The RSR and  $R^2$  of the optimized simulations for the six studied rainfall events using different modelling approaches are presented by the radar charts (Fig. 6). The RSR and  $R^2$  values are presented in Table S3.

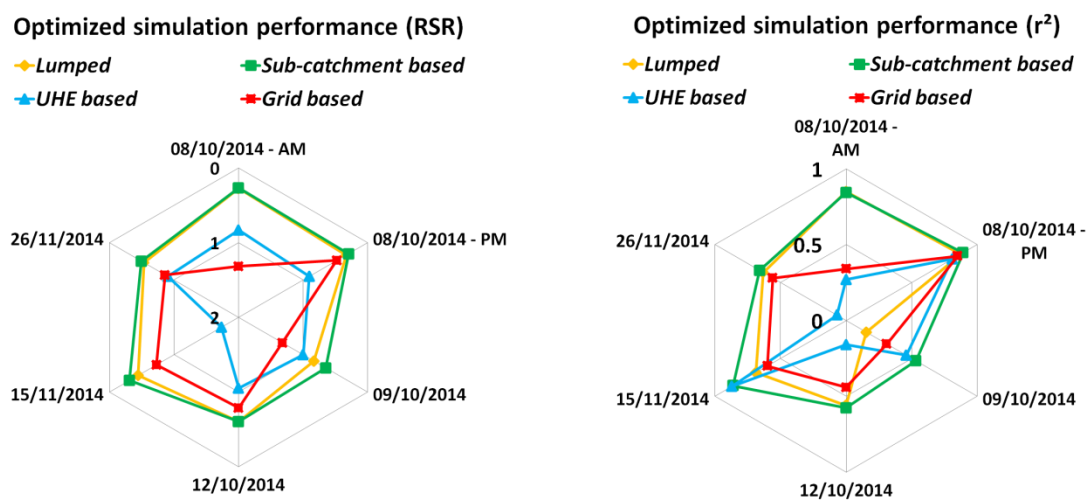


Fig. 6 Radar chart with reverse scale of (a) RSR and (b)  $R^2$  for the optimized simulations of six studied rainfall events using different modelling approaches.

According to Fig. 6, the sub-catchment based model has the best performance of TSS simulation in calibration for all the studied rainfall events, along with the lumped model. The UHE based and grid based models has lower performance. The lumped and sub-catchment based models are calibrated with the genetic algorithm which optimizes the parameters after 4000 simulations for one rainfall event. However, the parameters for UHE are not optimized;

they are randomly chosen for 10 simulations while the parameters of the grid-based model are optimized using simple trial and error method after only 8 simulations. Since the UHE based and grid based models are relatively less studied in the existing literature, simple artificial trial and error methods are commonly applied by researchers and practitioners for calibrating such modelling approaches. Performing a large number of simulation runs based on this calibration method is not feasible due to computational time issues. Therefore, the optimized simulation performance of different modelling approaches in this study could represent the calibration results in general operational applications.

**5.2.2. Predictive power**

The predictive power of each approach is presented in Fig. 7 using a radar chart with reverse scale of RSR and a radar chart of R<sup>2</sup>. RSR and R<sup>2</sup> values are also presented in Table S4.

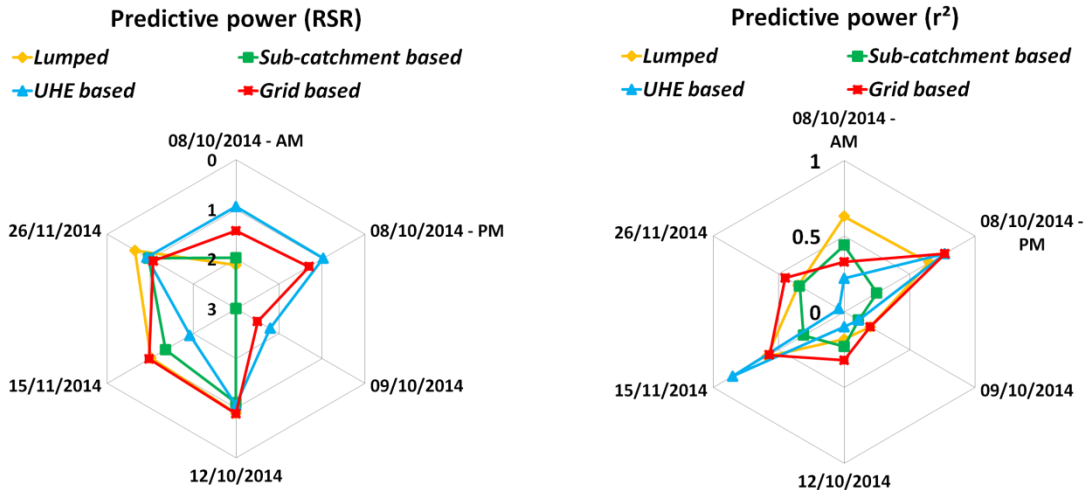


Fig. 7 Radar charts with reverse scale of (a) RSR and (b) R<sup>2</sup> for the predictive power of six studied rainfall events using different modelling approaches. For two events, the RSR values for the lumped approach are not presented in the figure for clarity reasons, the corresponding values can be found in Table S4.

The grid based model has the best performance for predicting TSS concentrations for various rainfall events, and it especially succeeds in simulating the TSS dynamic trends (R<sup>2</sup>). The UHE based model also shows good predictive power when evaluated in terms of RSR. However, it fails in predicting the trends of TSS fluctuations except for two rainfall events. The sub-catchment based model has the least predictive power comparing with other modelling approaches, while the lumped model showed different results based on the rainfall event.



Moreover, the modelling performance of the lumped and sub-catchment based models declines significantly for both RSR and  $R^2$  when comparing the results of the predictions (Fig. 7) with the optimized simulations (Fig. 6); while the performance coefficient, especially the  $R^2$ , remains at a similar level for the UHE based and grid based models. This indicates that when using UHE and grid based models the TSS dynamic trends can be well reproduced, benefiting from the spatially distributed representation of physical processes in these approaches.

### 5.2.3. Reliability of model outputs

Simulations with the least diversity of RSR and  $R^2$  indicate the best reliability performance for the applied modelling approaches. A radar chart with reverse scale of RSR and  $R^2$  changes are presented in Fig. 8. RSR and  $R^2$  values are listed in Table S5.

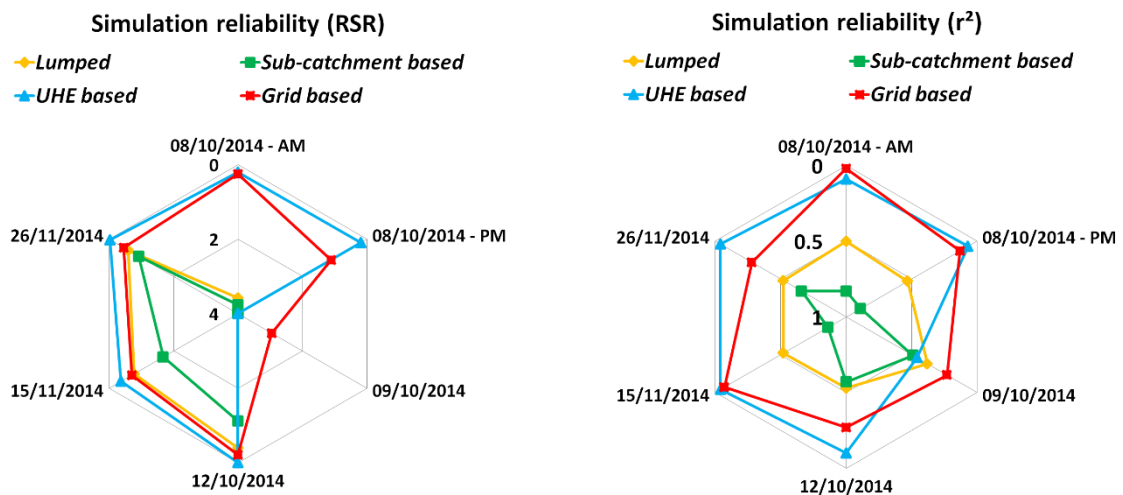


Fig. 8 Radar charts with reverse scale of (a) RSR and (b)  $R^2$  for the simulation reliability of six studied rainfall events using different modelling approaches.

It is shown in Fig. 8 that the UHE and grid based models perform better concerning simulation reliability, particularly for the modelling of TSS dynamics ( $R^2$ ). In general, the very limited variations of RSR and  $R^2$  imply that the UHE and grid based models are quite reliable for urban stormwater quality simulations of different rainfall events. The modelling results do not vary significantly when using different parameter values. In the contrary, parameter values for the lumped and sub-catchment based models should be carefully considered, in order to achieve acceptable simulation results. Although these simulations of the TSS dynamic trends with the grid based model are trustworthy for all the studied rainfall events, the deviations between simulations and measurements are still remarkable for certain rainfall events (for example, the event of 09/10/2014). This is mainly related to the incomplete

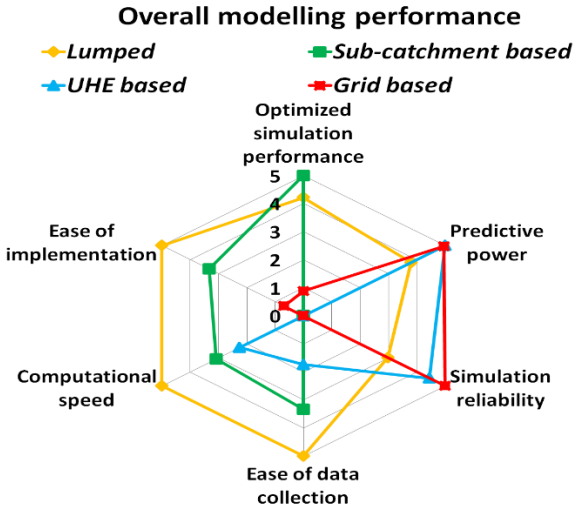
understanding of the physical mechanisms for urban stormwater quality processes, especially the urban pollutant build-up formulations.

### 5.3. Benchmarking the overall modelling performance

The overall comparison of the investigated modelling approaches is done based on the radar chart of the scores of the characteristics for each modelling approach shown in Fig. 9. Values of the metrics used to calculate the overall score are presented in Table 2.

**Table 2. Values of the performance Indicators for assessing the optimized simulation deviation, prediction deviation, simulation variability, data requirement, computational time, and setup time, of different modelling approaches.**

	Optimized simulation deviation (Mean RSR)	Prediction deviation (Mean RSR)	Simulation variability (Mean RSR)	Data requirement (Data point)	Computational time (min)	Setup time (week)
Lumped	0.50	2.16	3.43	15	3	1
Sub-catchment based	0.44	9.76	23.21	257	15	2
UHE based	1.07	1.34	1.34	3965	30	8
Grid based	0.92	1.36	0.95	76689	200	6



**Fig. 9 Radar chart of the logarithmic standardized scores of the optimized modelling performance, predictive power, simulation reliability, ease of data collection, computational speed, and ease of implementation for lumped, sub-catchment based, UHE based and grid based modelling approaches.**

As can be seen from Table 2 and Fig. 9, the lumped model has the best performance regarding the ease of implementation, the computational speed, and the ease of data collection. The sub-catchment based model is featured with its optimized simulation performance.

Furthermore, it is surprising to observe that the predictive power and the simulation reliability of the lumped model are not as poor as expected, but rather better than that of the sub-catchment based model. This result can be explained by the linearity of the urban catchment studied in this paper, where the added sub-catchments in the modelling configuration improves slightly the optimized simulation performance, but introduce huge uncertainties to the simulation reliability and diminish the prediction performance. This finding can be also referred to (Bonhomme and Petrucci, 2017; Orth et al., 2015).

Generally, the results of Fig. 9 show that the ideal modelling approach which can have all expected qualities, does not exist. However, according to the available data, computational and human resources, different modelling approaches can be adapted in accordance with the modelling objectives. Since the lumped model does not account for the spatial variability of the flow and water quality processes inside an urban catchment, it is easy to execute and is particularly suitable for total control problems. The sub-catchment model can achieve the best optimized simulation performance with straightforward calibration efforts, it is applicable for the common uses of practitioners, however, the uncertainty and prediction performance of this type of model should be carefully considered. Besides, the UHE and grid based models realize good performances in predictive power and simulation reliability. Nevertheless, these models require large amount of data and are relatively difficult to apply which limits their current use to research purposes.

## 6. Future outlook for urban stormwater quality modelling practice

Taking knowledge from the radar charts that clearly displayed the strengths and weaknesses for each modelling approach, suggestions to identify the suitable model for different modelling objectives, as well as the future directions for overcoming the current drawbacks are presented.

Lumped models are generally simpler and faster than other approaches, which is particularly useful when limited data is available. They can provide a first assessment of the urban water system at the catchment outlet without any spatially distributed information,

hence they can be used for global control management of urban stormwater quality. Furthermore, lumped models can be easily adapted for Real Time Control (RTC) modelling since they have high computational speed. However, when applied in the context of real time data assimilation, they should be calibrated using advanced optimization methods such as the auto-calibration system (Schou Vorndran Lund et al., 2014). Sub-catchment based models are attractive tools widely used by the practitioners due to their good performance with respect to several characteristics including simplicity, fast implementation and good calibration. However, their results can be accompanied with important uncertainties, especially when the number of sub-catchments is exaggerating. The added complexity of the same type of model does not necessarily lead to improved performance of urban stormwater quality models, which can vary greatly from one rainfall event to another (Bonhomme and Petrucci, 2017; Orth et al., 2015). The application of this approach should be thus accompanied with an uncertainty analysis (Dotto et al., 2009; Vezzaro and Mikkelsen, 2012), to better evaluate its outcomes.

The UHE based models include highly detailed spatial information to describe the morphology of the urban catchments based on urban databanks. This approach have strong potentials regarding stormwater quality estimations based on its relatively good performance with respect to several characteristics. Future studies should focus on the improvement of its optimized modelling performance and ease of setup. User-friendly tools for streamlining model setup and training courses could help the practitioners to better understand and handle the modelling calculations. The optimized modelling performance can be enhanced by implementing calibration methods such as the standardised regression coefficients (SRCs) method (Saltelli et al., 2008) since the computational speed of the model is relatively fast. Integrating these enhancements might lead to the replacement of the sub-catchment based models by the UHE based models, to support practitioners for designing conceptual operations and strategic plans. Additionnally, urban databanks will be more and more available in many cities, which should favor this kind of vector-based modelling approach.

The spatial variability provided by GIS maps and remote sensing can be best exploited by the grid based model, which performs calculations for each grid cell. The level of complexity varies with respect to the spatial resolution of the input data and with the internal description of the process. In this study, the selected 5-metre resolution is a widely accepted resolution for urban modelling applications (Dehotin and Braud, 2008; Leandro et al., 2016).

Excluding the predictive power and the simulation reliability, the grid based model performs poorly in all the other characteristics. However, this type of model is the unique approach, which can be used specifically for the assessment of risks and extreme event impacts, such as finding hidden pollutants flow pathways and simulating water depth of urban flooding. Moreover, since this type of model is relatively complicated, when it is operated inappropriately by unprepared users, it will lead to untrustworthy results. To avoid this issue, the model should be accompanied by a user-friendly modelling interface, for streamlining the model setup, visualizing the configurations and simulated processes, and analyzing the simulation results. Moreover, trainings are recommended for the potential adopters of this type of model. As for the data requirement issues, wider use of the grid based models must hinge on a more systematic approach for mining existing data repositories from governmental and/or commercial sectors. Similar as for the UHE based model, advanced calibration method is also necessary. Since the computational time is mostly quite important, variance based (e.g. Sobol', 1967) or regression based (e.g. SRCs, Saltelli et al., 2008) methods are not suitable for optimizing this type of model. However, the meta-modelling method (Liao et al., 2017; Xiu and Karniadakis, 2003), could be adapted with more considerations on convergence problems. More generally, code parallelization is an essential requirement to reduce computational times for large scale problems.

The suited application fields and the outlook of the lumped, sub-catchment based, UHE based and grid based models are listed in Table 3.

**Table 3. Suggested application fields and future development for lumped, sub-catchment based, UHE based and grid based models.**

<b>Model type</b>	<b>Reference models</b>	<b>Suggested application fields</b>	<b>Future development</b>
<b>Lumped</b>	BASINS (Brun and Band, 2000); KAREN (Dotto et al., 2011)	Preliminary assessment; Total control; RTC;	Auto-calibration system; Real-time data assimilation;
<b>Sub-catchment based</b>	SWMM (Rossman, 2010); InfoWORKS (Innovyze Ltd, 2011)	Regular operations; Conceptual design;	Advanced model uncertainty analysis;
<b>UHE based</b>	URBS (Rodriguez et al., 2008); CWB (Mackay and Last, 2010)	Conceptual design; Strategic planning;	Model setup tools; Regression based calibration methods; Trainings;
<b>Grid based</b>	MIKE-Flood (DHI, 2008); LISEM-SWMM (Hong et al., 2017)	Risk & impact assessment; Strategic planning;	Modelling interface; Meta-modelling calibration methods; Open data; Code parallelization; Trainings;

## 7. Conclusion

In this study, we proposed a radar chart method for quantitatively benchmarking urban stormwater quality models of varying spatial discretizations, including lumped, sub-catchments based, UHE based and grid-based models, that were applied to an urban catchment near Paris. Comprehensive comparisons of the modelling approaches were conducted with respect to different characteristics: (i) simulation performance, including (a) optimized simulation performance, (b) predictive power, and (c) simulation reliability; (ii) data requirement; (iii) demanded computational speed; and (iv) ease of implementation.

The results show that lumped and sub-catchment based models are generally easier and faster than the other approaches, and can achieve good simulation performance with limited calibration efforts. However, these models suffer significant uncertainty and low predictive ability. On the contrary, UHE and grid based models performs satisfactorily for predictive power and simulation reliability; nevertheless, they are not easy to execute, and difficult to achieve optimized parameters.

Based on the strength and weakness of each modelling approach, application fields and improvements for each model are suggested. The ideal approach for water quality modelling that covers all the characteristics does not exist yet. The appropriate model must be chosen mainly with respect to the modelling objectives and the available data. Complementary improvements to minimize the weaknesses of the model should be also developed.

## Appendix

Table S1. Summary of the studied rainfall events.

Rainfall date; begin time	Rainfall depth (mm)	Mean intensity (mm/hr)	Maximum intensity (mm/h)	Duration (hour)	Antecedent dry days (day)	
10/08/2014; 04:53	9.4	1.67	6.89	5.64	0.4	
10/08/2014; 17:30	7.5	2.06	10.1	3.63	0.3	
10/09/2014; 20:17	4.5	3.64	42	0.58	1.23	
10/12/2014; 13:24	3.60	1.68	6.9	2.14	1.8	
11/15/2014; 00:16	9.27	2.1	5.54	4.41	0.5	
11/26/2014; 00:42	2.86	1.1	4.99	2.6	9	
<b>D10</b>	1.55	0.5	2.57	0.70	0.24	
<b>Summary of the 56 rainfall events</b>	<b>D50</b>	3.35	2.27	7.15	3.29	1.82
	<b>D90</b>	8.65	16.36	56	7.51	10.18

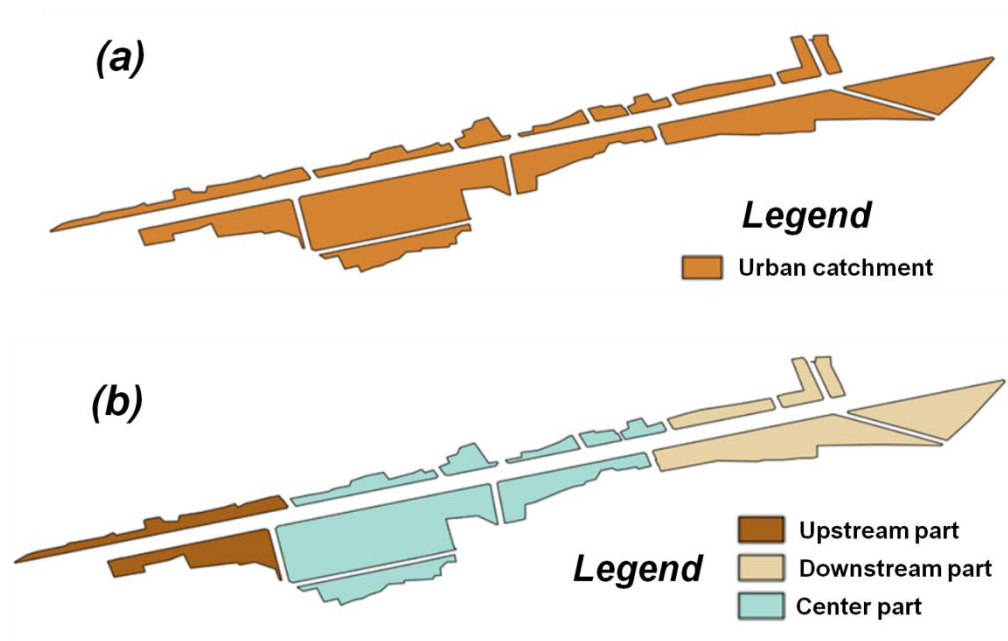


Fig. S1 Spatial discretization of the lumped (a) and sub-catchment (b) models.

## Spatial distribution of the basin based on UHE

- Internal parcel
- Parcel



Fig. S2 The spatial discretization of the basin in terms of UHE. The white parcels represents the UHEs including a fraction of the adjacent street. Red dashed parcels represent internal UHE.

Table S2. The corresponding intervals for the EMC and the wash-off parameters for the road and the roof.

Parameter	Road	Roof
EMC (mg/l)	[82 – 200]	[13 – 60]
C3		[0.01 – 1.5]
C4		[0.8 – 1.9]

Table S3. RSR and R<sup>2</sup> of the optimized simulations using different modelling approaches for the six studied rainfall events.

rainfall	RSR				R <sup>2</sup>			
	Lumped	Sub-catchment based	UHE based	Grid based	Lumped	Sub-catchment based	UHE based	Grid based
08/10/2014- AM	0.27	0.27	0.83	1.31	0.85	0.84	0.27	0.34
08/10/2014- PM	0.33	0.30	0.90	0.48	0.87	0.89	0.81	0.85
09/10/2014	0.83	0.65	1.00	1.32	0.15	0.53	0.46	0.31
12/10/2014	0.60	0.60	1.05	0.79	0.56	0.58	0.16	0.44
15/11/2014	0.44	0.31	1.73	0.73	0.69	0.86	0.87	0.60
26/11/2014	0.53	0.49	0.91	0.86	0.63	0.66	0.07	0.56



**Table S4. Averaged RSR and R<sup>2</sup> by applying the optimized parameters of other rainfall events to each event for lumped and sub-catchment based models; mean RSR and R<sup>2</sup> of the tested simulations for UHE and grid based models.**

rainfall	RSR				R <sup>2</sup>			
	Lumped	Sub-catchment based	UHE based	Grid based	Lumped	Sub-catchment based	UHE based	Grid based
08/10/2014 – AM	2.12	1.97	0.95	1.44	0.63	0.44	0.22	0.33
08/10/2014 – PM	4.94	45.88	0.97	1.31	0.65	0.25	0.77	0.77
09/10/2014	3.32	7.26	2.21	2.50	0.2	0.11	0.11	0.2
12/10/2014	0.90	1.11	1.06	0.88	0.18	0.23	0.1	0.32
15/11/2014	1.02	1.36	1.93	0.97	0.59	0.31	0.85	0.57
26/11/2014	0.65	0.96	0.93	1.07	0.35	0.34	0.04	0.45

**Table S5. Variations of RSR and R<sup>2</sup> by applying the optimized parameters of other rainfall events to each event for lumped and sub-catchment based models; mean RSR and R<sup>2</sup> of the tested simulations for UHE and grid based models.**

rainfall	RSR				R <sup>2</sup>			
	Lumped	Sub-catchment based	UHE based	Grid based	Lumped	Sub-catchment based	UHE based	Grid based
08/10/2014 - AM	3.58	3.76	0.20	0.25	0.5	0.83	0.09	0.02
08/10/2014 - PM	9.59	108.62	0.19	1.11	0.53	0.89	0.07	0.13
09/10/2014	5.66	23.19	7.24	2.95	0.38	0.49	0.46	0.23
12/10/2014	0.39	1.12	0.01	0.21	0.53	0.57	0.1	0.27
15/11/2014	0.77	1.68	0.37	0.70	0.52	0.86	0.04	0.07
26/11/2014	0.59	0.92	0.03	0.45	0.52	0.66	0.04	0.28

## 8. References

Al Ali, S., Bonhomme, C., Chebbo, G., 2016. Evaluation of the Performance and the Predictive Capacity of Build-Up and Wash-Off Models on Different Temporal Scales. *Water* 8, 312. doi:10.3390/w8080312

Bonhomme, C., Petrucci, G., 2017. Should we trust build-up/wash-off water quality models at the scale of urban catchments? *Water Res.* 108, 422–431. doi:10.1016/j.watres.2016.11.027

Brun, S., Band, L., 2000. Simulating runoff behavior in an urbanizing watershed. *Comput. Environ. Urban Syst.* 24, 5–22. doi:10.1016/S0198-9715(99)00040-X

Dehotin, J., Braud, I., 2008. Which spatial discretization for distributed hydrological models? Proposition of a methodology and illustration for medium to large-scale catchments. *Hydrol Earth Syst Sci* 12, 769–796. doi:10.5194/hess-12-769-2008

- DHI, 2008. MIKE by DHI Software. Reference Manuals for MIKE FLOOD.
- Dotto, C.B.S., Deletic, A., McCarthy, D.T., Fletcher, T.D., 2011. Calibration and Sensitivity Analysis of Urban Drainage Models: Music Rainfall/Runoff Module and a Simple Stormwater Quality Model. *Aust. J. Water Resour.* 15, 85–94. doi:10.1080/13241583.2011.11465392
- Fletcher, T.D., Andrieu, H., Hamel, P., 2013. Understanding, management and modelling of urban hydrology and its consequences for receiving waters: A state of the art. *Adv. Water Resour.* 51, 261–279. doi:10.1016/j.advwatres.2012.09.001
- Geotechdata.info, 2014. Cohesion. <http://www.geotechdata.info/parameter/cohesion>.
- Göbel, P., Dierkes, C., Coldewey, W.G., 2007. Storm water runoff concentration matrix for urban areas. *J. Contam. Hydrol.* 91, 26–42. doi:10.1016/j.jconhyd.2006.08.008
- Hairsine, P.B., Rose, C.W., 1992. Modeling water erosion due to overland flow using physical principles: 2. Rill flow. *Water Resour. Res.* 28, 245–250. doi:10.1029/91WR02381
- Hong, Y., Bonhomme, C., Bout, B.V. den, Jetten, V., Chebbo, G., 2017. Integrating atmospheric deposition, soil erosion and sewer transport models to assess the transfer of traffic-related pollutants in urban areas. *Environ. Model. Softw.* 96, 158–171. doi:10.1016/j.envsoft.2017.06.047
- Hong, Y., Bonhomme, C., Le, M.-H., Chebbo, G., 2016a. A new approach of monitoring and physically-based modelling to investigate urban wash-off process on a road catchment near Paris. *Water Res.* 102, 96–108. doi:10.1016/j.watres.2016.06.027
- Hong, Y., Bonhomme, C., Le, M.-H., Chebbo, G., 2016b. New insights into the urban washoff process with detailed physical modelling. *Sci. Total Environ.* 573, 924–936. doi:10.1016/j.scitotenv.2016.08.193
- Innovyze Ltd, 2011. InfoWorks 2D - Collection Systems Technical Review.
- Krause, P., Boyle, D.P., Bäse, F., 2005. Comparison of different efficiency criteria for hydrological model assessment. *Adv Geosci* 5, 89–97. doi:10.5194/adgeo-5-89-2005
- Leandro, J., Schumann, A., Pfister, A., 2016. A step towards considering the spatial heterogeneity of urban key features in urban hydrology flood modelling. *J. Hydrol.* 535, 356–365. doi:10.1016/j.jhydrol.2016.01.060
- Legates, D.R., McCabe, J., 1999. Evaluating the use of “goodness-of-fit” measures in hydrologic and hydroclimatic model validation. *Water Resour. Res.* 35, 233–241. doi:10.1029/1998WR900018
- Liao, Q., Zhang, D., Tchelepi, H., 2017. A two-stage adaptive stochastic collocation method on nested sparse grids for multiphase flow in randomly heterogeneous porous media. *J. Comput. Phys.* 330, 828–845. doi:10.1016/j.jcp.2016.10.061
- Mackay, R., Last, E., 2010. SWITCH city water balance: a scoping model for integrated urban water management. *Rev. Environ. Sci. Biotechnol.* 9, 291–296. doi:10.1007/s11157-010-9225-4

Moriasi, D.N., Arnold, J.G., Van, L., Bingner, R.L., Harmel, R.D., Veith, T.L., 2007. Model evaluation guidelines for systematic quantification of accuracy in watershed simulations. *Trans. ASABE* 50, 885–900.

Nelson, E.J., Booth, D.B., 2002. Sediment sources in an urbanizing, mixed land-use watershed. *J. Hydrol.* 264, 51–68.

Obropta, C.C., Kardos, J.S., 2007. Review of Urban Stormwater Quality Models: Deterministic, Stochastic, and Hybrid Approaches1: Review of Urban Stormwater Quality Models: Deterministic, Stochastic, and Hybrid Approaches. *JAWRA J. Am. Water Resour. Assoc.* 43, 1508–1523. doi:10.1111/j.1752-1688.2007.00124.x

Orth, R., Staudinger, M., Seneviratne, S.I., Seibert, J., Zappa, M., 2015. Does model performance improve with complexity? A case study with three hydrological models. *J. Hydrol.* 523, 147–159. doi:10.1016/j.jhydrol.2015.01.044

Paparoditis, N., Papelard, J.-P., Cannelle, B., Devaux, A., Soheilian, B., David, N., Houzay, E., 2012. Stereopolis II: A multi-purpose and multi-sensor 3D mobile mapping system for street visualisation and 3D metrology. *Rev. Fr. Photogrammétrie Télédétection* 69–79.

Petrucci, G., Bonhomme, C., 2014. The dilemma of spatial representation for urban hydrology semi-distributed modelling: Trade-offs among complexity, calibration and geographical data. *J. Hydrol.* 517, 997–1007. doi:10.1016/j.jhydrol.2014.06.019

Rauch, W., Seggelke, K., Brown, R., Krebs, P., 2005. Integrated approaches in urban storm drainage: where do we stand? *Environ. Manage.* 35, 396–409. doi:10.1007/s00267-003-0114-2

Refsgaard, J.C., 1990. Terminology, Modelling Protocol And Classification of Hydrological Model Codes, in: *Distributed Hydrological Modelling*, Water Science and Technology Library. Springer, Dordrecht, pp. 17–39. doi:10.1007/978-94-009-0257-2\_2

Rodriguez, F., Andrieu, H., Morena, F., 2008. A distributed hydrological model for urbanized areas – Model development and application to case studies. *J. Hydrol.* 351, 268–287. doi:10.1016/j.jhydrol.2007.12.007

Rossman, Lewis A., 2010. Storm water management model user's manual version 5.0. National risk management research and development U.S. environmental protection agency, Cincinnati, OH 45268.

Saltelli, A., Ratto, M., Andres, T., Campolongo, F., Cariboni, J., Gatelli, D., Saisana, M., Tarantola, S., 2008. *Global sensitivity analysis: the primer*. John Wiley & Sons.

Salvadore, E., Bronders, J., Batelaan, O., 2015. Hydrological modelling of urbanized catchments: A review and future directions. *J. Hydrol.* 529, Part 1, 62–81. doi:10.1016/j.jhydrol.2015.06.028

Schou Vorndran Lund, N., Pedersen, J.W., Borup, M., Grum, M., Mikkelsen, P.S., 2014. Auto-Calibration for Data Assimilation in Linear Reservoir Models Used in Flow Forecasting of Urban Runoff. *Proc. 13th Int. Conf. Urban Drain.*

Schueler, T., 1994. THE COMPONENTS OF IMPERVIOUSNESS.

Sobol', I., 1967. On the distribution of points in a cube and the approximate evaluation of integrals. *USSR Comput. Math. Math. Phys.* 7, 86–112. doi:10.1016/0041-5553(67)90144-9

Vezzaro, L., Mikkelsen, P.S., 2012. Application of global sensitivity analysis and uncertainty quantification in dynamic modelling of micropollutants in stormwater runoff. *Environ. Model. Softw.* 27–28, 40–51. doi:10.1016/j.envsoft.2011.09.012

Xiu, D., Karniadakis, G.E., 2003. Modeling uncertainty in flow simulations via generalized polynomial chaos. *J. Comput. Phys.* 187, 137–167. doi:10.1016/S0021-9991(03)00092-5

Zoppou, C., 2001. Review of urban storm water models. *Environ. Model. Softw.* 16, 195–231. doi:10.1016/S1364-8152(00)00084-0

## Chapitre 7. Bilan des messages principaux dans cette partie

L'application d'une approche stochastique, qui tient compte de la variabilité temporelle et spatiale des processus de production et de transfert des contaminants à l'échelle du bassin versant quartier, est promettant pour l'estimation des niveaux de pollution à l'exutoire. La performance de cette approche intégrée dans le modèle distribué basé sur les éléments hydrologiques URBS, en termes de pouvoir prédictif et de fiabilité des simulations, est comparable à celle d'un modèle physique maillé qui nécessite des bases de données et des temps d'implémentation et de calcul très importants. L'amélioration de cette approche pourra se faire en y associant des méthodes avancées de tirage qui permettent d'avoir un nombre plus grand de simulations.

Si cette approche avec l'approche physique distribuée sont les meilleures à utiliser pour faire des prédictions, elles ne sont pas souvent utilisées par les gestionnaires qui préfèrent les modèles simples conceptuels. Les modèles globaux et les modèles semi-distribués, malgré les simplifications qu'engendrent leurs structurations (surtout les modèles globaux), leurs performances dépassent les modèles distribués en calage, en temps d'implémentation et de calcul, ainsi qu'en nombre de points nécessaires pour la mise en œuvre. Cependant ces modèles ne doivent pas être appliqués pour des fins de développement des outils de control sans tenir compte explicitement des incertitudes qui y sont associés.

Ainsi, il n'existe pas une approche idéale qui couvre tous les critères pour avoir la meilleure simulation de la qualité des eaux de ruissellement en milieu urbain. La complexité n'est pas forcément la solution pour avoir des meilleurs résultats. Le choix du modèle doit se faire en fonction des objectifs, des données et des ressources tout en tenant compte des points faibles qui doivent être adressés proprement.



## Partie 6. Conclusions et Perspectives

### 6.1. Rappel des objectifs

Cette thèse s'inscrit dans le cadre de la quatrième phase du projet de recherche OPUR et bénéficie des bases de données collectées sur le site du « Perreux sur Marne » dans le cadre du projet ANR Trafipollu. Elle a pour objectifs principaux d'améliorer les connaissances sur les processus de production et de transfert des contaminants particuliers dans le milieu urbain notamment l'accumulation et le lessivage en se basant sur des bases de données en continu, et de contribuer au développement de nouvelles approches de modélisation conceptuelle de la qualité des eaux de ruissellement.

### 6.2. Principaux résultats

#### 6.2.1. Synthèse sur les connaissances acquises sur les processus d'accumulation et de lessivage

Les bases de données riches acquises dans le cadre du projet Trafipollu à l'échelle du bassin versant locale routier ont permis de mener des études exhaustives sur les processus d'accumulation et de lessivage.

L'étude des dynamiques d'émissions de MES sur le boulevard d'Alsace Lorraine en utilisant les modèles conceptuels usuels d'accumulation-lessivage a montré que ces modèles sont incapables de reproduire les variations temporelles des concentrations de MES pour des longues périodes. La complexité et la variabilité du phénomène d'accumulation, qui n'est représenté qu'avec une formulation simplifiée en fonction de la durée de temps sec, sont vraisemblablement responsables des faibles performances du modèle. Les jeux de paramètres optimaux obtenus sur les périodes où le calage est performant varient largement d'une période à l'autre indiquant l'impossibilité d'avoir un jeu de paramètre unique qui pourrait reproduire les comportements observés en réalité. Ces résultats remettent largement en cause les capacités des approches déterministes de modélisation de la qualité.

Le couplage des modèles de qualité air-eau dans le cas des bassins versants très fréquentés et situés à proximité immédiate des voies de circulation est mis à l'épreuve des

données expérimentales en évaluant la contribution des retombées atmosphériques sèches à la contamination des eaux de ruissellement. Les résultats suggèrent que le rôle que joue l'atmosphère en tant que source de contamination des eaux de ruissellement n'est pas significatif ni pour les HAPs, ni pour les métaux avec des pourcentages de contributions potentielles moyennes ne dépassant pas 11% et 4% respectivement. Pour que l'intégration des sorties des modèles de qualité atmosphérique comme données d'entrées dans les modèles de qualité de l'eau soit plus pertinente, il est recommandé de modifier la définition de la « contamination atmosphérique », pour tenir compte des dépôts directs émis du trafic. Ce qui permet de quantifier la contamination qui se dépose à proximité immédiate du lieu d'émission.

Les mécanismes de mobilisation des particules et la relation qui existe entre le stock accumulé et le stock mobilisé sont investigués à la micro échelle pour deux types de surfaces (un trottoir et un parking). L'eau de ruissellement est obtenue à partir d'une pluie artificielle simulée par un simulateur de pluie innovant qui présente non seulement l'avantage de pouvoir être utilisé sur des sites réels car il est mobile mais aussi la possibilité d'avoir des mesures en ligne du débit et de turbidité. Les résultats montrent le rôle crucial des particules fines dans la contamination des eaux de ruissellement. La sélectivité du lessivage n'est pas basée uniquement sur les tailles des particules mais elle varie aussi en fonction du type de la surface et de l'intensité de pluie. Les dynamiques de transport mesurées qui montrent l'occurrence d'un premier flot même sous débit constant fait la lumière sur la capacité des modèles conceptuels de lessivage à reproduire ce comportement.

## 6.2.2. Synthèse sur la modélisation à l'échelle du quartier

### 6.2.2.1. Modélisation conceptuelle stochastique couplée au modèle hydrologique URBS

La variabilité et la complexité des processus observés à travers l'investigation de l'accumulation et du lessivage à l'échelle locale, ont orienté les efforts vers le développement d'un modèle de qualité basé sur une approche stochastique pour simuler les dynamiques des polluants à l'exutoire qui est couplée au modèle hydrologique distribué URBS.

L'intégration de la variabilité des processus à l'échelle de l'élément hydrologique et la distinction des émissions provenant des différentes occupations du sol en tirant au sort les



concentrations moyennes de MES et les paramètres de lessivage, constitue une approche prometteuse pour simuler des niveaux de concentration à l'exutoire ainsi que la tendance générale des fluctuations intra-événement des polluants. Si cette approche est intéressante car elle est appliquée sans calage à partir de peu d'informations et prédit l'état de contamination à l'exutoire, elle nécessite des approfondissements pour optimiser ses résultats. Ainsi, l'intégration plus explicite de l'effet de la granulométrie des particules et de l'intensité des précipitations sur la fraction mobilisée, dans la procédure de tirage des paramètres de qualité peut être envisagée. L'application d'une méthode de tirage automatique est aussi intéressante comme elle permet d'explorer un nombre plus important de possibilités, surtout dans le cas où peu d'information a priori sur les niveaux de concentrations de polluants sont disponibles. Cela permet aussi de minimiser la liberté donnée au modélisateur dans le choix des intervalles de tirage des paramètres.

#### **6.2.2.2. Comparaison des différentes approches de modélisation de qualité**

La comparaison de quatre approches de modélisation de la qualité des eaux de ruissellement, qui diffèrent dans la description des processus et la discrétisation spatiale du bassin versant urbain, à l'échelle du quartier montre que le modèle idéal qui couvre toutes les caractéristiques de la modélisation de la qualité n'existe pas. C'est par rapport à l'objectif du modélisateur, aux données et aux ressources humaines et informatiques disponibles, que l'approche de modélisation appropriée doit être choisie. Des améliorations complémentaires doivent être également développées pour renforcer les points faibles de l'approche qui sera retenue.

Les résultats ont montré que les modèles globaux et semi-distribués (sous bassins versants) sont les plus simples et rapides à implémenter et ils nécessitent peu de données d'entrée pour leur mise en œuvre. Ils donnent aussi les meilleurs ajustements des pollutogrammes quand ils sont calés avec des algorithmes de calage puissants. Cependant, l'application de ces modèles, dans lesquels les processus sont très simplifiés, doit être accompagnée d'analyse des incertitudes pour une meilleure interprétation de leurs résultats. Si les modèles basés sur les éléments hydrologiques et sur un maillage fin de l'espace sont les plus difficiles à mettre en œuvre et nécessitent un temps d'implémentation et de calcul important, ils restent les plus puissants en termes de fiabilité et de prédiction. L'intégration des méthodes d'optimisation automatique dans ces modèles permettra d'améliorer leurs

résultats en calage. L'entraînement des personnels et la mise en ligne des guides d'utilisation de ces modèles permettront aussi de réduire les difficultés liées à leurs implantations.

### 6.3. Perspectives

Le travail de recherche mené pendant ces trois années a combiné le travail expérimental avec l'aspect modélisation et a fait surgir plusieurs réflexions qui orientent vers des nouvelles perspectives dans le domaine de la gestion de la qualité des eaux de ruissellement dans le milieu urbain.

#### 6.3.1. Pour une meilleure compréhension des processus

L'utilité du travail expérimental et de l'acquisition des bases de données à petite échelle sont soulignées dans cette recherche. L'investigation des processus à l'échelle élémentaire permet de réduire le grand nombre de variables qui sont associés à la recherche sur la qualité de l'eau et permet aussi d'assurer l'homogénéité spatiale ce qui est essentiel au développement des concepts de modélisation et des relations fondamentales qui gouvernent les processus responsables de la génération de la contamination. Ce type d'expérimentation présente aussi une solution au problème de transférabilité des résultats obtenus dans le cas des études à grande échelle. L'expérimentation menée dans le cadre de cette thèse en utilisant le simulateur de pluie et en collectant les dépôts directs sur la surface présente une première étape dans ce chemin. L'avantage de la portabilité du simulateur est de permettre de répéter cette expérimentation en différents points du bassin versant et pour différents types de surfaces urbaines ce qui permet d'acquérir une base de donnée importante en peu de temps ; ceci pourrait être exploité pour élaborer des cartographies dynamiques de la contamination et pour visualiser la répartition spatiale des contaminants.

L'étude des processus responsables de la contamination dans le milieu urbain s'est focalisée sur les processus physiques de dépôts et de mobilisation qui décrivent le comportement de la contamination liée aux particules. Cependant les processus chimiques et biologiques ont aussi une forte influence sur la qualité des eaux de ruissellement. Les caractéristiques physico-chimiques des eaux précipitées et des eaux de ruissellement influencent les processus d'adsorption et de solubilité ce qui entraîne des changements dans la biodisponibilité des polluants et dans la cinétique de lessivage. Cela met en évidence le fait

que certains polluants au cours de leur transport peuvent facilement passer d'un état à l'autre. Par conséquent, l'extension des concepts et des processus communément adoptés pour l'étude de la qualité des eaux de ruissellement afin d'inclure les corrélations entre les charges polluantes et les caractéristiques chimiques des eaux semble essentielle pour une meilleure compréhension des niveaux de contamination et une meilleure représentation des processus.

### 6.3.2. Modélisation de la qualité : où va t'on ?

Un problème central qui se présente par rapport à la modélisation de la qualité de l'eau est le manque d'une vision claire des objectifs attendus des modèles ce qui conduit à avoir des jugements falsifiés par des choix du modèle et des critères d'évaluation inappropriés.

Dans un cadre opérationnel, les efforts doivent s'orienter vers les modèles les plus simples, les modèles statistiques, qui nécessitent le moins d'effort en termes de temps de calcul et d'implémentation. Le développement de tels modèles nécessite la mise en place des stations de mesure en continu ce qui est favorisé par le développement de capteurs intelligents ayant des capacités de stockages énormes et dont les données peuvent être analysées à l'aide des algorithmes d'apprentissage automatique. Ces modèles cependant ne peuvent pas être appliqués dans le contexte d'avoir des prévisions à long terme, car ils sont incapables de tenir compte des scénarios de changement climatique ou de transformation de l'occupation du sol qui entraînent des changements dans la morphologie des bassins versants et qui auront un impact sur les niveaux de contamination.

Pour ce qui concerne la compréhension des processus, deux choix de modélisation se présentent : les modèles physiques et les modèles conceptuels. Les modèles physiques permettent certainement d'avoir la meilleure description des processus d'érosion, cependant les données nécessaires à leur implémentation doivent être disponibles avec une résolution très fine, ce qui engendre des coûts d'acquisition et des coûts informatiques très élevés. Une solution intelligente serait d'intégrer les connaissances acquises sur les processus à partir des modèles physiques dans des modèles conceptuels, étant donné que les modèles conceptuels mis en œuvre même dans un contexte stochastique ne donnent pas toujours des résultats satisfaisants. Le rôle crucial des particules fines dans la contamination des eaux de ruissellement peut être éventuellement intégré plus explicitement dans le modèle de qualité stochastique développé à l'échelle du quartier. Le développement plus poussé de cette

approche est promettant non seulement dans un cadre de recherche mais aussi dans un cadre opérationnel.

Face aux enjeux environnementaux qui menacent la qualité de l'eau, il faut agrandir l'espace de rencontre et d'échange entre les chercheurs et les gestionnaires de différents domaines pour orienter les recherches permettant d'aboutir à des outils de gestion fiables qui répondent aux attentes de la société et qui limitent éventuellement les niveaux de contamination des eaux.

